Synthesis and Characterization of High Performance Polytetrahydrofuran Based Polyurethane-urea and Ionene Elastomers

by

Bin Lee

Dissertation submitted to the Faculty of the

Virginia Polytechnic Institute and State University

in partial fulfillment of the requirements for the degree of

Doctor of Philosophy

in

Materials Engineering Science

APPROVED:

Dr. James E. McGrath, Chairman

Dr. David W. Dwight

Dr. Kenneth L. Reifsnider

Dr. Garth L. Wilkes

Dr. James F. Wolfe

May, 1987

Blacksburg, Virginia

Synthesis and Characterization of High Performance Polytetrahydrofuran Based Polyurethane-urea and Ionene Elastomers

by

Bin Lee

(ABSTRACT)

In this thesis, the effect of interphase bonding on the cohesiveness of domain structure was addressed. The interchain attractive forces between rigid segments and the phase separation between hard and soft segments have been improved by introducing either urea groups or ionic units. The urea linkages have the possibility of extensive hydrogen bonding while ionic units interact with each other by coulombic interactions, which provide even stronger interchain associations than the hydrogen bonding effects.

This thesis addressed the preparation and characterization of polytetrahydrofuran based segmented polyurethane-urea and ionene elastomers. The urea linkages were effectively introduced to the polyurethane elastomers through an unconventional route which was based on carbamate-isocyanate interactions. The carbamates were generated principally from isocyanate functional prepolymers and tertiary alcohols. The carbamates were rearranged thermally and/or catalytically to produce amines which were rapidly converted to ureas. The effects of varying the size of the rigid and flexible segments in polyurethane elastomers on physical behavior were investigated. The importance of hydrogen bonding interactions in promoting phase separation of hard and soft segments and the cohesiveness of hard segment domain structure was demonstrated. Living, difunctional polytetrahydrofuran dioxonium ions were prepared via triflic anhydride initiation. The direct coupling of these "living" polytetrahydrofuran dioxonium ions with a ditertiary amine was used to produce a novel segmented ionene elastomer. The ionenes thus synthesized displayed interesting solution behavior and could be molded, or cast to

produce good physical properties. Photochromic as well as thermochromic phenomena were also noticed in these systems.

ACKNOWLEDGEMENTS

My sincere thanks and appreciation are extended to Dr. James E. McGrath for his guidence and patience throughout the years. I also wish to thank Drs. Wilkes, Dwight, Wolfe and Reifsnider for their helpful comments.

I am thankful to all my colleagues who have offered me helpful suggestions during the course of this investigation. My special thanks are due to Mrs. Tulin Morcol who is responsible for some of the thermal characterization results. Gratitude are also extended to Dr. Tyagi and Mr. Daan Feng for their coorporation in the polymer morphology studies.

Finally, I would like to express my deep appreciation to my parents and my wife for their constant support and encouragement especially during the final stages of the work.

This thesis is dedicated

to my parents, Pei-Hua and Shi-Lin,

my sisters, Pei and Hon,

my brother, Jeh,

my wife, Bih-Shiuan,

who all have been sources of inspiration and strength

throughout this thesis work.

Dedication

TABLE OF CONTENTS

LIST OF FIGURES

LIST OF TABLES

1. INTRODUCTION

Three types of molecular structure can lead to thermoplastic elastomer characteristics [1-5]

1. ABA triblocks in which an elastomer block, B, is capped on both ends by a hard block, A;
2. graft copolymers in which the backbone is an elastomer and the branches are hard segments or vice versa;
3. $(AB)_n$ type of segmented copolymers in which hard and soft blocks are randomly distributed in the backbone itself.

The "soft" segment is an amorphous polymer above its glass transition temperature (T_g). The "hard" segment is usually a polymer below its T_g or its T_m, that is capable of undergoing thermally reversible intermolecular associations. These segments do not mix uniformly, but instead, segregate and result in domain formation. They behave as rubbers because of this unique morphology. The intermolecular association within the domains function as pseudocrosslinks to provide dimensional

stability and recovery after mechanical deflection. This type of elastomer is usually termed as thermoplastic elastomer. Above a certain temperature the "hard" segments soften and the copolymer can be processed in conventional plastics equipment such as extruders and injection-molding machines.

The polytetrahydrofuran (PTHF or PTMO) based polyurethaneureas and ionenes fall into the catagory of $(AB)_n$ type of segmented copolymers. These polymers are of interest not only for academic study but also for their commercial potential.

1.1. POLYURETHANE ELASTOMERS

Polyurethane elastomers exhibit a two-phase microstructure and are composed of blocks of soft and hard segments [6,7]. The polymer structure can vary its properties over a very wide range of strength and stiffness by modification of its three basic building blocks: the polyol, diisocyanate, and chain extender. Properties are related to segmented flexibility, chain entanglement, interchain forces and crosslinking.

The usual route of chemical formation for all urethanes is illustrated in Figure 1.1. This is referred to as the prepolymer method, as the final polymer is formed in two separate steps. Initially, the excess diisocyanate and polyol are reacted together to form an low molecular weight intermediate polymer which is called a "prepolymer" and is normally a thick viscous liquid or low melting point solid of low or no strength. This prepolymer is then converted into the final high molecular weight polymer by further reaction with a low molecular weight diol or a diamine chain extender. This step is usually referred to as the chain extension stage. Alternatively, the entire polymer

formation may be carried out by simultaneously mixing together polyol, diisocyanate, and chain extender (in the presence of catalyst), whereupon the reaction is referred to as the "one shot process". Generally speaking, the prepolymer method produces polymer with better defined copolymer structure (e.g., hard segment size distribution) than the one shot process.

The mechanical and thermal properties of the polyurethanes are determined by a number of factors including the molecular weight and type of soft and hard segment, interactions between the hard and soft phases and crystallinity. It is preferable to describe the relationships between the chemical structure of the polyurethanes and the resultant physical properties.

The hard (rigid) segment consists of a diisocyanate chain extended with a low molecular weight diol or diamine. Generally, polymers based on the aromatic diisocyanates such as most commonly used TDI (toluene diisocyanate) and MDI (4,4'-diphenylmethane diisocyanate) possess a higher softening temperature than their aliphatic counterparts. TDI is less expensive than MDI, however, MDI has superior reactivity and polymers based on MDI may have better properties. TDI is usually prepared as an isomeric mixture of 2,4-TDI and 2,6-TDI. MDI based polyurethanes are of interest since the hard segments can readily crystallize under the right conditions, which imparts good thermal and mechanical properties.

Because aromatic diisocyanates and polymers made from them are somewhat unstable toward light, aliphatic isocyanates have found wide use in coating applications. In addition to greater light stability, polyurethanes based on aliphatic isocyanates possess an increased resistance to hydrolysis and thermal degradation.

The reaction of equimolar quantities of macroglycol and diisocyanate generally results in a polymer that exhibit very poor physical properties. The "chain extender",

usually a low molecular weight diol or diamine, was utilized to tailor the polymer properties. The proportion of macroglycol to chain extender can be varied to produce polymers with widely differing mechanical properties due to the variation in the weight fraction of hard segment material in the block copolymers. In general, aliphatic chain extenders yield softer materials than do aromatic chain extenders.

The materials that are chain extended with diamines produce urea linkages, which usually exhibit superior properties when compared to similar polymers prepared with the equivalent diol chain extender. In viewing the chemical structure, the urethane chains contains the -O- "swivel", thus they are more flexible and have a large ΔS_f and therefore a lower T_m is expected than for the urea chains (for crystalline hard segments). This generalization is on the basis of the Gibbs free energy of melting which is given by

$$\Delta G_m = \Delta H_f - T\Delta S_f$$

At the crystalline melting point T_m, ΔG_m is equal to zero, so

$$T_m = \frac{\Delta H_f}{\Delta S_f}$$

Moreover, the urea linkage has the extra -NH- which form stronger or more extensive hydrogen bonds and therefore have a higher ΔH_m than the urethane linkage. An empirical estimation of the interaction energies of urea and urethane groups leads to

values of 59.9 and 36.5 KJ/mole respectively [8]. The cohesion of urea groups in the rigid blocks is largely responsible for the strength of the network structure.

However, many diamines are too reactive toward isocyanates in the preparation of bulk elastomers, as insufficient time is available for adequate mixing and pouring before gelation occurs. The preferred diamine for elastomers is MOCA (3,3'-dichloro-4,4'-diaminodiphenylmethane). Derivatives of 4,4'-diaminodiphenyl (benzidine), although providing elastomers having excellent physical properties, are to be avoided if possible, due to the fact that many present carcinogenic hazards, and MOCA also is suspected of constituting a health hazard.

The soft (flexible) segment is a long-chain macroglycol, with a molecular weight between 500 and 5000. Polyols available for elastomer synthesis include polyethers, polyesters, polydienes or polyolefins, and polydimethylsiloxanes. Their chemical structures and some corresponding literature references are listed in Figure 1.2. Traditionally, polyurethanes have been produced with polyether and polyester soft segments. Polyester based urethanes possess relatively good material properties; however, they are susceptible to hydrolytic cleavage of the ester linkage [9,10]. The polyether based urethanes exhibit a relatively high resistance to hydrolytic cleavage. Polyethylene oxide (PEO) based materials show poor water resistance due to the hydrophilic nature of the soft segments. Polypropylene oxide (PPO) has been widely used mostly due to its low cost, reasonable hydrolytic stability and balanced properties.

The polyether that results in a polyurethane with the best physical properties is polytetramethylene oxide (PTMO). Despite its relatively high cost, it is valued as a precursor leading to elastomers with outstanding hydrolytic stability, good low-temperature flexibility, outstanding thermal stability at elevated temperatures and high

fungus resistance, combined with excellent abrasion resistance and resiliency [11].

When envioromental stability is a major concern, hydrocarbon based glycols offer an alternative to the relatively less stable polyester and polyether soft segments. Polyisobutylene based polyurethanes show excellent resistance to light and thermal degradation and hydrolysis. Unfortunately, the synthesis of these materials is difficult, and the physical properties of the resulting polymers are poor relative to those of conventional polyurethanes. The use of polydimethylsiloxane glycol (PDMS) as a soft segment leads to polyurethanes with improved low-temperature properties. The glass transition temperature of PDMS is about -123^{o}C, which allows the use of these materials at very low temperatures.

The molecular weight of soft segment used in the synthesis of polyurethanes has an important influence on copolymer properties [12]. For example, a PTMO of about 1000 molecular weight leads to copolymers with the best overall properties, especially resistance to stiffening. When PTMO polyols of 3000 molecular weight or more are used, the copolymers contain crystalline polyether regions at room temperature. At approximately 2000 molecular weight, stress-induced crystallization occurs on stretching to 100% or more at room temperature.

In recent years, much work has been carried out to elucidate the physical structure of urethanes. In particular, thermal analysis and X-ray scattering investigations have been found to show evidence for a two phase structure. It is now generally accepted that the hard segments separate to form discrete domains in a matrix of soft segments. The rigid domains formed act both as tie down points (being chemically linked to the soft matrix) and as filler particles, reinforcing the soft segment matrix.

The extent of phase separation can affect many important properties of the segmented materials [3]. It is well accepted that thermal history [13,14],

stereoregularity [15], block length [16,17], and distribution of block length [17] play important roles in determining the degree of phase separation, as well as the degree of order in hard and soft segment domains. Higher degrees of phase separation are favored when non-polar soft segments [18,19] such as PBd and PIB, and/or a longer sequence length of the hard and soft segments is employed.

1.2. IONENE ELASTOMERS

Ionenes are those polyquaternary ammonium compounds where the ammonium cation integral in the main chain, as opposed to those materials where the bound positive sites are pendant to the chain. Integral quaternaries can be either on a linear chain or a cyclic (aliphatic or aromatic) species; in any case they form part of the backbone.

Ionenes synthesized from low molecular weight dialkyl halides and ditertiary amines are generally brittle and lack mechanical strength. For most industrial applications, it is desirable to have a polymer which possesses good film-forming properties which can be shaped by conventional processes such as compression molding and solvent casting. The incorporation of flexible chains, such as polypropylene oxide (PPO) and polytetra- methylene oxide (PTMO), into the matrix polymer has been generally utilized [52, 53-54, 55-58].

Elastomeric ionenes can be considered as a relatively new class of polymer in the sense that only limited articles have reported in the literature related to this subject so far. Common ionene elastomers reported actually are copolymers of urethane with some quaternary ammonium groups distributed along the polymer backbone. Only

until recently, pure ionene elastomers with interesting properties were prepared by the reaction of dimethylamino-terminated polytetrahydrofuran oligomers and p-xylene dibromide. This system is certainly of interest from academic point of view besides its potential commercial applications. One can now differentiate the contributions from hydrogen bonding (e.g., urethane and urea linkages) and ionic associations to the elastomer properties (thermal and mechanical properties, phase separation, etc.).

Elastomeric ionenes based on the dimethylamino-terminated polytetrahydrofuran and p-xylene dibromide have been prepared by Kohjiya et al. [56,57]. The reaction scheme they used is shown as follows

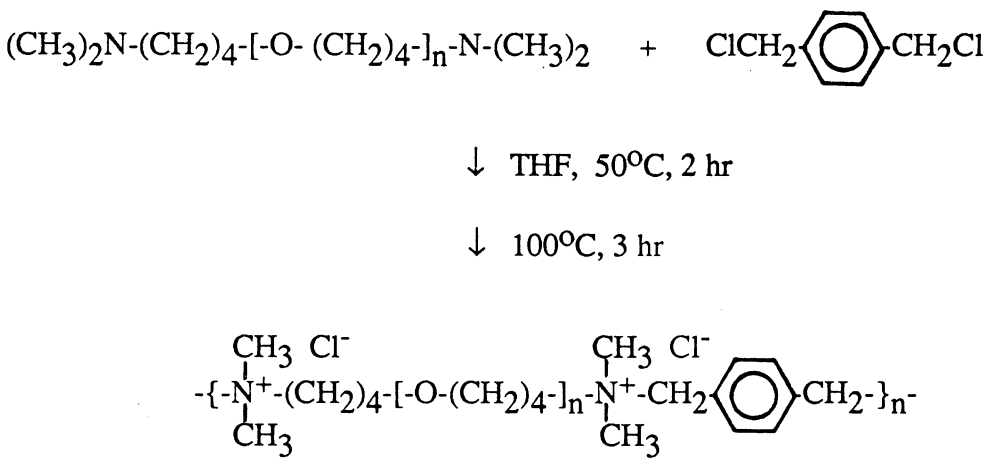

Dimethylamine terminated polytetrahydrofurans were prepared by the living cationic polymerization of THF terminated by dimethylamine. Basically, poly-THF with any molecular weight can be prepared and molecular weight increases with conversion. The functionality is found to be approximately two, which indicates dimethylamino groups are located at the both ends of poly-THF. The difunctional initiator utilized in the THF polymerization is trifluoromethanesulfonic acid anhydride, which was first reported by Smith and Hubin [59]. The detailed initiation mechanisms of this novel

initiator will be discussed in the Chapter 5.

1.3. RESEARCH OBJECTIVES

The principal goal to be achieved here was to develop novel polyurea or thermomechanical stable hard segments which would provide good heat resistance for possible short term high temperature (ca.150^{o}C) applications.

The reason for the choice of polytetrahydrofuran (PTHF or PTMO) as the soft segment is three fold. Firstly, good hydrolytic stability allows the polymer to be used in a wet enviroment. Secondly, a low glass transition temperature of about -80^{o}C provides low temperature flexibility. Finally, the ability to crystallize on extension is due to structural regularity and this is thought to be an important factor contributing to the high tensile strength.

The performance of elastomers at elevated temperatures is very dependent on the structure of the rigid segments and their ability to remain associated at these temperatures. Hard segments significantly affect mechanical properties, particularly modulus, hardness, and tear strength. Two approaches were utilized to improve the softening temperatures of hard segments. Firstly, the use of bulky aromatic diisocyanates having a symmetrical molecular structure such as MDI along with a bulky chain extender, presumably will result in a rigid structure with high distortion temperature. Secondly, the interchain attractive forces between rigid segments is expected to be improved by introducing either urea groups or ionic units. The urea linkages have the possibility of extensive hydrogen bonding while ionic units interact with each other by columbic interactions, which may provide even stronger interchain

associations than the hydrogen bonding effects.

The synthesis and physical properties of two types of elastomer, polyurethane-ureas and ionenes, based on the PTHF soft segment were studied. The effect of varying the size of the rigid and flexible segments in polyurethane elastomers were investigated. The ionic concentrations and the molecular weight of PTHF soft segment in ionene elastomers are also altered in order to study their effects on ionomer properties.

Structural identification of polymers was accomplished by using spectroscopic techniques such as FT-IR, ^{1}H-NMR, and Mass Spectroscopy. Thermal analysis techniques such as DSC (Differential Scanning Calorimetry), TMA (Thermomechanical), and TGA (Thermogravimetric Analysis) were utilized extensively to characterize the polymer thermal behavior. Dynamic mechanical experiments provided information on first- and second-order transitions (T_m and T_g, respectively), phase separation, and mechanical behavior of polymers. Finally, the stress-strain analysis was conducted on these elastomers to determine the mechanical response on extension.

1.4. FORMAT

This thesis is divided into two parts. The first part, comprised of Chapter 2,3, and 4, is related to polyurethane elastomers. Chapter 5 constitute the second part which describes the preparation and physical behaviors of ionene elastomers.

In Chapter 2, a new method for polyurea synthesis is introduced and discussed, which has been termed a carbamate-isocyanate interaction. Chapter 3 describes the

application of the methods for the preparation of polyurethaneurea elastomers and the physical properties of the resulting polymers.

The phase mixing between the soft and hard segments in polyurethane elastomers has been a general concern in the field. A better phase separation is usually translated to better polymer properties. In Chapter 4, a new concept was introduced in which a "phase demixing agent" was utilized to improve the phase separation of the polyurethane elastomers.

Part two (Chapter 5) discusses in considerable detail the synthesis, characterization, and properties of the novel PTHF-ionene elastomers. The approach to the ionene synthesis is quite unconventional and utilized the direct coupling of living PTHF dioxonium ions with ditertiary amines.

Within each of the chapters, a brief literature review related to the entitled subject will be given along with detailed experimental procedures and results and discussion, as well as conclusions. The cited references will be attached at the end of each chapters for the purpose of easy reading. Finally, in Chapter 6, general conclusions for the entire thesis will be given.

REFERENCES

1. A. Noshay and J.E. McGrath, "Block Copolymers: Overview and Critical Survey", Academic Press, New York (1977).
2. D.C. Allport and W.H. Janes, Eds., "Block Copolymers", Wiley, New York (1973).
3. J.J. Burke and V. Weiss, Eds., "Block and Graft Copolymers", Syracuse

University Press, New York (1973).

4. S.L. Aggarwal, Ed., "Block Copolymers", Plenum Press, New York (1970).
5. I. Goodman, Ed., "Development in Block Copolymers", Vol.1, Applied Science Publishing, Essex, UK (1982); Vol. 2 (1985).
6. C. Hepburn, "Polyurethane Elastomers", Applied Science Publishing, New York (1982).
7. M.D. Lelah and S.L. Cooper, "Polyurethane in Medicine", CRC Press, Inc., Boca Raton, Florida (1986).
8. D.W. Van Krevelen and P.J. Hoftyzer, "Properties of Polymers: Their Estimation and Correlation with Chemical Structure", Elsevier Scientific Publishing Company, New York (1976).
9. P. Wright and A.P.C. Cumming, "Solid Polyurethane Elastomers", Gordon and Breach, New York (1969).
10. D.W. Brown, R.E. Lowry, and L.E. Smith, Macromolecules, 13, 248 (1980).
11. P. Dreyfuss, "Poly(tetrahydrofuran)", Gordon and Breach Science Publishers, New York (1982).
12. J.R. Wolfe, Jr., Rubb. Chem. Technol., 50, 688 (1977).
13. G.L. Wilkes and J.A. Emerson, J. Appl. Phys., 47, 4261 (1976).
14. G.L. Wilkes, S. Bagrodia, W. Humphries, and R. Wildnauer, J. Polym. Sci., Letters, 13, 321 (1975).
15. K. Onder, R.H. Peters, and L.C. Spark, Polymer, 18, 155 (1977).
16. L.L. Harrell, Jr., Macromolecules, 2, 607 (1969).
17. G. Lunardon, Y. Sumida, and O. Vogl, Die. Angew. Makromol. Chemie., 87, 1 (1980).
18. S.B. Clough and N.S. Schneider, J. Macromol. Sci., Phys., B2, 553 (1968).

19. T.A. Speckhard and S.L.Cooper, Rubb. Chem. Technol., 59 (3), 405 (1986).

20. C. T. Chen, R.F. Eaton, Y.J. Chang, and A.V. Tobolsky, J. Appl. Polym. Sci., 16, 2105 (1972).

21. J.T. Koberstein and T.P. Russell, Macromolecules, 19, 714 (1986).

22. G.A. Senich and W.J. MacKnight, Macromolecules, 13, 106 (1980).

23. M. Watanabe, K. Sanui, and N. Ogata, Macromolecules, 19, 815 (1986).

24. C.S. Paik Sung, T.W. Smith, and N.H. Sung, Macromolecules, 13, 117 (1980).

25. H. Ishihara, I. Kimura, and N. Yoshihara, J. Macromol. Sci., Phys. Ed., B22(5), 713 (1983).

26. C.B. Hu, R.S. Ward, Jr., and N.S. Schneider, J. Appl. Polym. Sci., 27, 2167 (1982).

27. S.C. Yoon and B.D. Ratner, Macromolecules, 19, 1068 (1986).

28. H. Ishihara, J. Macromol. Sci., Phys. Ed., B22(5), 763 (1983).

29. M.F. Rubner, Macromolecules, 19, 2114 (1986).

30. T.A. Speckhard, G. Ver Strate, P.E. Gibson, and S.L. Cooper, Polym. Eng. Sci., 23(6), 337 (1983).

31. T.A. Speckhard, S.L. Cooper, V.S.C. Chang. and J.P. Kennedy, Polymer, 25, 55 (1984).

32. T.A. Speckhard, K.K.S. Huang, S.L. Cooper, V.S.C. Chang. and J.P. Kennedy, Polymer, 26, 70 (1985).

33. T.A. Speckhard, S.L. Cooper, V.S.C. Chang. and J.P. Kennedy, Polymer, 26, 55 (1985).

34. R.M. Houghton and D.A. Williamson, SPE J. 27, 43 (1971).

35. C.H.Y. Chen-Tsai, E.L. Thomas, W.J. Macknight, and N.S. Schneider, Polymer, 27, 659 (1986).

36. Y.S. Lipatov, N.V. Dmitruk, V.V. Tsukruk, V.V. Shilov, L.S. Priss, and L.I. Dashevsky, J. Appl. Polym. Sci., 29, 1919 (1984).

37. P.W. Ryan, Brit. Polym. J. 3(3), 145 (1971).

38. D.M. French, Rubb. Chem. Technol., 42, 71 (1969).

39. C.M. Brunette, S.L. Hsu, W.J. Macknight, and N.S. Schneider, Polym. Eng. Sci., 21(3), 163 (1981).

40. J. Foks and G. Michler, J. Appl. Polym. Sci., 31, 1281 (1986).

41. G. Rehage, R. Lamour, J. Fuhrmann, and T. Wilhelm, Makromol. Chem., 187, 1313 (1986).

42. R.W. Seymour, A.E. Allegrezza, Jr., and S.L. Cooper, Macromolecules, 6(6), 896 (1973).

43. R.W. Seymour, G.M. Estes, and S.L. Cooper, Macromolecules, 3(5), 579 (1970).

44. J.W.C. Van Bogart, P.E. Gibson, and S.L. Cooper, J. Polym. Sci., Phys. Ed., 21, 65 (1983).

45. C.G. Seefried, Jr., J.V. Koleske, F.E. Critchfield, and J.L. Dodd, Polym. Eng. Sci., 15(9), 567 (1975).

46. A. Balas, G. Palka, J. Foks, and H. Janik, J. Appl. Polym. Sci., 29, 2261 (1984).

47. J.P. Pascault and Y. Camberlin, Polym. Communications, 27, 230 (1986).

48. Y. Camberlin and J.P. Pascault, J. Polym. Sci., Polym., Phys. Ed., 22, 1835 (1984).

49. D. Tyagi, G.L. Wilkes, I. Yilgor, and J.E. McGrath, Polym. Bull., 8, 543 (1982).

50. D. Tyagi, I. Yilgor, J.E. McGrath, and G.L. Wilkes,Polymer, 25, 1807 (1984).

51. Y. Xuuhai, M.R. Nagarayan, T.G. Grasel, P.E. Gibson, and S.L. Cooper, Polymer, (1986).

52. C.M. Leir and J.E. Stark, 3M Company, to be published.

53. M. Watanabe, N. Toneaki, Y. Takizawa, and Isao Shinohara, J. Polym. Sci. Chem. Ed., 20, 2669 (1982).

54. M. Watanabe, N. Toneaki, and Isao Shinohara, Polym. J., 14(3), 189 (1982).

55. M. Watanabe, K. Nagaoka, M. Kanba, and Isao Shinohara, Polym. J., 14(11), 877 (1982).

56. S. Kohjiya, T. Ohtsuki, and S. Yamashita, IUPAC 6th International Symposium on Cationic Polymerization and Related Processes, Ghent, Belgium, Abstracts, 169 (1983).

57. S. Kohjiya, T. Ohtsuki, and S. Yamashita, Makromol. Chem., Rapid Commun., 2, 417 (1981).

58. S. Kohjiya, T. Hashimoto, S. Yamashita, and M. Irie, Chem. Lett., 1497 (1985).

59. S. Smith and A.J. Hubin, J. Macromol. Sci. Chem., 7, 1399 (1973).

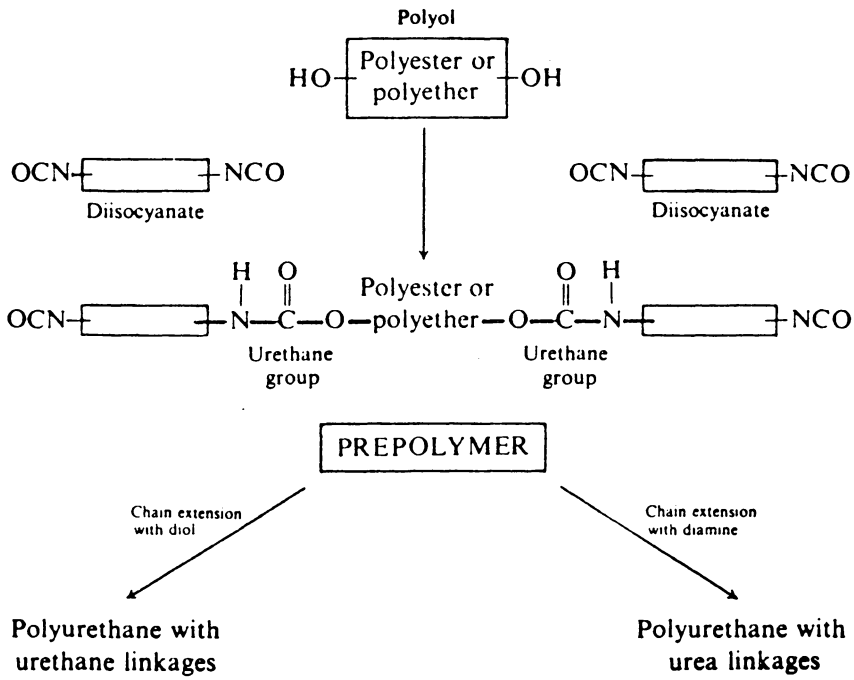

FIGURE 1.1. Two-Step Synthesis of Polyurethane Elastomers. [6]

TABLE 1.1. Chemical Structure of Typical Polyol Soft Segments.

POLYOL	ABBREVIATION	CHEMICAL STRUCTURE	REFERENCE
Polyethylene oxide	PEO	$HO\text{-}(CH_2CH_2O\text{-})_n\text{-}H$	20
Polypropylene oxide	PPO	$HO\text{-}(CH_2\text{-}\underset{\displaystyle CH_3}{\underset{\vert}{CH}}\text{-}O\text{-})_n\text{-}H$	21-23
Polytetramethylene oxide	PTMO	$HO\text{-}(CH_2\ CH_2\ CH_2\ CH_2O\text{-})_n\text{-}H$	24-29
Polyisobutylene	PIB	$HO\text{-}(\overset{\displaystyle CH_3}{\overset{\vert}{C}}\text{-}CH_2\text{-})_n\text{-}OH$ $\underset{\displaystyle CH_3}{\vert}$	30-33
1,4-Polybutadiene diol	PBd	$HO\text{-}(CH_2\text{-}CH{=}CH\text{-}CH_2\text{-})_n\text{-}OH$ *	34-39
Polyethylene adipate	PEA	$HO\text{-}[\text{-}(CH_2)_4\text{-}O\text{-}\overset{\displaystyle O}{\overset{\Vert}{C}}\text{-}(CH_2)_2\text{-}\overset{\displaystyle O}{\overset{\Vert}{C}}\text{-}O\text{-}]_n\text{-}H$	40,41
Polytetramethylene adipate	PTMA	$HO\text{-}[\text{-}(CH_2)_4\text{-}O\text{-}\overset{\displaystyle O}{\overset{\Vert}{C}}\text{-}(CH_2)_4\text{-}\overset{\displaystyle O}{\overset{\Vert}{C}}\text{-}O\text{-}]_n\text{-}H$	42,43
Polycaprolactone	PCL	$HO\text{-}[\text{-}(CH_2)_5\text{-}\overset{\displaystyle O}{\overset{\Vert}{C}}\text{-}O\text{-}]_n\text{-}H$	44-46
Polydimethylsiloxane (hydroxybutyl terminated)	PDMS	$HO\text{-}(CH_2)_4\text{-}(\underset{\displaystyle CH_3}{\underset{\vert}{Si}}\text{-}O\text{-})_n\text{-}\underset{\displaystyle CH_3}{\underset{\vert}{Si}}\text{-}(CH_2)_4\text{-}OH$	47-51

* cis, trans, and 1,2- addition possibilities are not shown.

2. POLYUREA SYNTHESIS VIA CARBAMATE-ISOCYANATE INTERACTION:

2.1. INTRODUCTION

Polyureas have been of interest in many areas such as thermoplastics and / or as a hard block in thermoplastic elastomers, due to their excellent mechanical properties and relatively good thermal stability. The chemistry of urea is of interest because which can be pursued in a variety of ways. Conventionally, the polyaddition reaction of diisocyanates with diamines has been used to produce polyureas [1]. Due to the rapid reaction of diisocyanate with most diamines, low temperature solution polymerization is usually essential. The solvent used in solution polymerization reactions must be not only unreactive towards both the diamine and diisocyanate, but it must also be a good solvent for both reactants and polymer. Clearly, the choice of solvent could influence the degree of polymerization due to side reactions or the possible premature

precipitation of the polymer. Mechanically weak materials would be obtained if the molecular weight of the polymer is low. Premature precipitation of polyurea from solution is generally recognized as the consequence of extensive hydrogen-bonding between urea linkages. Therefore, polar solvents are usually utilized in the synthesis of polyureas in order to achieve high molecular weight. A relatively low polymerization temperature is necessary to minimize several significant side reactions. It has, in fact been shown [2] that isocyanates react with even very dry polar solvents such as N,N-dimethylformamide (DMF), N,N-dimethyl- acetamide (DMAC), N-methyl-2-pyrrolidone (NMP), tetramethylurea (TMU), hexamethylphosphoramide (HMPA), and dimethylsulfoxide (DMSO) at relatively modest temperatures.

Katz [3] and others have attemped to reduce the aforementioned difficulties by using a 5 % solution of LiCl in N,N-dimethylformamide (DMF) as reaction solvent. Such a system is capable of improving the solvent power of the polyureas probably by forming a complex with urea linkages which reduces self-hydrogen bonding.

High molecular weight of polyureas have also been synthesized by hydrolysis of silyl-substituted polyureas [4]. The silyl-substituted ureas on treatment with ethanol produce the unsubstituted polyureas. The solubility properties of the silyl-substituted polyureas differs remarkably from those of their parent unsubstituted analogs, mainly due to decreased hydrogen-bonding.

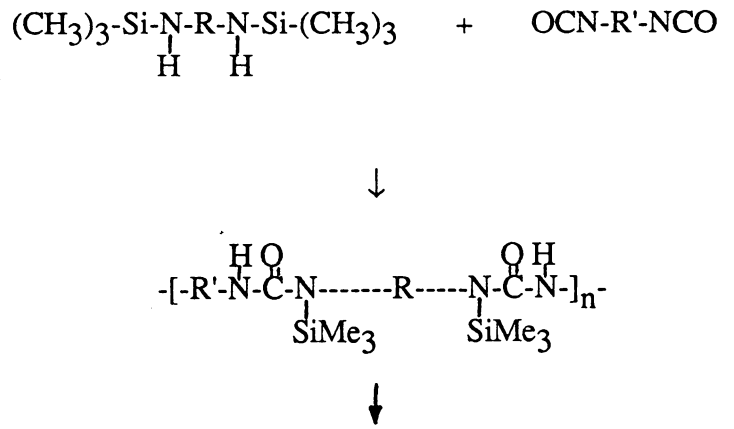

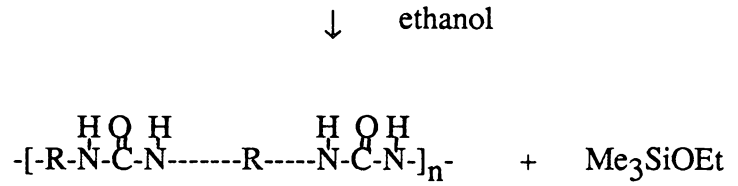

Sorenson [5] has demonstrated that high molecular weight polyureas can be prepared quantitatively by reacting diisocyanates with monocarboxylic acids in dimethylsulfoxide (DMSO). The polar solvent, DMSO, enters into the reaction as shown in the following reaction scheme and carbon dioxide and α-benzoyloxy-dimethyl sulfide are reaction by-products.

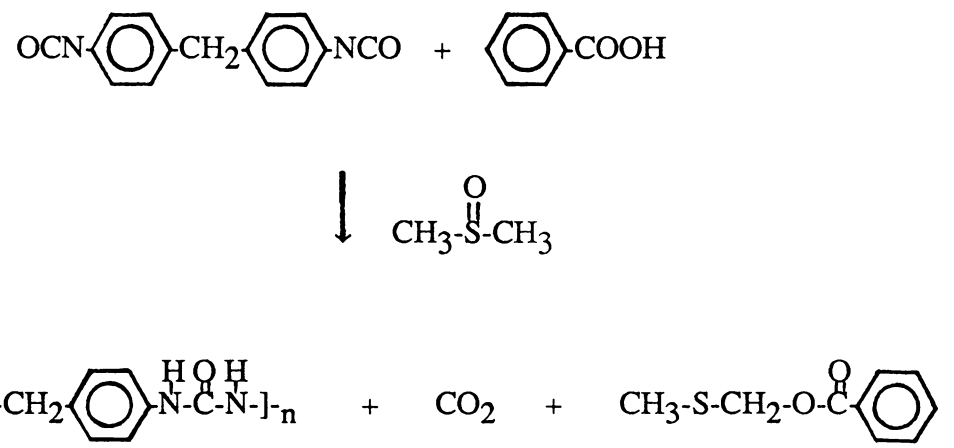

Chain extension of the isocyanate terminated prepolymer with water is well known to also lead to the formation of urea linkages (along with the evolution of carbon dioxide) as illustrated below [1].

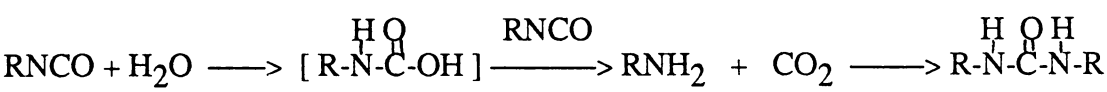

Water extended polyurethane systems, have been investigated for many years. However, one major problem with adding water directly into the system is its extremely low solubility in the reacting medium. Thus, a wide variation in reactivity occurs, which translates to a rather heterogeneous hard segment structure.

Two novel synthetic routes to polyalkylureas which involve the use of organosilicon reagents have been studied [6]. As an example of the first method, 1,6-hexane-diamine was reacted with trimethylisocyanatosilane in a sealed tube at elevated temperature. In the second, the 1,1'-hexamethylenediurea was heated with hexamethyldisilazane (HMDS). In either case a good yield of the corresponding polyhexamethyleneurea was obtained.

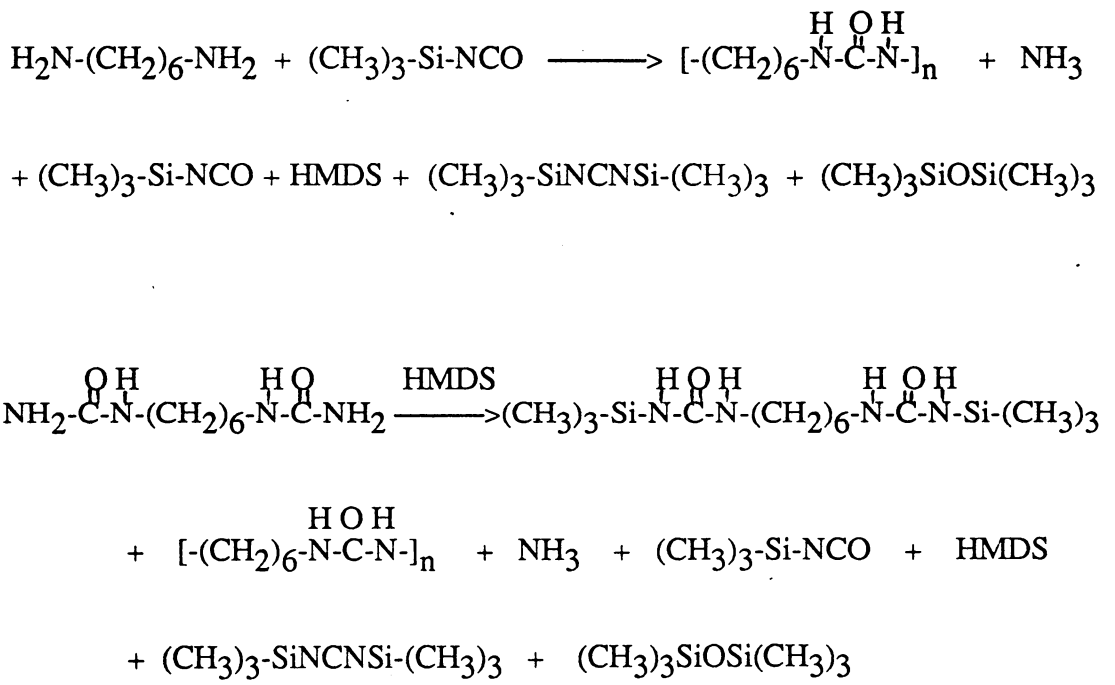

The preparation of high molecular weight polyureas has also been achieved by the polycondensation of carbon dioxide under a pressure of 20 atm with various diamines

using either triphenylphosphite [7,8] or ethylene chlorophosphite [19] in pyridine solution, in the presence of pyridine hydrochloride as catalyst. In the absence of pyridine, no polyurea was obtained. Pyridine appears to participate in the polyurea formation as indicated in the following reaction scheme.

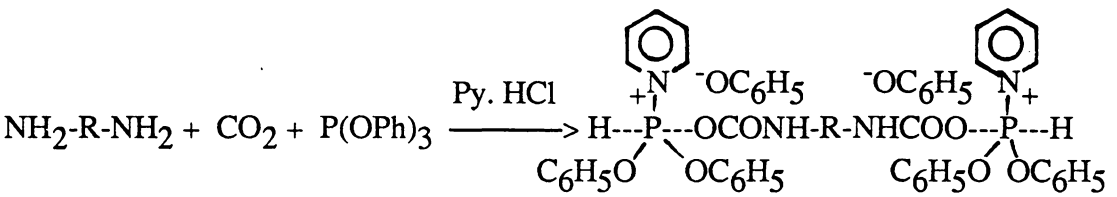

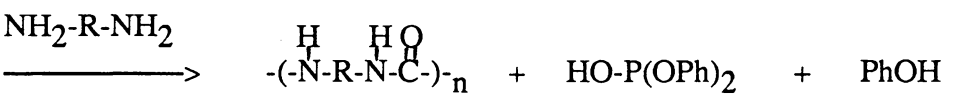

More recently, Ogata et al. [9,10] reported that polyureas can be prepared by polycondensation of aromatic diamines and lithium carbonate (Li_2CO_3) in the presence of triphenylphosphine (Ph_3P) and a polyhalo compound such as hexachloroethane (C_2Cl_6) in pyridine solution.

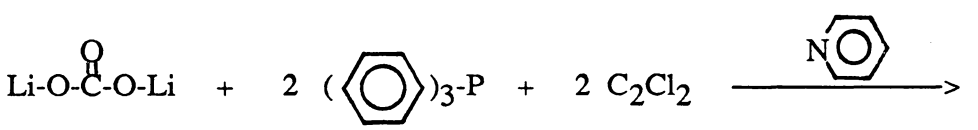

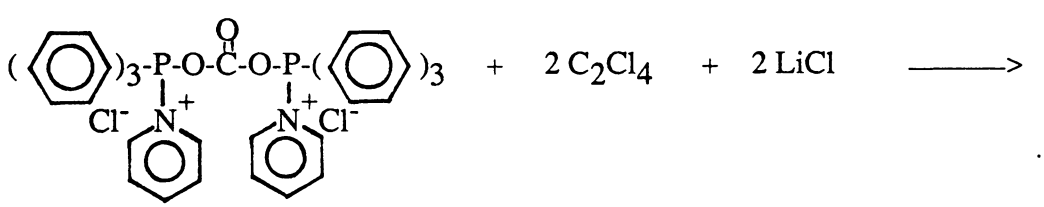

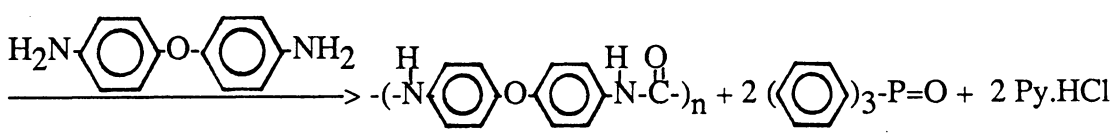

While the synthetic methods cited above involve the use of solvents and unstable reagents, there has been no potential application in the bulk synthesis of polyurethane-urea elastomers which is of particular interest to our research group. It is the purpose of this thesis to further describe a new method for preparing polyureas in bulk via what is termed carbamate-isocyanate interactions. Tertiary alcohols are an unusual type of "chain extender" investigated in our laboratory recently. It has been observed that carbanilide and the corresponding olefin are formed by heating tertiary alcohols with phenyl isocyanate [11,12,18]. The urea formation mechanism has not been clarified in the literature. However, it has been postulated that tertiary alcohols may be dehydrated by heating with isocyanates [11]. Isocyanates are then hydrolyzed by water with the formation of disubstituted ureas. However, we suggested that the ureas are generated by the interaction between tertiary alcohol derived carbamates and isocyanates. It is known that the carbamate derived from phenylisocyanate and t-butylalcohol can be thermally dissociated at temperatures over 200°C. The dissociation products of such a carbamates are found to be aniline, carbon dioxide and corresponding alkene [16].

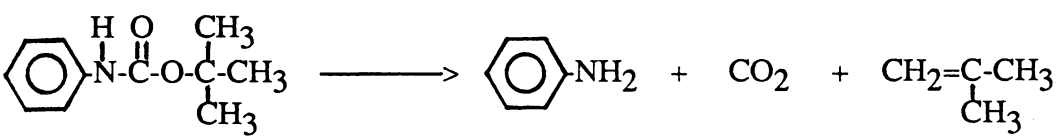

Thus the approach discussed herein for the synthesis of polyureas is based on the above observations. It is thought that ureas could be obtained by heating tertiary alcohol derived carbamates with isocyanates. Since the temperatures described above

are rather high, relative to temperatures applicable to the cure of coatings, one might consider the route impractical. However, Abbate et al. [17] found that the dissociation temperature of alkyl N-phenyl-urethanes can be significantly lowered, even to as low as 130^{o}C, in the presence of amine catalysts. Such a finding certainly should be of interest from the technical point of view.

In this study, the tertiary alcohol structure and the type of catalyst have been varied in order to study the influence on the dissociation temperature of carbamates. The feasibility of bulk and solution synthesis of polyureas by using tertiary alcohols are also reported.

This interesting characteristic of tertiary alcohols (either mono- or di- functional) can be utilized synthetically to produce polyureas in the presence of diisocyanates and a suitable catalyst. The morphological and physical properties of MDI based urea-polyether-urethanes have been investigated and very attractive physical properties as well as thermomechanical stability have already been reported [13-15].

2.2. EXPERIMENTAL

2.2.1. Reagents:

Phenyl isocyanate (Aldrich), t-butyl alcohol (Alfa Products) and 2-phenyl-2-propanol (Aldrich) were purified by vacuum distillation. 1,1-Diphenylethanol (DPE) was used as received. Three catalysts employed were used as received: 1,8-diazobicyclo [5.4.0]-undec-7-ene (DBU) (Aldrich), tin octoate (TOC) and

dibutyltin dilaurate (DBTDL) (Pfaltz & Bauer, Inc.). 4,4'-Dianilinemethane (DAM) (Aldrich) was purified by recrystallization from boiling water. 4,4'-Methylene-diphenylisocyanate (MDI) (Mobay Chemical Co.) was vacuum distilled and stored in a desiccator at 0°C before use. Dimethylformamide (DMF) was dried over calcium hydride and distilled under reduced presure.

2.2.2. Model reaction:

0.03 Moles of distilled phenylisocyanate were reacted with 0.03 moles of tertiary alcohol in bulk at 70°C in the presence of approximately 0.1 wt. % of catalyst. Reactions were conducted in a 50 ml two-neck round-bottom flask under nitrogen atmosphere for various time periods. The reaction mixtures are homogeneous clear liquids at these conditions, before catalyst is added. In most cases, precipitation occurred as soon as the catalyst was added. The model compounds were produced in high yields and were further purified by recrystallization three times from either acetone (for carbanilide) or hexane (for carbamates) before structure determination.

2.2.3. Polyurea synthesis:

Four polyureas with identical chemical structures were prepared by two different approaches. First, equal molar quantities of 2-phenyl-2-propanol and MDI were reacted in bulk at 140°C for 10 minutes. Secondly, 2-phenyl-2-propanol was reacted with equal molar amounts of MDI in purified 1,2-dichlorobenzene (DCB) at 140°C for 15 hours. Finally, stoichiometric amounts of 1,1-diphenylethanol and MDI were reacted in bulk at 140°C for 10 minutes. Reaction products were washed successively

with methanol in order to remove the reaction by-product, α-methylstyrene and possibly unreacted materials, then dried under reduced pressure. As a control, polyurea was synthesized more conventionally with MDI and DAM in distilled DMF at 10°C for about 4 hours. All reactions were conducted under nitrogen atmosphere in a two-neck round-bottom flask.

2.2.4. Characterization:

Infrared spectra were recorded on a Nicolet MX-1 FT-IR Spectrometer linked to a Nicolet Data Station. Nuclear magnetic resonance spectra were measured with a IBM 270SY Spectrometer. The model compounds were dissolved in $CDCl_3$ (~ 10% wt./vol.) and tetramethylsilane (TMS) was used as the internal reference. Mass spectral analyses were done at the Biochemistry Department of Virginia Tech on a VG 7070E-HF GC-MS system. Melting points were taken on a Laboratory Devices MEL-TEMP melting point apparatus and are uncorrected. DSC (differential scanning calorimetry) thermograms were recorded by a Perkin-Elmer DSC II over the temperature range of 25 to 400°C. A constant flow of nitrogen gas was used to purge the system and a heating rate of 10°C/min was employed throughout the measurements. Isothermal and dynamic TGA (thermogravimetric analysis) runs were performed under nitrogen on a Perkin-Elmer TGS-2. Samples used were finely grounded powders, weighing about 5-7 mg. Samples were run at five different isothermal temperatures, chosen to be in the range 100-180°C and for a period of 60 minutes. The initial rate of weight loss was determined over the first 2.5 min of each run. Dynamic runs on polyureas were performed over a temperature range of 50 - 450 °C with a heating rate of 10°C/min.

2.3. RESULTS AND DISCUSSION

2.3.1. Model Reactions:

The use of polar solvents was avoided to minimize complications arising from possible side reactions. In considering the low reactivity of sterically hindered tertiary alcohols toward phenyl isocyanate, a variety of catalysts were utilized to accelerate the reactions. It was of some concern that tertiary alcohol derived carbamates may not be thermally stable in the presence of certain catalysts as stated before. A reaction temperature of 70°C, at which a homogeneous reaction mixture was insured, was applied in all cases in order to not only isolate the tertiary alcohol derived carbamate for further thermal analysis but also to prevent the possible dimerization of phenyl isocyanate under such conditions.

A test of the possibility that the cumyl alcohol could undergo self-dehydration to α-methylstyrene at 150°C with and without the presence of catalysts (DBU and TOC) was conducted. There was no evidence from IR spectra that supported the formation of α-methylstyrene even after a period of 2 hours reaction time. Common acid catalysts for the dehydration of tertiary alcohols have not been taken into consideration nor utilized since they cannot be applied to polyurea elastomer synthesis.

Some results from the model reactions are summarized in Figure 2.1. All the ureas formed in less than one minute. The completion of reactions is judged visually by the formation of solid product. The melting points of carbanilide and tertiary alcohol derived carbamates as expected, all exceed 100°C, which is higher than the reaction

temperature. All products were produced in high yields. Since reactions are carried out in bulk, there is a possibility that reactions were hampered due to solidification of products.The yields could also be misleading due to physical loss after three recrystallizatons.

The type of catalyst was found to have a significant effect on the urea formation at 70°C. In reaction II, III and IV, the reaction of 2-phenyl-2-propanol (cumyl alcohol) and phenyl isocyanate catalyzed by DBU and TOC afforded urea, CO_2 and alkene while the reaction catalyzed with DBTDL yielded the urethane (carbamate). Obviously, DBU and TOC not only effectively catalyzed the urethane formation but also accelerated the dissociation of the resulting urethane. On the contrary, DBTDL is not an effective catalyst for the cumyl alcohol and phenyl isocyanate reaction, as indicated by a relatively long reaction time. There is also no evidence for the formation of carbanilide in reaction IV, which implies that DBTDL is not affecting the dissociation of the carbamate under the conditions used. The products were characterized by Mass spectroscopy, ^{1}H-NMR and IR analysis and by comparison of their melting points. Olefin formation also has been identified by FT-IR and HPLC.

2.3.1.1. Spectroscopic Analysis:

Mass spectra of model compounds are shown in Figure 2.2. The Mass spectrum of 2-phenylpropyl-N-phenyl carbamate showed M^+ at m/e 255 with a base peak at 119. A significant observation is the fragmentation of 2-phenyl-N-phenyl carbamate to m/e 119, 93, and 44, indicating the formation of cumyl cation, aniline and carbon dioxide, respectively. The other peak from m/e 211 may be explained by the formation of the secondary amine, N-phenyl-cumylamine.

The Mass spectrum of t-butyl-N-phenyl carbamate is shown in Figure 2.2, with M^+ at m/e 193 and a base peak at 57. The fragmentation of t-butyl-N-phenyl carbamate to m/e 93, 57 and 44 is observed, indicating the formation of aniline, t-butyl cation and carbon dioxide, respectively. Again, the peak at m/e 149 may be attributed to the formation of the secondary amine, N-phenyl-t-butylamine.

The FT-IR spectra of carbanilide, t-butyl-N-phenyl carbamate and 2-phenylpropyl- N-phenyl carbamate are shown in Figure 2.3. The peak at 1640 cm^{-1} is attributed to the urea absorption, while the peak at 1700 cm^{-1} is due to the urethane absorption.

The ^{1}H-NMR spectrum of 2-phenylpropyl- N-phenyl carbamate is given in Figure 2.4. The singlet at 1.8 ppm is assigned to the methyl protons and the broad singlet at 6.6 ppm is due to the presence of an imino proton (-NH-). The triplet appearing at 7.0 ppm results from H_c of phenyl ring on the tertiary carbon and the remaining phenyl protons were assigned as a group at 7.2 - 7.5 ppm. This is in accordance with the integration of signals observed at 1.8 (6H), 6.6 (1H), 7.0 (1H), and 7.2 -7.5 (9H) ppm, respectively.

2-Phenylpropyl-N-phenyl carbamate, the product obtained in reaction IV, was reacted with phenyl isocyanate at 130°C with (reaction VII) and without (reaction VIII) catalyst in order to study the thermal stability of such urethane linkages. Initially, we have had some concern about the formation of allophanate, where the isocyanate could add to the nitrogen atom of the urethane linkage as shown in the following reaction.

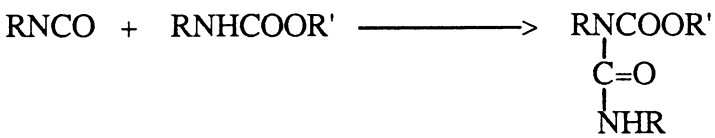

However, carbanilide was only obtained in high yield within 30 minutes in our uncatalyzed reaction, while it takes as short as about 1 minute to obtain the same result in catalyzed reaction. Two possibilities could be considered. First, the carbamate could dissociate to give aniline which could then further react with phenylisocyanate to generate carbanilide. Secondly, phenyl isocyanate could initially react with carbamate to afford allophanate and simultaneously eliminate carbon dioxide and α-methyl styrene. Allophanate formation reaction is not catalyzed strongly by tertiary amines, it requires stronger bases or temperatures of approximately 120-140°C in uncatalyzed systems in order to provide a significant reaction rate [20]. Therefore, the allophanate route is unlikely to be important here, otherwise we would not be able to obtain carbanilide in such short period of time in the tertiary amine catalyzed reaction.

It is interesting to make a comparison among reaction I, II and V where the same amine catalyst, DBU, was utilized. By changing the number of phenyl groups from 0 to 2 on the tertiary carbon, carbamate was obtained in reaction I, while the rest gave carbanilide. This probably indicates that the phenyl group on the tertiary carbon is playing an important role in the thermal stability of tertiary alcohol derived carbamates. t-Butyl alcohol derived carbamate is most stable which can be obtained in high yield at conditions described. TOC is the only catalyst, among those studied, which favored the formation of 2-phenylpropyl-N-phenyl carbamate. One might expect that reaction V should generate carbanilide at a faster rate than reaction II, since it has more phenyl groups on the tertiary carbon. However, a little slower carbanilide formation rate was observed in reaction V. We believe that this is due to the steric effect of the 1,1-diphenyl-ethanol on the urethane formation reaction with phenyl isocyanate, while the dissociation of such a carbamate still can proceed very rapidly.

On the basis of our observations, we propose the following mechanism for the

urea formation, here illustrated using cumyl alcohol as tertiary alcohol as shown in Figure 2.5. In this mechanism, the decomposition of carbamate **I** proceeds by two pathways to give a primary amine in **A** and a secondary amine in **B**. Carbon dioxide is evolved in both cases. Carbamate **I** dissociated at high temperatures affords an intermediate **II** which then could rearrange to produce aniline. Carbanilide, the major product, is probably formed by reacting aniline with free isocyanate (path **A**). It is this part of the sequence that accounts for polymer formation in the case of the diisocyanate which will described later. Dyer et el. [23] have reported the formation of primary and secondary amine, as well as olefin formation from urethane decomposition. The possibility of the formation of secondary amine **III**, by the combination of tertiary cumyl cation and amine anion, in this mechanism therefore cannot be eliminated (path **B**). Secondary amine **III** species (m/e 211) are also found in our Mass spectrum (Figure 2.2). However, we do not know at this point how the presence of phenyl isocyanate would possibly affect the formation of the secondary amine. Secondary amine **III**, if present, still could react with phenyl isocyanate to produce a substituted urea **IV**. However, we have no proof of this.

Aniline may also be produced by an intramolecular cyclic mechanism, as suggested for the thermal degradation of many esters [21] including chloesteryl carbamate [22].

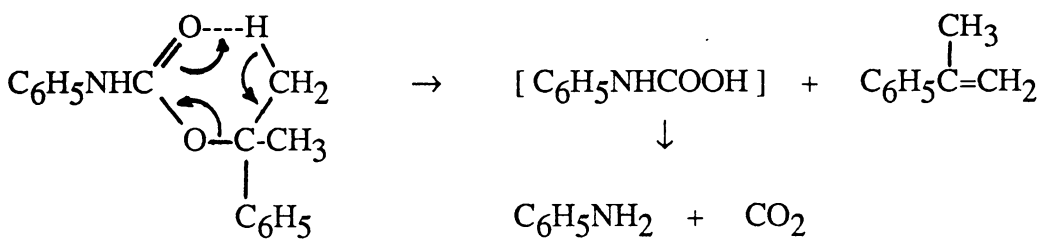

If this is the pathway to the formation of aniline, carbanilide should be the only type of urea produced, i.e. there would be no secondary amine formation.

2.3.1.2. Thermogravimetric Analysis:

Since the synthesized carbamate **I** discussed here and the approach to the synthesis of polyurea are new, it was of interest to investigate the thermal stability. Therefore, carbamate **I** has been investigated using isothermal thermogravimetric analysis. The sample was run at five different isothermal temperatures, chosen to be in the range 100-180^{o}C for a period of 60 minutes. The results are shown in Figure 2.6. There is no observable weight loss at 100^{o}C for a period of 60 minutes, while a complete weight loss in one hour was observed at temperature of about 175^{o}C. This result conflicts with the data we obtained from model reaction VII, where urea produced in high yield within 30 minutes at 130 ^{o}C. However, one could be misled from the weght loss data if dissociation products are not volatile at the temperature studied. The boiling points of the dissociation products, aniline and α-methylstyrene, are 184^{o}C and 167^{o}C, respectively. Therefore, only the initial rate of weight loss due to the evolved of carbon dioxide over the first 2.5 min was considered for each isothermal temperature. The energy of activation for the carbamate **I** was calculated to be 24.8 kcal/mole, which is calculated using the following form of the Arrhenius equation: - ln Rate = ln A - E/RT (Figure 2.7).

2.3.2. Polyurea synthesis:

Polyureas prepared by using carbamate-isocyanate interaction and conventional amine-isocyanate condensation reaction are summarized in Figure 2.8. In reaction A, B, and C, poly-MDI-urea was obtained by reacting MDI with monofunctional tertiary alcohols. The urea formation mechanism has been postulated by the authors as discussed in model compound studies. It would of course be impossible to prepare a "polymer" via a conventional alcohol-isocyanate reaction since one of the reagents would be, nominally at least, monofunctional. However, moderate molecular weight polymer was in fact obtained in all cases where "monofunctional" tertiary alcohols were used.

In reaction A , polyurea is synthesized in 1,2-dichlorobenzene by reacting MDI with CA at 150°C. A slower polymerization rate in solution was observed as compared with in bulk. This is due to the low monomer concentration, ~10%, in solution. Polar solvents such as DMF were avoided due to possible side reactions with isocyanates at high temperatures. 1,2-Dichlorobenzene (DCB) was utilized not only because its high boiling point, 180°C, but also because of its low reactivity with isocyanates. High molecular weight polymers were not anticipated from DCB solution, since it is not a good solvent for polyureas. In case of polar solvents, catalysts can be added in order to lower the reaction temperature, possibly below 80°C as described in the model compound studies.

Tertiary alcohols are very effective in bulk synthesis of polyureas (reaction B and C). Polymers are formed in a short period of time at 150°C even without the presence of catalyst. That carbon dioxide was evolved from the reaction was established by passing the evolved gas from a typical reaction through a calcium hydroxide solution. The familiar milky precipitate formed, but no quantitative measure was made. Olefin formation was identified by FT-IR as a reaction by-product . For comparison, poly-MDI-urea also was synthesized by a more conventional way, by reacting MDI

with DAM in DMF at 10°C (reaction D).

Due to the regular structure and interchain hydrogen bonding of poly-MDI-ureas, a high crystallinity was expected for those polymers. High crystallinity of poly-MDI-ureas have been confirmed by wide-angle x-ray diffraction reflections. As a consequence of this high crystallinity, the polymers are not soluble in common solvents, or even in a 5% LiCl/DMF solution. IR analysis was not clearly able to demonstrate that those polyureas have identical chemical structures. The authors can only make the statement that those polymers possess identical chemical structure on the basis of our model reaction studies.

Since a small amount of secondary amine also may be possibly formed in reaction A, B, and C as discussed in model reaction studies, this will result substituted urea linkages along the polymer backbone as indicated below.

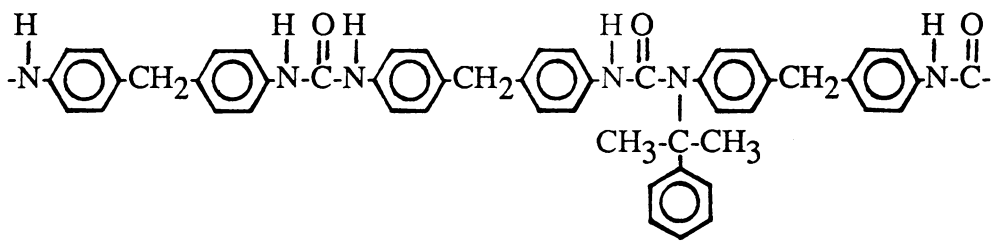

If this is true, the polyurea synthesized by using carbamate-isocyanate interaction would have a lower crystallinity than the polyurea prepared by conventional approach, since branching affects the packing efficiency of polymer chains. This statement has been confirmed by using WAXS (wide-angle X-ray Diffraction), in which the poly-MDI-urea prepared by using conventional approach shows sharp lines pattern while the polymer prepared by carbamate-isocyanate interactions shows mostly diffuse halos. To further confirm this statement, DSC (differential scanning calorimetry) measurements were conducted on those polyureas prepared by different approaches.

DSC thermograms are shown in Figure 2.9. The DSC scans provided are only the first runs since polymers are degraded above T_m. A sharp endotherm peak at around 370°C was observed in all polymers and calculated ΔH_f's are unusually high and are in the range of 80 to 110 cal/gram. It has been reported in the literature [24] that polyurea prepared by polycondensation of MDI and MDA has a melting temperature at 370°C. Althought a similar endotherm temperature was observed in our polyurea D, we were concerned by its unrealistically high ΔH_f for a polymer. The sharp endotherm may possibly be due to a contribution from the thermal degradation of polyurea. Therefore, dynamic TGA (thermogravimetric analysis) was conducted in nitrogen in order to study the thermal stability of those poly-MDI-ureas. TGA thermograms are shown in Figure 2.10. At a temperature of 370°C, the polyureas lost most of their weights. This result further demonstrated that the sharp endotherm peak appearing in the DSC thermogram is not a true melting behavior of polymer. However, we believe that the observed T_g (around 160°C) and the exotherm (T_c) at around 250°C are real. Unfortunately, the melting temperatures are too close to the degradation temperatures to be quantified.

The polyurea prepared by polycondensation of MDI and MDA shows better thermal stability than those polyureas prepared by carbamate-isocyanate interaction as judged by the initial weight loss temperature. It is interesting to note that there is a significant difference in the percentage of char yields. The char yield could be as high as 35 % in the case of DPE-MDI (polymer C) system while there is only 15 % char yield in the case of DAM-MDI system (polymer D). We have no good explanation for this phenomenon yet.

2.4. CONCLUSION

Polyureas have been efficiently prepared via carbamate-isocyanate interaction. Carbamates, or "blocked amines" in this case, are derived from tertiary alcohols and isocyanates and tend to dissociate at high temperature to give the corresponding amines. The reaction temperature can be lowered, if the carbamate contains aryl groups and / or if catalysts are utilized. Branching might also be occurring due to the formation of secondary amines.

REFERENCES

1. C. Hepburn, "Polyurethane Elastomers", Applied Science Publishers, New York (1982).
2. H. Ulrich, J. Polym. Sci.: Macromol. Rev., 11, 93 (1976).
3. M. Katz, U. S. Pat. 2,888,438 (1957).
4. J. F. Klebe, J. Polym. Sci., Part B, 2, 1079 (1964).
5. W. R. Sorenson, J. Org. Chem., 24, 978 (1959).
6. A. L. DiSalvo and J. H. Cornell, J. Polym. Sci. Chem. Ed., 13, 97 (1975).
7. N. Yamazaki, T. Iguichi, and F. Higashi, J. Polym. Sci. Chem. Ed., 13, 785 (1975).
8. F. Higashi, T. Murakami, and Y. Taguchi, J. Polym. Sci. Chem. Ed., 20, 103 (1982).

9. N. Ogata, K. Sanui, M. Watanabe, and Y. Kosaka, J. Polym. Sci. Polym. Letters, 24, 65 (1986).

10. Y. Kosaka, M. Watanabe, K. Sanui, and N. Ogata,J. Polym. Sci. Chem. Ed., 24, 1915 (1986).

11. J. H. Saunders and R. J. Slocombe, Chem. Rev., 43, 203 (1948).

12. W. J. Bailey and F. Cesare, Am. Chem. Soc. Meeting, April, 1956.

13. D. Tyagi, B. Lee, G. L. Wilkes, and J. E. McGrath, ACS Polym. Prepr., 26 (2), 12 (1985). Advances in Elastomers and Rubber Elasticity, J. Lal and J. E. Mark, Editors, 1987.

14. B. Lee, D. Tyagi, G. L. Wilkes, and J. E. McGrath, 32nd Sagamore Army Materials Research Conference, Elastomers, R. Singler, Editor, 1987.

15. B. Lee, D. Tyagi, G. L. Wilkes, and J. E. McGrath, Rubber Division Meeting, Los Angeles, April 23 (1985).

16. N. Yoshitake, S. Shigee, Y. Nagano, and T. Tanaka, Kyusho Daigaku Kogaku Shuko, 44 (3), 411 (1971); C.A., 77: 115666 (1972).

17. F. W. Abbate, W. J. Farrisey, Jr., and A. A. R. Sayigh, J. Appl. Polym. Sci., 16, 1213 (1972).

18. G. Karmas, U. S. Pat. 2,574,484 (to Ortho Pharmaceutical Corp.) (Nov. 13, 1951).

19. C. I. Chiriac, Polym. Bull., 16, 143 (1986).

20. D. J. David, and H. B. Staley, "Analytical Chemistry of The Polyurethanes", Robert E. Krieger Publishing Company, New York, 1979.

21. A. T. Blades, Can. J. Chem., 32, 366 (1954).

22. A. F. McKay and G. R. Vavasour, Can. J. Chem., 31, 688 (1953).

23. E. Dyer, G. E. Newborn, Jr., and G. C. Wright, "Thermal Degradation of Carbamates," Delaware Chemical Symposium, Feb. 1958.

24. H. Ishihara, I. Kimura, and N. Yoshihara, J. Macromol. Sci., Phys., B 22, 713 (1983).

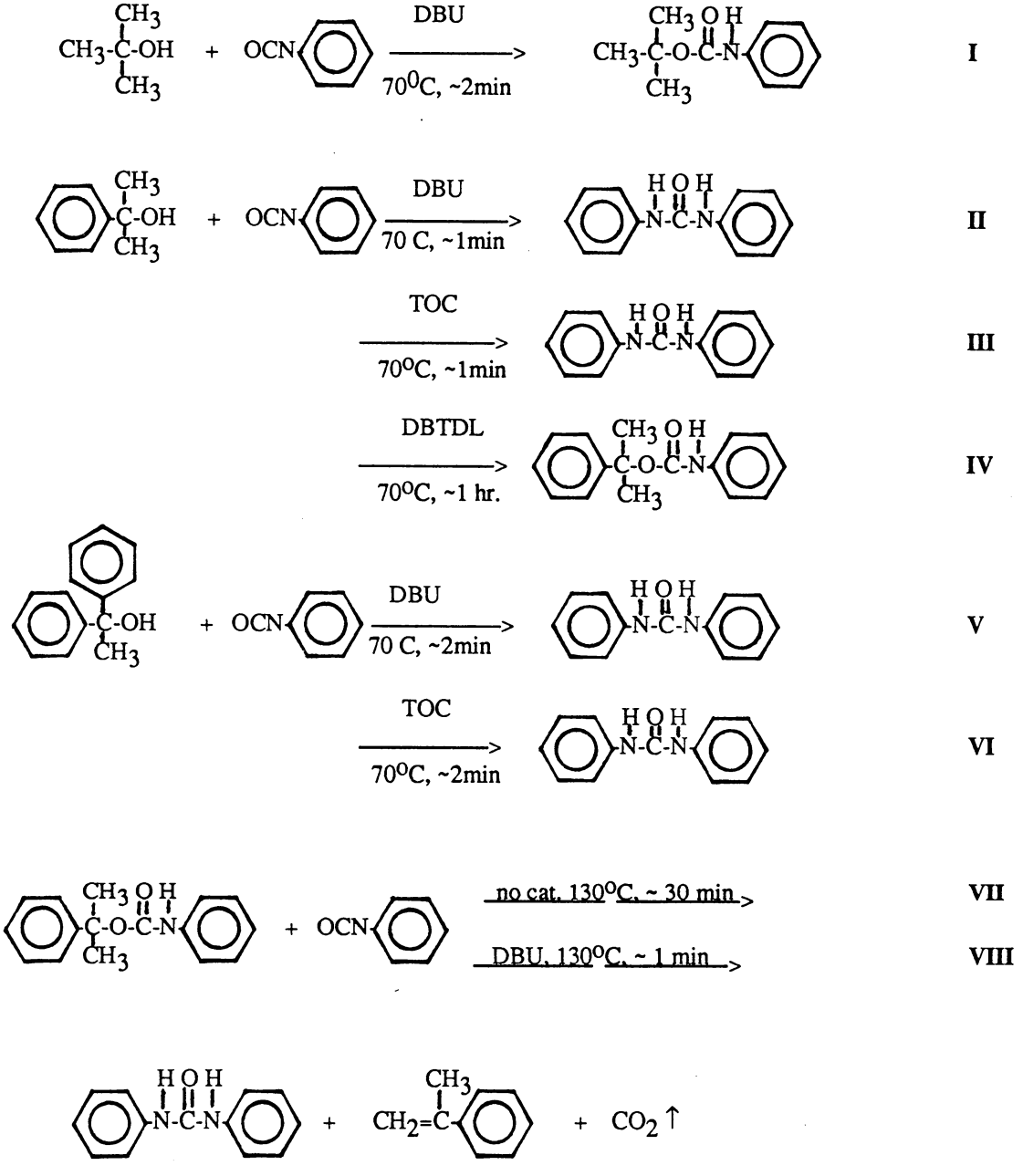

FIGURE 2.1. Model Reactions of Tertiary Alcohols with Phenyl Isocyanate.

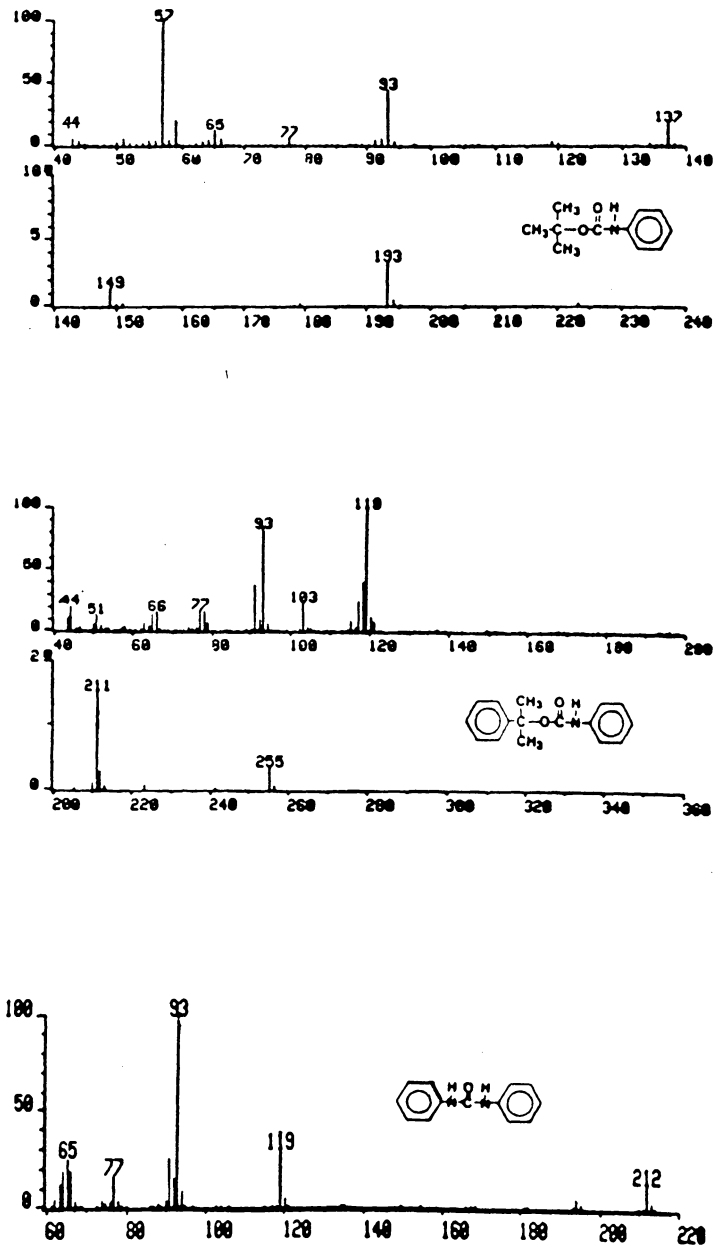

FIGURE 2.2. Mass Spectra of Model Carbamates and Carbanilide.

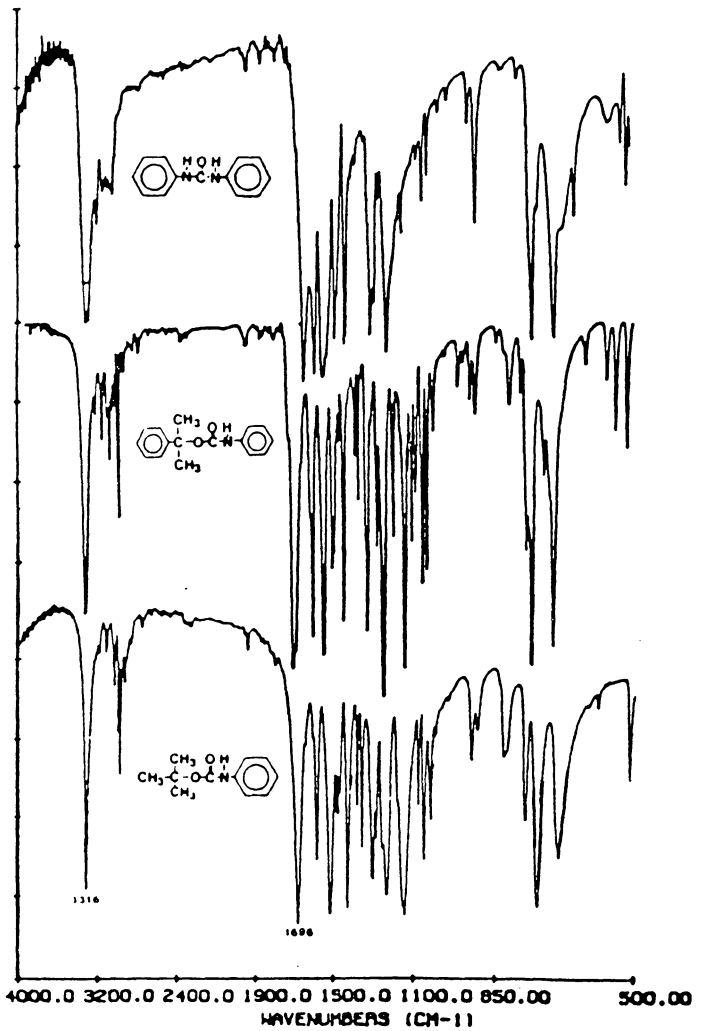

FIGURE 2.3. FT-IR Spectra of Model Carbamates and Carbanilide.

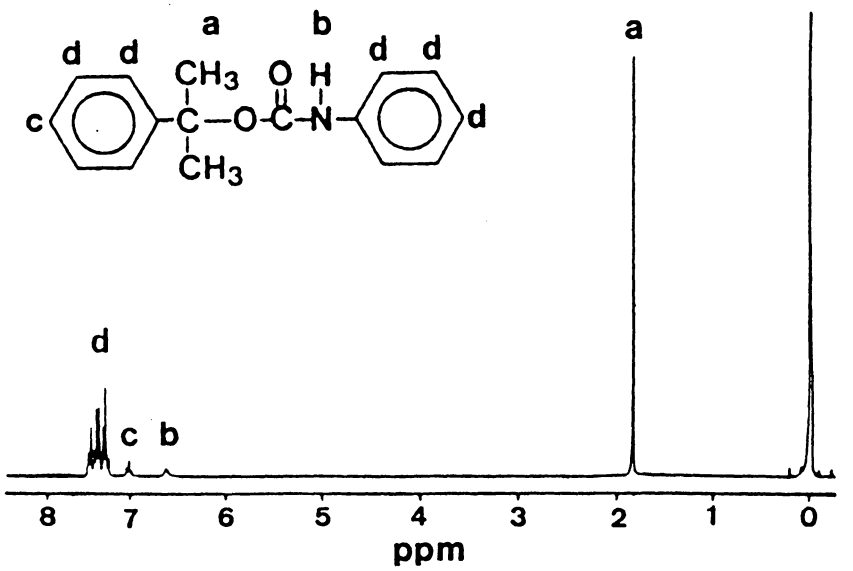

FIGURE 2.4. ^{1}H NMR Spectrum of 2-Phenylpropyl-N-Phenyl Carbamate.

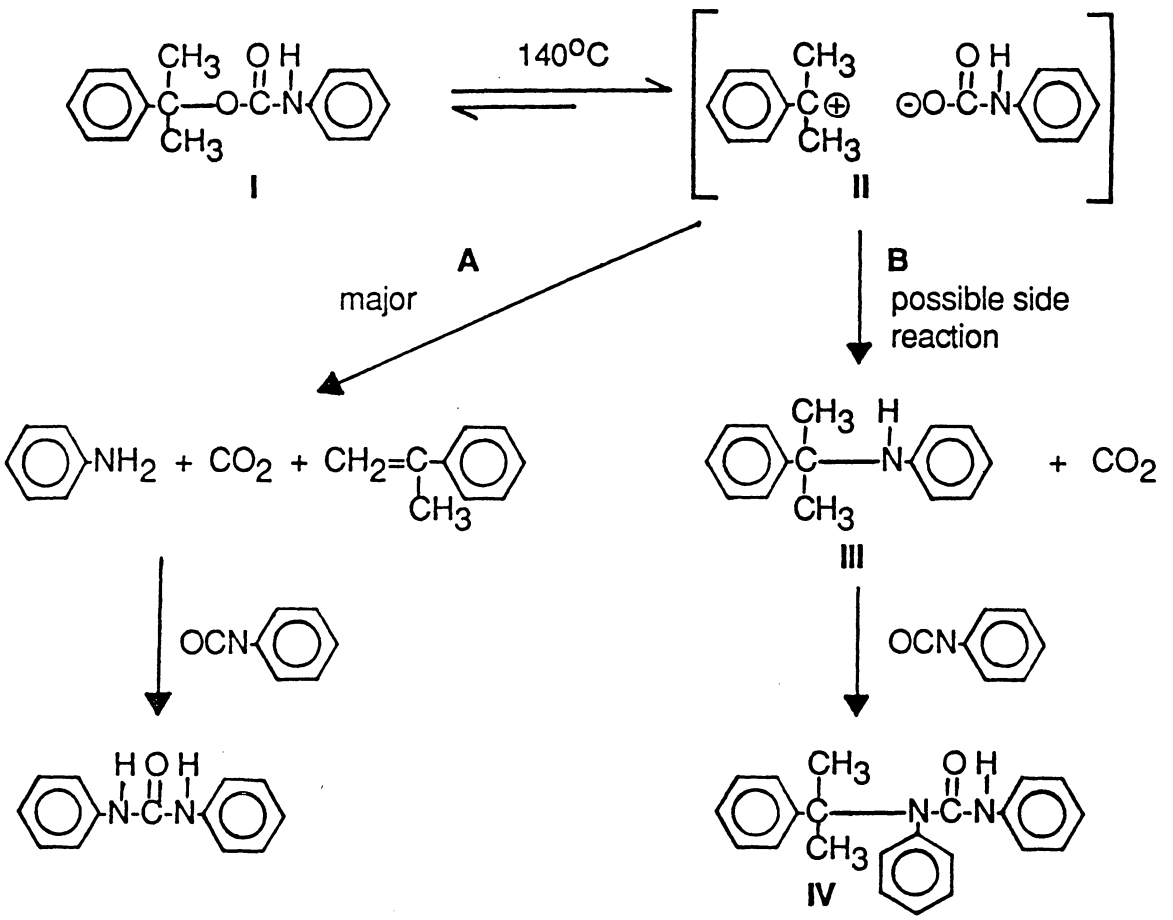

FIGURE 2.5. Urea Formation Via Carbamate-Isocyanate Interaction.

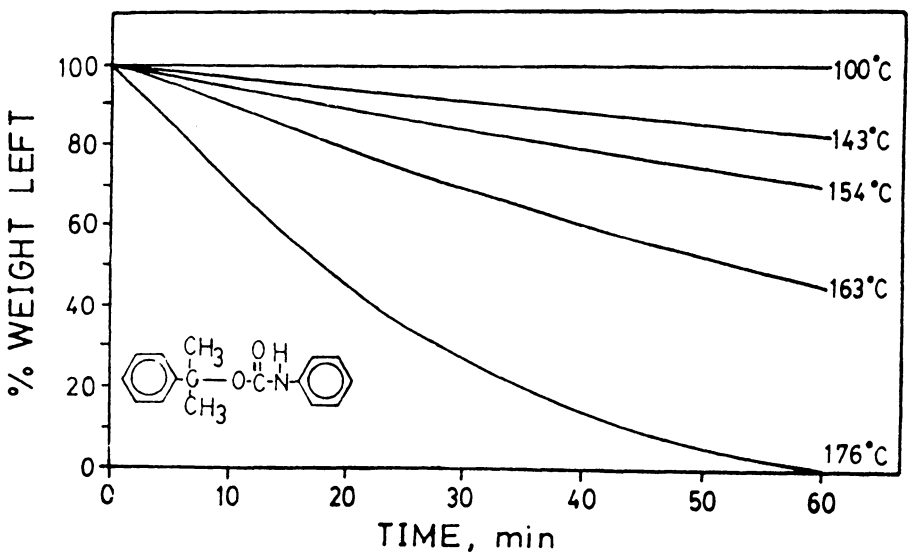

FIGURE 2.6. Isothermal TGA of 2-Phenylpropyl-N-Phenyl Carbamate.

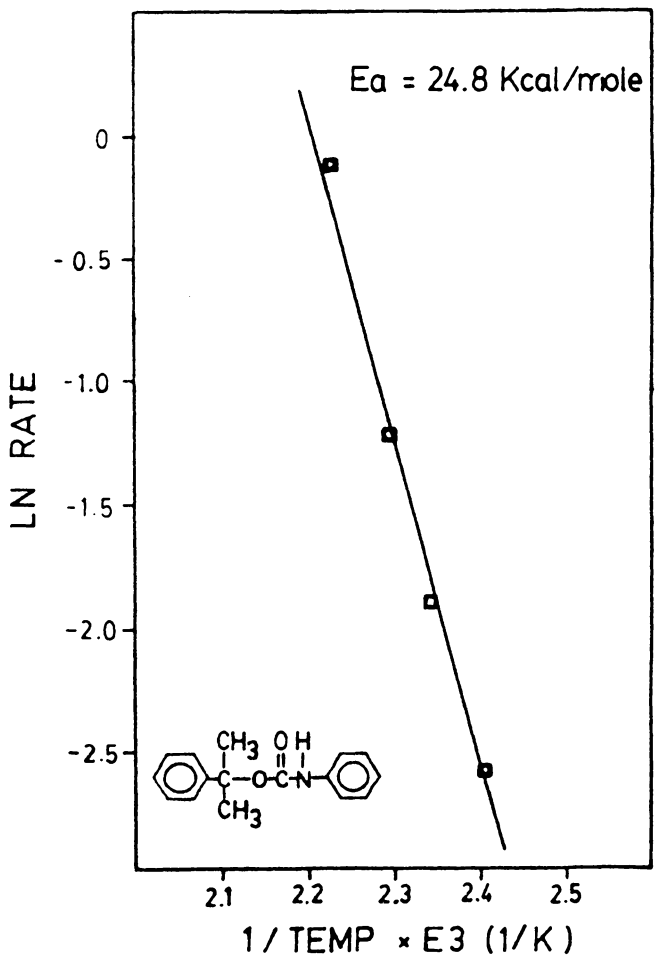

FIGURE 2.7. Arrhenius Plot.

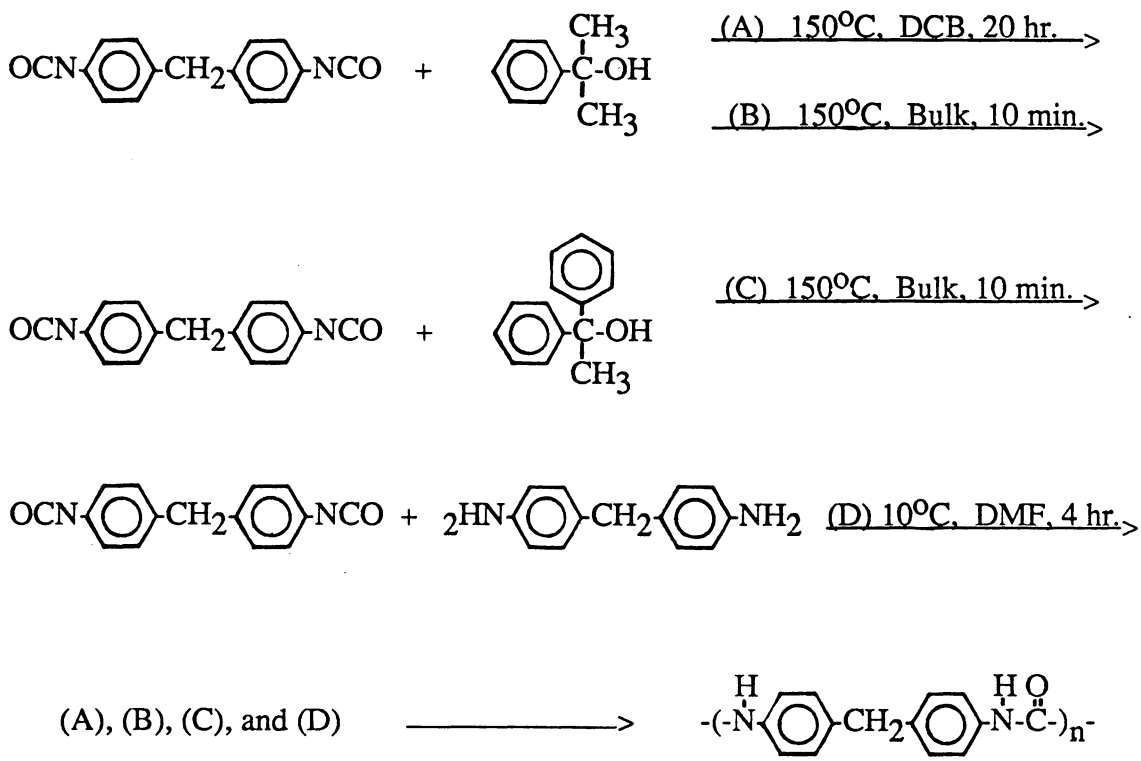

FIGURE 2.8. Poly-MDI-Urea Synthesis.

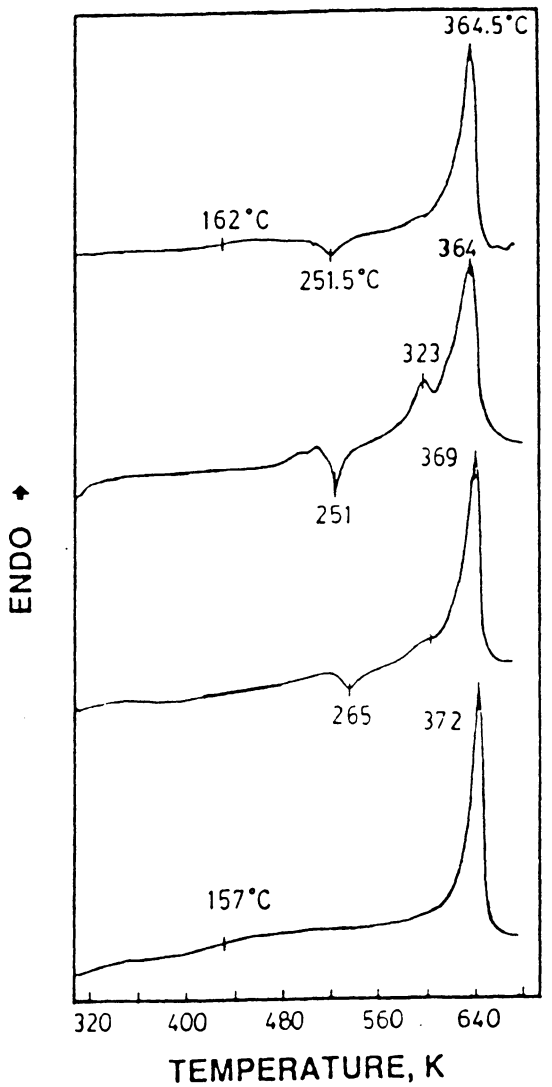

FIGURE 2.9. DSC Spectrum of Poly-MDI-Ureas.

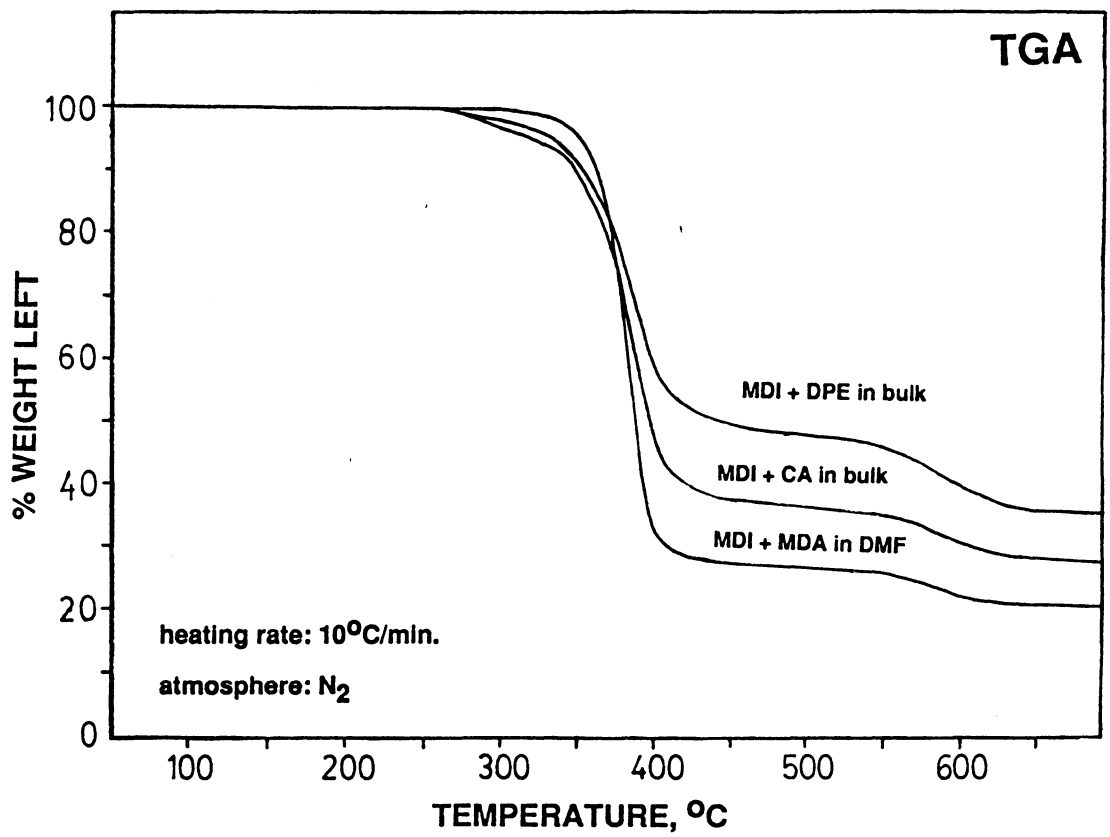

FIGURE 2.10. TGA Spectra of Poly-MDI-Ureas.

3. SYNTHESIS AND CHARACTERIZATION OF POLYETHER-URETHANEUREAS: "CHAIN EXTENSION" WITH TERTIARY ALCOHOLS AND SILANOLS

3.1. INTRODUCTION

Conventional urethane elastomers are well-known to have a number of desirable properties, but are not considered high temperature polymers [1]. Continuous service applications at temperatures above 100°C are not usually recommended. Softening and even thermal dissociation at high temperatures is an inherent characteristic of the urethane linkage. However, it has been recognized that the incorporation of urea linkages in the polyurethane hard segment has a profound effect on the phase separation and domain structure of polyurethaneureas. This is largely due to the high polarity difference between hard and soft segments and possibly to the development of

a three-dimensional hydrogen-bonding network.

The hard segments, in the polyurethaneurea elastomers, are often composed of an aromatic diisocyanate reacted with a diamine chain extender, while the soft segments are a low molecular weight hydroxy-terminated polyether or polyester. Due to the rapid diisocyanate reaction with diamine, solution polymerization is usually essential in the synthesis of polyurethaneurea elastomers. A relatively low polymerization temperature is necessary to prevent significant side reactions. However, the solution polymerization suffers from the difficulty of obtaining a good common solvent for both soft and hard segments (sometimes crystalline) which have a large difference in solubility parameter. Clearly, the choice of solvent affects the degree of polymerization due to premature precipitation of the polymer. A mechanically weak polymer would be obtained if the molecular weight of the segmented copolymer is low. Diamines having a substituent on the benzene ring, ortho to the amine group, such as 3,3'-dichloro-4,4'-diaminodiphenyl- methane (MOCA), provide an acceptable lowered diamine reactivity in the bulk preparation of polyurethaneurea elastomers. These chain extenders, as well as derivatives of 4,4'-diaminodiphenylmethane (DAM) should be avoided since they present well-known carcinogenic hazards.

From the literature it is obvious that a variety of polyurethaneurea elastomers have been prepared and studied [2-18]. Among the chain extenders studied, the DAM chain extended polyurethaneureas [2,5,10-12] have been of great interest. A symmetric MDI/DAM hard segment would have better packing efficiency than a TDI/DAM hard segment. As a result, much stronger hard segment domains would be expected to display a stronger mechanical response. Moreover, the "thermomechanical" stability of a MDI/DAM type hard segment domains is expected to be higher than a hard segment domain constructed by MDI/ED (ethylene diamine). Due to the all aromatic structure in

the MDI/DAM hard segment, a reasonable estimate of its transition temperature is in the range of 300 to 375°C as shown in Table 3.1. This thermal characteristic of MDI/DAM hard segment should provide better thermomechanical and heat resistance properties to polyurethane elastomer systems.

Chain extension of the isocyanate terminated prepolymer with water could also lead to polyurethaneureas with hard segment structure similar to the MDI/DAM system as already discussed in Chapter 2. Water extended polyurethane systems have been investigated for many years. However, one major problem with the addition of water directly into the system is its extremely low solubility in the reacting medium. Thus, a wide variation in reactivity occurs, which is no doubt related to the nature of the heterogeneous system (e.g. hard segment sequence distribution).

In Chapter 2, a new method, carbamate-isocyanate interaction, for preparing urea polymer has been described. This method potentially allows us to synthesize high molecular weight polyurethaneureas (PEUU) with MDI/DAM type hard segment by using bulk polymerization technique. In this chapter, the synthesis and characterization of PEUU's by using chain extenders such as tertiary alcohols and silanols will be discussed. The reactions of tertiary alcohol and isocyanate have been discussed thoroughly in Chapter 2. The chemistry of isocyanate and silanol reaction is interesting and also can be utilized synthetically to produce PEUU with hard segment structure similar to MDI/DAM. It has been observed that carbanilide and the corresponding siloxane are formed rather than silylurethanes by heating silanol with phenyl isocyanate [20,21].

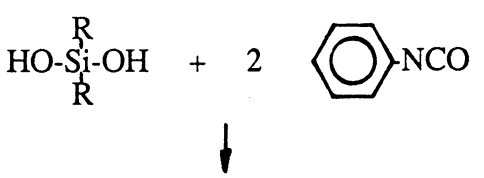

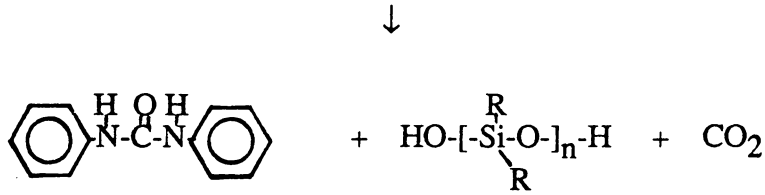

This phenomenon has been attributed to the self-condensation of silanols before they react with phenyl isocyanate. The water thus generated was molecularly dispersed in the reacting medium, which converts isocyanate to urea. It is certainly of interest to utilize such a characteristic in the synthesis of polyether-urethaneureas, since water can be efficiently and quantitatively introduced to the reaction without the immiscibility problems which are usually encountered in conventional water-extended PEUU systems. More interestingly, if a disilanol was utilized, a new multiphase polyurethaneurea / polysiloxane network can be formed in situ.

In the following section a brief literature review of the synthesis and characteristics of polyurethane elastomers is provided. However, it begins with the preparation of some important monomers.

3.2. LITERATURE REVIEW

3.2.1. Synthesis of Basic Urethane Building Blocks.

3.2.1.1. Diisocyanates.

The most important diisocyanates used in elastomer manufacturing are the 2,4-

and 2,6-toluene diisocyanate (TDI); 4,4'-diphenylmethane diisocyanate (MDI) and its aliphatic analogue 4,4'-dicyclohexylmethane diisocyanate (HMDI); 1,5-naphthalene diisocyanate (NDI); 1,6-hexamethylene diisocyanate (HDI); xylene diisocyanate (XDI); isophorone diisocyanate (IPDI); and 3-isocyanatomethyl-3,5,5-trimethyl-cyclohexyl isocyanate. The structures of these diisocyanates are given in Figure 3.1.

Isocyanates can be made in many ways. The chemical laboratory routes include the Lossen, Curtius, and Hoffman rearrangements, are may involve nitrene as an intermediate, are not suitable for large scale operation.

Lossen rearrangement

$$RCOOR' \xrightarrow{NH_2OH} R'OH + RCONHOH \xrightarrow{-H_2O} RCON \longrightarrow RNCO$$

Curtius rearrangement

$$RCOCl \xrightarrow{NaN_3} RCON_3 \xrightarrow{-N_2} RCON \longrightarrow RNCO$$

Hoffman rearrangement

$$RCONH_2 \xrightarrow{NaOBr} RCONHBr \xrightarrow{-HBr} RCON \longrightarrow RNCO$$

The use of azides in the Curtius reaction is hazardous and the utility of the Hoffman and Lossen rearrangements is limited to preparation of aliphatic isocyanates, as aqueous media are employed (aromatic isocyanates react readily with water to form substituted ureas). Tertiary butyl hypochlorite can be used for non-aqueous Hoffman rearrangements, but is costly.

In practice, only phosgenation of a primary amine is commercially important:

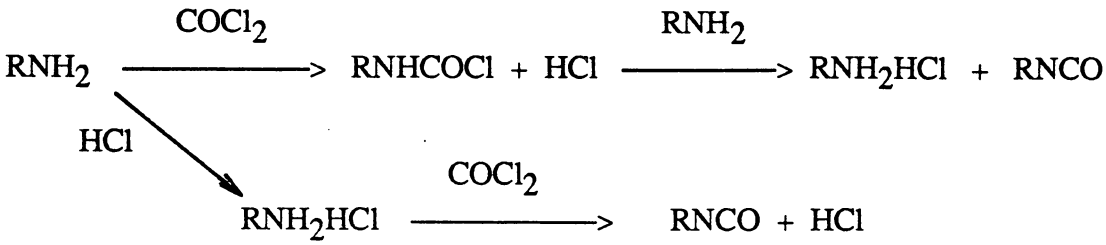

The phosgenation of the corresponding amines or amine hydrochlorides is usually conducted in an inert medium (o-dichlorobenzene). The reaction proceeds in two stages: first at room or somewhat higher temperature to generate the carbamyl chloride and HCl; further treatment with phosgene at temperatures of the order of 150- 170^{o}C then forms the isocyanate [22].

Toluene diisocyanates are prepared by direct nitration of toluene affording an 80:20 mixture of the 2,4- and 2,6-dinitro derivatives, followed by hydrogenation to the corresponding diaminotoluenes. The diamine mixtures are treated with phosgene at temperatures up to 140^{o}C and the derived diisocyanate mixture is isolated and purified by distillation. The two (2,4- and 2,6-) isomers differ considerably in reactivity, so the actual ratio of the two components can be quite important. For many purposes the 80:20 mixture is most widely preferred.

The diisocyanate MDI based on diaminodiphenylmethane is considerably safer to use than TDI, having a much lower volatility. However, the disadvantage that is less easily purified and consequently MDI is often used in the crude (undistilled) form. MDI is derived by phosgenation of the diaminodiphenylmethanes formed by condensation of aniline with formaldehyde which is illustrated in Figure 3.2.

According to the ratio of the reactants and the extent of purification adopted, smaller amounts of higher molecular weight products are also present, and on phosgenation a mixed isocyanate of functionality greater than 2 results. For example, a typical crude MDI may contain 55% of the 4,4'- and 2,4-diisocyanates and 20-25% of the triisocyanates, the remainder being polyisocyanates. When elastomers must possess maximum strength it is preferable to use the pure 4,4'-MDI to obtain maximum linearity in the elastomer.

The conventional phosgene process has several troublesome problems as follows:

1. The toxicity and corrosiveness features of phosgene are undesirable.
2. It produces large quantities of hydrogen chloride.

On the other hand, the market for pure 4,4'-MDI is expected to grow in next decade. On the basis of these demands, many attempts have been tried to develop a suitable method for the manufacture of MDI without using phosgene.

Recently, Asahi Chemical Co. of Japan developed a new route to synthesize MDI without using phosgene [23], and such a process is summarized in Figure 3.3. This process consists of three steps: (1) oxidative carbonylation of aniline to form ethyl phenylcarbamate (EPC), (2) condensation of EPC with formaldehyde and subsequent intermolecular transfer reaction with EPC to form methylene diphenyldiurethane (MDU) selectively, and (3) decomposition of MDU to form methylene diphenyl diisocyanate (MDI).

3.2.1.2. Polytetramethylene oxide (PTMO)

The synthesis and characteristics of PTMO will be discussed in detail in Chapter V.

3.2.2. Isocyanate Reactions

An outline showing some of the typical reactions of isocyanates is given in Figure 3.4 [24]. Reviews are available which treat the chemistry of isocyanates in considerable detail [25].

The electronic structure of the isocyanate group, as shown below, consists of several resonance structures:

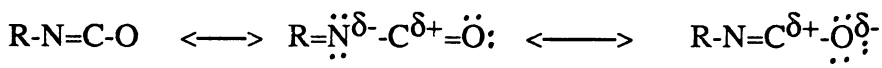

Because of the existence of multiple structures, several classes of reactions involving the isocyanate group are possible. Reaction can occur across the C=N bond in a variety of ways including adduct formation, oligomerization, cyclo-addition, and insertion reactions. Of these, only oligomerization and insertion are important in the formation of polyurethanes. Reactions involving the C=O bond are less important; the formation of carbodiimides is an exception.

The primary reaction in the polymerization of isocyanates is the insertion reaction. The reaction mechanism proceeds by a nucleophilic attack at the carbon atom in the isocyanate group, as shown below for the reaction of an alcohol with an isocyanate.

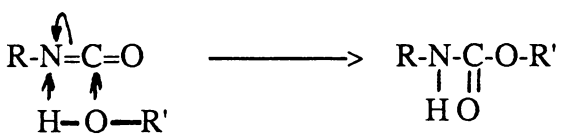

The product of this reaction is a carbamate ester linkage, which is more commonly known as a urethane linkage. Isocyanates can also react with amines in a similar fashion to form urea linkages:

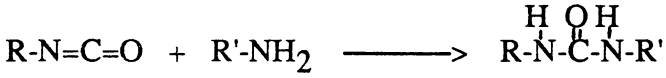

Polymers containing both urethane and urea linkages are called as polyurethaneureas.

Undesirable side reactions in the synthesis of polyurethanes include both insertion reactions and oligomer formation, and to a lesser extent the formation of carbodiimides. Both the urethane and urea linkages are capable of nucleophilic attack on the isocyanate, particularly at elevated temperatures. The products of these reactions are called allophanates and biurets, respectively. Their structures are shown as follows:

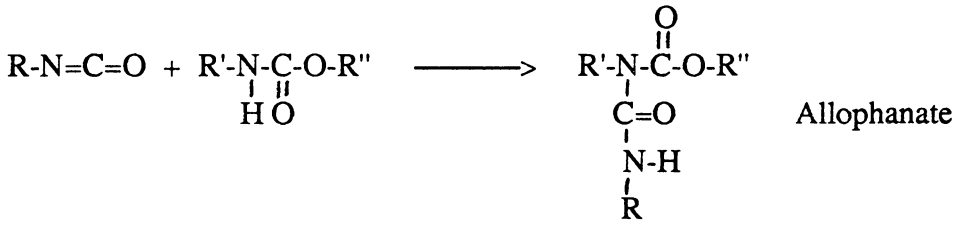

Allophanate

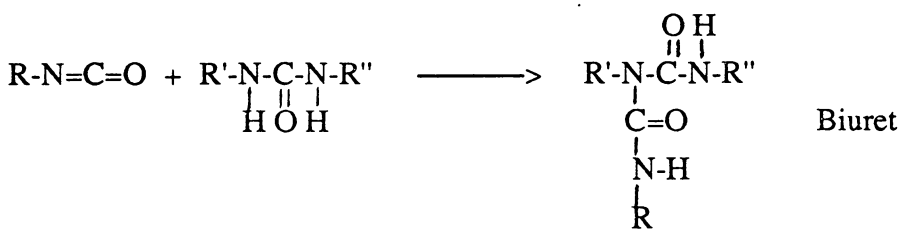

Biuret

Allophanate or biuret formation results in the chemical crosslinking of the polymer

chains. Often a small excess of isocyanate functionality is used in the polymerization to promote crosslinking in the postcuring period, after the product has been formed in its final state. Because the allophanate reaction is reversible at high temperatures, polyurethanes with a small amount of allophanate crosslinking can be melt processed with the dissociation of the allophanate bonds in the melt, followed by a reformation of the crosslinks as the material is slowly cooled. Recent work also suggests that transurethanifi- cation also takes place in polyurethane melts [26].

The second type of side reaction involving the isocyanate group is the formation under special conditions of oligomeric species. Dimers (uretidine diones) may be formed from aromatic isocyanates. Trimers (isocyanurates) can be produced from both aliphatic and aromatic isocyanates. The dimer reaction is readily reversible above 150^{o}C, whereas the trimer is a stable complex even at relatively high temperatures. It is therefore also possible to produce linear polyisocyanates using monoisocyanates, and crosslinked networks by using multifunctional isocyanates [27].

The catalysis of the insertion reaction in urethane formation can be accomplished with a variety of different catalyst systems. Tertiary amines and alkyl tin compounds are the most commonly used catalysts [28]. The tertiary amines catalyze both the hydroxy- isocyanate reaction as well as the water-isocyanate reaction. This is desirable when the final product is a urethane foam. Alkyl tin catalysts, on the other hand, are specific toward the hydroxy-isocyanate reaction in their catalytic activity. The efficiency of amine catalysts increases as the basicity of the amine increases and as the steric hindrance of the nitrogen decreases. Tin catalysts are more effective than amines for producing polyurethane elastomers. Dialkyl tin compounds are considerably more effective catalysts than are trialkyl and tetraalkyl tin catalysts. In addition, tin compounds with shorter alkyl groups have a higher activity than those with long alkyl

groups. Dimethyl tin is most effective catalyst, but because of toxicity considerations, alkyl groups shorter than butyl are rarely utilized commercially [29].

The divalent tin compounds act catalytically by coordinating first the hydroxyl group and then the isocyanate group. While the exact mechanism is not known, the following mechanism has been proposed [30]:

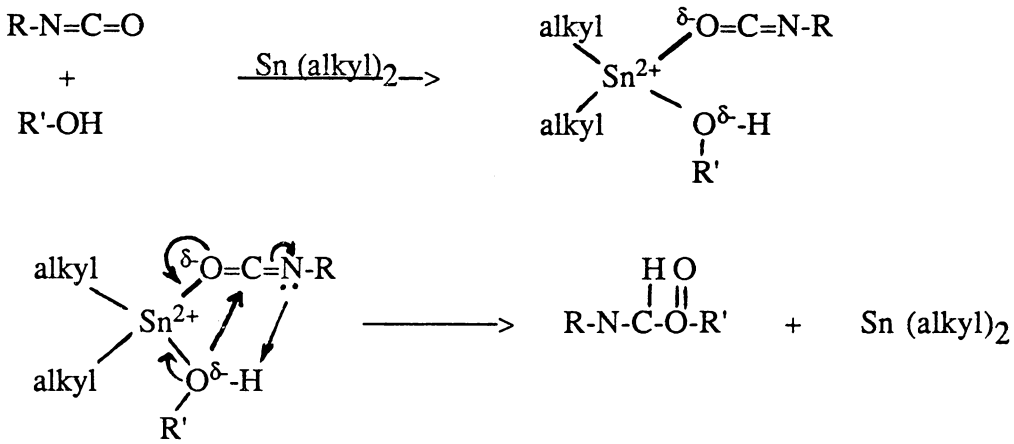

3.3. EXPERIMENTAL

3.3.1. Materials.

Hydroxy-terminated polytetramethylene glycols (PTMO, DuPont) were dehydrated at 70°C under vacuum for 24 hours before use. 2-Phenyl-2-propanol or cumyl alcohol (CA, F.W. 136, m.p. 32-34°C, b.p. 202°C, 97%, Aldrich) was purified by vacuum distillation. α,α'-Dihydroxy-p-diisopropylbenzene or dicumyl

alcohol (DCA, F.W. 194, m.p. 140°C, Goodyear Co.), 1,1-diphenylethanol (DPE, F.W. 198, m.p. 77-81°C, 98%, Aldrich), and triphenylmethanol (TPM, F.W. 260, m.p. 160-163°C, b.p. 360°C, 97%, Aldrich) were used as received. 4,4'-Bis-methylenediphenyl isocyanate (MDI, Mobay Co.) was vacuum distilled and stored in a desiccator at 0°C before use. DMSO was used as a solvent in some experiments and was purified by vacuum distillation over calcium hydride right before use. Diphenylsilanediol (DPSOL, F.W. 216, b.p. 140°C decomposed, Petrarch Systems, Inc.) and 1,4-bis(hydroxydimethylsilyl)benzene (HDSB, F.W. 226, b.p. 135°C) were used as received. 1,8-Diazobicyclo [5.4.0]-undec-7-ene (DBU, Aldrich) was used as a catalyst without further purification in the solution polymerization of DCA chain extended polyurethanes.

3.3.2. Synthesis of DCA Chain-Extended Polyurethanes By Solution Polymerization

Reactions were conducted in a three-neck round-bottom flask fitted with a gas inlet, a thermometer, a condenser, and a magnetic stirrer. MDI, 1.5g (6.2 mmoles), was added to the flask. Next, 5g (2.5 mmoles) of PTMO-2000 was transfered to the reactor. The reaction mixture was heated under N_2 atmosphere at 100°C and after one hour, a solution of 0.71g (3.7 mmoles) of DCA in 73 ml of DMSO was added into flask. The isocyanate-terminated PTMO prepolymer is soluble in DMSO and formed a homogeneous solution. The reaction temperature was maintained at 50°C and the catalyst, DBU (approximately 0.1 wt.%) was added when isocyanate-terminated prepolymer was completely dissolved.

A high molecular weight polymer was obtained about one minute after the addition of the catalyst. The product was precipitated out from DMSO and formed a big rubber-ball. The polymer is so tough that it was sometimes necessary to break the flask in order to remove it. The product was dried in a vacuum oven at 80°C for 24 hours.

3.3.3. Synthesis of Polyurethane-ureas By Bulk Polymerization.

3.3.3.1. Tertiary Alcohol Chain Extended System.

The segmented polyurethaneurea elastomers were synthesized by a step-growth reaction (Figure 3.5). MDI was charged into a N_2-filled resin kettle equipped with a high torque mechanical stirrer at room temperature. The reaction set-up is shown in Figure 3.6. PTMO was then slowly syringed into the reactor at 110°C over a period of 10 minutes. After reacting the prepolymer/MDI mixture at 110°C for 1 hour, CA or DCA was added and the temperature was increased to 150°C. At 150°C, the bulk viscosity gradually increases and the mechanical stirrer was stopped within 30 minutes, due to the high viscosity. Essentially, a solid polymer had been formed at this stage. The reaction was continued for two additional hours at 150°C in order to complete the reaction. In fact, the synthesis can be accelerated by adding a suitable catalyst, and high molecular weight polymer can be obtained in a very short time. The copolymers synthesized in this fashion was extracted with hot THF for 24 hours to remove any soluble by-products such as α-methylstyrene and were dried in a vacuum oven at 70°C for 36 hours.

The molar ratio of MDI and PTMO and soft segment molecular weight were altered in different experiments to produce samples with systematically varied hard segment content and block length. By using this approach, tertiary alcohols are not directly involved in the chain extension step. Thus, the hard segment in the copolymers will be totally derived from the diisocyanates. The theoretical hard segment content is equivalent to the weight percent of the diisocyanate charged.

$$\% \text{ Hard Segment Content} = \frac{\text{wt. of MDI}}{\text{wt. of MDI} + \text{wt. of PTMO}}$$

The theoretical percentage of urea content can be calculated by using the following relationship (note that possible side reactions are not considered):

$$\% \text{ urea content} = \frac{\text{urea linkages}}{\text{urea linkages} + \text{urethane linkages}}$$

$$= \frac{\text{\# moles of } NH_2}{\text{\# moles of } NH_2 + \text{\# moles of OH}}$$

$$= \frac{(\text{\# moles of MDI} - \text{\# moles of PTMO}) / 2}{(\text{\# moles of MDI} - \text{\# moles of PTMO}) / 2 + \text{\# moles of PTMO}}$$

$$= \frac{\text{\# moles of MDI} - \text{\# moles of PTMO}}{\text{\# moles of MDI} + \text{\# moles of PTMO}}$$

The characteristics of the various polyurethaneureas synthesized are listed in Table 3.2. A system obtained with 2000 molecular weight PTMO, MDI and CA is referred

to as PTMO-2000-MDI-X-CA, where X represents the weight percent of the hard segments and CA indicates the type of the chain extender. A similar nomenclature is employed for all other samples.

3.3.3.2. Silanol Chain Extended System.

The synthetic procedure is basically the same as that described in the tertiary alcohol chain extended system, except a relatively lower bulk reaction temperature, 110°C, was employed in the chain extension stage since DPSOL tends to decompose at 140°C. Approximately 0.1 wt. % of DABCO (triethylene diamine) was introduced after the addition of DPSOL, which functions as a catalyst for the self-condensation of DPSOL. DPSOL formed a clear mixture with the isocyanate-capped PTMO prepolymer at 110°C. Generally, the polymerizations proceed very fast. High molecular weight polymer was generated in about 30 seconds in the presence of tertiary amine catalyst. The copolymers synthesized in this fashion were extracted with hot THF for 24 hours to remove any soluble by-products such as low molecular weight polydiphenylsiloxane (PDPS) and were dried in a vacuum oven at 70°C for 36 hours. The extracts were collected for further analysis to identify the structure of the by-products.

Theoretically, the number moles of DPSOL required is equal to the one half of the number moles of free isocyanate remaining after the first stage capping reaction. This is assuming that an infinite high molecular weight of PDPS result. One mole of H_2O would be formed by the self-condensation of one mole of DPSOL. The amount of H_2O generated is taken into account during the calculation of the stoichiometry needed to obtain high molecular weight polymer. However, the self-condensation of DPSOL

only results low molecular weight PDPS, about 1000 molecular weight from VPO (vapor phase osmometry) studies, in the polyether-urethane medium due to its high crystalline nature. An excess amount of DPSOL was usually utilized.

Since the DPSOL is not part of the polymer backbone, the actual percentage of hard segment and urea content are calculated as the same way as in the CA chain extended system.

A butanediol chain extended PTMO-based segmented polyurethane elastomer with 31% hard segment content was also synthesized which was used as a control for the novel PEUU's.

3.3.4. Characterization Techniques

3.3.4.1. Sample Preparation

Films for physical testing were prepared by compression molding dry material at 200 to 240°C and 10,000 psi. The temperature was slightly higher when the hard segment was increased to high values. The material was first heated in the press for two to three minutes and the pressure was then raised slowly. The film was then kept in the press for another 5 minutes prior to the fast water cooling step. The pressure was released when the press temperature reading reached room temperature. This cooling process usually took 2 to 3 minutes. After removal from the press, all samples were placed under vacuum in a dessicator until further testing. No degradation of the materials at these high temperatures was observed and all the films retained their superior physical properties.

3.3.4.2. Spectroscopic Analysis

Structural determination of the segmented copolymers was obtained with a Nicolet MX-1 FT-IR Spectrometer linked to a Nicolet Data Station. IR spectra were taken on polymer films and the polymerization extracts. Since those materials are insoluble in common low boiling solvents such as THF, methanol, etc., the thin polymer films for IR analysis was prepared by using compression molding between two Teflon ® sheets at a pressure of about 20,000 psi.

3.3.4.3. Thermal Analysis

DSC thermograms were recorded by using a Perkin-Elmer DSC II over the temperature range of -100 to 50°C. A constant flow of helium gas was used to purge the system and a heating rate of 10°C/min was employed throughout the measurements. The data were derived from second cycles in order to provide a constant thermal history. Thermal mechanical analysis (TMA) on polymer films was performed on a Perkin-Elmer Thermal Mechanical Analyzer over the temperature range -100 to 300°C. The experiments were carried out at a heating rate of 10°C/min under a constant load of 10 grams. Thermal gravimetric analysis (TGA) was used for the thermal degradation studies, which began at 50°C and was increased to where the polymers degraded completely.

3.3.4.4. Dynamic Mechanical Analysis

The dynamic mechanical data were recorded using a Rheovibron DDV-IIC Viscoelastomer (Toyo Measuring Instruments) at a frequency of 110 Hz. The samples were rapidly cooled to -100°C and the measurements were made with a heating rate of 2°C/min. up to 300°C.

3.3.4.5. Tensile Testing

Uniaxial stress-strain experiments were performed on dog-bone specimens using an Instron Tensile Tester (Model 1122) at room temperature. These experiments were carried out at a strain rate of 200% per minute, based on the initial sample length.

3.4. RESULTS AND DISCUSSION

3.4.1. Synthesis

3.4.1.1. Dicumyl Alcohol Chain Extended PEUU

Dicumyl alcohol, a tertiary alcohol, is usually not of interest as a chain extender in the preparation of polyurethane elastomers, since it associated with a lower reactivity toward isocyanates when compared with a primary alcohol, due to the sterically hindered hydroxy groups. As a result of this, there is no information appearing in the open literature concerning this "bulky" chain extender. However, the general idea here

has been to utilize this bulky nature of di-tertiary alcohol to produce a high T_g hard segment in a polyurethane elastomer. In other words, a better heat resistant polyurethane elastomer hopefully can result due to the high stiffness of the hard segments.

The synthesis by using bulk polymerization was first investigated because it is simple and economical. Interestingly, it was found that the polymer formation was very temperature dependent, as shown in Figure 3.7. If the reaction was conducted in bulk at 110°C without catalyst, no increase in viscosity was observed for several hours. However, at higher temperatures, e.g., 150°C, an immediate increase in viscosity was observed which indicated an increase in polymer molecular weight. The high reaction temperature necessary is not surprising due to the effect of steric hindrance in these phenyl substituted tertiary alcohols. In fact, the synthesis can be accelerated by adding catalyst and high molecular weight polymer was formed in a very short period of time and at a lower temperature, ~100°C. It is also noted that the polymer formation was always accompanyed by "foaming" which indicated gas evolution. Besides that, there is always presence some liquid in the reactor after the polymerization which has a strong stench. The possibility of unreacted monomers was considered unlikely since it is necessary to have a perfect stoichiometry in order to obtain high molecular weight condensation polymers. An unbalanced stoichiometry will produce polymer with poor mechanical strength. However, all the dicumyl alcohol chain extension conducted in bulk at 150°C produced extremely strong polymeric film.

Extraction with hot THF was conducted after the polymerization by using Soxhlet apparatus to remove possible side-product. The polymer is not soluble in common low boiling solvents such as THF, chloroform, etc. A clear polymer solution was obtained

by dissolving the extracted copolymers in DMF at 100°C. This indicated that an essentially linear polymer was obtained.

In order to characterize the reaction mechanism, infrared spectra were obtained from the thin compression molded polymer films. The bottom FT-IR spectrum in the Figure 3.8 is for the DCA chain extended polymers prepared in bulk at 150°C, PTMO-2000-MDI-23-DCA. It is not surprising to see the urethane linkage absorptions which appear at 1730 and 1703 cm^{-1} and these correspond to the nonhydrogen bonded and hydrogen bonded C=O stretching mode of urethane groups, respectively. However, an additional absorption peak at 1640 cm^{-1} in the IR spectrum also appeared which is usually utilized as an indication of the formation of urea polymers. This intense peak is attributed to the hydrogen bonded urea carbonyl. The MDI based polyurethane prepared by using this approach gave a very similar IR spectrum with the MDI/DAM based PEUU prepared by Ishihara et al.[2]. This probably implies that those two polymers are structurally similar, despite the fact that two entirely different chain extenders are utilized.

Now, one of the critical question need to be answer here is how does the urea formation take place at high temperatures? It is speculated that the polyurethanes with tertiary alcohol derived carbamate linkages distributed along the polymer backbone are thermally unstable. However, the degradation products include an amine which is very reactive toward any free isocyanates, thus allowing an urea linkage to be obtained. It is also thought that such a dicumyl alcohol derived carbamate linkages may have a chance to survive at lower temperatures without degradation. If this is the case, it can be used as a control polymer for comparison with other urea polymers.

An attempt was made to incorporate DCA to the polymer backbone by using solution polymerization in DMSO at 50°C. The amount of reactants employed was

exactly the same as in the bulk polymerization case in order to provide a good comparison. Due to the relatively low reactivity of tertiary alcohols with isocyanates, a catalyst was added during chain extension. A high molecular weight polymer was obtained about one minute after the addition of the catalyst.

From IR studies, no absorption peak corresponding to the 1640 cm^{-1} due to the urea linkages was observed for the solution polymerized DCA chain extended polyurethane, PTMO-2000-MDI-DCA-31-S, as illustrated in the top spectrum of Figure 3.8. Under the conditions utilized, DCA is expected to react with MDI terminated prepolymer through a conventional alcohol-isocyanate mechanism, without observable degradation. The resulting urethane linkages apparently have reasonable thermal stability at 50°C. These observations were in good agreement with the model reaction studies, as described in Chapter 2.

3.4.1.2. Monofunctional Tertiary Alcohol "Chain Extended" PEUU's

As mentioned earlier in the introduction section of this chapter, the carbamates derived from tertiary alcohols and phenyl isocyanate are thermally unstable. On heating such a carbamate in the presence of isocyanate to 150°C, a thermally more stable urea linkage can be obtained. In other words, the tertiary alcohols in the polyurea synthesis are not directly incorporated into the polymer backbone. It is more likely that they convert the isocyanates to corresponding amines via a carbamate-isocyanate interaction, which then react with isocyanates to produce the polyurea. As a consequence, the basic structure of the polyureas should be independent to the type of the tertiary alcohol used (either mono- or di-functional) while the other starting materials are the same. The FT-IR spectra of both CA (monofunctional) and DCA

(difunctional) chain extended polymers are shown in Figure 3.9. Basically, there is no difference between the polymer in terms of IR absorptions. Both polymers show a very intense absorption at 1640 cm^{-1} which is due to the hydrogen bonded urea carbonyl. Moreover, it would of course be impossible to prepare a "polymer" via a conventional alcohol-isocyanate reaction if one of the reagents is a monofunctional material.

The reaction by-product resulting from the carbamate-isocyanate interaction was carbon dioxide and corresponding olefin. The gas evolution during the polymerization has been observed and that is believe to be carbon dioxide. More substantially, evidence of the formation of olefin (α-methylstyrene, in the case of CA chain extended systems) is given in Figure 3.10. Three IR spectra were taken on CA and α-methylstyrene control and the reaction by-products. The liquid by-products were collected from the inside wall of the reaction kettle during the reaction. Due to the volatility of CA and α-methylstyrene at 150°C, the collected liquid was actually a mixture of α-methylstyrene and CA as demonstrated by IR (bottom spectrum of Figure 3.10). Fortunately, even though most of the absorption peaks overlapped with the olefin, absorptions are able to be differentiated from the background. The absorption peaks appearing at 1640 and 850 cm^{-1} correspond to the C=C stretching and $=CH_2$ wagging, respectively, and compare well with an authentic IR spectrum for α-methylstyrene.

In this approach to polyurethaneureas, phenyl-substituted tertiary alcohols have been selected as a chain extender for the reason described in Chapter 2. The typical reaction temperature was observed to be about 140-150°C (in the absence of catalyst) for most of the polymerizations.

The majority of our experiments were carried out with CA and DCA, while DPE and TPM are utilized as chain extender instead in several experiments in order to verify our proposed urea formation mechanism. The reason for using DPE (1,1-diphenylethanol) is because there is two phenyl groups on the tertiary carbon. An extra phenyl group may provides further stabilization of carbonium ion intermediate. In other words, a faster rate of the amine formation is expected. However, the chain extension rate, as judged by the time required to generate high molecular weight polymer, is comparable with CA chain extended system. This is probably due to the steric hindrance of DPE. Despite a possible faster dissociation rate of the resulted carbamate, the rate of the formation of such a carbamate is lower than the case of CA.

Initially, no polymer is expected in the TPM chain extended system on the basis of our proposed urea formation mechanism. The two reasons for such expectation: first, there is no α-proton available for the formation of olefin; second, such highly sterically hindered hydroxy group is unreactive as according to the literature [31]. However, a high molecular weight polymer was obtained after 8 hours reaction time at 150°C. The chain extension of isocyanate-terminated prepolymer with TPM is characterized by dark-brown color formation. We know that dark-brown colors are not characteristic of either the isocyanate- terminated prepolymer or TPM itself. TPM is fairly thermal stable and can be distilled between 360 and 380°C without decomposition [32]. The color formation is unclear at this time. The FT-IR spectrum of the color polymer is shown in Figure 3.11. Clearly, the urea absorption is appeared at 1640 cm^{-1}. The possible route for the urea formation is pictured in Figure 3.12. It is speculated that TPM first reacted with isocyanate at a slow rate and the resulting carbamate was rapidly dissociated to corresponding triphenyl carbonium ion and aniline anion along with the evolution of carbon dioxide. A secondary amine therefore

results which might react with any other free isocyanate to generate a highly sterically hindered urea linkage.

The resulting highly colored polymer formed a transparent film after compression molding. A low temperature T_g of -49°C was observed from DSC which is considerably higher than the T_g, -79°C, of starting PTMO-2000 oligomer. The increased soft segment T_g suggests some phase mixing between soft and hard segment phases. Despite the possible urea formation as indicated by IR spectrum, the interchain hydrogen bonding is greatly reduced by the presence of sterically hindered triphenylmethane substituted urea linkages.

3.4.1.3. Silanol Chain Extended PEUU

Interesting urea polymers are obtained by using diphenylsilanediol as a "chain extender" as well. In this case, the formation of urea linkages is believed to occur as indicated in Figure 3.13. The pathway to the urea groups, using silanol thus seems to proceed differently from that of the tertiary alcohols. Diphenylsilanol tends to undergo self-condensation to give polydiphenylsiloxane and water in the presence of various catalysts such as tertiary amines [21]. By using this approach, "molecularly dispersed" water can be quantitatively introduced into the system without immiscibility problems which are usually encountered in conventional water-extended systems. Water presumably first reacts with isocyanate to form an thermally unstable carbamic acid intermediate, which is then converted to a corresponding amine.

The direct confirmation of the urea formation was provided by FT-IR analysis on dried polymer after extraction, as shown in Figure 3.14. An intense absorption at 1640

cm^{-1} is due to the hydrogen bonded urea carbonyl. This spectrum is basically identical with the PEUU spectrum provided in Figure 3.9, which suggests that they are similar polymers, although the chain extenders utilized are entirely different.

PDPS can be recovered almost quantitatively after extraction. This suggested that polyether-urethaneurea and PDPS are formed separately. Figure 3.15 provides spectra of collected extracts and starting DPSOL, and a genuine PDPS obtained from Aldrich Chemical Co. was also attached for comparison. There is no doubt that the reaction by-product is PDPS although it may be a low molecular weight product. Most of the DPSOL underwent self-condensation, as indicated by a drastically decreased -OH IR absorption at 3250 cm^{-1}.

The reaction by-product, polydiphenylsiloxane (PDPS), is a crystalline solid at room temperature. The difference in the crystallinity of polymers before and after removal of PDPS was investigated with the aid of the wide-angle x-ray diffraction (WAXS) technique. The WAXS diffraction patterns on the polymers before and after extraction are shown in Figure 3.16. A sharp ring appeared in the WAXS pattern for the polymer before extraction which indicated that the crystalline nature of the polymer. However, this ring disappeared after extraction with hot THF. Clearly, the crystalline behavior is attributed to the presence of PDPS, since PDPS is the only product extracted out by THF as demonstrated by IR analysis.

The GPC trace of the extracted PDPS is provided in Figure 3.17. A single peak appeared at relatively high elution volumes, which implies that it is a low molecular weight product. The extent of the self-condensation of DPSOL is low, which is due to the low solubility of crystalline PDPS in the polyetherurethane medium. On the other hand, the bulk polymerization temperature employed for the polymer synthesis may also limit the high molecular weight PDPS formation, since it is significantly lower

than the melting temperatures of the high molecular weight PDPS.

3.4.2. Chemical Structure of Polymers

3.4.2.1. PEUU's Via Carbamate-Isocyanate Interaction.

The approach we have taken for the design of unique polyether-urethane-urea polymers is based on the observation that urea is formed via a carbamate-isocyanate interaction. Therefore, the structure of the hard segments is solely dependent on the chemical structure of the isocyanate employed. For example, a MDI-urea type hard segment will result when MDI was utilized, its generalized chemical composition can be represented by the following:

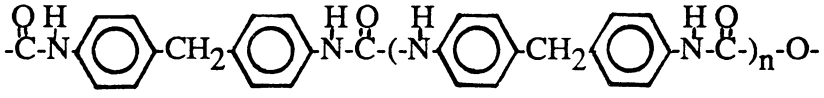

The exact hard segment chemical structure may be more complicated than the above generalized structure since branching may also possibly occur during the carbamate-isocyanate interaction. The reason for the speculation of the branching formation has been discussed in Chapter 2. If this is the case, a bulky side group will be formed randomly on the hard segment by substituting one of the active hydrogen on either urethane or urea linkages. The envisioned hard segment chemical structure that results can be depicted as

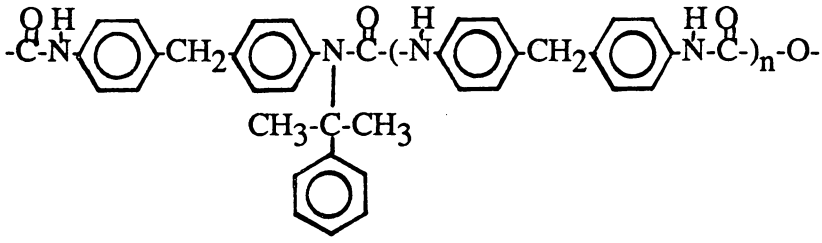

Although some degree of branching is believed to be presented, the amount of it is low on the basis of model compound studies as has described in the Chapter 2. The reason for pointing this possibility out is for better understanding the structure-property relationship on the basis of characterization results. The amount of side-chain branching certainly will affect the physical properties of the polymer. The efficiency of interchain hydrogen bonding between the urea linkages may be reduced due to the presence of the bulky side group which further retards the hard segment crystallization. A bulky side group gives a copolymer with a rigid hard segment, which is translated to a high softening temperature. However, polymer thermal stability may be decreased with the presence of branching.

In both cases of mono- and di-tertiary alcohol chain extended PEUU's via carbamate-isocyanate interaction, the resulting polymer will be similar in terms of chemical structure. However, a polymer derived from ditertiary alcohols (such as DCA) may be slightly crosslinked if side reactions are considered. This is because branching may occur in between the polymer chains and a lightly crosslinked material can result. The possible crosslinked structure can be represented as follows:

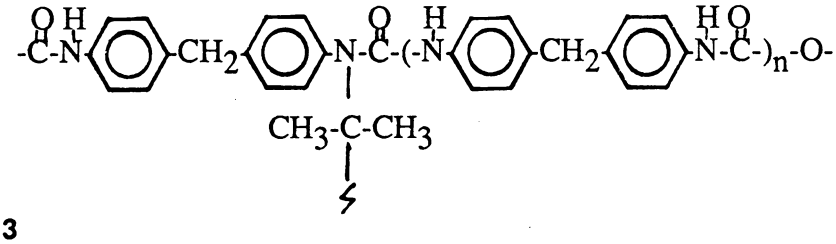

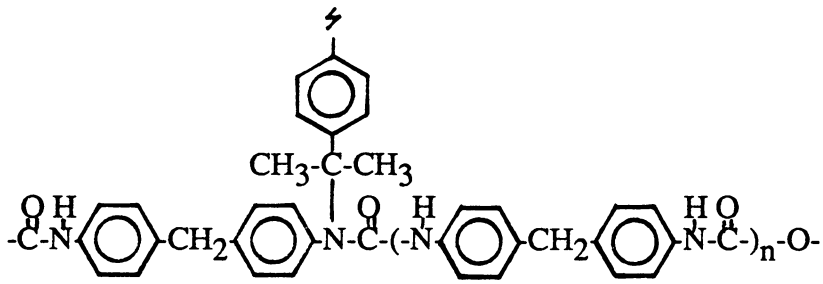

It is therefore clear that a mono-functional tertiary alcohol is usually preferred in the synthesis of PEUU via carbamate-isocyanate interaction, since it represents a generally linear PEUU structure, despite a small amount of branching may be present.

The microstructure of copolymers synthesized by the prepolymer method following chain extension can be altered and is a function of soft segment molecular weight and the percentage of hard segment content. For example, the urea linkage concentration (in the case of a diamine chain extender) will be increased in a system with fixed hard segment content when a higher molecular weight of PTMO is utilized. This is because that the -OH concentration is decreased with increasing PTMO molecular weight on the same weight basis. A larger number moles of low molecular weight diamine chain extender is therefore necessary to balance the stoichiometry in order to achieve a certain amount of hard segment content. On the other hand, urea concentration certainly will be increased when a higher weight percentage of hard segment is desired since more chain extender needs to be used. The relative urea concentrations in our PEUU's have been estimated on the basis of the above assumption and are listed in Table 3.2. Higher concentration of urea linkages presumably will improve the cohesiveness of the polymer chain, through the hydrogen bonding.

3.4.2.2. DCA Chain Extended Polyurethanes - Via a Conventional Approach.

It is also possible to incorporate DCA to the polymer backbone when the chain extension was conducted in a polar solvent at a relatively low temperature, ~ 50°C. The polymer thus prepared although may be thermally unstable at temperatures above 100°C due to the presence of tertiary alcohol derived carbamate linkages, this unique chemical structure (as shown below) is expected to provide polyurethanes with interesting properties.

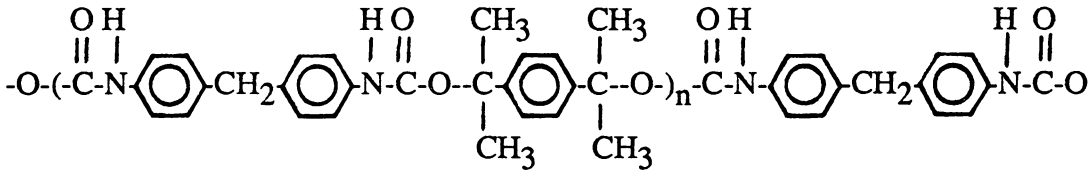

Hydrolytic stability of the polymer is expected to be improved due to the presence of the "protective" bulky aliphatic groups adjacent to the urethane linkages which protect the urethane linkages from moisture attack.

3.4.2.3. Silanol Chain Extended PEUU's.

This process can be considered as a special case of water-extended polyurethane-ureas. Virtually, molecularly dispersed water was produced in situ by the self condensation of silanols. Ideally, the chemical structure of PEUU synthesized by silanol chain extension should be similar as those PEUU's prepared by

carbamate-isocyanate interaction. Although this point has been supported by FT-IR spectra, some minor differences between two systems are undoubtedly present due to the nature of the polymer formation mechanism. Branching is less significant in the silanol chain extended polymers than in the case of the tertiary alcohol chain extended system. This linear characteristic should provide the silanol chain extended PEUU with superior physical properties in the later case, since the hard segment is more crystallizable in the absence of side chain branching. However, as described in the synthesis section, the extent of self-condensation of silanols in the polyurethane medium is usually low, the molecular water thus generated is less than stoichiometric amount. Nevertheless, a reasonable high molecular weight polymer can be obtained in short period of time.

In addition to using silanol to generate water in situ, the condensation product, a crystalline PDPS was originally thought to be a possible reinforcing agent for the polyurethane-urea matrix. However, this idea could not be confirmed experimentally due to some difficulty in preparing a "good" polymer film by compression molding for physical testing and further work was not continued.

3.4.3. Thermal and Mechanical Analysis

3.4.3.1. Differential Scanning Calorimetry (DSC)

a. PTMO Oligomers

It is always instructive to compare the low temperature DSC behaviors of starting oligomers with the resulting polymers. The DSC thermograms of PTMO's with

molecular weight ranging from 650 to 2900 are shown in Figure 3.18 and Table 3.3. For consistency glass transition temperature values were obtained at a heating rate of 10°C/min on the second heating cycle.

PTMO-650 is a sticky viscous fluid while the rest of the PTMO's are waxy materials at room temperature. This is understandable since PTMO is a highly crystalline material at temperatures below their T_m. Their melting temperatures are dependent on the PTMO molecular weight. The T_m of high molecular weight PTMO is about 50°C. From Figure 3.18, the T_m of PTMO oligomers are systematically increased with molecular weight. This is probably due to larger crystallites present in higher molecular weight PTMO. No crystallization exotherm was observed when the molecular weight of PTMO was higher than 650. This implies that PTMO crystallize rapidly even at a cooling rate of 320°C/min when the molecular weight reaches to 1000. The magnitude of the heat capacity change (ΔC_p) at the T_g, normalized to the weight of the material, is a function of both the relative amount of the participating amorphous phase and the difference of conformational entropy between the glassy and rubbery state. The ΔC_p of the PTMO-650 is significantly higher than the rest of PTMO's as shown in Table 3.3.

Interestingly, the T_g of the PTMO was increased with the molecular weight. This is quite unusual since it is generally thought that the longer the polymer chain the more flexible would be. As the molecular weight of the PTMO increases, the chain end -OH concentration decreases. Restricted motion of polymer chains was imposed by the interactions between the chain ends and chain ends with ether linkages, possibly through crystallinity. The consequence of this anchoring effect will be an increased T_g value. The PTMO crystallites formed during the cooling process greatly reduced the

flexibility of the soft segment. Thus, a higher value of T_g was obtained with higher molecular weight PTMO oligomers. Presumably, the restricted motion imposed by the crystallites is more effective with larger size of crystallites.

b. PEUU's via Carbamate-Isocyanate Interactions.

As mentioned earlier in the introduction, the phase separation in the polyurethane elastomers can be promoted by the incorporation of urea linkages. Both mechanical and thermal properties of the polyurethanes could be affected dramatically by phase mixing. Interaction between soft and hard segments can increase the glass transition temperature (T_g) of the soft segment and decrease the T_g of the hard segment. The degree of phase mixing is indicated by this shift of transition temperatures toward intermediate values. Both qualitative and quantitative evaluation of the degree of phase separation can be obtained by differential scanning calorimetry [12,33].

Table 3.4 presents a summary of the low temperature DSC results for the tertiary alcohol chain extended segmented PEUU copolymers. The low temperature thermograms contain the transitions associated with the soft segments are presented in Figure 3.19, Figure 3.20 and Figure 3.21. The thermograms in Figure 3.19 show the low temperature transitions indicated by various copolymers with different PTMO molecular weight but the same hard segment content. For PTMO-2000 and PTMO-2900 based PEUU's, the soft segment glass transition occurs at -74^{o}C and -78^{o}C, respectively. They are followed by an in situ crystallization exotherm at -36^{o}C and -52^{o}C, and melting endotherms at about 9^{o}C and 11^{o}C, respectively. The presence of a melting endotherm is observed as expected by virtue of the greater molecular weight of soft segment involved and that the hard segment solubilization in the soft segment matrix is minimal. At room temperature, those segments are just

above their melting point so that rapid cooling below room temperature is effectively a melt quench to an amorphous glassy state below T_g. When reheated, the soft segments crystallize above their glass transition temperature. The crystallization rate of PTMO-2000 segment in the copolymer is believed to be much slower than in the oligomeric state due to the imposed restriction by the hard segment domains.

A slightly higher T_m was observed for PTMO-2900 based PEUU than the PTMO-2000 based materials is probably due to the larger crystallites associated with the longer soft segment chains. A lower crystallization temperature was observed for PTMO-2900 based PEUU when compared with PTMO-2000 based PEUU's. Two reasons possibly attributed to such observation: firstly, the longer the PTMO chain is more flexible; secondly, a better phase separated system may result when larger molecular weight of PTMO was utilized. Here, the soft segment is less restricted by the solubilized hard segment. Crystallization and melting transitions were not observed for the lower soft segment molecular weight based materials. For PEUU samples with 650 and 1000 molecular weight PTMO, the T_g was observed at -38 and -48^{o}C respectively. These T_g's are substantially higher than the glass transition temperatures reported in Figure 3.18 and Table 3.3 for pure PTMO oligomers (-84 and -82^{o}C respectively). This indicates the existence of mixed hard segments in the soft segment matrix of these materials, the extent of which is likely determined by the amount and length of both segments. In addition, the anchoring of soft segments at the phase boundaries of a domain structure would also raise the T_g due to the restrictions imposed by coupling at the interface.

The width of the glass transition zone is also longer for low soft segment molecular weight based copolymer suggesting a higher degree of segment mixing.

Moreover, it is observed that the ΔC_p at the glass transition is increased, with the decrease of soft segment length which directly correlated to the amount of amorphous content in the soft segment matrix. The dissolved hard segment in the soft segment matrix will prevent the soft segment crystallization during the cooling process and therefore increase the amorphous content.

The high temperature DSC thermograms of PTMO-2000 based PEUU's, indicating the transitions associated with the hard segments are shown in Figure 3.22. These samples show a glass transition peak near 220°C corresponding to the hard segment. Interestingly, no melting endotherm at the temperature range studied was observed even with the highest hard segment content sample. This observation at first seems quite puzzling since the hard segment with MDI/DAM type structure is expected to be crystallizable due to its high chain regularity. As one may recall from the model compound studied in Chapter 2, side-chain branching possibly occurred during the polymerization. The crystallization of hard segment undoubtly will be reduced due to the presence of bulky branch unit and therefore with an increase the amorphous content of hard segment phase. Although melting endotherms were not detected by DSC up to 250°C, the possibility of a semicrystalline nature of hard segment cannot be eliminated since branching only believed to be presented in a small amount. The possible T_m of hard segment may exist at temperatures above 300°C which is in the neighborhood of the degradation temperature. This statement was on the basis of Skuches's work on model urea compounds [19]. One urea model compound they investigated is listed in Table 3.1 with the comparison similar to our hard segment structure. The T_m associated with their urea compound is reported as 330°C. A reasonable estimate on the T_m of our hard segment phase is in the neighborhood of

that temperature. or even higher.

c. DCA Chain Extended Polyurethanes.

First and second runs of DSC scans on DCA chain extended polyurethane with 31 wt % hard segment content are provided in Figure 3.23. In the first run scan, two sharp endotherms are observed at 18 and 40°C and partially overlapping with each other. This behavior is commonly observed only in the first run DSC scan of pure PTMO oligomers [3]. To illustrate this, the first and second run of DSC scans of PTMO-2000 was collected as shown in Figure 3.24. The low temperature endotherm is attributed to the melting of metastable PTMO crystallites. The higher temperature melting peak is associated with the crystalline PTMO segment close to their equilibrium state. These larger crystals are due to the nearly ideal annealing conditions that room temperature storage affords. The high temperature melting endotherm disappeared in the second scan after fast cooling from a temperature above PTMO's equlibrium T_m.

The low temperature DSC behavior of both DCA chain extended polymer and PTMO-2000 oligomer are suprisingly similar to each other with the exception that a crystallization exotherm was observed on the former at the second cycle. This suggests a high degree of purity within the soft segment matrix of DCA chain extended polymer. Although a clean soft phase was obtained, the PTMO-2000 segment in the copolymer is expected to crystallize at a much slower rate when compared with a PTMO-2000 oligomer. This is due to the fact that the chain ends of PTMO are chemically bonded to hard segments which restricted the soft segment mobility. A rapid cooling of copolymer after the first run becomes an effective melt quench to an amorphous glassy state below T_g. Therefore, soft segment crystallization was

observed when the reheated temperatures exceed T_g. The polymer soft segment T_g was observed at a temperature slightly higher than its starting oligomer also revealed the anchoring effect of hard segments.

Such pure phase separation as judged by DSC results have never been observed in the literature on polyurethane elastomers, even with PEUU's based on PTMO-2000 oligomer. It is speculated that the incorporation of DCA unit to the hard segment increased the solubility parameter difference between two phases. The contribution from hydrogen bonding on the phase separation may not be as significant in this system due to the presence of bulky groups next to the urethane linkages and is expected to greatly reduce the efficiency of hydrogen bonding. Further work was not continued due to the concerns of polymer thermal stability at high temperature.

d. Silanol Chain Extended PEUU's.

Figure 3.25 demonstrates the low temperature DSC behavior of silanol chain extended PEUU's of different hard segment contents based on the PTMO-2000. Again, an almost unchanged T_g of PTMO, when compared with the starting oligomer indicates that a good phase separated system was obtained. Certainly, it is of interest that to compare this series of polymer with similar PEUU's prepared previously by using carbamate-isocyanate interaction as already shown in Figure 3.20. The most noticeable difference comes from the location of melting endotherms. In the silanol chain extended series, the highest T_m was obtained on the sample with the lowest hard segment content. However, this trend was observed to be reversed in the case of PEUU's prepared by using carbamate-isocyanate interaction.

This difference may be viewed from the polymer chemical structure point of view. As mentioned previously, the MDI-urea hard segment structure is linear in the silanol

extended materials, while it contains some branching in PEUU's prepared by using carbamate- isocyanate interaction. A linear chain with MDI-urea type structure is expected to be more crystallizable than its branched forms. The crystallization of hard segment is thought to be one of the driving forces for a better phase separation. A relatively better phase separation is therefore assumed in PEUU's prepared by chain extension with silanol. When a good phase separation was assumed, larger PTMO crystallites may be produced in copolymers with higher soft segment content, due to the possibly smaller number of hard segment domains (i.e, smaller hard segment contents) which may restrict the soft segment mobility. On the other hand, phase separation is fairly good but may not be complete in branched PEUU's. The hard segment sequence length and urea concetration are increased with the hard segment content. The phase separation may be more effective as the hard segment length and urea concentration increase due to possibly increased solubility parameter difference between two phases. Therefore, an increased soft segment T_m was observed with the hard segment contents in the branched PEUU's.

3.4.3.2. Thermomechanical Analysis (TMA)

Thermomechanical analysis is a technique in which the deformation of a substance is measured under nonoscillatory load as a function of temperature as the substance is subjected to a controlled temperature program.

a. PEUU's via carbamate-isocyanate interactions.

The penetrometer mode for the thermomechanical spectrum was utilized for these PEUU's to observe the transitions associated with the hard and soft segments. Figure 3.26 compares the TMA measurements of three representative copolymers with

different hard segment content. The primary transition near -70°C is ascribed to the soft segment glass transition. The hard segment transition is indicated to be composition dependent and varies from 200 to 250°C as the hard segment content is increased from 23 to 41% by weight. These results are consistent with the DSC data as shown previously. One significant feature of conventional polyurethane materials (e.g. Estane®) is that they soften at relatively low temperatures, about 100°C, as expected. By contrast, both the strength and the service temperatures have been dramatically improved in these PEUU's. The TMA response is also affected when the molecular weight of soft segment is varied for constant hard segment (see Figure 3.27). The PTMO-2000 based copolymers show the highest softening temperature while PTMO-650 is the lowest. Two reasons may be given for this observaton. First, better phase separation was observed on polymers with higher soft segment molecular weights as demonstrated by DSC. The dissolved soft segments in the hard segment domain act as a plasticizer, which significantly lowers the softening temperature. On the other hand, the effective interchain hydrogen bonding could also be reduced by phase mixing. Secondly, urea concentration is significantly higher in PTMO-2000 based PEUU's when compared with PTMO-650 based polymers. This not only affects the degree of phase separation but also the cohesiveness of the hard segment structure. In other words, a higher temperature is necessary to disrupt the hard segment domain of a PTMO-2000 based polymer in order to promote flow.

b. Silanol chain extended PEUU.

Typical TMA thermograms of PEUU's before and after the removal of PDPS are shown in Figure 3.28. Both samples revealed the soft segment T_g around -70°C and the softening of the hard segment that occurred at temperatures beyond 200°C.

Noteworthy features of these scans are the extensive phase separation in these samples as indicated by a low T_g, which is in good agreement with DSC results, and the broadness of rubbery plateau which indicated the possible service temperature range. The softening temperature of these PEUU's are comparable with those prepared by carbamate-isocyanate interaction.

There is only a minor difference at the high temperature end in terms of the thermomechanical behavior on samples before and after the removal of the PDPS side product. The onset softening temperature of the sample which contains PDPS seems to be about 30°C lower than the sample without PDPS. This is mostly due to the low molecular weight PDPS present in the polymer. As indicated by DSC (Figure 3.29), such low molecular weight PDPS melts at around 160°C which is significantly lower than the MDI-urea hard segment softening temperature.

3.4.3.3. Thermogravimetric Analysis (TGA)

The TGA experiments were also conducted in order to investigate whether PEUU basically has a higher thermal stability than the polyurethanes. The results shown in Figure 3.30 demonstrate that PEUU is perhaps about 30 - 40°C more thermally stable than polyurethane at the same soft segment molecular weight and hard segment content as judged by TGA. Since the other components are identical, we believe this must reflect differences between the butanediol carbamates and the polyurea hard segment systems.

3.4.3.4. Tensile Properties (Stress-Strain Analysis)

a. PEUU's via carbamate-isocyanate interactions.

The engineering stress-strain curves for segmented MDI based PEUU's are shown in Figure 3.31 and Figure 3.32. All curves are shown up to the fracture stress of the sample. The Young's modulus, ultimate tensile strength, and ultimate elongation were determined from these results and are listed in Table 3.5 for each sample.

In Figure 3.31, the stress-strain behavior for materials with different soft segment molecular weight but the same hard segment content are shown. The results indicate that the Young's modulus and the tensile strength in these samples increases as the hard segment length is increased. This can be explained on the basis of the increase in the hard segment length necessary to maintain the same hard segment content with increasing molecular weight of the soft segments. Increasing the block length not only increases the aspect ratio of the dispersed hard domains but also leads to a higher degree of order in the hard domain since this results in more urea linkages per hard segment unit. Although the sample PTMO-650-MDI-31-DCA has a higher density of the hard segment units, the pseudo multifunctional cross-links formed by the hard domains are shorter and likely weaker. As a consequence of these poorly defined hard domains, the sample PTMO-650-MDI-31-DCA exhibits lower mechanical strength.

The stress-strain behavior for PEUU's based on PTMO-2000 with varying hard segment contents is shown in Figure 3.32. It is indicated that the mechanical response of these materials is strongly affected when the hard segment content is raised from 23 to 41% by weight. The observed behavior can be explained on the basis of the introduction of a higher volume fraction of hard segments as well as a higher degree of order in the hard segment domains. The higher modulus and tensile strength with increasing hard segment content in these samples is also consistent with their greater urea content which results in more cohesive hard domains. The dotted lines in Figure

3.32 depict the Estane® control (PTMO-2000-MDI-BD-31) which has no urea linkages in the polymer backbone. This sample shows the lowest ultimate tensile strength. Clearly, the weaker interdomain secondary binding forces result in less cohesive hard domains, poor hard/soft phase separation which may limit the development of a three dimensional hydrogen bonding network.

b. Silanol chain extended PEUU's.

The stress-strain behavior of silanol chain extended PEUU's before and after the removal of PDPS is shown in Figure 3.33. Both samples show respectable ultimate tensile strength with an elongation of break at 800%, which implies that the polymer is a reasonable high molecular weight product.

The Young's modulus of the sample contains PDPS (before extraction) was initially expected to be higher than the same sample without PDPS (after extraction) since PDPS is a highly crystalline material which possibly acts as a filler in the polyurethane-urea matrix. However, a reverse trend was observed instead. The polymer which contains no PDPS is apparently stiffer than its counterpart. This may be due to the low molecular weight nature of the PDPS.

One interesting feature appeared when comparing the value of Young's modulus of PEUU's with the same composition prepared by using different type of chain extenders (e.g. PTMO-2000-MDI-31 series). It is noted that the PEUU's modulus increased in the order of chain extenders utilized, silanol (in Figure 3.33) > cumyl alcohol (CA, in Figure 3.32) > dicumyl alcohol (DCA, in Figure 3.31). This can be explained by comparing the chemical structure of polymers which has been discussed previously in section ***3.4.2***. The MDI-urea hard segment is more linear, while branched or even lightly crosslinked structure may result for the tertiary alcohols chain

extended polymers. Apparently, branch points or crosslink sites will not easily fit into a lattice so either of these will lead to smaller and more imperfect crystals. On the other hand, the MDI-urea hard segment of silanol chain extended PEUU is more crystallizable due to its linear characteristics. This may be attributed to the reason why the Young's modulus of silanol chain extended PEUU is significantly higher than the tertiary alcohols chain extended PEUU's with the same composition.

3.4.3.5. Dynamic Mechanical Analysis

Dynamic mechanical spectra were obtained to investigate the compositional dependence of the local scale motion as well as the cooperative segmental motion which may exist in these segmented polyurethane-urea copolymers. It was also of interest to determine the mechanical and thermal properties in light of the role of the variety of hydrogen bonding possibilities in these materials. Figure 3.34 and Figure 3.35 show the overall dynamic behavior in terms of storage modulus (E') and loss modulus (E") as a function of temperature. The transitions observed by dynamic mechanical testing are in good agreement with DSC results. Figure 3.34 demonstrates the effect of hard segment content for PTMO-2000 based polyurethane-ureas. A rubbery plateau, from the E' curves, is observed to be composition dependent and extends to 200^{o}C for 23% hard segment content material and over 250^{o}C for the sample with 41% hard segment content. The plateau modulus increases with hard segment content in the sample. An increase in the order of hard domains or in hard segment content results in the formation of a stiffer material which is reflected in the E' behavior. Interestingly, the plateau modulus in these polyurethane-ureas is nearly one

order of magnitude higher than the reported for a MDI/ED based PEUU with a similar hard segment content [3].

The secondary loss peak near -120°C is designated as the γ relaxation. This peak has been ascribed to the short chain motion of methylene sequences in PTMO soft segment [3]. The γ relaxation temperatures observed in these copolymers are in excellent agreement with the reported value (-120°C) at the same frequency for polyolefin systems. This indirectly suggests that the degree of phase separation achieved in these copolymers may be very high. This is expected because of the highly polar nature of the aromatic urea linkages that form the hard segments in these coplymers.

The primary relaxation observed near -55°C in the dynamic mechanical spectra at 110 Hz for these copolymers is designated as the α_a relaxation and has been assigned to the glass transition temperature of the soft segment [3]. On the high temperature side of the α_a peak, a mechanical dispersion is indicated as a shoulder near 0°C. This transition is designated as α_c and is related to the melting of crystalline for the PTMO soft segments.

The existence of δ relaxations in dynamic mechanical behavior has been observed for conventional MDI/BD based polyurethanes, and shown to be associated with the hard segments of the copolymer [34]. The high temperature relaxation near 200°C in the dynamic mechanical spectra has been attributed to the melting of the hard segment microcrystallites with urea linkages and this dispersion is designated as δ. An endotherm at these temperatures was also observed by DSC. The melting point of the poly-MDI-urea control is about 375°C as described in the experimental section, although we are not certain that this represents the value associated with very high

molecular weight components.

Figure 3.35 shows the dynamic mechanical behavior of segmented PEUU's as a function of PTMO molecular weight. The results indicate that α_a transition shifts to a lower temperature as the molecular weight of the soft segments is increased. This shift can be explained on the basis of a longer, more ordered and well defined domain structure which results when the molecular weight of the PTMO is increased at constant hard segment content. PTMO-650 and PTMO-1000 based PEUU,the α_c relaxation was not observed. The higher hard/soft segment mixing present in these systems may prevent the crystallization of the soft segments. The γ relaxations appear to be molecular weight dependent as they shift to low temperatures, for high molecular weight PTMO based PEUU's of the same hard segment content. This may indicate a higher degree of phase mixing as the molecular weight of the PTMO soft segment is lowered for the same hard segment content.

The length and extent of the rubbery plateau is also shown to depend on the molecular weight of the PTMO soft segment. The plateau modulus is higher for samples where PTMO-2000 is utilized as compared to samples where the soft segment molecular weight is lower. For PTMO-2000 based copolymers, better phase separation is obtained and enhanced physical cross-linking and/or filler effects dominate the properties. Additionally, for samples with the same hard segment content, the concentration of urea groups is higher for samples with higher PTMO molecular weight. This higher concentration of urea groups, provides strong hydrogen bonding which improves interdomain cohesion.

Similar dynamic mechanical data were obtained with PTMO-2900 based PEUU (Figure 3.36). No significant drop in storage modulus was observed until temperature

goes beyond 10°C. This is unexpected since it is known that PTMO-2900 based PEUU has a low glass transition temperature around -78°C (see Figure 3.19). There were at least one order of magnitude of storage modulus difference between the glassy state and the rubbery state as were observed on PEUU's based on shorter PTMO molecular weight (2000 or lower). However, this contradiction can be explained in conjunction with the first run DSC results on the same polymer, which is similar to the second scan shown in Figure 3.19. By comparing the ΔC_p values and those corresponding to the crystallization and melting peaks, it is apparently that the material may be highly crystalline at temperatures below its soft segment T_m. This was indicated by a higher value of ΔC_p associated with T_m. As the molecular weight of PTMO increases, the PTMO segments become more flexible in a rather clean soft phase and crystallization occured even at a fast cooling rate of 320°C/min to a temperature below its T_g. The amorphous content associated with the soft phase of PTMO-2900 based PEUU is believed to be low at subzero temperatures. This may be responsible for the observation of a small loss modulus peak at the low T_g.

Interestingly, an additional transition was observed at 170°C which was not found in the samples with shorter PTMO molecular weights. The rubbery plateau modulus was decreased somewhat at 170°C and returned to a similar level upon further heating. The polymer was completely melted at around 250°C. This behavior is very similar to that observed in a semi-crystalline material. The material becomes softer at T_g and the modulus may be increased when crystallization occured. To further confirm this speculation, DSC analysis was conducted on this sample and the result is shown in Figure 3.37. Unfortunately, no convincing T_g and T_c conclusions can be made. However, the endotherms appeared at around 250°C are likely due to the melting of

hard segment crystallites. If this is the case, it shows good agreement with the catastrophic drop in G' at 250°C.

3.5. CONCLUSION

Two new routes to urea linked polyurethane systems have been investigated. It has been shown that it is possible to synthesize novel polyurethane ureas by utilizing either the rearrangement characteristics of phenylcarbamate-isocyanate interactions at a sufficiently high temperature or the silanol modified water-extended method. FT-IR spectra show the urea linkages have been efficiently incorporated into the polymer backbone. From the spectroscopic point of view, there is basicallly no difference in structure among mono- and di- functional tertiary alcohol and silanol chain extended PEUU's. Thus, it strongly suggests these novel "chain extenders" are not directly involved in the chain extension step.

In the case of tertiary alcohols, carbamates forms with isocyanates tend to dissociate at high temperatures to give the corresponding amines. Phenyl substituted carbamates significantly reduce this temperature, probably by stabilizing the intermediate carbocation. The introduction of a suitable catalyst may also be greatly reduce this rearrangement temperature.

In the case of silanol chain extended system, molecularly dispersed water was introduced through the self-condensation of silanols. The water thus generated converts isocyanate to urea. By using this approach, water can be efficiently and quantitatively introduced to the reaction without the immiscibility problems which are

usually encountered in conventionally water-extended PEUU system. More interestingly, if a disilanol was utilized and can be converted to high molecular weight material in the polyurethane medium, a new multiphase polyurethaneurea/polysiloxane network can be formed in situ.

By using these approaches, the hard segment in the copolymer will be totally derived from the diisocyanates. Althought one is suspicious that some branching may be present in the PEUU synthesized by carbamate-isocyanate interactions, the amount of branching is believed to be small on the basis of model compound studies described in Chapter 2.

Good agreement with dynamic mechanical measurements was observed for DSC and TMA results as well. The PEUU's based on PTMO-2000 exhibited a much higher upper temperature relaxation than the PEUU's based on PTMO-1000 and PTMO-650 or the control polyurethane. This is also reflected by a much lower soft segment T_g in the PEUU-2000 series. This has no doubt reflected some significant differences in phase separation as well as possible sequence length effect in the hard segment.

The mechanical properties were observed to depend primarily on the degree of order in the hard domains. It was shown that this order can be improved by increasing either the hard segment content at constant molecular weight of the soft segment or soft segment molecular weight at the same hard segment content. Both approaches increase the concentration of urea linkages in the PEUU's and hence the tensile properties. At comparable hard segment content, all materials indicated superior mechanical strength over polyether-urethane controls chain extended with butanediol.

REFERENCES

1. K. Hepburn, "Polyurethane Elastomers", Halstead Press, New York (1982).
2. H. Ishihara, I. Kimura, K. Saito, and H. Ono, J. Macromol. Sci., Phys. Ed., B 10(4), 591 (1974).
3. C.B. Wang, S.L. Cooper, Macromolecules, 16, 775(1983).
4. K. Nakayama, T. Ino, and I. Matsubara, J. Macromol. Sci., Chem. Ed., A3(5), 1005 (1969).
5. H. Suzuki and H. Ono, Bull. Chem. Soc., Japan, 43, 682 (1970).
6. V.A. Khransovskii, Polym. Sci. USSR, 22(6), 1516 (1980).
7. C.S.Paik Sung, C.B. Hu, and C.S. Wu, Macromolecules, 13, 111 (1980).
8. C.S.Paik Sung, T.W. Smith, and C.S. Wu, Macromolecules, 13, 117 (1980).
9. C.S.Paik Sung, andC.B. Hu, Macromolecules, 14, 212 (1981).
10. I. Kimura, H. Ishihara, H. Ono, N. Yoshihara, N. Nomura, and H. Kawai, Macromolecules, 7, 355 (1974).
11. H. Ishihara, I. Kimura, K. Saito, and H. Ono, J. Macromol. Sci., Phys. Ed., B 22, 713 (1983).
12. C.B. Hu, R.S. Ward, Jr., and N.S. Schneider, J. Appl. Polym. Sci., 27, 2167 (1982).
13. R.E. Lyon, D.X. Wang, R.J. Farris, and W.J. Macknight, J. Appl. Polym. Sci., 29, 2857 (1984).
14. A. Takahara, J.I. Tashita, T. Kajiyama, and W.J. Macknight, Polymer, 26, 978 (1985).
15. A. Takahara, J.I. Tashita, T. Kajiyama, and W.J. Macknight, Polymer, 26, 987 (1985).
16. R. Bauart, L. Mobitzer, and H. Rinke, Kolloid-Z. Z. Polym., 240, 807 (1970).

17. V.A. Khranovskii and L.P. Gul'ko, J. Macromol. Sci., Phys. Ed., B22(4), 497 (1983).

18. V.A. Khranovskii and L.P. Gul'ko, J. Polym. Sci., USSR. 25(1), 123 (1983).

19. G.S. Skuches and P.S. Carleton, J. Appl. Polym. Sci., 29, 3431 (1984).

20. V.N. Kotrelev, D.A. Kochkin, S.P. Kalinina, and V.V. Borisenko, J. Appl. Chem., USSR (Engl. Transl.), 31(6), 944 (1958).

21. W. Noll, "Chemistry and Technology of Silicones", Academic Press, New York (1968).

22. W. Siefken, Annalen, 562, 75 (1949).

23. M. Chono, S. Fukuoka, and M. Kohno, J. Cellular Plastics, 385 (1983).

24. E.G. Arnold, J.A. Nelson, and J.J. Verbanc, J. Chem. Educ., 34(4), 158 (1957).

25. S. Patai, "The Chemistry of Cyanates and Their Thio Derivatives", Part I and II, The Chemistry of Functional Group Series, John Wiley & Sons, New York (1977).

26. C.D. Eisenbach, "Synthesis and Properties of Model Urethane Oligomers and Monodisperse Soft Segments for Segmented Polyurethanes", Workshop on the Structure of Polyurethane Elastomers, Brighton, Mass. (1984).

27. W.J. Farrissey, L.M. Alberino, and A.A.R. Sayigh, Polymers from Unconventional Reactions of Isocyanates, J. Elast. Plast., 7, 285 (1975).

28. S.L. Reegan and K.C. Frisch, "Catalysis in Isocyanate Reactions". Adv. Urethane Sci. Technol., 1, 1 (1971).

29. L.R. Brecker, Plast. Engr., 33(3), 39 (1977).

30. J.H. Saunders, "Elastomers by Condensation Polymerization, A. Polyurethane Elastomers" in "High Polymers", Vol. 23, Part 2, John Wiley & Sons, New York

(1969).

31. J.H. Saunders and K.C. Frisch, "Polyurethanes: Chemistry and Technology", Vols. I and II, Interscience, New York (1962).
32. M. Windholz, Ed., "The Merck Index, An Encyclopedia of Chemicals, Drugs, and Biologicals", 10 th. Ed., Merck & Co., Inc., Rahway, N. J. (1983).
33. Y. Camberlin and J.P. Pascault, J. Polym. Sci., Chem. Ed., 21, 415 (1983).
34. H.N. Ng, A.E. Allegrezza, R.W. Seymour, and S.L. Cooper, Polymer, 24, 255 (1973).
35. B. Lee, M.S. Thesis, Virginia Polytechnic Institute and State University (1985).

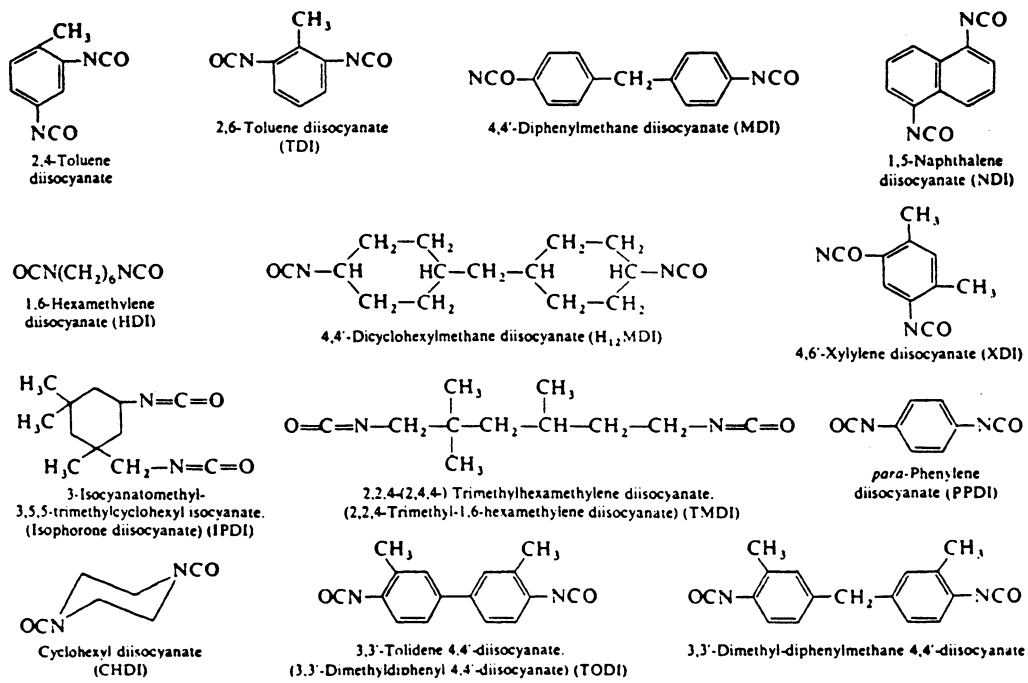

FIGURE 3.1. Structure Formulae of diisocyanates used in Polyurethane Elastomer Synthesis.

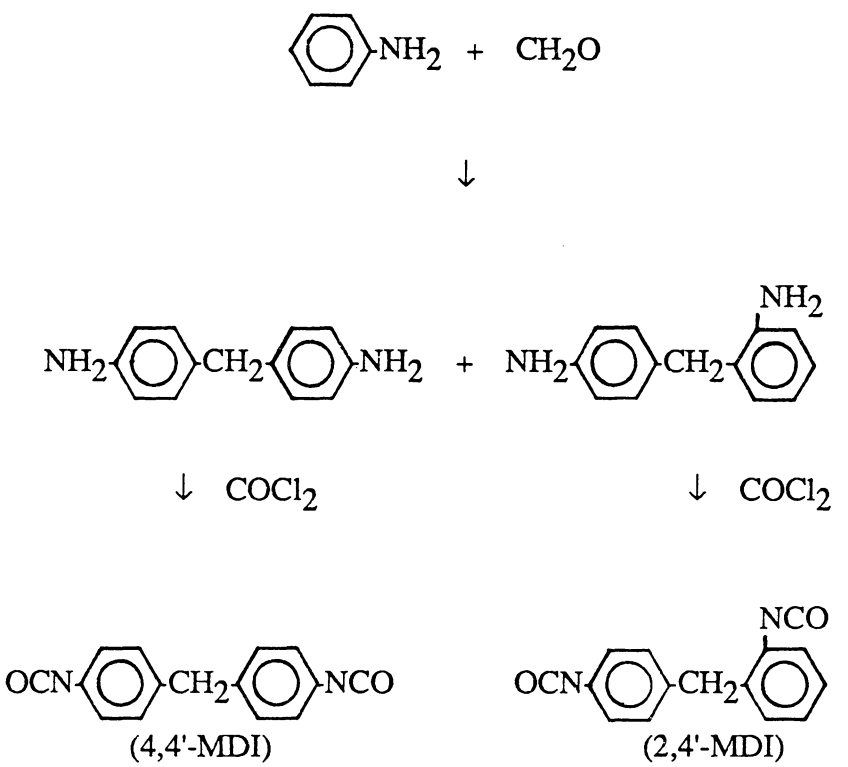

FIGURE 3.2. Synthesis of MDI Through Phosgenation Route.

1. CARBONYLATION

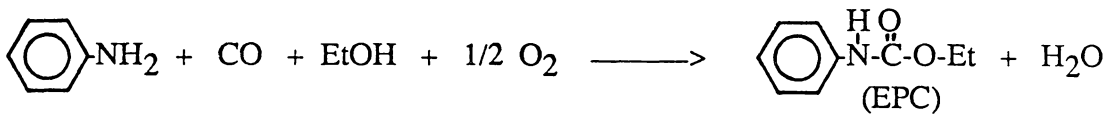

2. CONDENSATION

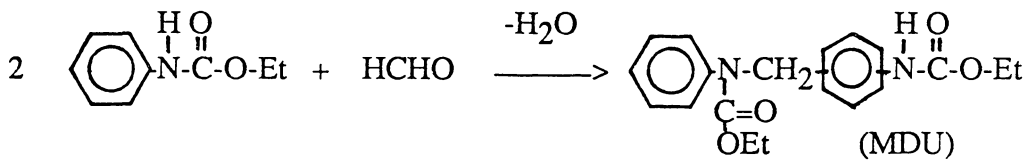

3. INTERMOLECULAR TRANSFER REACTION

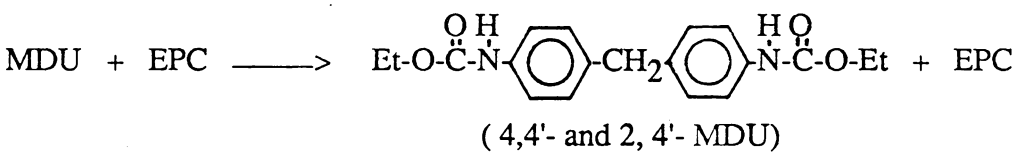

4. DECOMPOSITION

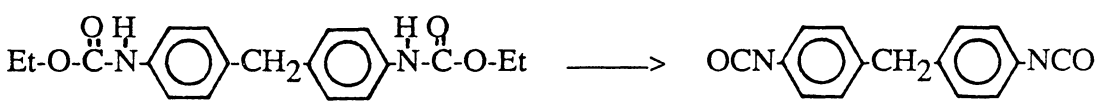

FIGURE 3.3. MDI Synthesis By Asahi Chemical Co. Process.

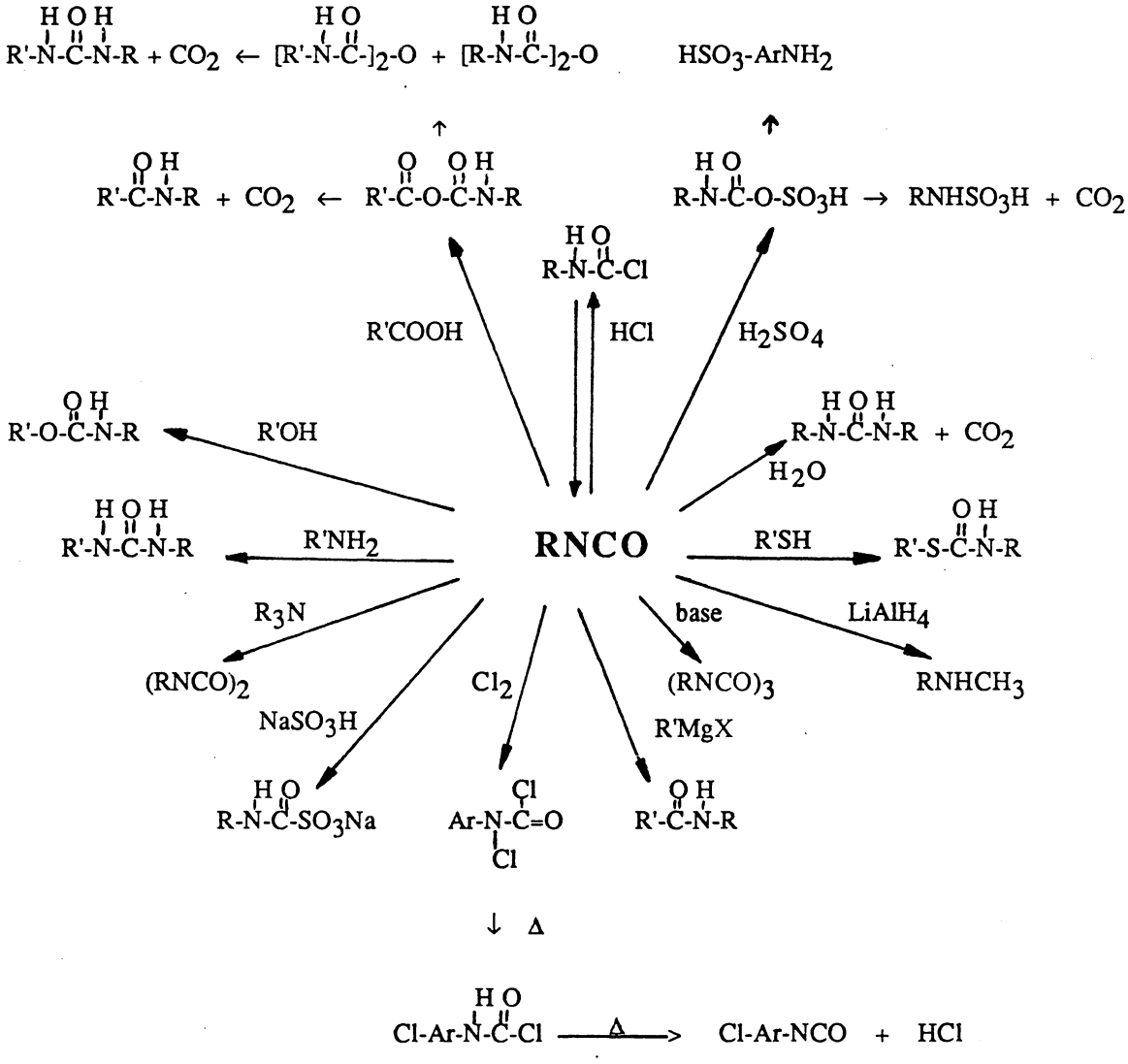

FIGURE 3.4. Typical Isocyanate Reactions.

1. Capping Reaction

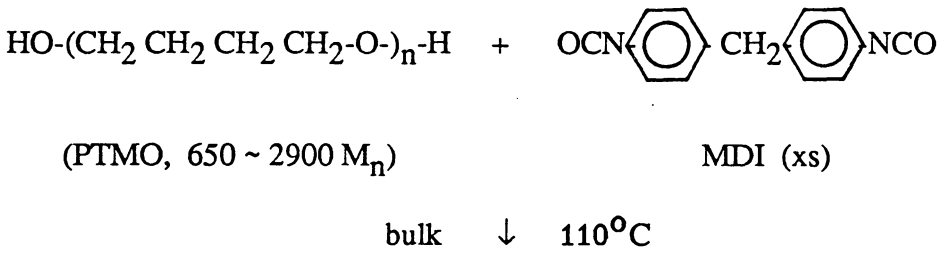

2. Chain Extension with CA or DCA

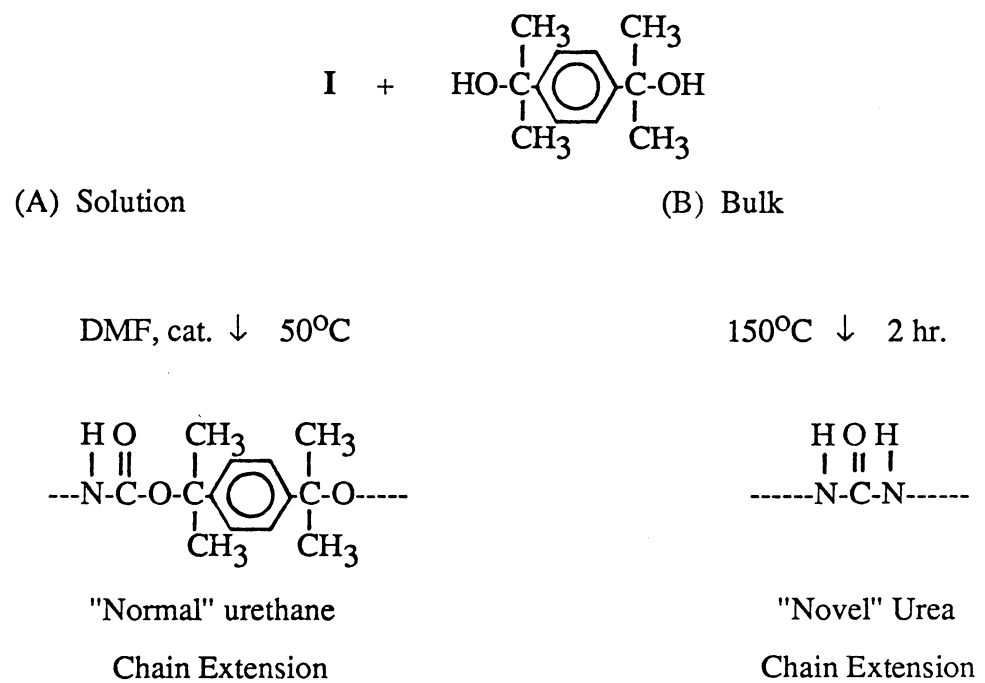

FIGURE 3.5. Reaction Scheme of Di-Tertiary Alcohol Chain Extended Polyurethanes.

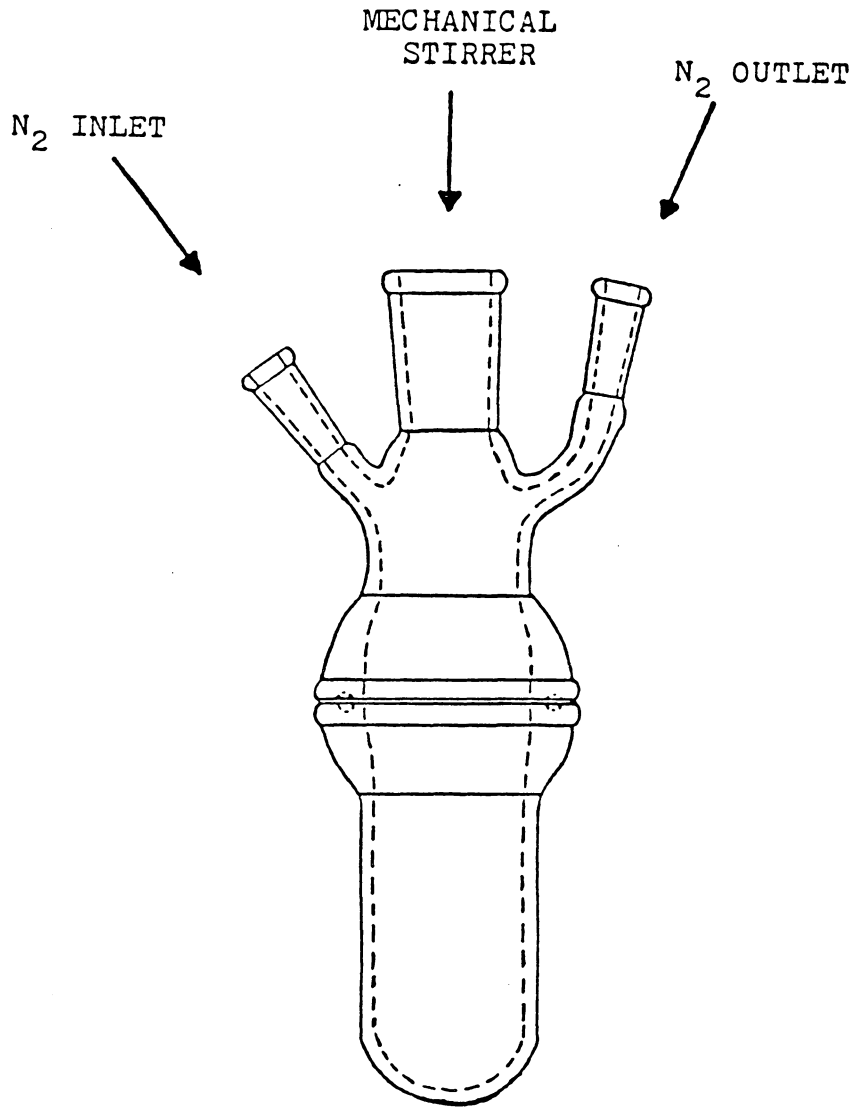

FIGURE 3.6. Reaction Set-Up for PEUU Synthesis.

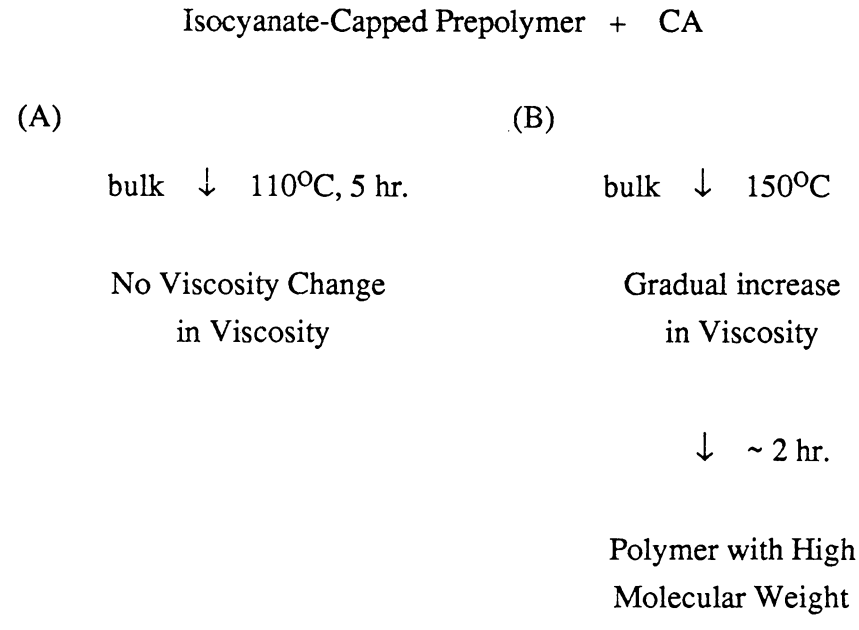

FIGURE 3.7. Temperature Effects on the Chain Extension Reaction.

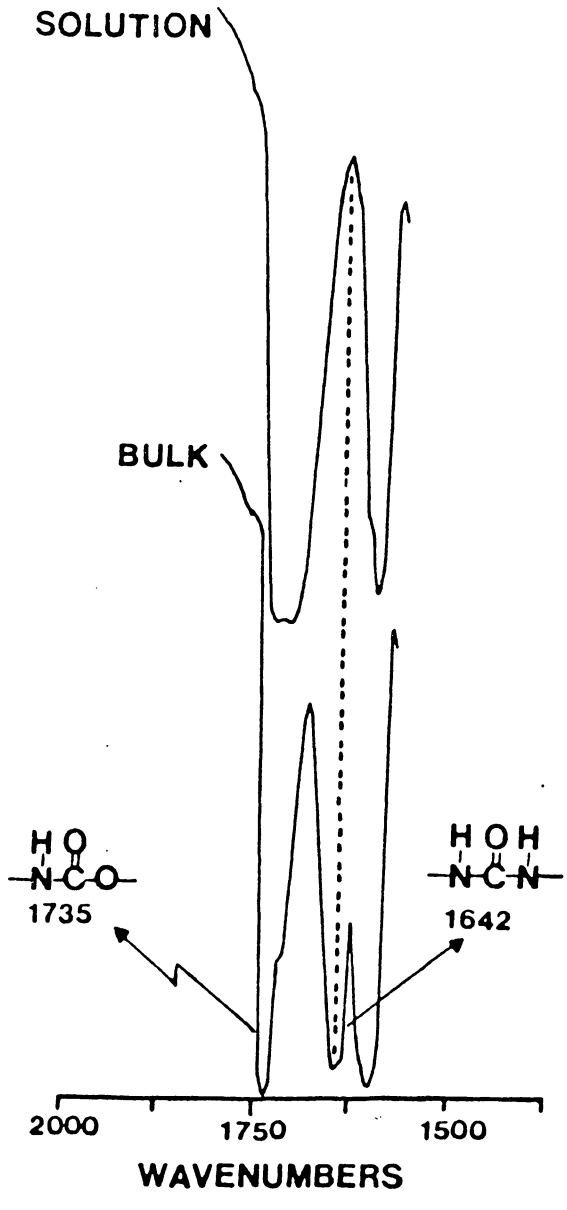

FIGURE 3.8. FT-IR Spectra of DCA Chain Extended Polyurethanes Prepared at Different Conditions.

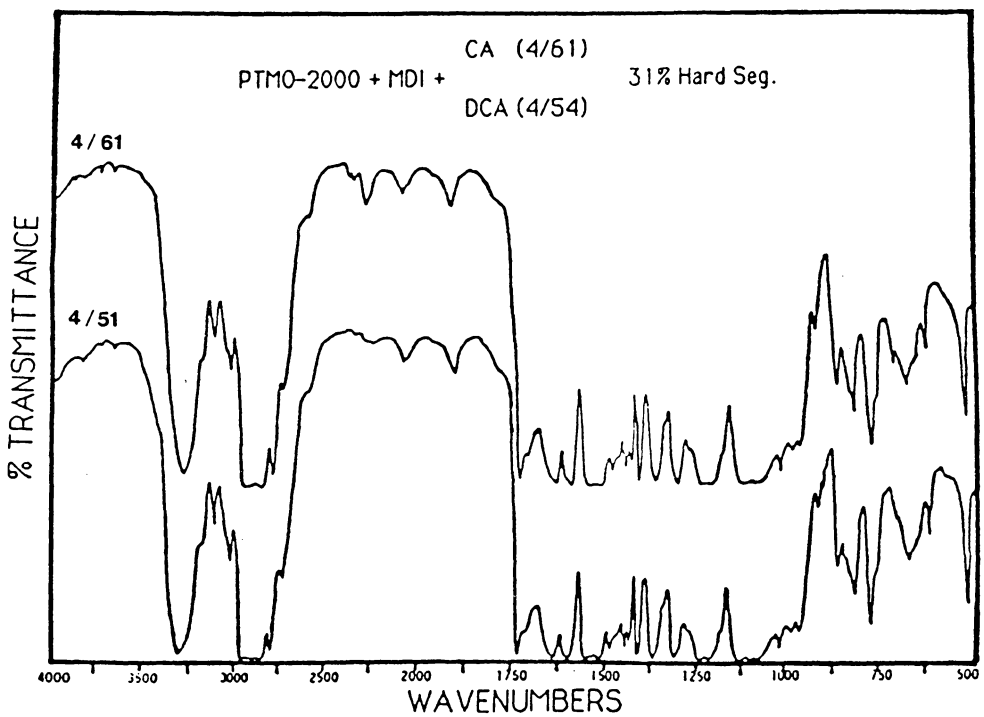

FIGURE 3.9. FT-IR Spectra of Mono- and Di- Tertiary Alcohols Chain Extended PEUU's.

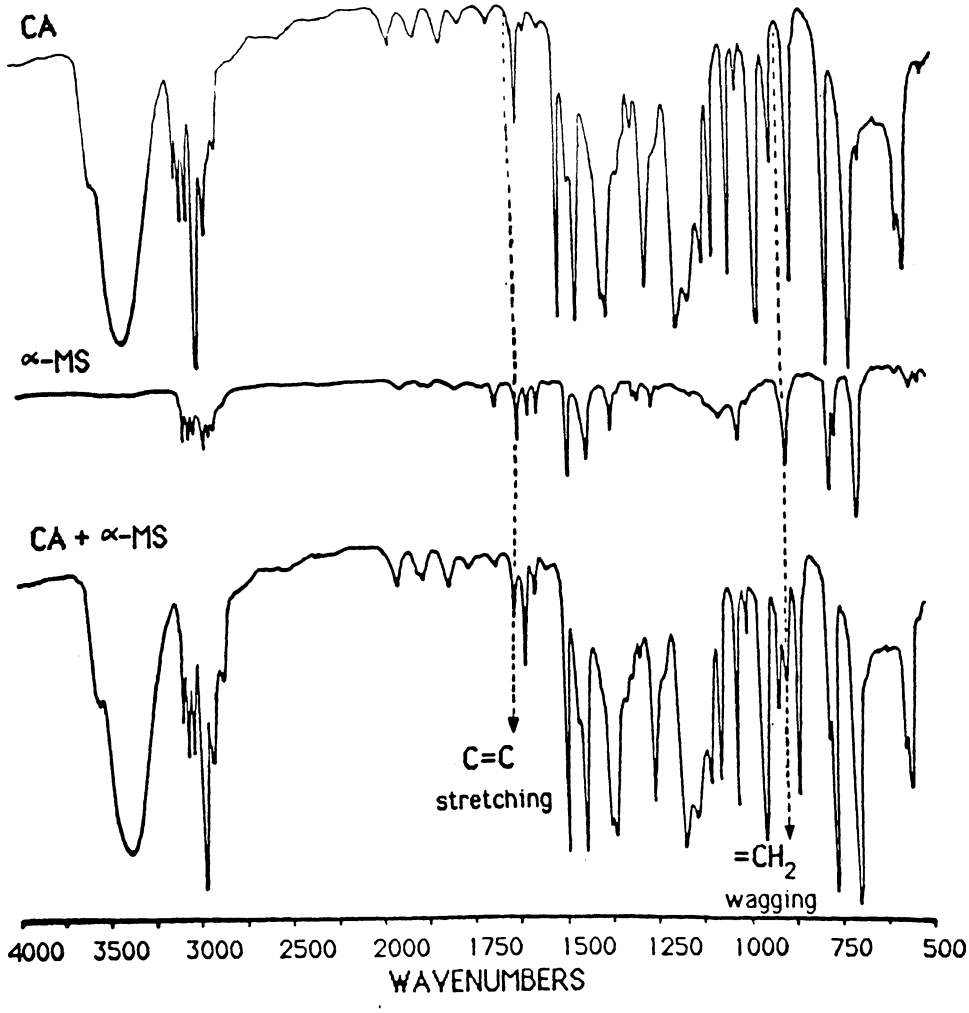

FIGURE 3.10. Evidences for the Olefin Formation.

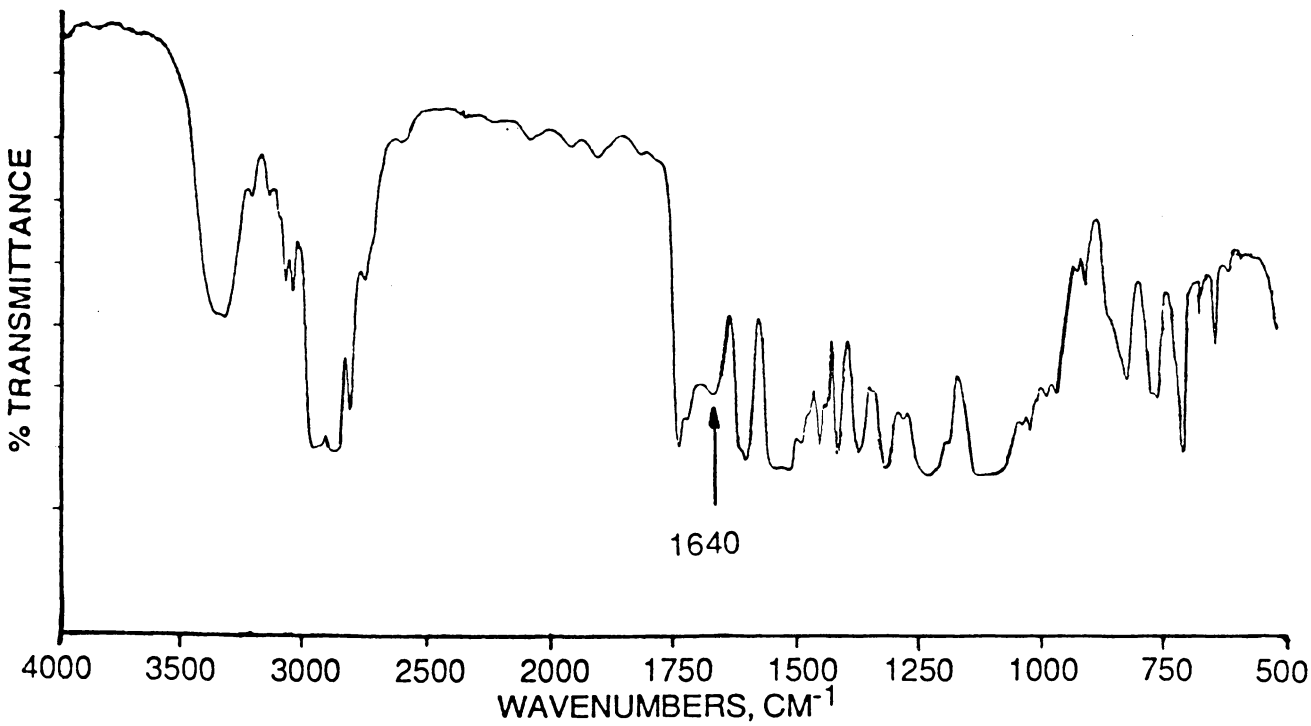

FIGURE 3.11. FT-IR Spectrum of TPM Chain Extended PEUU.

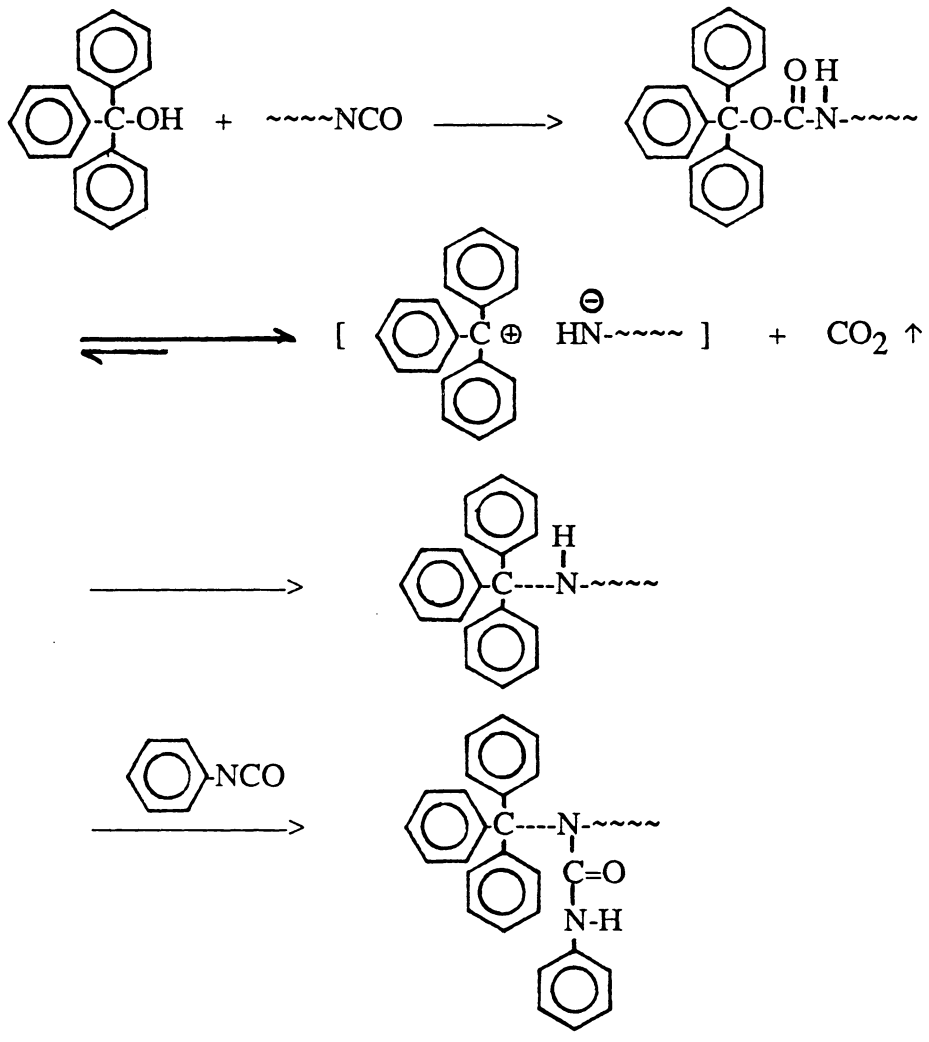

FIGURE 3.12. The Possible Route for the Urea Formation in TPM Chain Extended System.

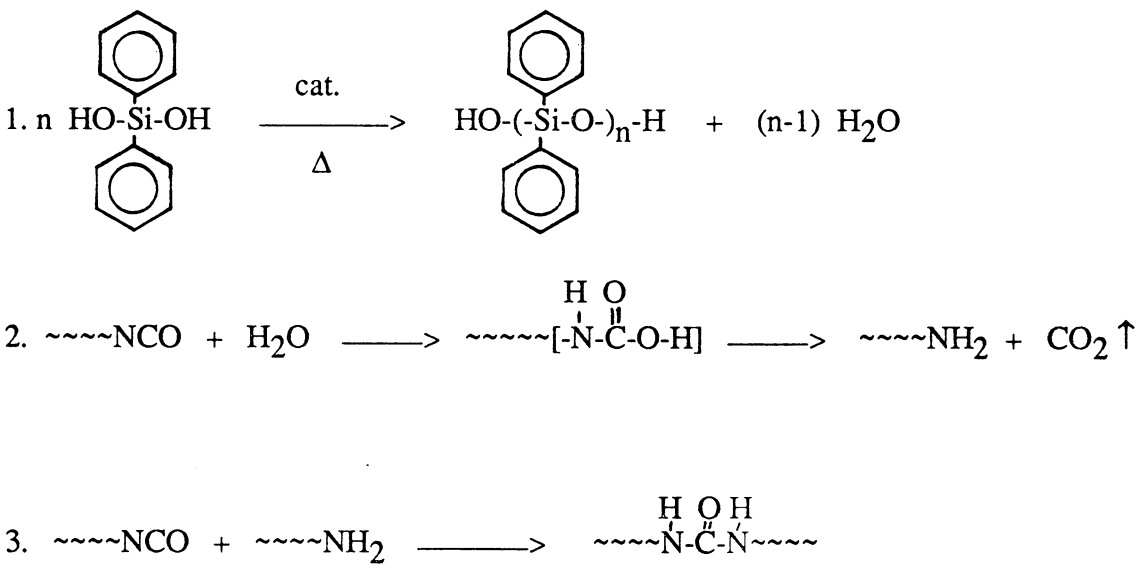

FIGURE 3.13. Proposed Urea Formation Mechanism in DPSOL Chain Extended System.

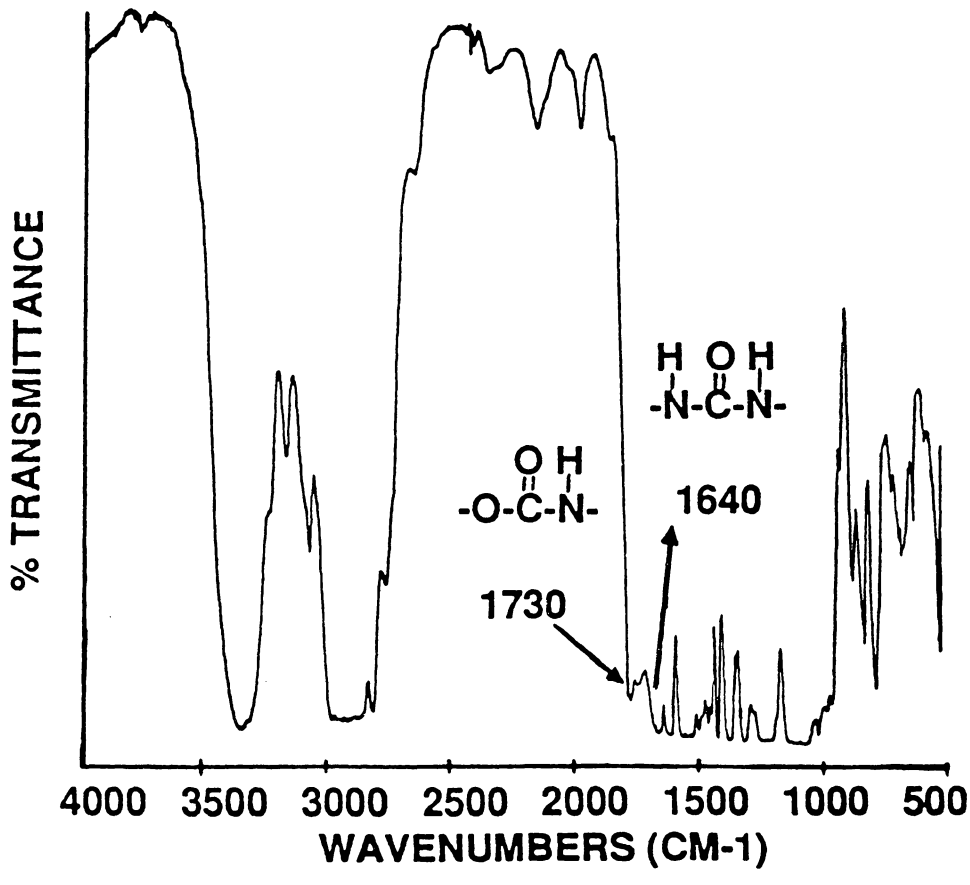

FIGURE 3.14. FT-IR Spectrum of DPSOL Chain Extended PEUU.

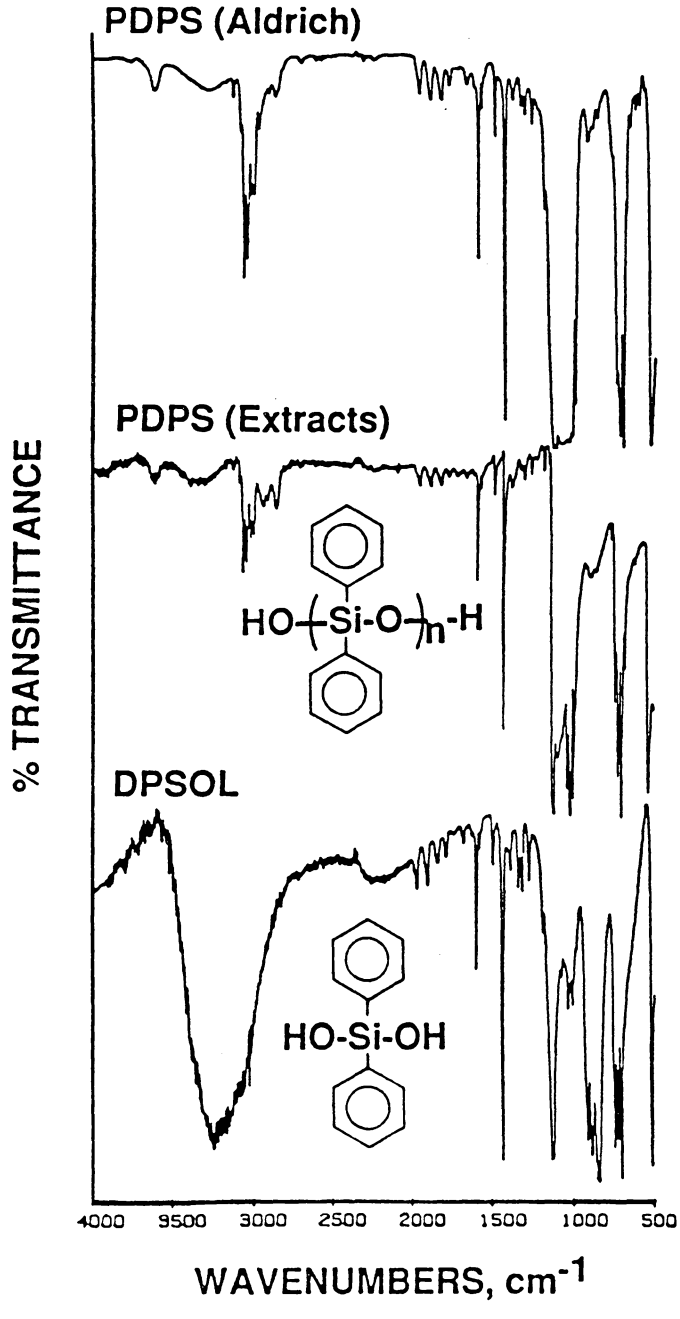

FIGURE 3.15. FT-IR Spectra of PDPS (Aldrich), PDPS (Extracts), and DPSOL.

Before Extraction

After Extraction

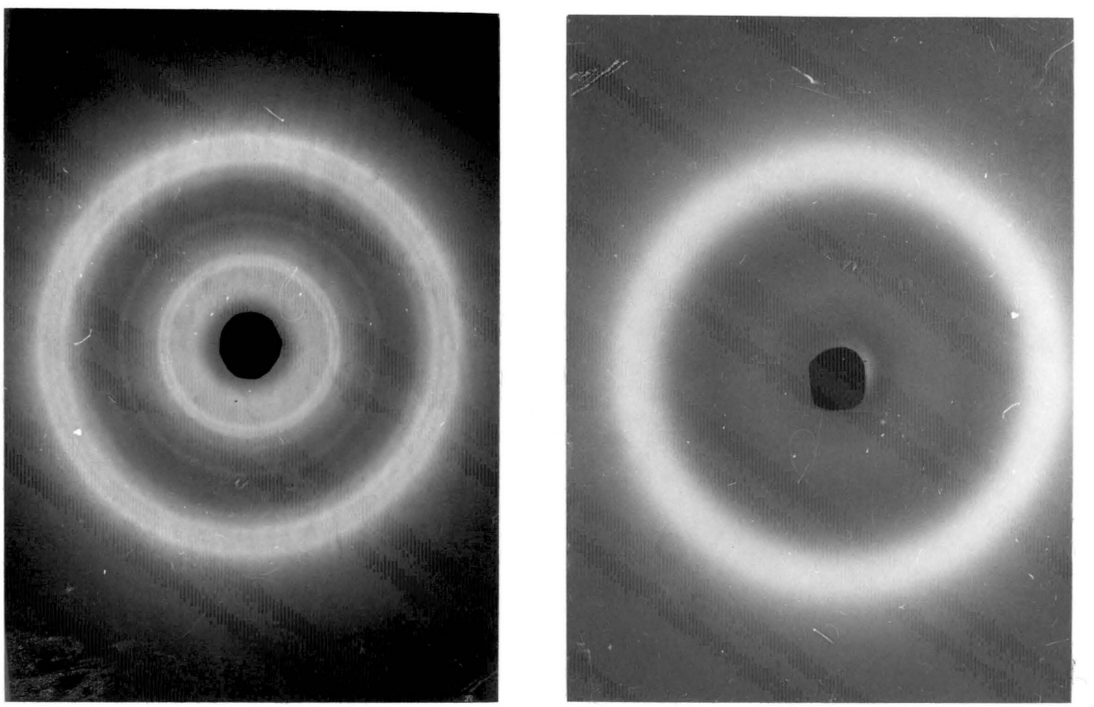

FIGURE 3.16. Wide-Angle Diffraction Patterns for PEUU's Before and After the Removal of PDPS.

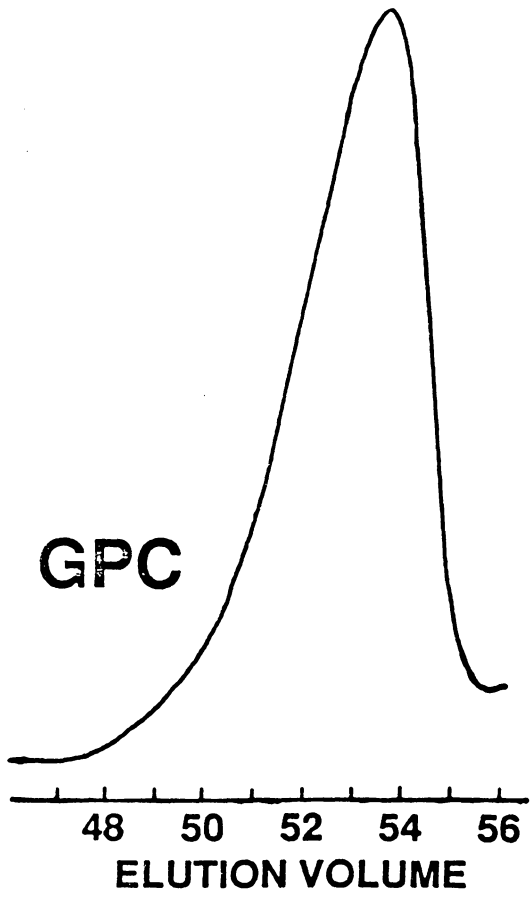

FIGURE 3.17. GPC Trace of The PDPS Extracts.

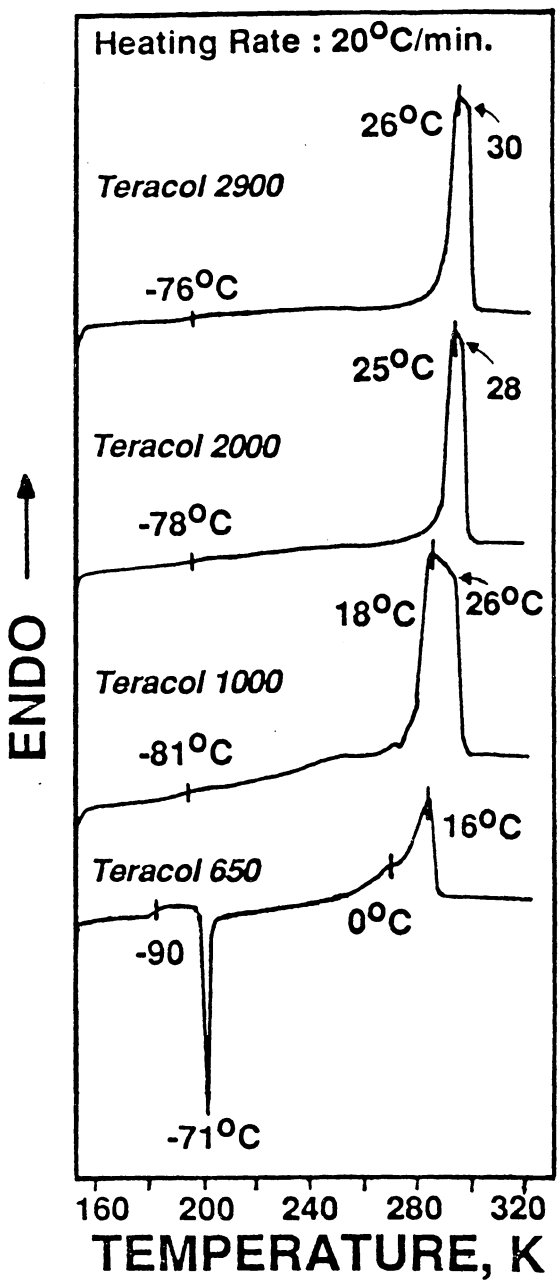

FIGURE 3.18. Low Temperature DSC (2nd runs) Characteristics of Teracol® Polyether Polyols.

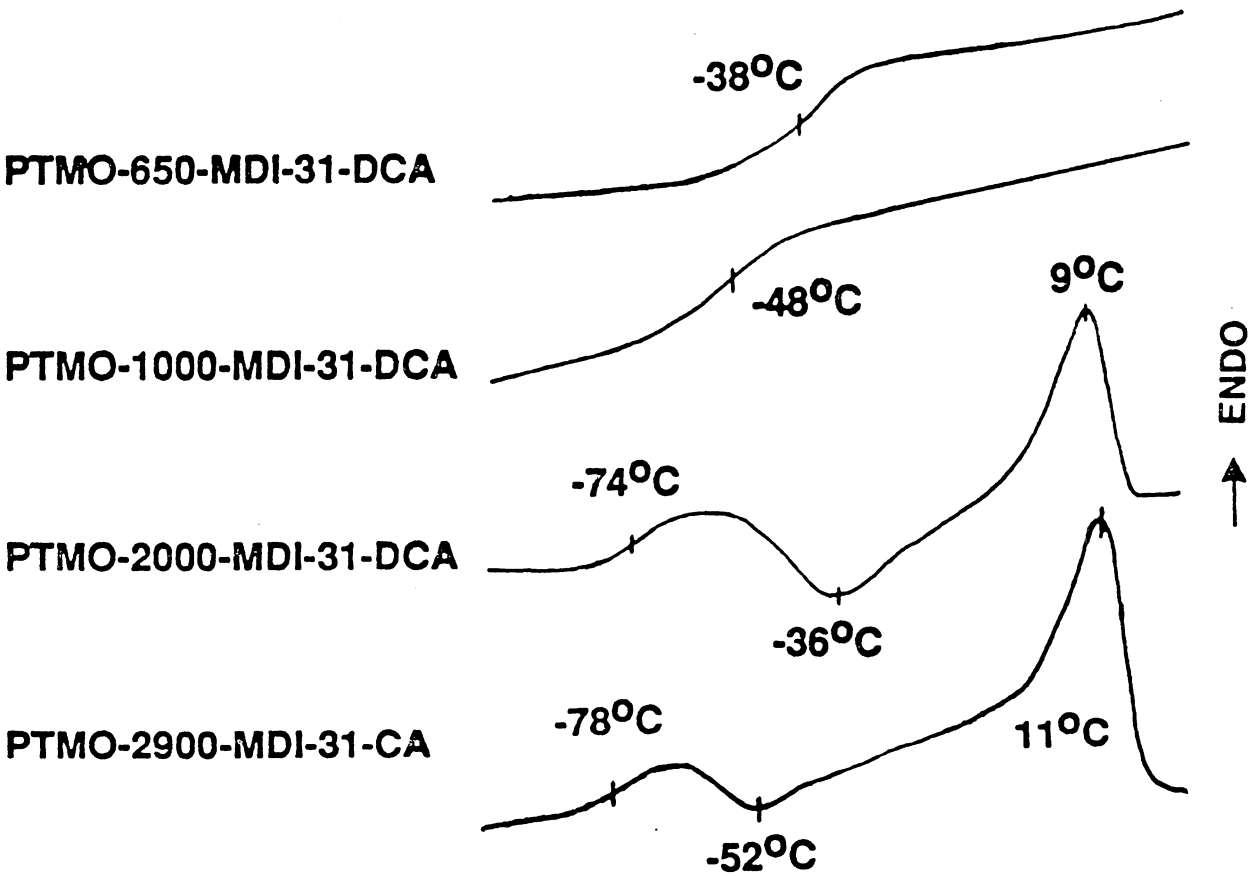

FIGURE 3.19. DSC Scans of PEUU's Based on Different Soft Segment Length.

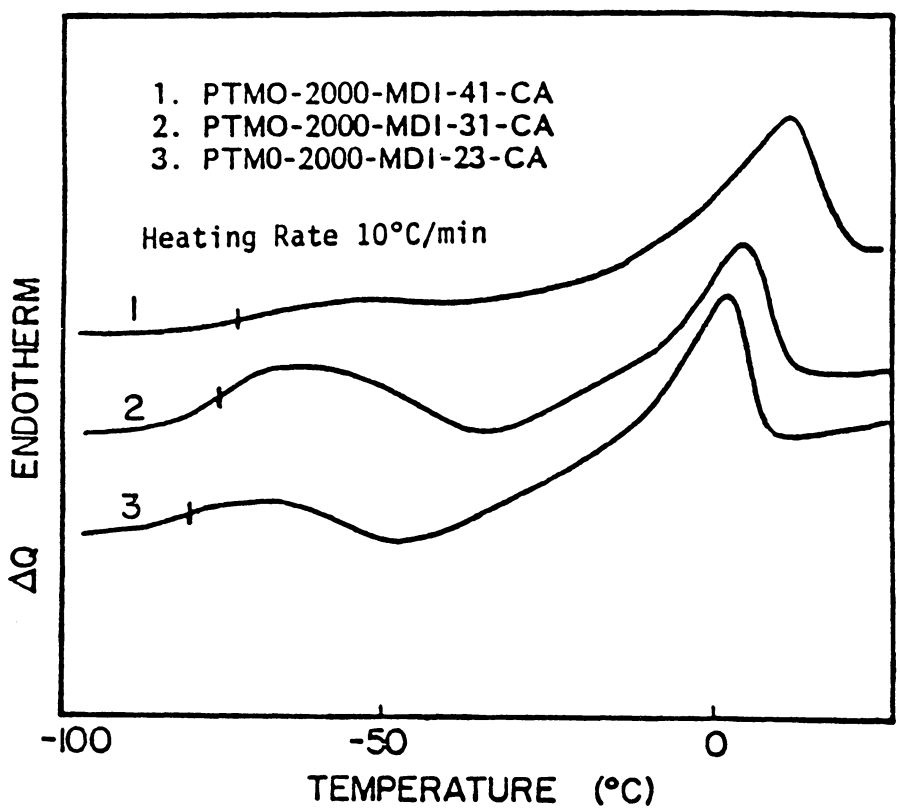

FIGURE 3.20. DSC Scans of PTMO-2000 Based PEUU's with Various Amount of Hard Segment Content.

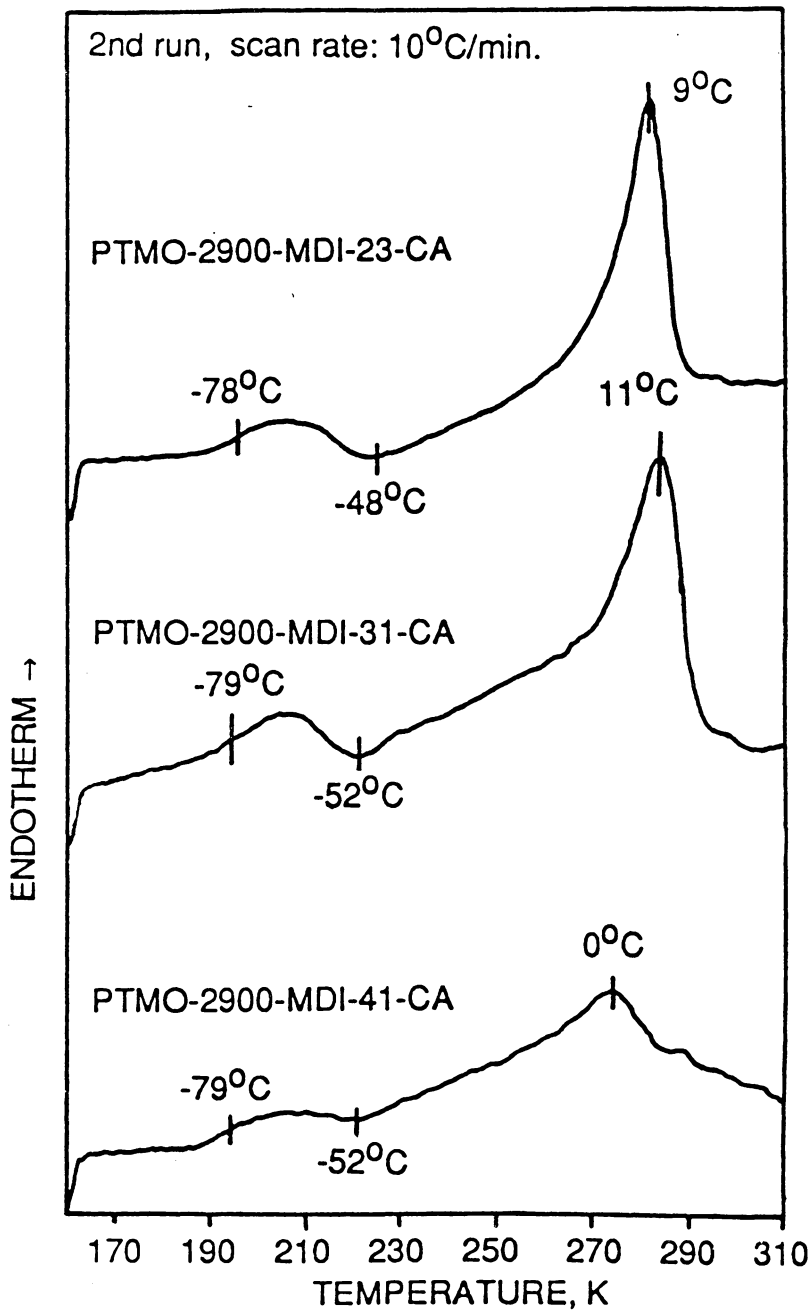

FIGURE. 3.21. DSC Scans of PTMO-2900 Based PEUU's with Various Hard Segment Content.

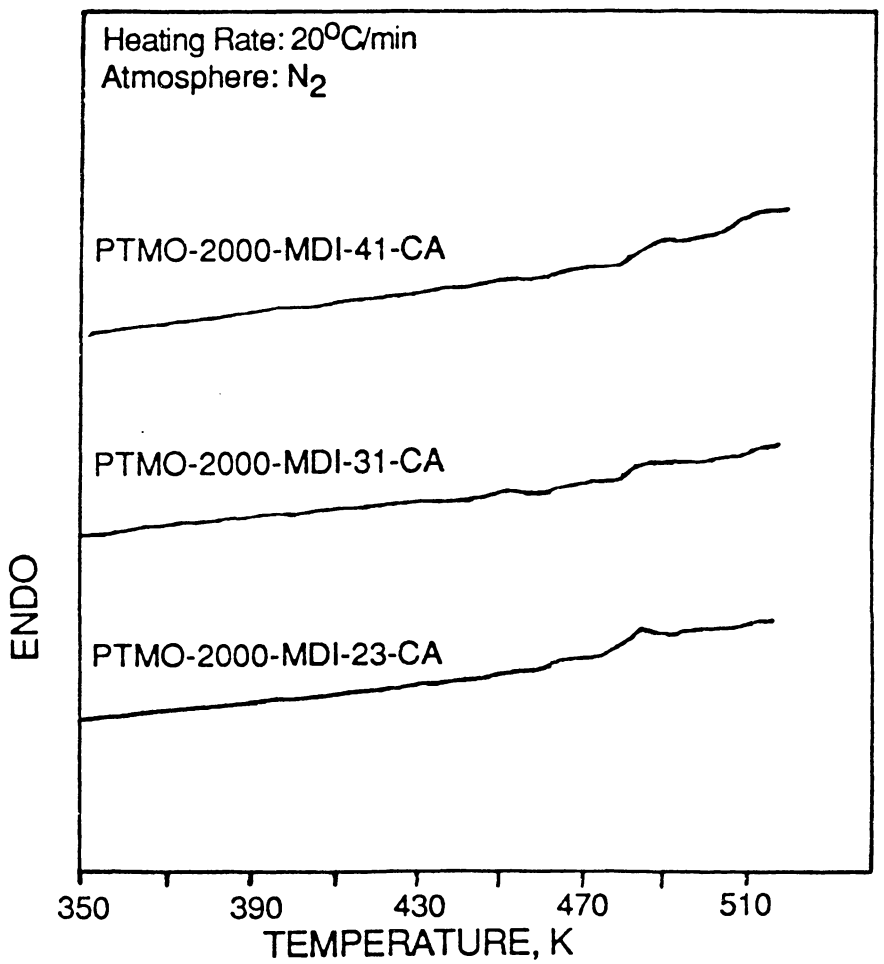

FIGURE 3.22. High Temperature DSC Characteristics of PTMO-2000 Based PEUU's with Various Hard Segment Content.

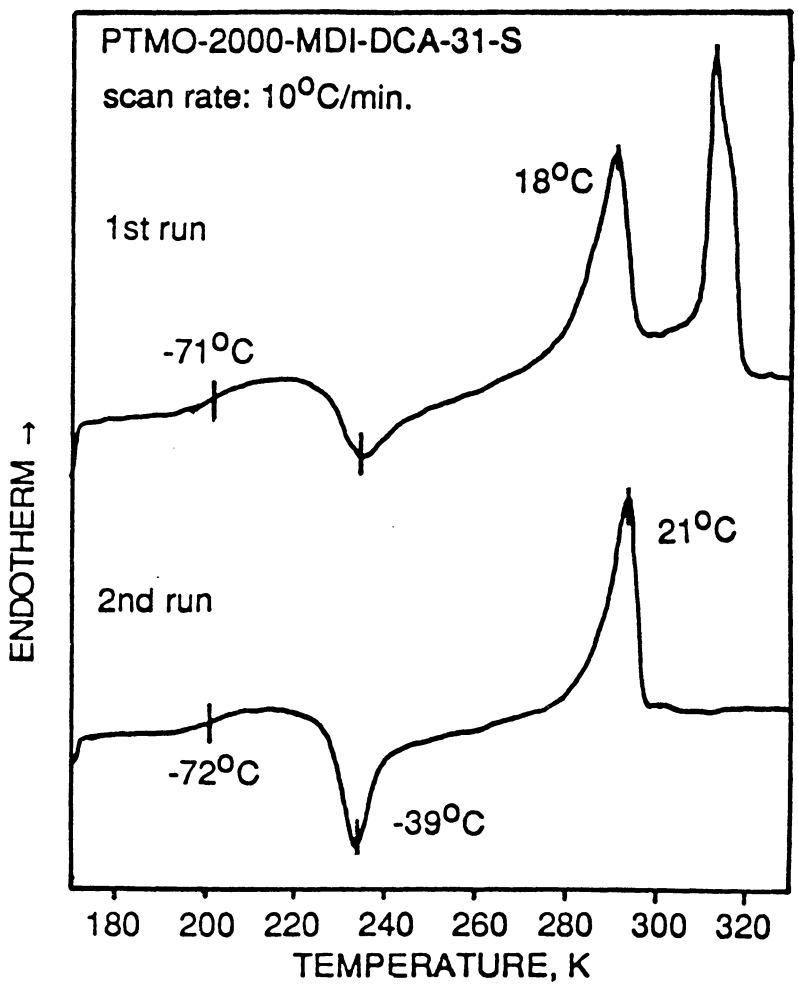

FIGURE 3.23. Thermal History Dependence of Solution Polymerized DCA Chain Extended Polyurethane on Low Temperature DSC Behaviors.

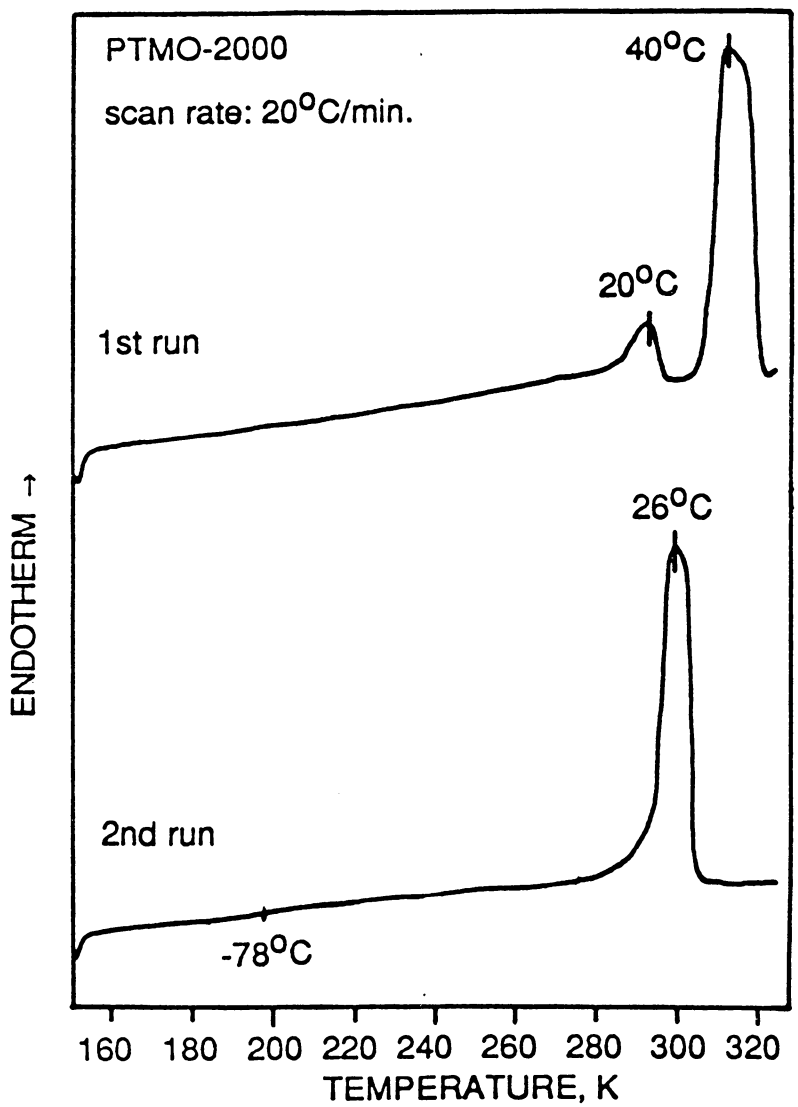

FIGURE 3.24. First and Second Run of Low Temperature DSC Scans of PTMO-2000.

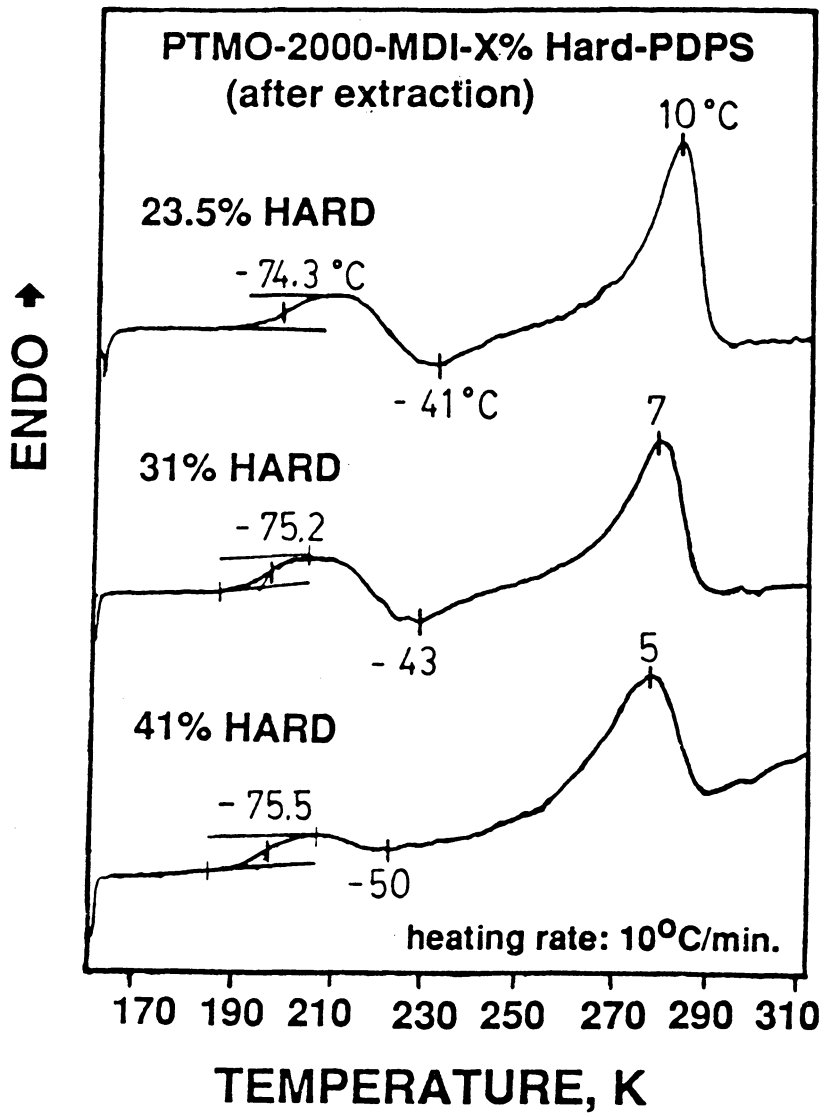

FIGURE 3.25. Low Temperature Behaviors of Silanol Chain Extended PEUU's with Various Hard Segment Content.

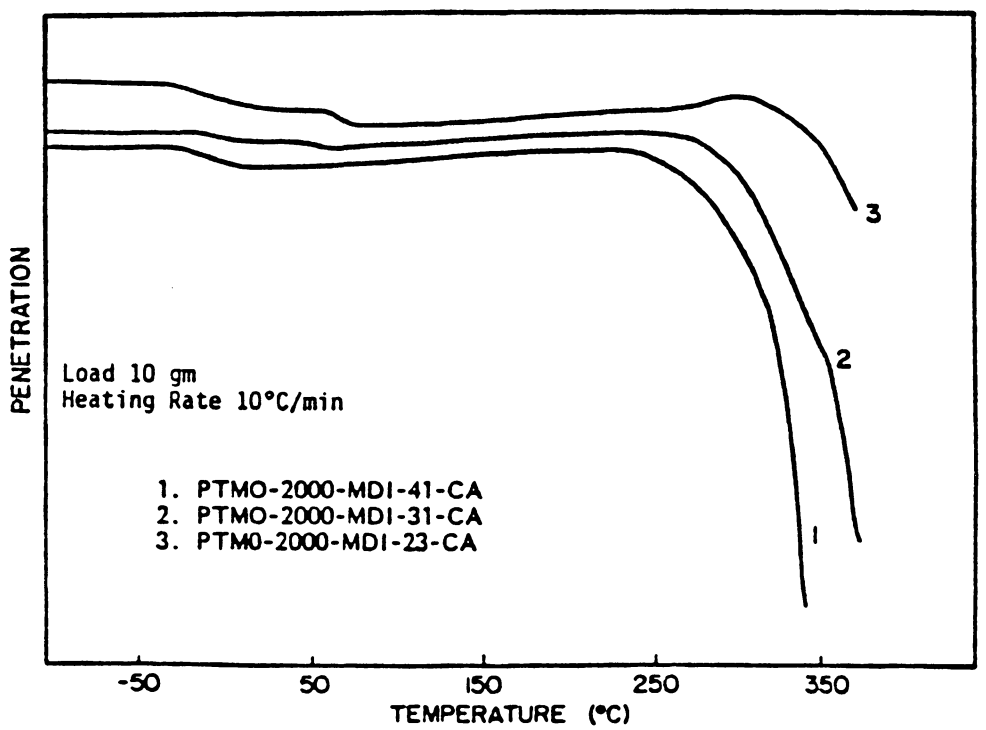

FIGURE 3.26. TMA Spectra of PTMO-2000 Based PEUU's with Various Hard Segment Content.

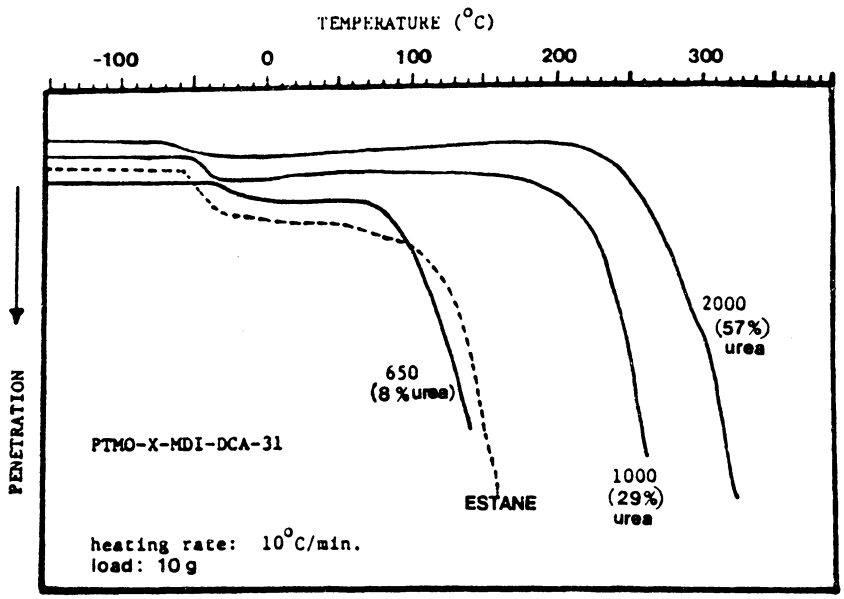

FIGURE 3.27. TMA Spectra of PEUU's Based on Different Soft Segment Length.

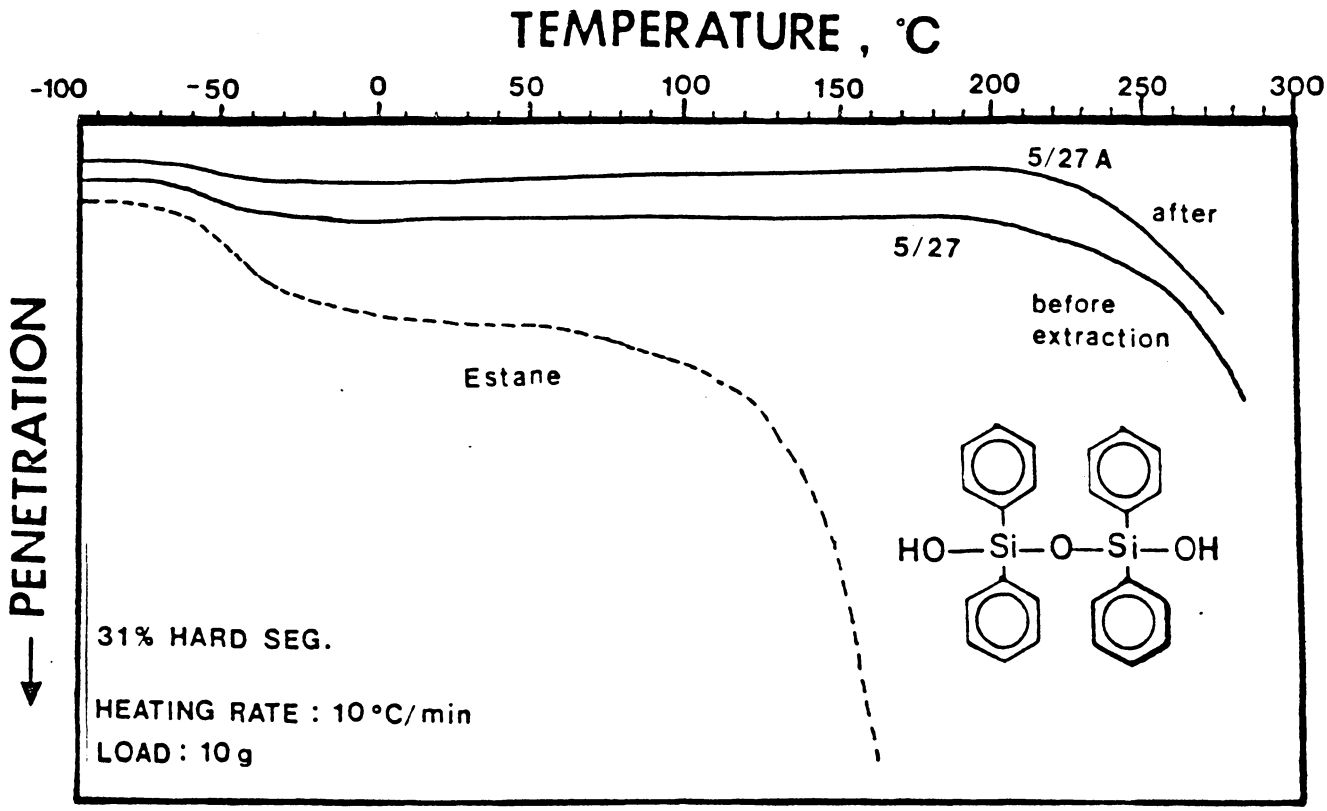

FIGURE 3.28. TMA Spectra of Silanol Chain Extended PEUU's (Before and After Extraction).

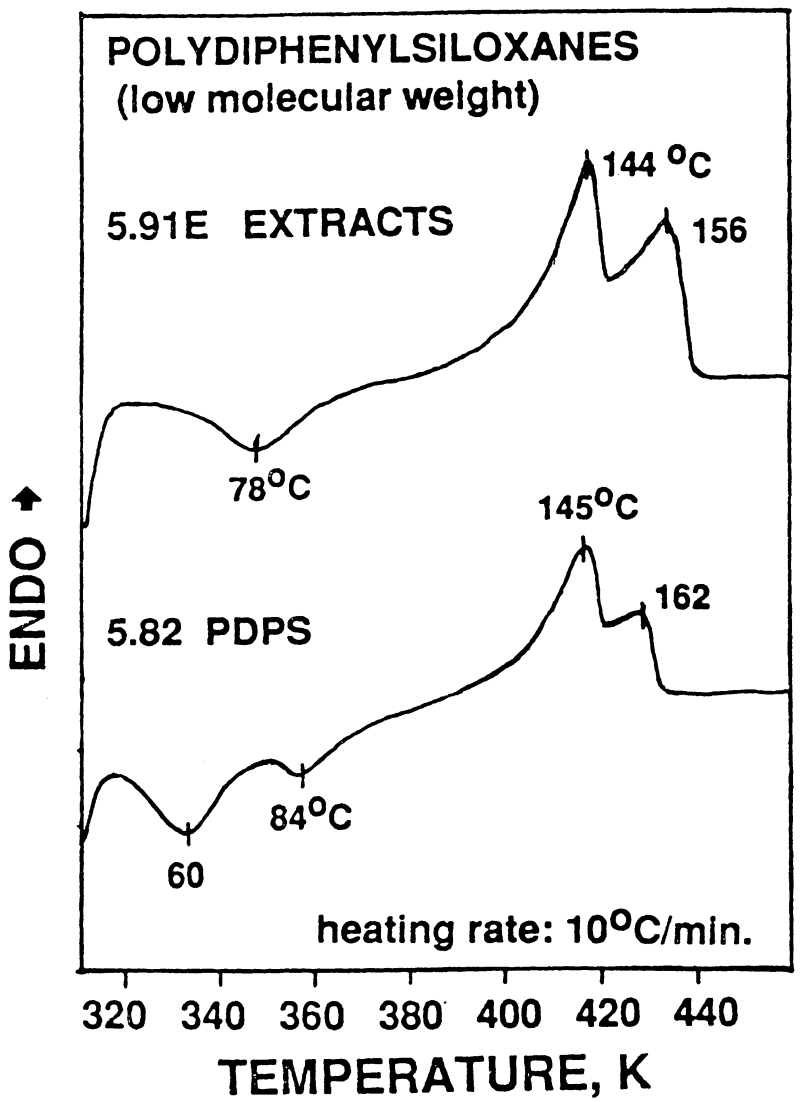

FIGURE 3.29. DSC Scans of Low Molecular Weight PDPS (Extracts and Control).

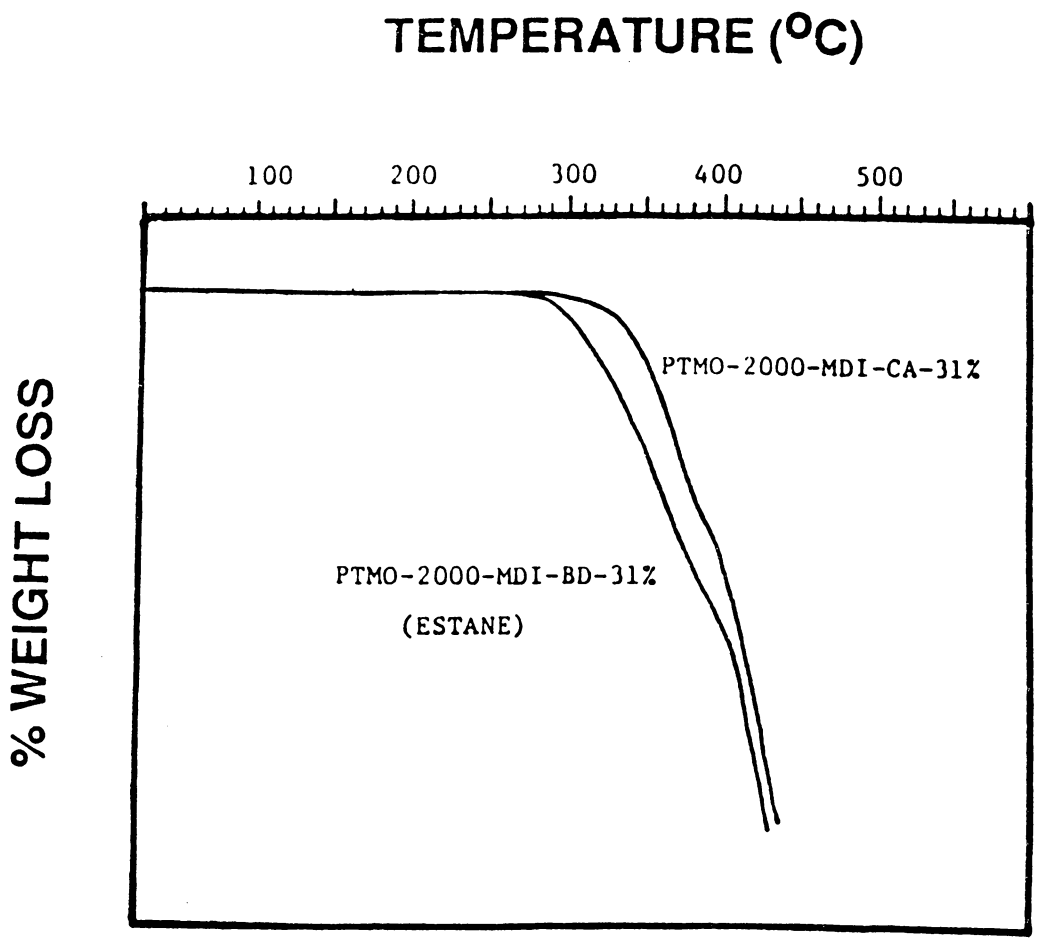

FIGURE 3.30. TGA Spectra of Polyurethanes.

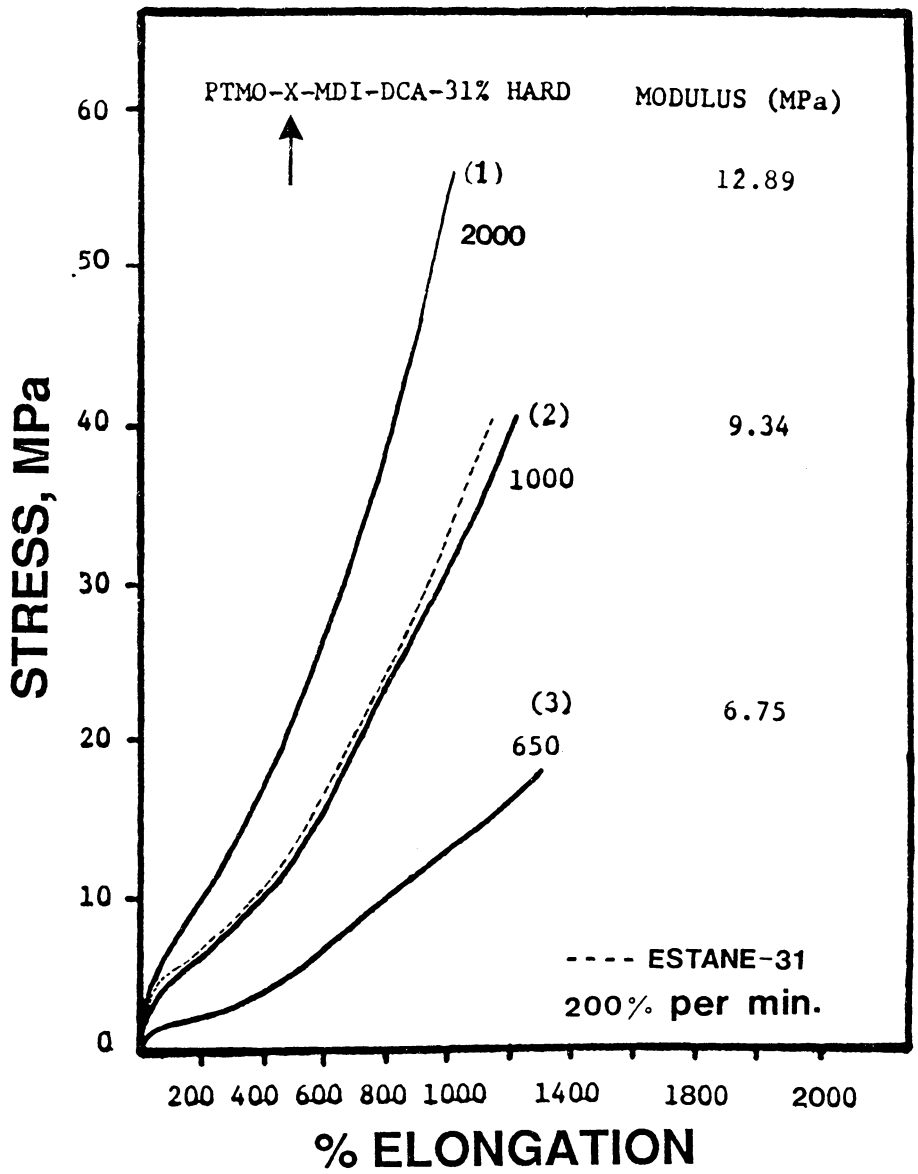

FIGURE 3.31. Tensile Properties of PEUU's Based on Different Soft Segment Length.

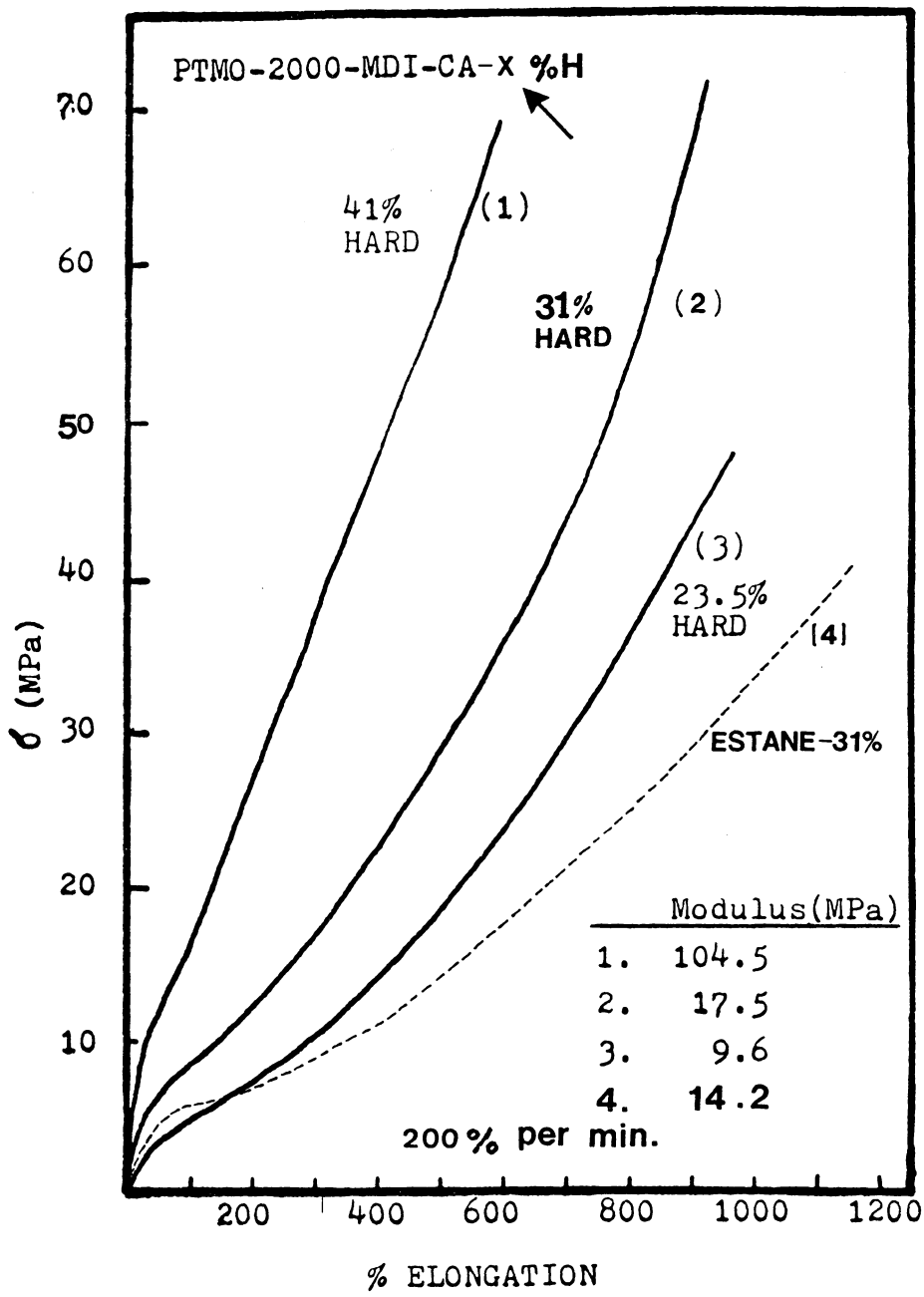

FIGURE 3.32. Stress-Strain Analysis of PTMO-2000 Based PEUU's with Various Hard Segment Content.

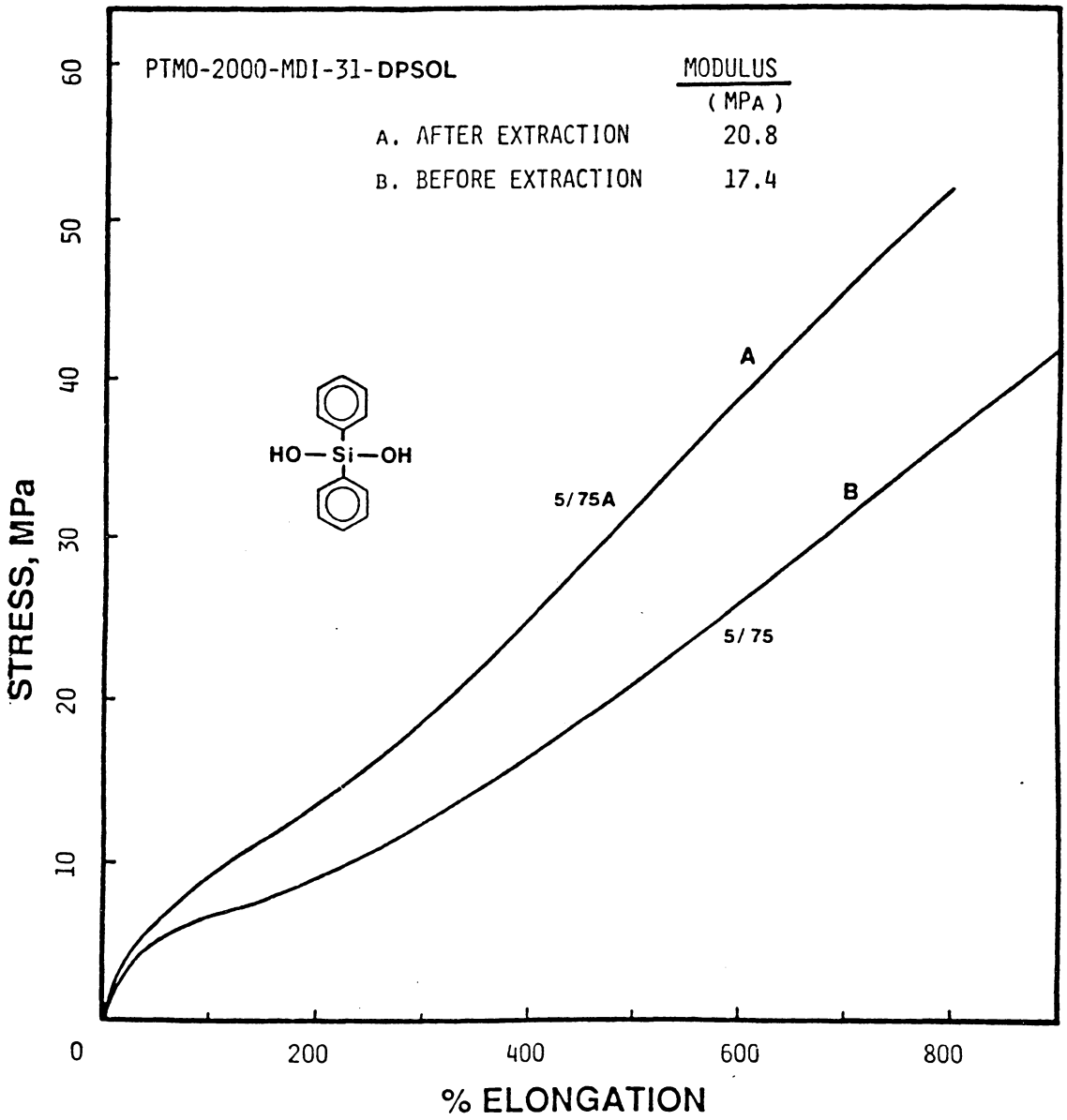

FIGURE 3.33. Stress-Strain Curves of Silanol Chain Extended PEUU's (Before and After Extraction).

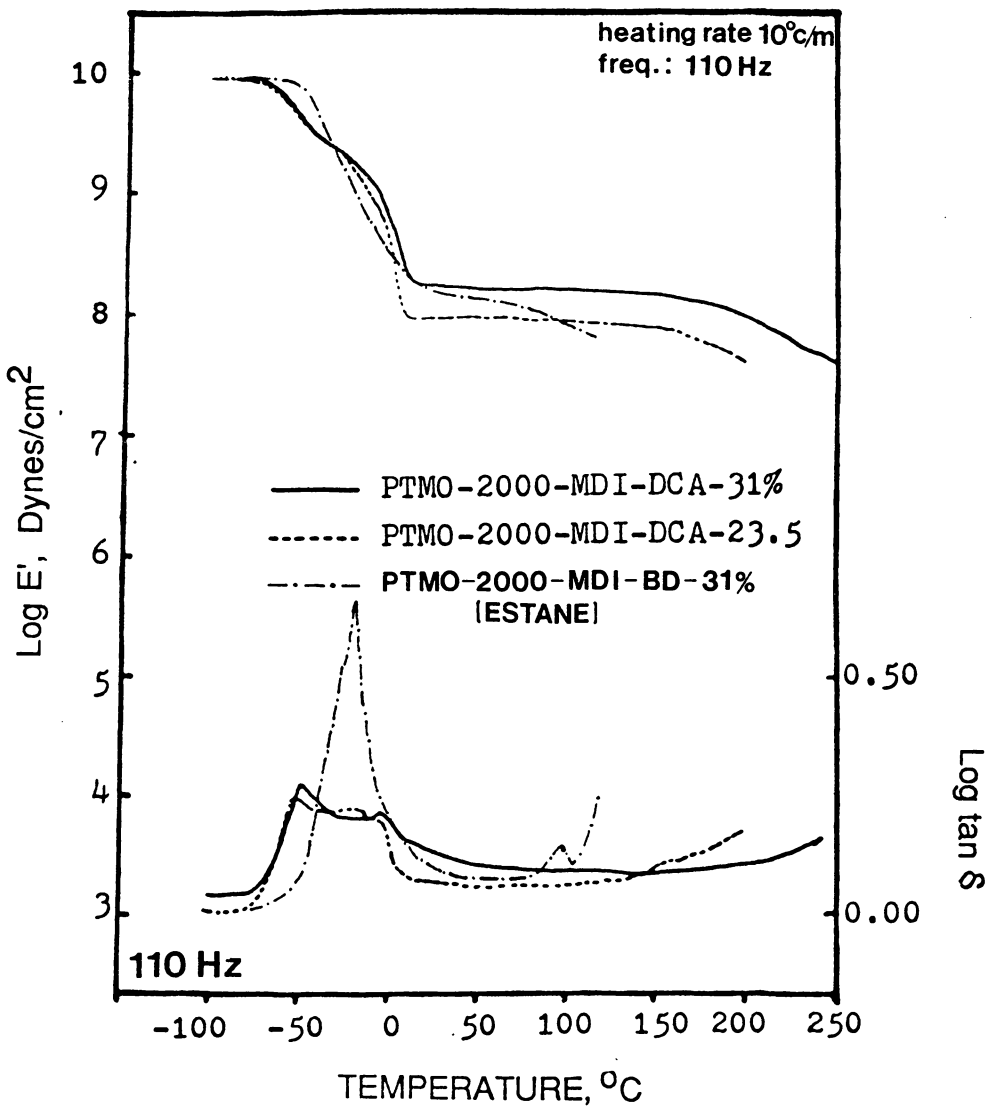

FIGURE 3.34. Dynamic Mechanical Properties of PTMO-2000 Based PEUU's with Various Hard Segment Content.

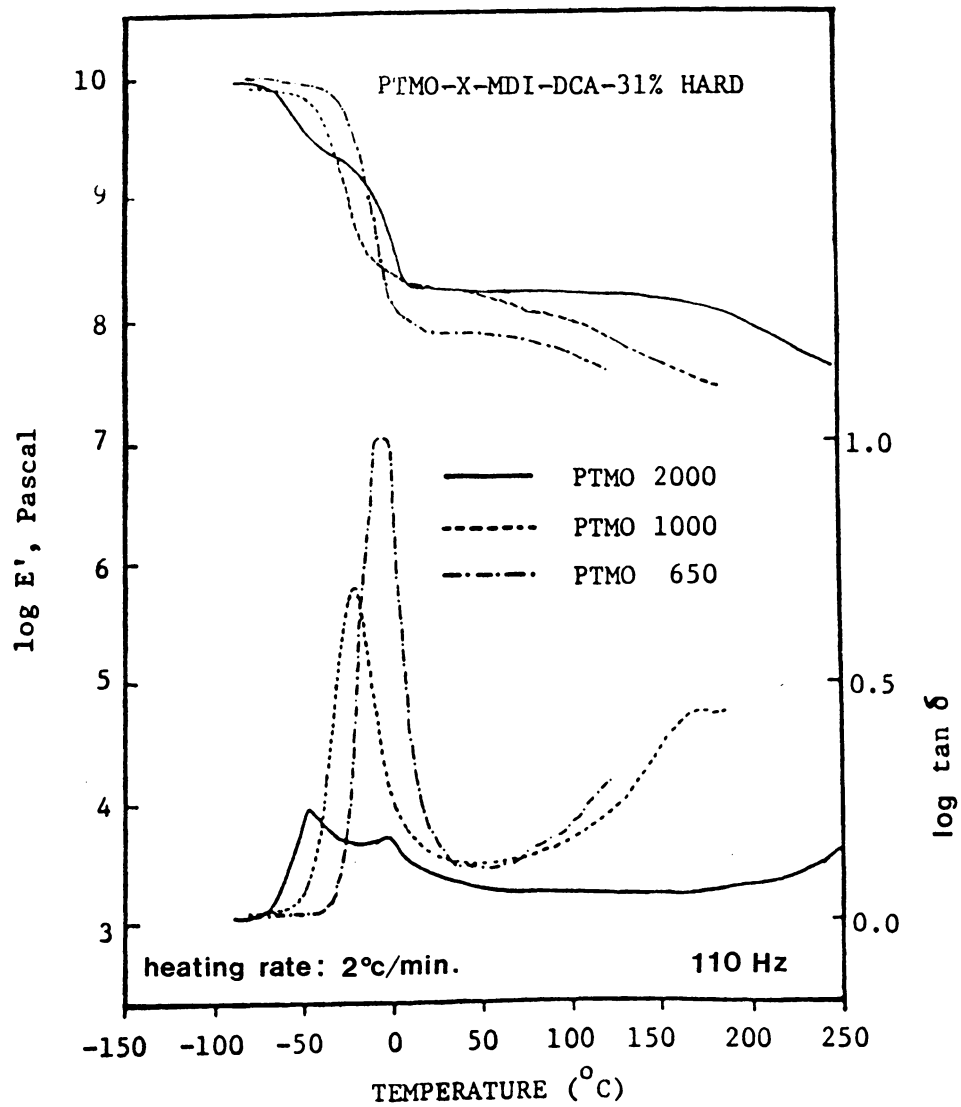

FIGURE 3.35. Effect of Soft Segment Molecular Weight on the Dynamic Mechanical Behaviors of PEUU's.

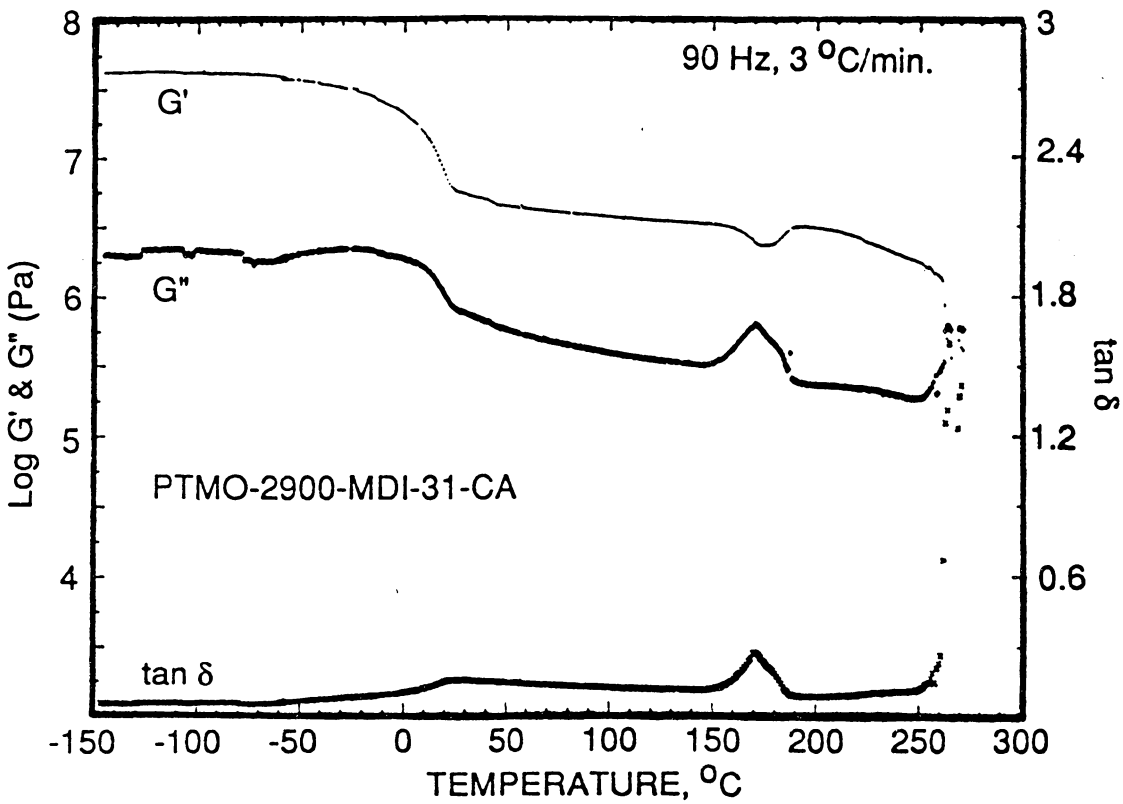

FIGURE 3.36. DMTA Spectra of PTMO-2900 Based PEUU.

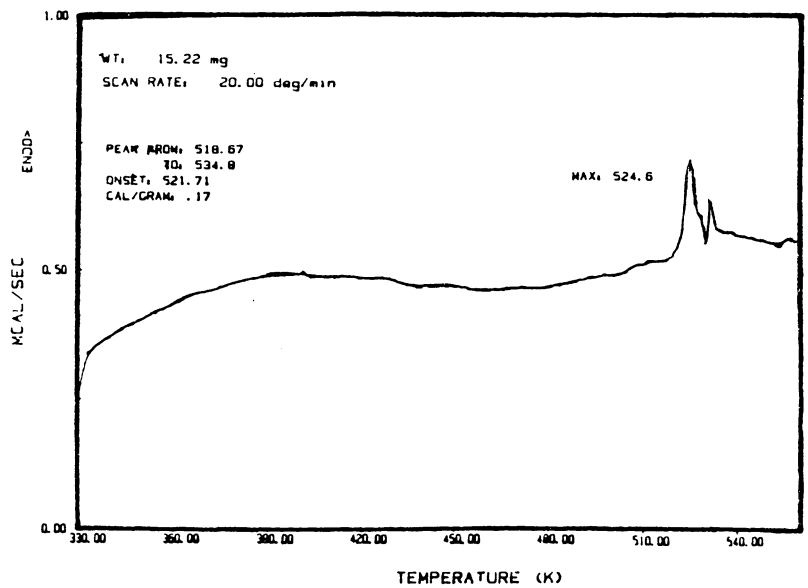

FIGURE 3.37. High Temperature DSC Curve on PTMO-2900 Based PEUU.

TABLE 3.1. Characteristics of Short and Long Chain MDI/DAM ureas.

Structure	T_m, °C Experimental	Reference
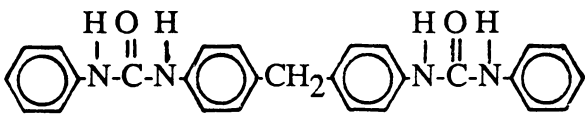	330	19
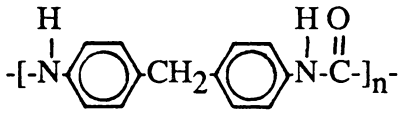	375	11

TABLE 3.2. Characteristics of Various Polyurethane-Ureas Synthesized.

Sample	Mole Ratio MDI/PTMO/CA or DCA	% Urea Content
PTMO-2000-MDI-23-CA	2.5/1/1.5	43
PTMO-2000-MDI-31-CA	3.7/1/2.7	57
PTMO-2000-MDI-41-CA	5.6/1/4.6	70
PTMO-2000-MDI-31-DCA	3.7/1/1.35	57
PTMO-1000-MDI-31-DCA	1.8/1/0.4	29
PTMO- 650-MDI-31-DCA	1.2/1/ 0.1	9

TABLE 3.3. Characteristics of Teracol™ Polyether Polyols.

PTMO	T_g, (°C)					Tc	Tm	
M.W.	onset	mid.	end	width	$\Delta C_p x 10^{-2}$	°C	°C	ΔH_f
650	-97	-90	-86	13	14.3	-71	0, 16	23
1000	-90	-81	-73	17	3.0	-	18, 26	18
2000	-84	-78	-68	16	4.0	-	25, 28	23
2900	-83	-76	-67	16	3.6	-	26, 30	22

TABLE 3.4. Low Temperature DSC Behaviors of Tertiary Alcohols Chain Extended PEUU's.

Sample	T_g, °C					T_c		T_m	
	onset	mid[1]	end	width	$\Delta C_p x10^{-2}$*	°C	ΔH_c*	°C	ΔH_f*
PTMO-2000-MDI-23-CA	-87	**-75**	-65	22	5.5	-43	4.4	3	5.8
PTMO-2000-MDI-31-CA	-86	**-76**	-65	21	10	-35	3.4	4	3.4
PTMO-2000-MDI-41-CA	-88	**-72**	-58	30	8.8	-35	1.0	12	7.0
PTMO-2900-MDI-23-CA	-91	**-78**	-69	22	6.6	-49	3.1	9	9.7
PTMO-2900-MDI-31-CA	-91	**-78**	-70	21	5.7	-52	1.9	11	8.5
PTMO-2900-MDI-41-CA	-87	**-79**	-68	19	12.1	-53	0.5	0	8.1
PTMO-2000-MDI-31-DCA	-93	**-74**	-61	32	12.2	-36	4.8	9	5.3
PTMO-1000-MDI-31-DCA	-63	**-48**	-33	30	11.3	--	--	--	--
PTMO- 650-MDI-31-DCA	-62	**-38**	-23	39	15.2	--	--	--	--

1. The midpoint at the transition was taken as the glass transition temperature.

* mcal/mg, All values of ΔC_p, ΔH_c, and ΔH_f have been normallized to the weight of the soft segment.

TABLE 3.5. Mechanical Properties of Segmented Polyurethaneureas.

SAMPLE	Ultimate Tensile Strength, MPa	Modulus MPa	Elongation %
PTMO-2000-MDI-23-CA	49.0	15.1	1000
PTMO-2000-MDI-31-CA	67.5	17.6	900
PTMO-2000-MDI-41-CA	59.0	104.5	600
PTMO-2000-MDI-31-DCA	59.0	11.4	1000
PTMO-1000-MDI-31-DCA	40.5	9.3	1100
PTMO- 650-MDI-31-DCA	17.5	6.8	1300
PTMO-2000-MDI-31-DPSOL	52.0	20.8	800
PTMO-2000-MDI-BD-31*	41.0	13.2	1000

* Estane® control.

4. PHASE DEMIXING STUDIES IN POLY-URETHANE ELASTOMERS

4.1. INTRODUCTION

Polyurethane elastomers with an $(AB)_n$ structure, typically exhibit a two-phase microstructure in which hard segment domains are distributed in the soft segment matrix. The driving force for the segregation into domains is provided by the chemical incompatibility of the hard and soft segments. This is a consequence of the well-known relationship for free energy (ΔG) given by the equation: $\Delta G = \Delta H - T\Delta S$. The equilibrium domain size and shape are a result of the balance of these three free energy terms.

1. In a material composed of units of type A and B which have a positive heat of mixing, there is a tendency toward phase separation. However, the topology of the block copolymer molecules imposes restrictions on this segregation, leading to microdomain formation.

2. From a thermodynamic point of view, there is a positive surface free energy associated with the interface between the A and B phases. This serves as a driving force toward growth of the domains.

3. There is a loss of entropy (decrease in randomness of the system) in two ways. One is attributed to the confinement of the joints to the interface. The other has its origin in maintaining the virtually constant overall polymer density by the suppression of a vast number of polymer conformations.

Thermodynamic theories for phase separation in block copolymers have been developed by Krause [1,2], Meier [3,4], Helfand [5,6], and Le Grand [7]. Krause analyzed microphase separation from a strictly thermodynamic approach based on macroscopic variables, with an assumption of complete phase separation with sharp boundaries. Meier developed criteria for the formation of domains and their sizes in terms of molecular and thermodynamic variables. Helfand formulated a useful statistical thermodynamic model of the microphases similar to that of Meier. Le Grand developed a model to account for domain formation and stability based on the change in free energy which occurs between a random mixture of block copolymer molecules and a micellar domain structure. This model also considers the interfacial boundary between the phases.

In addition to the effects of the number, size, and interactions of the copolymer blocks, temperature can affect phase separation. A higher temperature will decrease the free energy of mixing of the system, and thus enhance phase mixing. Wilkes and Emerson [8] have demonstrated that considerable phase mixing in segmented polyurethanes take place at 160^{o}C. However, upon cooling, phase separation occurs gradually until the original domain structure is restored. This thermally reversible process can be studied kinetically by a variety of techniques such as small-angle X-ray

scattering (SAXS), differential scanning calorimetry (DSC), mechanical methods, and others.

The miscibility of hard and soft segments can be estimated by using the Flory-Huggins interaction parameter:

$$\chi_{HS} = \chi_{(\Delta S)} + V_r (\delta_H - \delta_S)^2 / RT$$

Here $\chi_{(\Delta S)}$ is an entropy term [43] and can be neglected for polymer blends. Thus

$$\chi_{HS} \cong (\delta_H - \delta_S)^2 / 6$$

for $T = 298K$, with RT in calories, and the reference volume V_r taken as 100 cm^3/mol. Although the quantitative use of χ may be questionable for block copolymers, this parameter has been used to compare polyurethanes [9]. Here δ_H and δ_S are the solubility parameters, respectively, of hard and soft segments. Even though there is a well-known uncertainty in solubility parameters, relatively good estimates can be obtained from several references [10-14]. The average values of δ obtained for the soft segments are listed in Table 4.1 [9].

The case of the hard blocks is more complex. However, δ_H can be estimated from group contributions [10] in the glassy state. The glassy state was assumed since hard block crystallinity in polyurethanes is always much lower than in model hard segments [15,16]. The interaction parameters χ_{HS} listed in Table 4.1, vary widely from one soft segment to another. The critical condition for miscibility is

where i is the degree of polymerization and subscripts H and S denote hard and soft blocks. With $i_H \cong 2.5$ and $i_S \cong 28$, $(\chi_{HS})_{cr}$ becomes 0.34. Since χ_{HS} is much greater than $(\chi_{HS})_{cr}$ all the blends should be immiscible and theoretically have two fully separated phases [14].

One of the most easily accessible methods of measuring the perfection of phase separation are the measurements of changes in the glass transition temperature obtained from DSC [9,17-28] and dynamic mechanical analysis [29-37]. Quantitative information on the volume or weight fraction of the hard domains and on the domain interface is especially valuable. This information can be achieved by SAXS measurements in favorable cases [38-47]. Similar results can be obtained from pulsed NMR investigations [48-50]. The utility of NMR technique stems from its sensitivity to the molecular dynamics of polymers. The general conclusion of these studies has been that microphase separation is not complete. In most cases, an elevation in the soft segment glass transition temperature is observed as a result of the presence of "dissolved" hard segments. In addition, the dissolution of a hard segment lowers the effective filler content and leads to a loss of two physical crosslink sites for the soft segment at the microdomain interface. These effects consequently affect the modulus of the material. It is therefore thought that polyurethane elastomers would display their optimum properties when a "complete" phase separation was achieved.

The general strategy utilized to improve the phase separation in the literature is by increasing the solubility parameters difference between soft and hard segments. A high degree of phase separation has been observed when non-polar soft segments (compared with the highly polar urethane hard segments) such as PBd (polybutadiene) and PIB (polyisobutylene) were utilized. Unfortunately, the resulting polymers

polyurethanes. While the utilization of polyether or polyester soft segments is desirable, the incorporation of urea linkages to the polymer backbone became as an important approach to improve the phase separation. A better phase separation has been observed in polyurethane-urea elastomers in comparison with analogous polyurethanes. Enhancement in phase separation can be attributed to the extensive hydrogen-bonding in urea polymers.

On the basis of foregoing discussions, one question which may arise, is concern over the location of the urea linkages. Do urea linkages have to be chemically linked to the polymer backbone in order to improve the phase separation? In other words, can better phase separation be achieved by physically blending low molecular weight urea compounds with polyurethane elastomers? This question led to our objective of the work discussed in Chapter 4.

For this preliminary study, N-N'-dimethylurea (DMU) was introduced at the chain extension stage along with butandiol (BD) chain extender during the polymerization. DMU serves as the purpose what we termed "phase demixing agent" (PDA). It was postulated that this blended small urea compound would behave similarly as those urea linkages on the polyurethane backbone. Although DMU possesses two active hydrogen and may be reacted with isocyanates to produce biuret on prolonged heating at high temperature, it can be considered inert at 100°C for 10 minutes due to its lower reactivity toward isocyanates in comparison with butanediol chain extender.

4.2. EXPERIMENTAL

4.2.1. Materials

PTMO-2000 was dehydrated at 70°C under vacuum for 24 hours before use. 1,4-Butanediol (BD; F.W. 90; b.p. 230°C; DuPont) and 4,4'-bis-methylenediphenyl isocyanate (MDI; F.W. 250; Mobay Co.) were purified by vacuum distillation. 1,3-Dimethylurea (DMU; F.W. 88; m.p. 101-104°C; b.p. 268-270°C) was purified by recrystallization from acetone.

4.2.2. Preparation of Well Phase-Separated Polyurethane Elastomers

Well phase-separated polyurethane elastomers were synthesized by a two-step condensation reaction (Figure 4.1). MDI was charged into a N_2-filled resin kettle equipped with a high torque mechanical stirrer at room temperature. The reaction set-up is pictured in Figure 3.6. PTMO-2000 was then slowly syringed into the reactor at 100°C over a period of 20 minutes. After reacting the PTMO-2000/MDI mixture at 100°C for one hour, BD and DMU were added. The mechanical stirrer was stopped within one minute after the addition of BD and DMU due to the solid polymer formation. The reaction was continued for one additional hour at 100°C in order to complete the reaction. The amount of DMU was varied from 0.5 to 2 wt. % in separate experiments and a control with no DMU added also prepared in order to serve as a base point for the improvement in phase separation.

4.2.3. Characterization

DSC was the primary characterization technique utilized to observed the phase separation behavior in these polyurethanes. DSC thermograms were recorded by using a Perkin-Elmer DSC II over the temperature range of -100 to 30°C. A constant flow of helium gas was used to purge the system and a heating rate of 10°C/min was employed throughout the measurements. The data were derived from second cycles in order to provide a constant thermal history.

4.3. RESULTS AND DISCUSSION

4.3.1. Synthesis

High molecular polymers were obtained in very short time after the addition of BD and DMU (PDA). This implies that PDA is not participating in the chain extension, otherwise a low molecular weight polymer would have be resulted due to the unbalanced stoichiometry. It is found that the polymerization proceeds faster when the PDA was added in comparison to a regular butanediol chain extension. Although relatively low basicity is associated with DMU, it may still possess some catalytic effect for the isocyanate-alcohol reaction.

Theoretically, the number moles of urethane units on the polymer backbone will be equivalent to the the number moles of charged MDI, and they will be segregated from the soft segment phase to form hard segment domains. Since a partial phase mixing was postulated as illustrated in Figure 4.3, some of the urethane units were dissolved in the soft segment matrix. However, the percentage of dissolved urethane

units is unknown. Therefore, the amount of DMU was varied from 0 to 2.0 wt % in separate experiments which is equivalent to about 6 to 24 % of the urethane linkages in terms of its mole ratio with MDI. It is proposed that DMU will hydrogen bond with formed urethane linkages during polymerization as illustrated below:

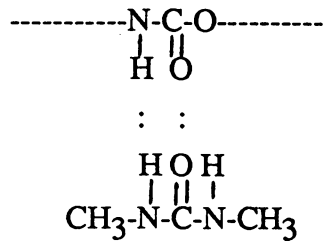

A better phase separation may be achieved by using this approach since the association of DMU with urethane linkages of hard segments provided could increase the polarity difference between the soft and hard segments. On the other hand, DMU might be considered as a nucleating agent for the hard segment as well. Thus, the phase separation might also be improved by the enhanced crystallization of the hard segments.

4.3.2. Characterization

It is difficult to know if "complete" phase separation of the hard and soft segments has been achieved after the addition of phase demixing agent (PDA), but the relative extent of phase separation can be easily visualized by mechanical and thermal analysis. The examples provided in this section will be on the basis of DSC and dynamic mechanical analysis results.

4.3.2.1. Differential Scanning Calorimetry (DSC)

Figure 4.4 collects some of the DSC spectra and Table 4.2 lists some of the characteristics of the resulting polymers. The T_g of the soft phase and the transition width are decreased with increasing the PDA content, suggesting that a purification of the soft segment phase occurs by removal of dissolved hard segments. The T_g variation is too small (less than 2°C) to conclude there is an improvement in phase separation. However, the transition width at T_g became significantly narrower as one increased the amount of PDA, which suggests a higher degree of structural homogeneity in the soft segment phase.

The magnitude of the heat capacity change (ΔC_p) at the soft segment T_g, normalized to the weight of soft segment, is a function of both the relative amount of the participation of the amorphous phase and the difference of conformational entropy between the glassy and rubbery state. At constant polymer composition, it was observed that ΔC_p is systematically decreased with the increase in PDA. This is probably caused by the fact that lesser amounts of hard segment impurity was present in the soft phase when a larger amount of PDA was utilized.

Crystallization and melting endotherms are observed in addition to glass transitions on those samples containing PDA, while the control sample (0 % PDA) shows only a glass transition. This observation can be directly related to the purity of the soft phases. As the purity of soft phase increased (less solubilized hard segment), the PTMO segment became less restricted and packing occurs more easily when the

temperature is above T_g. This was reflected by the appearence of the crytallization and melting endotherms.

The T_m and ΔH_f are larger for polymers with higher level of PDA which implies a larger size of PTMO crystallites as well as possibly a higher soft segment crystallinity. This, however, can only possibly be achieved when the purity of soft phase is high.

The addition of PDA clearly improves the purity of soft phase and of course will also be reflected in the hard segment phase. Figure 4.5 shows the high temperature DSC thermograms on the same series of polymers. Multiple endotherms were observed for these polymers. In control sample (0 % PDA), a broad peak with a shoulder were observed at 171 and 188°C, respectively. The intensity of the peak at 171°C was reduced, while the peak at 188°C is increased in intensity after the addition of PDA. Interestingly, as the PDA content reaches 1 wt %, a new endotherm was developed at 205°C and the ΔH_f of that is increased with the PDA content. This would indicate that greater phase separation and better ordered hard segment structures are responsible for the development of possibly long range ordering endotherms.

On the basis of the aforementioned discussion, the one speculated that the ultimate softening temperature of a well phase separated butanediol chain extended polyurethane elastomer could be as high as 200°C. The long range ordering of the hard segments clearly can be induced by the PDA. The DMU has to be removed in order to achieve this goal since DMU melts at 102°C and will be act as a plasticizer for the hard segment at high temperatures.

4.3.2.2. Dynamic Mechanical Properties

DMTA spectra for control sample and the sample contains 2 wt% of DMU are illustrated in Figure 4.6. The storage modulus, G', representing the modulus of

elasticity of the material as function of temperature, and tan δ, showing the occurence of relaxation processes within the material, are plotted on the same graph. In general, two relaxation processes can be observed within this material. The transition at roughly -40°C corresponds to the T_g of the PTMO segment. The peak intensity is related to the amount of soft segment involved in the transition. The soft segment contents in these two polymers are equal. Therefore, the observed difference in intensity might occur due to the difference in the amount of amorphous phase presented which can be indirectly related to the degree of phase separation. The phase separation may be greater in the phase demixed polymer since a somewhat lower T_g and a less intense peak were observed.

Above T_g, all samples show an extended rubbery plateau region in the storage modulus spectra, followed by a rapid drop at the hard segment softening point. For the control sample, the polymer was completely softened around 170°C. This observation agrees with DSC results, suggest the melting of hard segment crystallites.

A higher plateau modulus usually reflects more effective physical crosslinking. Qualitatively, the plateau modulus is significantly higher in the case of the polymer containing 2 wt% of DMU, as opposed to the control sample. Two reasons may be attributed for this result: first, the extent of dissolved soft segment in the hard segment domains is believed to be smaller in the phase demixed polymer; secondly, it could be due to the presence of a small amount of low molecular weight crystalline DMU, which is still a solid at temperatures below 100°C.

The hard segment domain cohesion should be stronger for a "cleaner" phase structure and thus the higher hard segment softening point. However, phase demixed polymer shows a lower softening temperature than the control sample. This is

probably solely the consequence of the presence of DMU in the hard segment phase. The DMU will melt as the temperature go beyond 100°C, and may then act as a plasticizer for the hard segment phase. This results in a modulus drop and a lower softening temperature, as is seen in the G' curves.

4.3.2.3. Solution Properties

It is thought that phase segregation increased, the product should be less soluble due to the strong physical interaction between hard segments. The polymers prepared by using the PDA technique, were initially soluble in THF and became insoluble after heating in the vacuum oven at 120°C for 24 hours. This implies that DMU has been possibly removed and a better cohesiveness of hard segment domain was achieved. The presence of DMU may be greatly reduced the packing efficiency of polymer chains. Thus, the solvent molecules may easily penetrate into the hard segment phase and reduce the interchain interaction.

4.4. CONCLUSION

The N,N'-dimethyl-urea (DMU) has been found to be an effectively novel "phase demixing agent" (PDA) for the polyurethane elastomers. The polar DMU molecules are presumably hydrogen bonded with urethane linkages of hard segments and thus increase the polarity difference with the soft segment which is certainly one of the important criteria of phase separation. The DMU also possibly served as an added nucleating agent, that promoted the crystallization of hard segments and the phase

separation process.

In this study, DSC and DMTA have been utilized as a means of verifying the proposed idea. The results obtained on both techniques are generally in good agreement with each other. The improvement in phase separation are shown by a lower and more sharply defined soft segment T_g and a higher rubbery plateau modulus.

The low molecular weight DMU has to be removed from the polymer after the polymerization in order to achieve ultimate physical properties. The research discussed in this chapter are only preliminary studies. It is realized that more work needs to be done before a solid theory can be developed. Nevertheless, the "phase demixing" phenomenon by the action of DMU is believed to be valuable in further understanding the phase separation behavior of polyurethane elastomers.

REFERENCES

1. S. Krause, J. Polym. Sci., Part A2, 7, 249 (1969).
2. S. Krause and P.A. Reismiller, J. Polym. Sci., Part A2, 13, 663 (1975).
3. D.J. Meier, "Block Copolymers", Academic Press, New York (1979).
4. D.J. Meier, J. Macromol. Sci., Phys. Ed., 17, 181 (1980).
5. E. Helfand and Y. Tagami, J. Polym. Sci., B9, 741 (1971).
6. E. Helfand and Z.R. Wasserman, Macromolecules, 11, 683 (1978).
7. A.D. Le Grand, G.G. Vitale, and D.G. Le Grand, Polym. Eng. Sci., 17, 598 (1977).
8. G.L. Wilkes and J.A. Emerson, J. Appl. Phys., 47, 4261 (1976).

9. Y. Camberlin and J.P. Pascault, J. Polym. Sci., Polym. Phys. Ed., 22, 1835 (1984).

10. D.W. Van Krevelen and P.J. Hoftyzer, "Properties of Polymers: Their Estimation and Correlation with Chemical Structure", Elsevier Scientific Publishing Company, New York (1976).

11. J. Brandrup and E.H. Immergut, "Polymer Handbook", Interscience, New York (1966).

12. "Encyclopedia of Polymer Science and Technology", Vol. 3, pp.833-861, Interscience, New York (1969).

13. C.M. Hansen, J. Paint Technol., 39, 505 (1967).

14. A. Chapiro, M. Lamothe, and T. Le Doan, Eur. Polym. J., 14, 647 (1978).

15. Y. Camberlin and J.P. Pascault, J.M. Letoffe, and P. Claudy, J. Polym. Sci., Polym. Chem. Ed., 20, 383 (1982).

16. Y. Camberlin and J.P. Pascault, J.M. Letoffe, and P. Claudy, J. Polym. Sci., Polym. Chem. Ed., 20, 1445 (1982).

17. G.L. Wilkes and R. Wildnauer, J. Appl. Phys., 46, 4148 (1975).

18. C.G. Seefried, J.V. Koleske, and F.E. Critchfield, J. Appl. Polym. Sci., 19, 2503 (1975).

19. C.S. Paik Sung, C.B. Hu, and C.S. Wu, Macromolecules, 13, 111 (1970).

20. W. Nierzwicki and E. Wysocka, J. Appl. Polym. Sci., 24, 739 (1980).

21. T.R. Hesketh, J.W.C. Van Bogart, and S.L. Cooper, Polym. Eng. Sci., 20, 190 (1980).

22. J.W.C. Van Bogart, D.A. Bluemake, and S.L. Cooper, Polymer, 22, 1428 (1981).

23. Y. Camberlin and J.P. Pascault, J. Polym. Sci., Polym. Chem. Ed., 21, 415

(1983).

24. N.S. Schneider and C.S. Paik Sung, J. Polym. Sci., Polym. Chem. Ed., 17, 73 (1977).
25. N.S. Schneider, C.S. Paik Sung, R.W. Matton, and J.L. Illinger, Macromolecules, 8, 62 (1975).
26. C.S. Paik Sung and N.S. Schneider, Macromolecules, 8, 68 (1975).
27. R.W. Seymour and S.L. Cooper, Macromolecules, 6, 48 (1973).
28. L.M. Leung and J.T. Koberstein, Macromolecules, 19, 706 (1986).
29. G.A. Senich and W.J. Macknight, Adv. Chem. Ser., 176, 97 (1979).
30. C.M. Brunette, S.L. Hsu, W.J. Macknight, and N.S. Schneider, Polym. Eng. Sci., 21, 163 (1981).
31. D.S. Huh and S.L. Cooper, Polym. Eng. Sci., 11, 369 (1971).
32. S.L. Samuels and G.L. Wilkes, J. Polym. Sci., Polym. Symp., 43, 149 (1973).
33. R.J. Zdrahala, F.E. Critchfield, R.M. Gerkin, and S.L. Hager, J. Elast. Plast., 12, 184 (1980).
34. T. Kajiyama and W.J. Macknight, Macromolecules, 2, 254 (1969).
35. T. Kajiyama and W.J. Macknight, Trans. Soc. Rheol., 13(4), 527 (1969).
36. J.L. Illinger, N.S. Schneider, and F.E. Karasz, Polym. Eng. Sci., 12, 25 (1972).
37. H. Ng, A.E. Allegrezza, R.W. Seymour, S.L. Cooper, Polymer, 14, 255 (1973).
38. R. Bonart and E.H. Mueller, J. Macromol. Sci., Phys. Ed., B10, 177 (1974).
39. R. Bonart and E.H. Mueller, J. Macromol. Sci., Phys. Ed., B10, 345 (1974).
40. Z. Ophir and G.L. Wilkes, J. Polym. Sci., Polym. Phys. Ed., 18, 1469 (1980).
41. L.M. Leung and J.T. Koberstein, J. Polym. Sci., Polym. Phys. Ed., 23, 1883 (1985).
42. J.T. Koberstein and R.S. Stein, J. Polym. Sci., Polym. Phys. Ed., 21, 1439

(1983).

43. J.W.C. Van Bogart, P.E. Gibson, and S.L. Cooper, J. Polym. Sci., Polym. Phys. Ed., 21, 65 (1983).
44. S. Abouzahr, G.L. Wilkes, and Z. Ophir, Polymer, 23, 1077 (1982).
45. N.S. Schneider, C.R. Desper, J.L. Illinger, A.O. King, and D. Barr, J. Macromol. Sci., Phys. Ed., B11, 527 (1975).
46. P.E. Gibson, J.W.C. Van Bogart, and S.L. Cooper, J. Polym. Sci., Polym. Phys. Ed., 24, 885 (1986).
47. Yu.S. Lipatov, N.V. Dmitruk, V.V. Tsukruk, V.V. Shilov, and L.I. Dashevsky. J. Appl. Polym. Sci., 29, 1919 (1984).
48. R.A. Assink and G.L. Wilkes, Polym. Eng. Sci., 17, 606 (1977).
49. R.A. Assink, J. Polym. Sci., Polym. Phys. Ed., 15, 59 (1977).
50. W. Nierzwicki, J. Appl. Polym. Sci., 29, 1203 (1984).

Table 4.1. Solubility Parameters of Soft Segments and Interaction Parameters with the MDI-Butanediol Hard Segment at 25°C. [9]

Type of Soft Segment	δ_s (± 0.1) ($cal^{1/2}/cm^{-3/2}mol^{-1}$)	$(\chi_{HS})_{25°C}$*
Hydrogenated 1,2-Polybutadiene	7.90	4.68
1,2-Polybutadiene	8.20	4.17
1,4-Polybutadiene	8.27	4.05
Poly(tetramethylene oxide)	8.70	3.37
Poly(propylene oxide)	9.10	2.80

* Relative error can be estimated to about ± 6%.

PTMO-2000 + MDI

bulk ↓ 110°C

Isocyanate Capped Prepolymer

bulk ↓ 110°C

add ↓ BD and DMU

↓ ~ 1 min.

Well Phase-Separated
Polyurethane Elastomers

FIGURE 4.1. Preparation of Well Phase-Separated Butanediol Chain-Extended Polyurethane Elastomers.

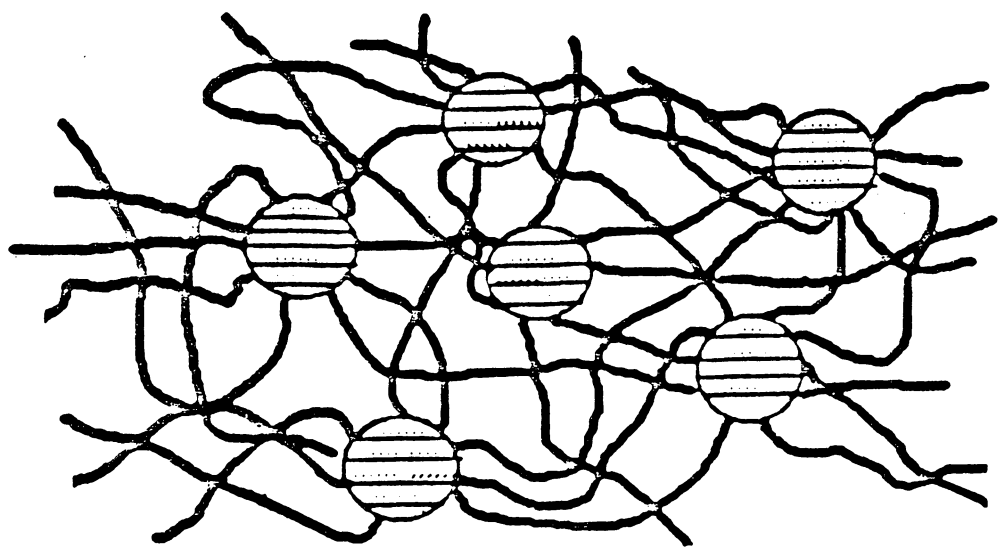

-------- Phase Demixing Agent (PDA)

——— Hard Segments

Soft Segments

FIGURE 4.2. Well Phase Separation (after "PDA" Addition).

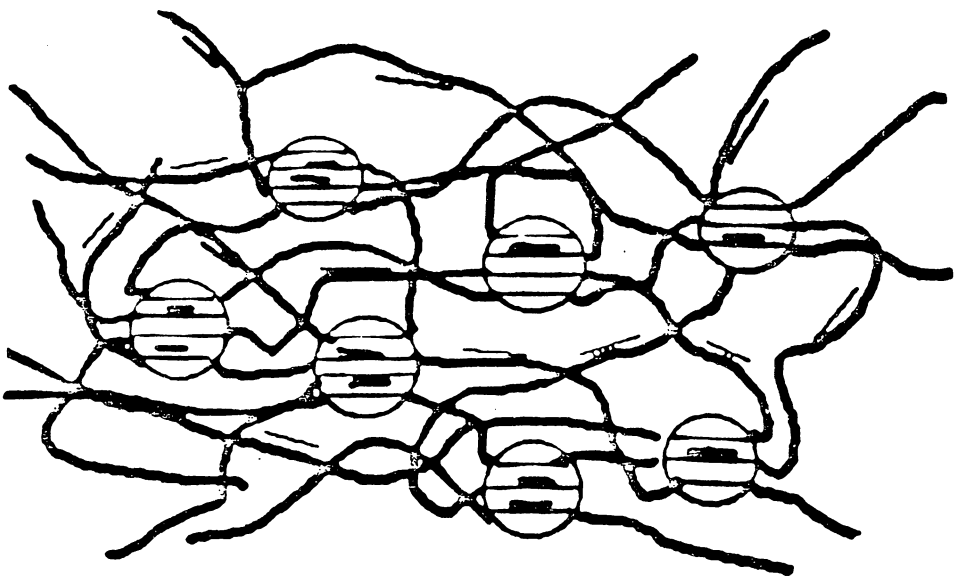

Hard Segments

Soft Segments

FIGURE 4.3. Partial Phase Mixing.

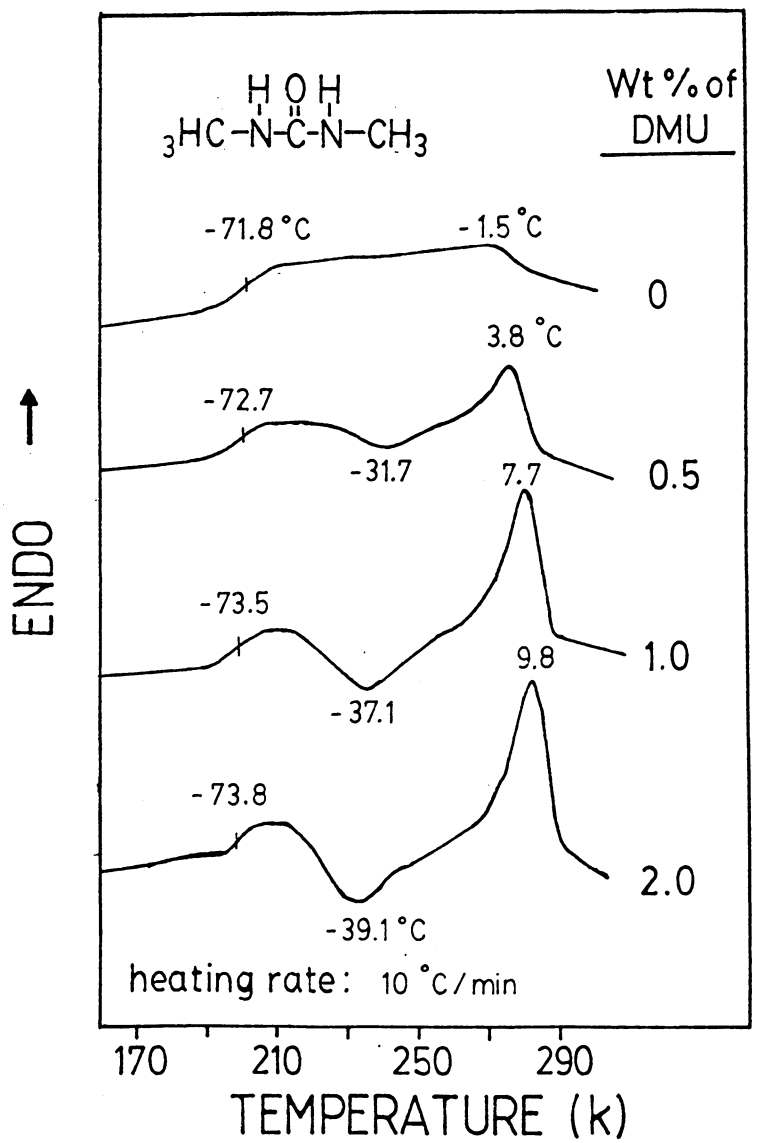

FIGURE 4.4. Effects of PDA on the Low Temperature DSC Behaviors of Butanediol Based Polyether-urethanes.

Table 4.2. Characteristics of Polyether-Urethanes with the MDI-BD Hard Segment Before and After the "PDA" Added

sample	amt. of PDA		mole ratio	T_g, °C					T_m	
#	wt %	# moles x 10^3	PDA/MDI*	onset	mid.	end	width	$\Delta C_p x 10^2$	°C	ΔH_f
control	0	0	0	-83	-72	-63	20	7.05	-2	0.45
1	0.5	1.25	0.06	-83	-73	-63	20	7.00	4	2.65
2	1.0	2.51	0.12	-82	-74	-67	15	6.91	8	3.67
3	2.0	5.03	0.24	-78	-74	-70	8	5.53	10	4.29

* # moles of MDI is equivalent to the # moles of urethane linkages present on the polymer backbone.

** The unit for ΔC_p and ΔH_f is mcal/mg.

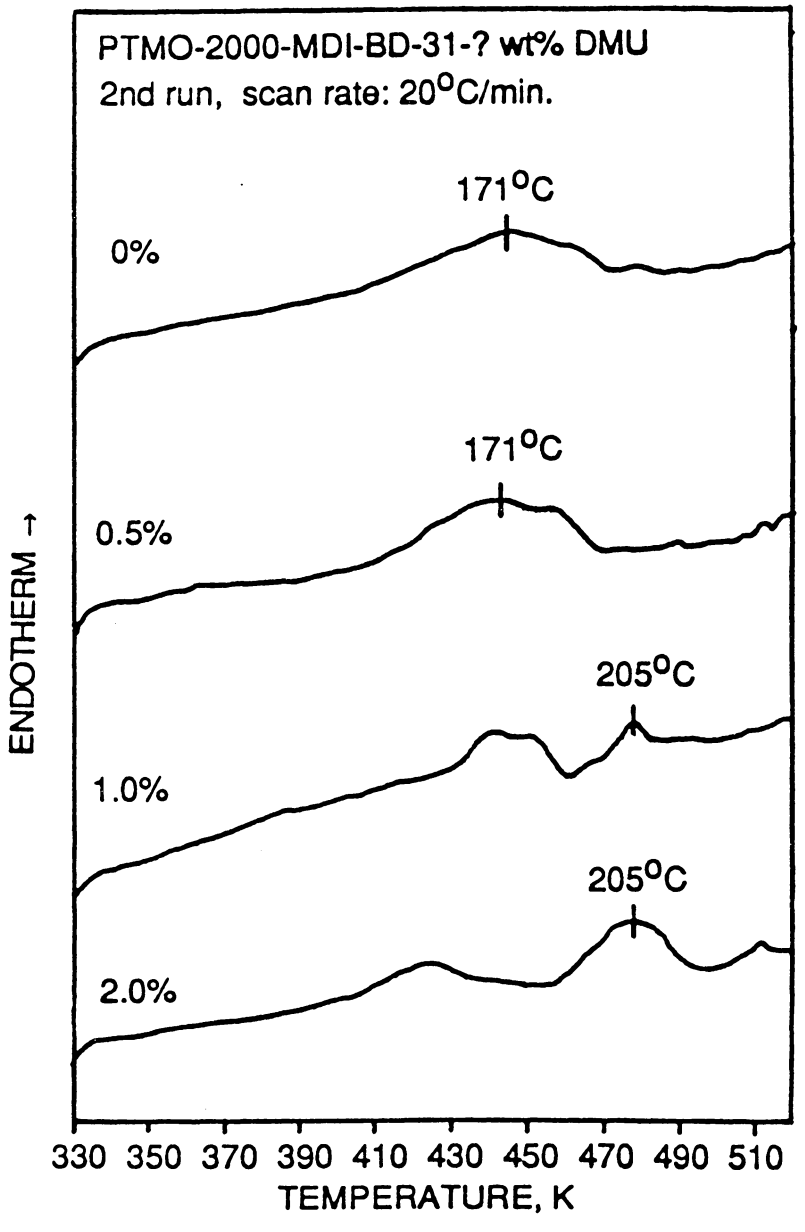

FIGURE 4.5. High Temperature DSC Scans of Butanediol Chain Extended Polyether-Urethanes Prepared by Using PDA Technique.

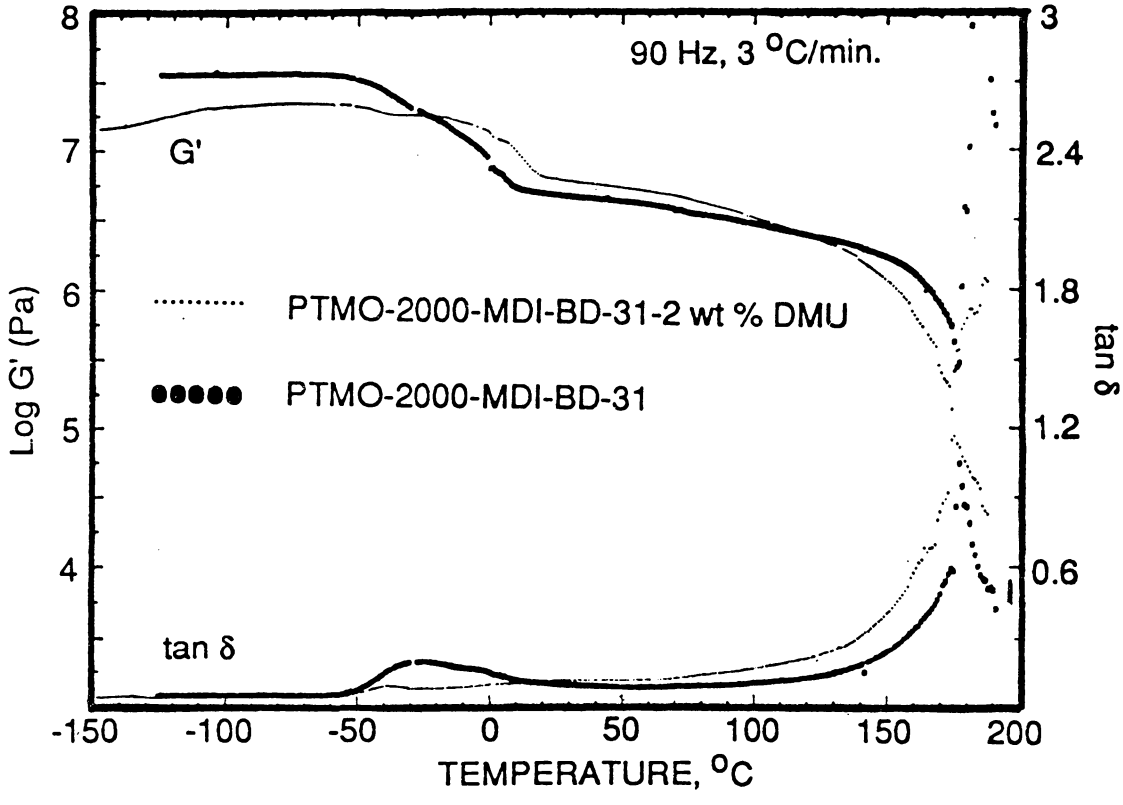

FIGURE 4.6. DMTA Spectra of Butanediol Chain Extended Polether-urethanes with and without Containing PDA.

5. DIRECT SYNTHESIS OF POLYTETRA-HYDROFURAN-IONENE ELASTOMERS BY COUPLING REACTIONS OF "LIVING" POLY-THF DIOXONIUM IONS WITH DITERTIARY AMINES

5.1. INTRODUCTION

In Chapter 2 to 4, the synthesis of polyurethane elastomers and their outstanding physical properties have been extensively reviewed. Generally speaking, the hydrogen-bonding of urethane linkages enhanced the phase separation by way of increasing the polarity difference between hard and soft segments in polyurethane elastomers. Both thermal and mechanical properties could be greatly influenced by the extent of phase separation as discussed in Chapter 4. By the same token, phase separation could be possibly increased by the incorporation of ionic bonding to the polyurethane

backbone due to the highly polar characteristics of ionic bonds.

This chapter will be focused on the synthesis and characterization of a rather new type of elastomer - ionenes based on the polytetrahydrofuran soft segment. Ionenes are those polyquaternary ammonium compounds where the ammonium cation is an integral part of the main chain. A new approach to the synthesis of PTHF ionene elastomers will be discussed and their physical properties will also be reported. Conventional approach to the ionene synthesis is by using Menschutkin reaction between a diprimary alkyl halide and a ditertiary amine. An elastomeric segment is generally introduced in order to provide good film-forming properties to the ionenes. The ionene chemistry is utilized frequently in the literature to prepare polyurethane ionenes. Therefore, a review on the synthesis of polyurethane ionomers and their physical properties also will be given in this chapter which could be helpful in understanding the structure-property relationship of the new ionene polymers. Since the polytetrahydrofuran soft segment is the primary interest in this research, its preparation and properties are also reviewed.

5.2. LITERATURE REVIEW:

5.2.1. Polyurethane Ionomers:

Ion-containing polymers exhibit a wide range of physical properties, many of which are due to the ionic groups contained in the polymer. They have proven utility in solving solids/liquid separation problems related to water pollution and are used extensively in

paper manufacturing, textile finishing, oil production, plastics, coatings, biomedical applications, etc. This wide range of applications, in turns, has sparked a tremendous growth in research for new ion-containing monomers and ion-containing polymer systems. They are generally referred to as "polyelectrolytes" when they have sufficient ionic charge to be soluble in water and as "ionomers" when the concentration of ion-containing groups is too low for water solubility.

Polymer containing low concentrations of ions can be prepared by copolymerization of a nonionic monomer with an ionizable or ionic monomer; alternatively, many nonionic polymers can be modified by appropriate chemical techniques to yield partly ionic materials. Both approaches can be considered to result in the same end product - copolymers whose major component is nonionic and whose minor component is ionizable or ionic.

One of the important and useful class of polymers whose properties can be modified by the introduction of ionic forces are the rubber-forming polymers such as polyether-urethanes. The most prominent characteristic of the family of polyurethane elastomers is that they exhibit a two-phase microstructure. It is this microstructure that is responsible for the novel and sometimes unique properties of these materials. These polymers have the general structure of $-(A-B-)_n-$ where the soft segment is usually formed from a polyether or polyester macroglycol of molecular weight between 600 and 3000. The hard segment is formed by extending an aromatic diisocyanate with low molecular weight diol.

The morphology and properties of polyurethane segmented copolymers have been subjected to extensive investigations over the past decade. Introducing ions into polyurethane elastomers is a useful way to alter polymer morphology, and physical properties. Synthesis and limited mechanical data were reported for polyurethane ionomers

[1-7]. In polyurethane ionomers, in addition to the hydrogen bonding system, ionic association must be considered. The importance of ionic interactions has been demonstrated in studies of random copolymers containing ionized acid groups, for example, the carboxylic rubbers [8,9,53]. These materials show the enhanced rubbery modulus and other mechanical properties characteristic of block copolymers. This has been attributed to clustering of ionic groups, similar to the microphase separation in block copolymers. The microstructure in a block copolymer ionomer may be quite complex and easily varied by changing the degree of ionization, hydration, and casting solvent system.

An interesting property of many polyurethane ionomers is the ability to emulsify or dissolve in water. Solvents with low polarity tend to solvate the hydrocarbon portions of a polyurethane ionomer, whereas solvents with a very high polarity, such as water, tend to solvate the ionic groups. Thus very interesting viscosity and emulsification behavior is observed upon varying solvent composition in mixed solvent systems, such as acetone and water [1]. Such systems may find applications in coatings, adhesives, and paints.

Polyurethane ionomers may be conveniently prepared by using a chain extender containing a secondary or tertiary amine. The tertiary amine may by quaternized with alkyl halides to produce a polyurethane cationomers. Chain extenders with secondary amines can be further reacted with sultones or lactones to give sulfonic acid or carboxylic acid side groups. These acid groups may be subsequently neutralized with various cations to produce anionomers. When a chain extender containing a tertiary amine is reacted with a sultone, a quaternary ammonium sulfonate zwitterionomer is formed.

5.2.1.1. Polyurethane Cationomers:

The thermoplastic polyurethane containing tertiary amine along the polymer backbone can be "vulcanized" with bifunctional quaternizing agents such as 1,4-bis(chloromethyl)benzene [1] and dibromohexane [11]. This type of chemical linkages with quaternary amine cation on the polymer backbone has been named as "ionene" which was coined by the late Dr. Rembaum et al. [6].

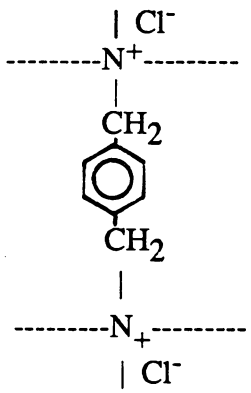

If a monofunctional quaternizing agent such as dimethyl sulfate or methyl chloride was used, chemical crosslinking is impossible. Nevertheless, this again gives an elastomer which shows drastically improved physical properties.

Dieterich et al. [1] found that those cationomers can be obtained readily by the action of acids than by quaternization. Neutralization of the basic polyurethane takes place when the polymer is dissolved into a polar organic solvent with a strong acid such as hydrochloric acid. The resulting ionomer forms colloidal solutions in water and yields films having the same properties as the quaternized products.

More recently, Hsu et al. [5] examined the effect of polyols, diisocyanates, tertiary amine-containing diols, and the chain lengths of the polyol on their mechanical properties. In summarizing their work, the mechanical properties of polyurethane cationomers were

improved with decreasing molecular weight of the polyol and increased concentration of quaternary ammonium ions and degree of quaternization. The soft segment glass transition temperatures of polymers increased both with an increase in the quaternary ammonium ion concentration and with degree of quaternization.

5.2.1.2. Polyurethane Anionomers:

Since free carboxyl groups can react with the isocyanates, it is difficult to use carboxyl containing diol chain extenders in the preparation of polyurethane elastomers with free carboxyl pendant groups on the backbone. Therefore, polyurethane anionomers are usually prepared by postreaction of polyurethane or polyureas with cyclic compounds such as sultones, lactones, or anhydrides in the presence of strong bases [10].

A procedure of greater practical interest is the modification of existing polyurethanes containing urea groups [1].

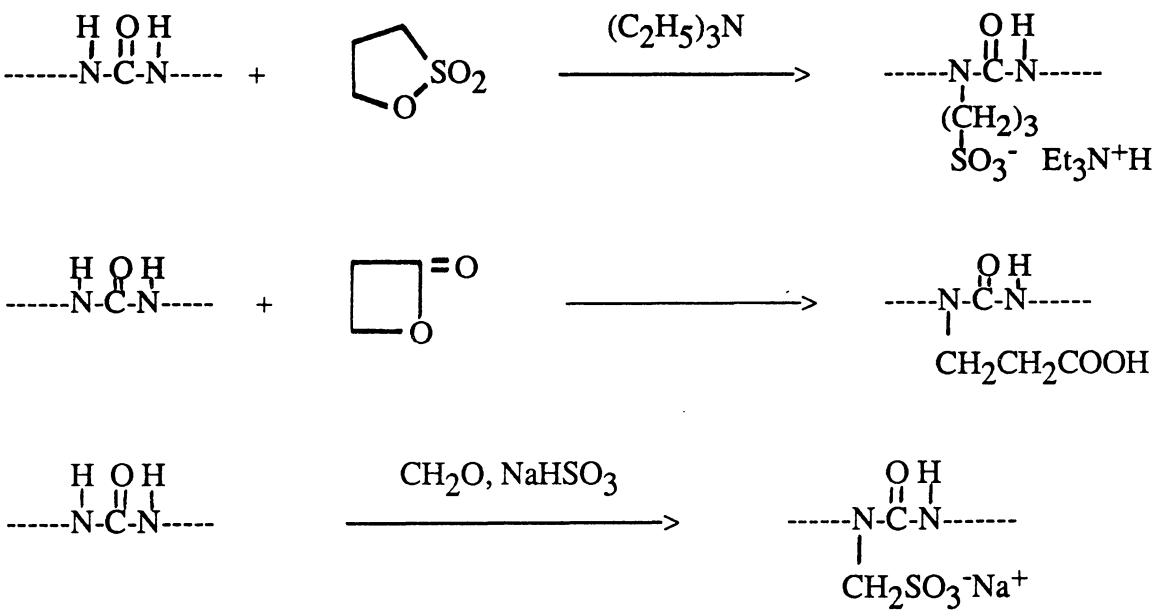

The segmented polyurethane anionomers containing carboxylate or sulfonate groups also have high tensile strength and elasticity with predominantly linear structures.

5.2.1.3. Polyurethane Zwitterionomers:

A zwitterionomer results by reacting a polyurethane elastomer containing tertiary amine groups with a sultone in polar solvents.

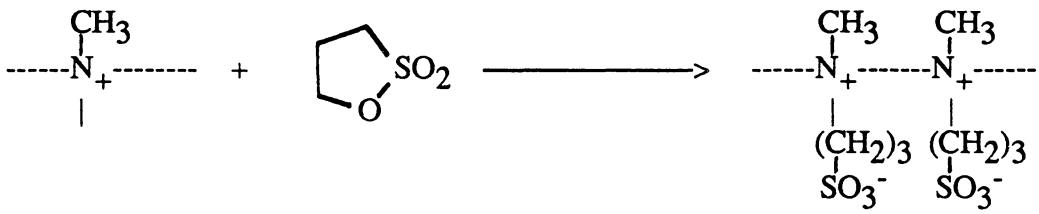

The dynamic mechanical properties of the ET-37 (PTMO-1000-37 % hard segment) series of zwitterionomer is shown in Figure 5.1 [2]. The hard segment cohesiveness is markedly enhanced by coulombic interactions among the ionic sites in the zwitterionomer which indicated by an increase in breadth and modulus of the rubbery plateau with increasing degree of ammonium sulfonation.

Miller et al. [3] and Yu et al. [12,13] studied the conversion of a zwitterionomer to an anionomer and the reaction is illustrated as follow:

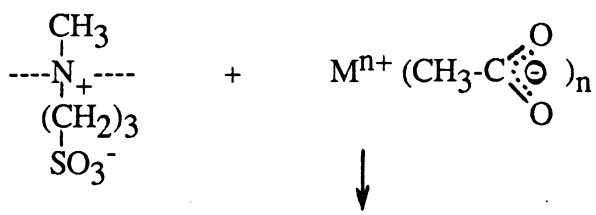

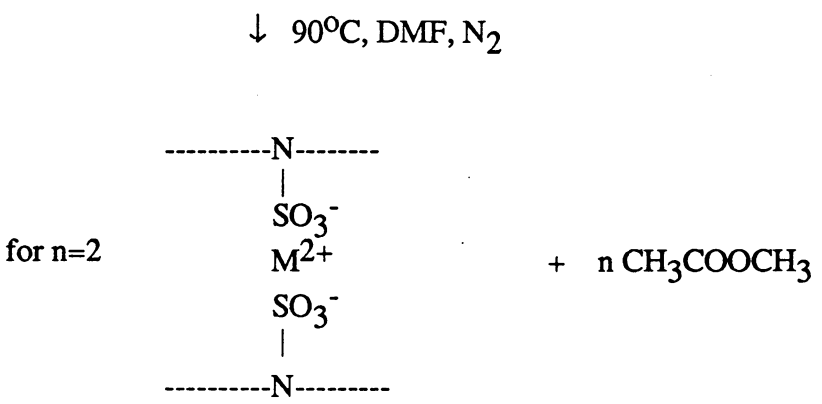

They found that polymers differing in composition and cation type exhibited markedly different properties. In general, material strength was found to increase as the neutralizing cation charge increased, provided that the system exhibited a two-phase interlocking morphology. The improved strength is due to increased hard domain cohesiveness caused by the aggregation of ionic groups.

5.2.1.4. Metal Dicarboxylate Containing Polyurethanes:

Previously discussed polyurethane ionomer synthesis involves the postreaction on a high molecular weight polymers containing either a secondary or tertiary amine. However, Kothandaraman et el. [14] took a rather reverse approach in which a low molecular weight metal dicarboxylate-containing diols (as shown below) was reacted with diisocyanates.

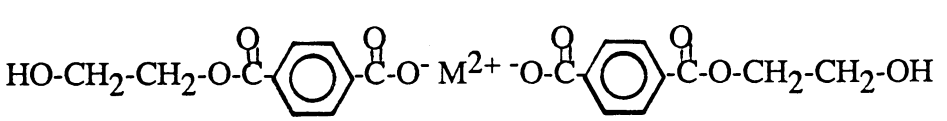

The feature which distinguishes the metal dicarboxylates from other polymers is the presence of the highly ionic metal bonds in the main chain of the polymer. The ability of these metal dicarboxylates to display both polymeric and salt-like properties appears to be unique. The term "halatopolymers" has been introduced to describe that group of materials which can display salt and polymer properties [9,15].

The presence of metal dicarboxylates in the main chain results in a strong dipole interaction between chains and a corresponding brittle behavior. Regarding the brittleness of halatopolymers, one could possibly overcome that by introducing some flexible segments, such as polytetramethylene oxide (PTMO) or other common types soft segment used for the polyurethane elastomers synthesis, to the polymer backbone [16].

5.2.2. IONENES:

Ionenes are those polyquaternary ammonium compounds where the ammonium cation is integral part of the main chain, as opposed to those materials where the bound positive sites are pendant to the chain. Integral quaternaries can be either on a linear chain or a cyclic (aliphatic or aromatic) species; in any case they form part of the backbone. Three examples follow:

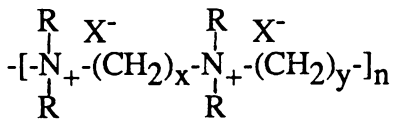

X, Y, Ionene

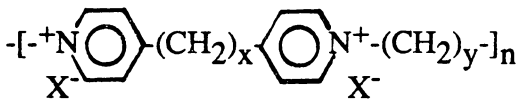

Aromatic Ionene

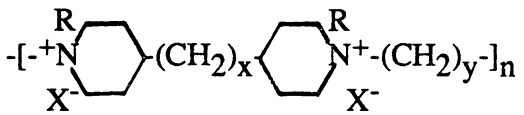

A Polypiperazine

The name "ionene", which was coined by Rembaum et al. [23,24], has been widely accepted and generally is used to describe this type of materials.

5.2.2.1. Synthesis:

Ionenes have been known for over half a century since the work of Gibbs and Marvel [18-22] in the early 1930s with ω-haloalkyldialkylamines. Their research is summarized as the following reactions:

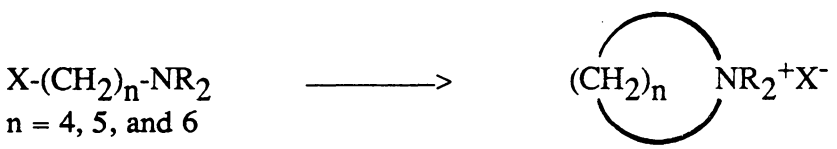

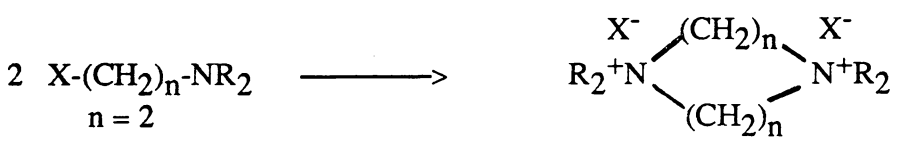

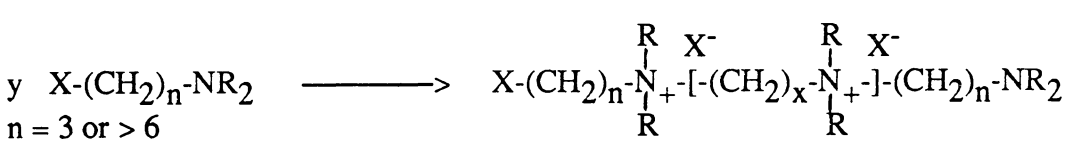

They demonstrated that the number of methylene groups separating the halide from the dialkylamine functional group was the major factor governing whether stable cyclic structures or linear polymer would form. It appears to be most favored for the formation of linear polymer, when the number of methylene groups is equal to 3 or is greater than 6. Ionenes prepared by this fashion will be limited to symmetrical structures.

The Menschutkin reaction between a diprimary alkyl halide and a ditertiary amine has been widely used to prepare ionenes [23-29].

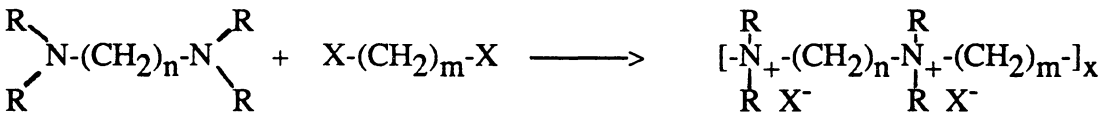

In this way, either symmetrical or unsymmetrical ionene structures can be synthesized. The distance between the positive ions can be changed almost at will. Therefore, one can tailor the hydrophilic and hydrophobic characteristics of the ionene by altering the number of methylene groups (either n or m).

Initial ionene synthesis by using Menschutkin reaction was done by Kern and Brenneisen [27]. They were be able to obtain hygroscopic, polymeric salts varying in molecular weight from 3,000 to 10,000 where R = methyl, X = bromo, n = 2, or 3, and m = 3, 5, or 10.

Rembaum et al. [24, 30-34] have been major investigators in this field. They have further elucidated mechanisms involved in the step growth polymerization of both the A-A/B-B (diamine/dihalide) reaction sequence and the A-B (dialkylaminoalkylhalide) reaction to form ionenes of well defined character. Rembaum has shown that the reaction of both diamine/dihalides and haloalkylamines goes through a cyclic intermediate stage involving cyclic ammonium salts (azetidinium ions) which he confirmed by NMR studies.

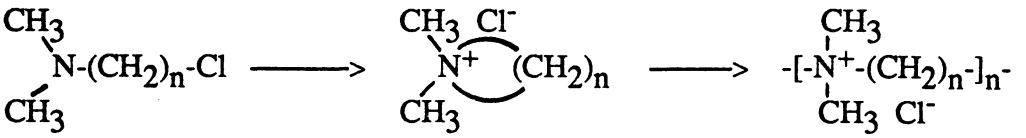

They also have reported that for the Menschutkin reaction, where R was typically a methyl group and X was a bromo group, polymers with a weight average molecular weight of 10,000 - 15,000 were usually obtained when n and m were greater than three [29]. When n and m were less than three, either cyclic or unexpected linear compounds normally resulted.

Aromatic diamines such as 4, 4'-dipyridine (where n = 0) and 1,3-dipyridylpropane (where n = 3) have also been used to prepare aromatic ionenes with interesting properties [36].

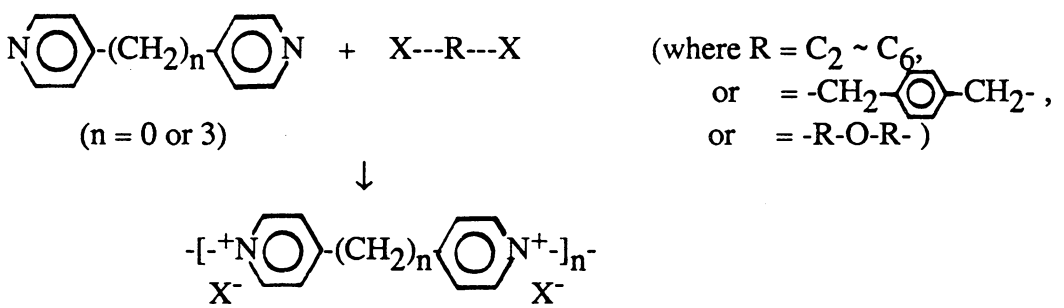

These materials are useful redox polymers, especially in aqueous solutions, but films made by casting techniques are brittle and difficult to work with unless bodying polymers are used.

Simon et al. [35] tried to design film-forming aromatic ionenes by preparing N,N'-bis-aminoalkyl-4,4'-dipyridinium salts and converting to polyamides by

condensation with difunctional acid chlorides. The Schotten-Baumann reaction was carried out at room temperature by interfacial condensation.

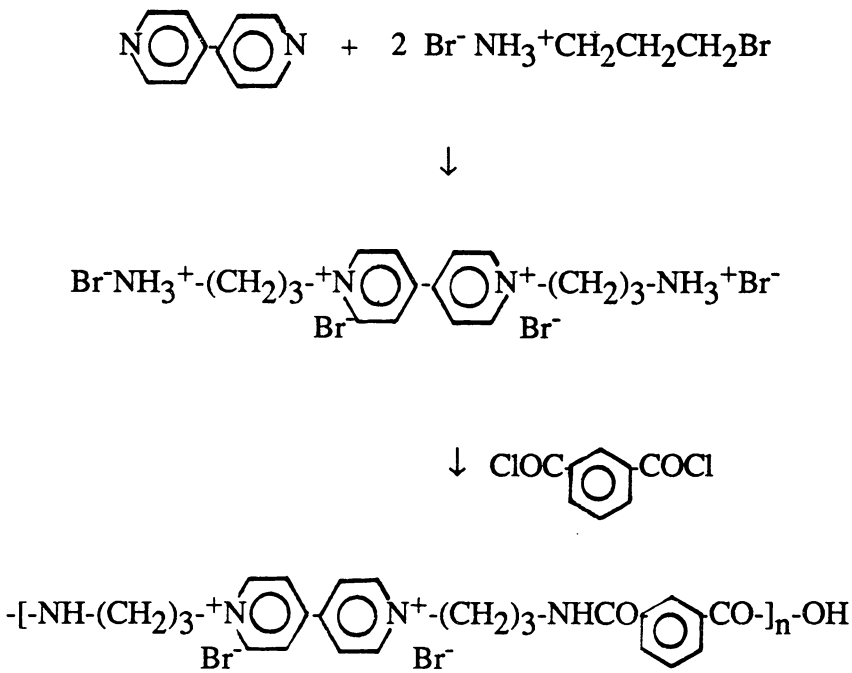

The resulting polymers gave somewhat viscous solutions in water and could be cast to form tractable films.

Salamone and Snider [25] prepared ionenes by using rigid bicyclic tertiary amines such as triethylene diamine and normal primary aliphatic dibromides or xylene dibromide to yield ionene polymers with the following structure:

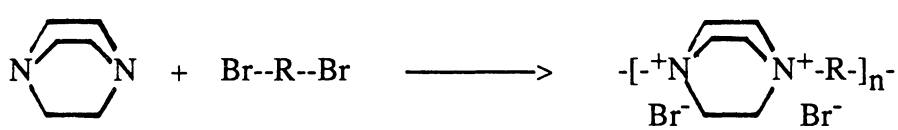

The purpose of the use of bicyclic tertiary amines is twofold which are to reduce the possibility of cyclization as cited by Rembaum [29] and also to use a highly nucleophilic amine, due to the fully exposed nitrogen lone-pair electrons.

Due to its high rigidity, It could be considered to be in a rod-like conformation in dilute water solutions. Therefore, it has been utilized as a preoriented matrix media in which p-styrene sulfonic acid was polymerized on matrix polymer backbones [40]. The estimated distance between two consecutive charges (4.5 Å) is such that the two double bonds of successive monomeric gegenions are within suitable proximity for easy polymerization [42]. This provides a simple model system to study the kinetic and structural factors in "template" polymerization. Many naturally occurring reactions such as the synthesis of nucleic acids, proteins, and polysaccharides take place by means of "template" or "matrix" polymerization. The complexity of the natural polymerization processes is responsible for the scarcity of data in this field.

More recently, Sugiyama et al. [41] prepared an interesting ionene polymer system containing aza-crown ethers and phosphatidylcholine analog moieties, which they expected might be useful as a potential biomedical material.

5.2.2.2. Properties of Ionenes:

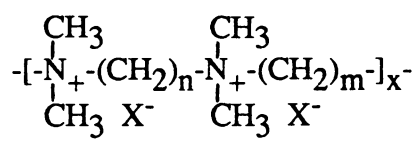

Because their regular structures, ionenes are often highly crystalline. A direct

determination of the glass transition is therefore impossible. In addition, ionenes are generally hydrophilic and cannot be dried completely without serious decomposition. Water contents in the polymers caused even more difficulty on the glass transition studies, since they plasticized the polymer. One approach has been to plasticize each particular ionene to various extents, measure the T_g values as a function of composition, and extrapolate to zero plasticizer content. The extrapolation procedure employed the following relationship [37].

$$T_g = w_1 T_{g1} + w_2 T_{g2} - \kappa w_1 w_2$$

where w is the weight fraction, T_g, and T_{g1} and T_{g2} are the glass transition temperatures of the polymer and diluent, and κ is a constant. The solvents used in the study included water, glycerine, and formamide, for which the glass transition temperatures are either known or can be determined by extrapolation.

It is found that [38] the solvent used to plasticize ionenes has a drastic effect on the glass transition values. The value for the 6,8-ionene is -4 ^{o}C with water, in contrast to the -82 ^{o}C obtained with glycerine. This effect has been related to the conformational change of ionene structures in different plasticizer with wide range of dielectric constants. The glass transition temperature of 6,8-ionene obtained by using various plasticizers is plotted versus dielectric constant of the plasticizer as shown in Figure 5.2 [38]. This illustrates dramatically that a determination of the T_g of an ionic polymer by data obtained from solutions must be interpreted with caution.

The viscoelastic properties of ionene polymers have also received attention. Tsutsui et al. [39] studied the properties of a system termed x,y-oxyethylene ionene (x,y-OEI) (structure as shown below), where x and y varied from 2 to 5.

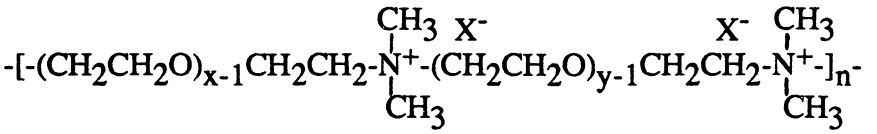

The temperature dependence of the dynamic mechanical properties of these materials was studied by torsional braid analysis over the range -170 to +150 ^{o}C. For each polymer, except 2,2-OEI, two dispersions were observed, as seen in the examples shown in Figure 5.3 [39]. The temperature of T_{α} of the primary dispersion was found to be linearly dependant on the charge density along the ionene backbone and was identified with the T_g of the amorphous phase of the polymer. The low temperature or ß dispersion showed as no regular temperature dependence. It was associated with a "local mode" dispersion. Both relaxation regions were greatly influenced by the presence of absorbed water.

Most standard texts of organic chemistry state that the decomposition of quaternary tetraalkylammonium salts yields an alkylhalide and tertiary amine, when the dry salt is heated to fairly high temperatures.

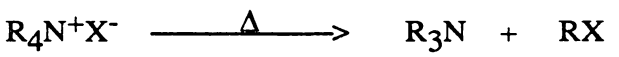

The reaction is thus the reverse of the Menschutkin reaction. This unique character of ionenes has been proposed to be advantageous in ionene processing [47]. Melt viscosity of ionenes expected to be very low, by virtue of the depolymerization at elevated temperatures. Polymer may be regenerated by a repolymerization of ditertiary amine and dihalide at lower temperatures. However, this concept has not been very successful.

The decomposition of ionene salts in solution has also been studied, e.g. in

chloroform [44-46] and in aqueous solution [43]. It is found that tertiary amine and halide are the only products after decomposition. Fujii's results [43] show that the longer the methylene chain between neighboring charges on the polymer backbone, the greater is the degree of dissociation, as Manning's theory predicts. Manning's theory [48] states that a fraction of the counterions of polyelectrolytes in aqueous solutions condense on the polymer when the quantity ξ, defined by the equation

$$\xi = q^2 / \varepsilon \kappa T b$$

is greater than unity. Here q is the protonic charge, ε is the bulk dielectric constant of the solvent, κ is Boltzmann's constant, T is the Kelvin temperature, and b is the distance between neighboring charges on the polymer molecule in its configuration of maximum extension. The degree of dissociation of the counterions in a salt-free solution at infinite dilution is ξ^{-1}.

Solution properties of ionenes have been investigated by many authors [26, 49-52]. Polyelectrolyte behavior has been observed as seen in Figure 5.4 [26]. As the concentration of the polymer decreases in salt-free or extremely dilute salt solutions, the charges on the backbone become less shielded by the counterions, leading to an increase in intramolecular repulsion. This caused the polymer to expand, resulting in a dramatic rise in reduced viscosity. As the ionic strength of the aqueous solution increased by the addition of small amount of salt such as KBr, ionenes behave as a nonionic solutes. Therefore, with some special precautions, molecular weights of ionic polyelectrolytes may be measured by light scattering and equilibrium ultracentrifugation, and intrinsic viscosity-molecular weight relations may be established, in the presence of added salt.

Knapick et al. [26, 49] observed that aliphatic ionenes behave as an electrolyte when quaternary N-alkyl groups is small and as a polysoap when the length of the N-alkyl group increases. Polysoap behavior was indicated by a decreasing overall reduced viscosities and the steepness of the reduced viscosity / concentration curves. The charge density of the polyelectrolyte seems less important than the length of the pendant alkyl group in the onset of polyelectrolyte-polysoap transition. In general, a polysoap can be defined as a polymer in which soap molecules are part of the covalent structure. It is an interesting and useful subclass of polyelectrolytes.

Ionene polymers have been interesting for many years due to their unusual properties. It has been reported that ionenes exhibit certain biological properties, such as acting as bacteriocidal and antiheparin agents [29]. Photochromic [35,36] and thermochromic behaviors have also been observed while ionene polymers containing viologen groups in the main chain. They can used in variable light filtering devices which may be actuated by the action of light or by heat. The discovery [11] of high electronic conductivity of positive polyelectrolytes complexed with 7,7,8,8,-tetracyanoquino-dimethane (TCNQ) has stimulated the research on the electronic transport properties of ionene polymers [29, 55, 56]. Several patents have been issued on the application of ionene polymers to produce cationic permselective membranes by incorporation into other polymeric binder systems [57].

5.2.3. Ionene Elastomers:

Ionenes synthesized from low molecular weight dialkyl halides and ditertiary amines are generally brittle and lack mechanical strength. For most industrial applications, it is

desirable that a polymer possess good film-forming properties which allows it to be shaped by conventional processes such as compression molding and solvent casting. The incorporation of flexible chains, such as polypropylene oxide (PPO) and polytetramethylene oxide (PTMO), into the matrix polymer has been generally utilized [47, 55, 56, 58-61].

Elastomeric ionenes based on the dimethylamino-terminated polytetrahydrofuran and p-xylene dibromide have been prepared by Kohjiya et al. [59, 60]. The reaction scheme is shown as follow

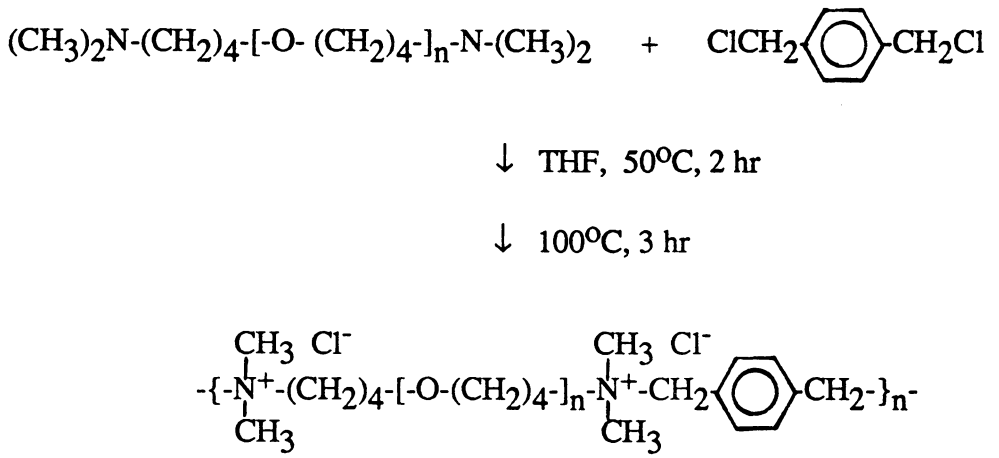

Dimethylamine terminated polytetrahydrofurans were prepared by the living cationic polymerization of THF terminated by dimethylamine. Basically, poly-THF with any molecular weight can be prepared and molecular weight is increase with conversion. The functionality was found to be approximately two, which indicates dimethylamino groups are located at the both ends of poly-THF. The difunctional initiator utilized in the THF polymerization was trifluoromethanesulfonic acid anhydride which was first reported by Smith and Hubin [62]. Detailed initiation mechanism of this novel initiator will be discussed in the next section.

Solution properties of ionene elastomers are very interesting as shown in Figure 5.5

[59], which shows an ordinary viscosity behavior in $CHCl_3$ while behaving as a polyelectrolyte in CH_3OH. This may be the first example that a polymer shows both electrolytic and non-electrolytic behaviors according to the solvent without any salt addition. As the polymer ionic concentration goes up, i.e. decreased molecular weight of poly-THF between two quaternary ammonium groups, an enhancement of polyelectrolyte behavior was observed.

The tensile properties of poly-THF ionene elastomers are also promising. The ionene with the poly-THF segment molecular weight of 4400 shows a tensile strength of 27 MPa and an ultimate elongation larger than 1000 %. Strain-induced crystallization of polyoxytetramethylene units was observed after 500% elongation which was indicated by a sharp rising stress during stretching. However, the polymer is poor in terms of recovery properties (permanent set of ca. 500%).

Leir and Stark of the 3M Company [47] studied the effects of dihalide structure on the polymerization rate with dimethylamino terminated poly-THF. They found that the reactivity of all benzyldihalides can be enhanced by the electron donating substituents on the benzene ring. However, the polymerization rate and ultimate polymer molecular weight were most influenced by the type of the leaving group (halides), which increased in the order of Cl < Br < I. Although their polymers show excellent mechanical strength at room temperature, the use as a thermoplastic elastomer was hampered by irreversible degradation during molding.

Watanabe et al. [55,56,58] have extensively investigated the ionene elastomers based on polypropylene oxide (PPO) for possible applications such as ionic and electronic conductors. The preparation of PPO based ionenes is shown in Figure 5.6 [56]. They modified commercial available hydroxy terminated polypropylene oxide by reacting with excess toluene- diisocyanate (TDI) to form an isocyanate terminated prepolymer.

Dimethylamino terminated PPO was obtained by the end-capped reaction of isocyanate terminated PPO with stoichiometric amount of 2-dimethyl-aminoethanol. Successively, polymerization proceeded by the Menschutkin reaction between dimethylamino terminated PPO and a chain extender, either 4,4'-bipyridine or 1,2-bis(4-pyridyl) ethylene. The same procedure was also applied for the synthesis of polytetramethylene oxide urethane ionenes [58].

The simple TCNQ (7,7,8,8-tetracyanoquinodimethane) salts of the elastomeric ionenes were prepared by the reaction of the ionenes with LiTCNQ in a methanol-ethanol mixture at room temperature under nitrogen atmosphere [55].

It was confirmed by electronic spectra that bromine ions of the elastomeric ionenes were completely exchanged by $TCNQ^{-}$ of LiTCNQ. Complex salts were obtained by evaporating DMF under reduced pressure after dissolving the simple salt and neutral $TCNQ^{o}$ in DMF.

The TCNQ salts of the elastomeric ionenes contained 4,4'-bipyridinium or 1,2-bis(4-pyridinum)ethylene rings showed low resistivity of ~10 Ωcm and could be obtained as flexible films. Mechanical strength was improved by introducing flexible polyether chains into the ionene without decreasing the electronic conductivity. Furthermore, they found [63] that the drawn films of these TCNQ salts showed conductivity anisotropy.

Several interesting features of ionenes have made them special as a conducting

material. First, the complex of polycation and TCNQ is known as an organic semiconducting polymer. The ionene TCNQ salts containing 4,4'-bipyridinium or 1,2-bis(4-pyridinium)ethylene rings show the highest conductivity among the polycation-TCNQ salts obtained [65]. Second, it contains N^+ atoms in the main chain and the intervals between N^+ atoms are fixed to 6 - 8 Å by rigid ring structure, which allows the complex formation of $[TCNQ^o]$ / $[TCNQ^-]$ = 1.0 [64]. This brings about simultaneously a lowering of the Coulomb repulsion between carrier electrons and an increase in the overlap of π-electrons of TCNQ molecules.

Unaware of the work of Kohjiya and his coworkers [61], the author prepared two series of polytetrahydrofuran ionene elastomers by the coupling reactions of "living" PTHF dioxonium ions with either 4,4'-bipyridine or 1,2-bis (4-pyridinium)ethylene. All of those polymers show excellent mechanical properties while 4,4'-bipyridine based ionenes show superior thermal stability relative to the 1,2-bis (4-pyridinium) ethylene based polymer. Thus, although we were not the first to disclose this novel idea in the literature, our work does provide a systematic study of the structure-property relationship of PTHF ionene elastomers.

Kohjiya et al. [61] were interested in the incorporation of organic photochromic groups such as 4,4'-bipyridine into the polymers. They utilized 4,4'-bipyridine to terminate, (actually chain extend), the living PTHF dioxonium ions in which the ring-opening polymerization of THF was initiated by trifluoromethanesulfonic acid anhydride. Both polyelectrolytic and photochromic behavior were observed in this material. However, no systematic study of those phenomena has been reported yet.

In the literature, Cunliffe et al. [66] have reported that they failed to couple bipyridine with living dioxonium ions. Their difunctional initiator utilized for the ring-opening polymerization of THF was the combination of silver hexafluorophosphate

with p-xylene dibromide.

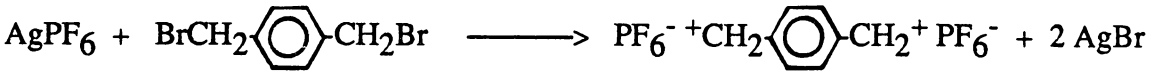

Perhaps, their failure may be due to the unstability of the counterion [67].

5.2.4. POLYTETRAHYDROFURAN:

Polytetrahydrofuran (PTHF) is a linear polymer consisting of a chain of methylene

$$-[-CH_2CH_2CH_2CH_2O-]_n-$$

groups with an oxygen atom inserted after every fourth methylene unit. The polymer is also referred to as poly(tetramethylene oxide) or polyoxytetramethylene. PTHF is a low melting, crystallizable polymer and is characterized by a low glass transition temperature, T_g. It is possible to synthesize PTHF of almost any molecular weight. Due to its low melting temperature, ca 50°C, high molecular weight PTHF homopolymer hardly finds any practical utility. It is only the low molecular weight hydroxy-terminated PTHF that has commercial application.

This material, when incorporated as flexible segments in a polyurethane or polyester, impart favorable and useful properties. In the United States, diprimary diols

from PTHF are available in commercial quantities from DuPont and Quaker Oats under the trade names Teracol polyether glycols and Polymeg Polyols, respectively. In 1981, annual consumption of such glycols was ca 27,000 metric tons in the United States and ca 1400 -2300 tons each in Japan and Europe. The typical 1981 price, depending on the molecular weight and quantity purchased, was $ 3.11 - 3.62 / Kg fob. The price of PTHF is dominated by the cost of the monomer which, in 1981, cost $ 1.76 / Kg fob in tank-car lots. Due to the high cost of THF monomer relative to that of monomers like butadiene, ethylene and propylene, PTHF does not compete as a general-purpose rubber. If, and when, a more economical route to the production of THF is obtained, this economic picture could change.

5.2.4.1. Monomer Synthesis:

a. Furfural Route - The oldest synthetic route to THF is based on furfural as feedstock [68]. This method is still being used in the US by the Quaker Oats Co., which produces large quantities of furfural.

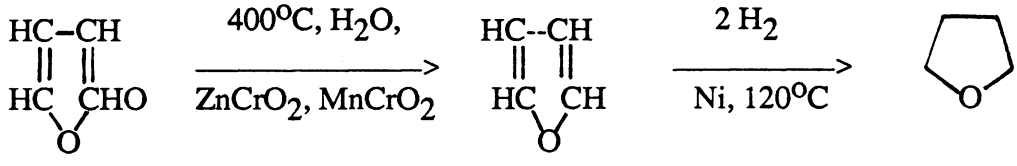

The furfural route has been largely replaced by other synthetic routes based on acetylene/formaldehyde, maleic anhydride and butadiene as feedstocks.

b. Reppe Process - This process is based on acetylene/formaldehyde.

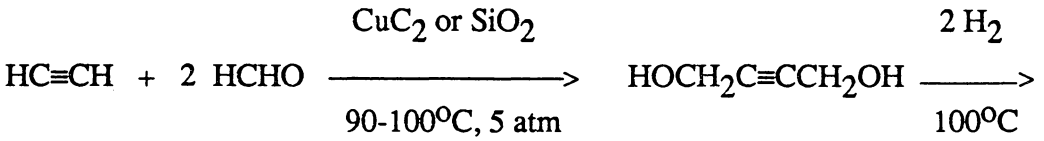

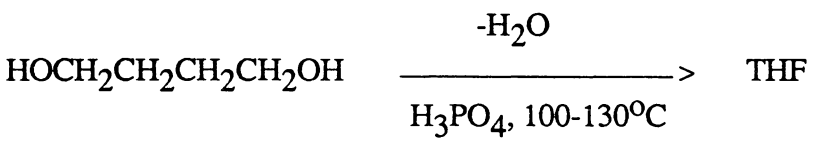

The Reppe route was originally developed by BASF of Germany. The Company claims that this route is the most economical one for large-scale production with greater than 5,000 tons/year capacity. DuPont, the only US producer of THF besides Quaker Oats, also uses this process [69].

c. Maleic-Anhydride Route - It is based on the direct catalytic hydrogenation of maleic anhydride and was developed by Mitsubishi Petrochemicals of Japan [69].

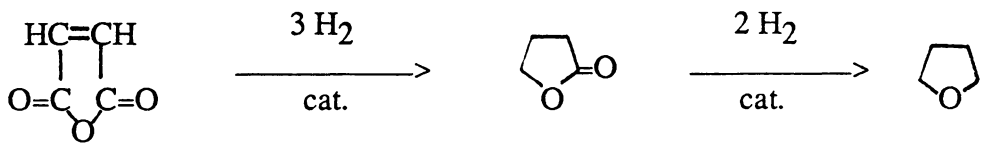

The choice of catalyst is very important. However, the nature of the commercial catalyst has not been revealed in the open literature.

d. 1,4-Dichlorobutene Route - The newest route with industrial potential, developed

by Toyo Soda Co., uses butadiene as feedstocks and also yields chloroprene, a valuable monomer [69].

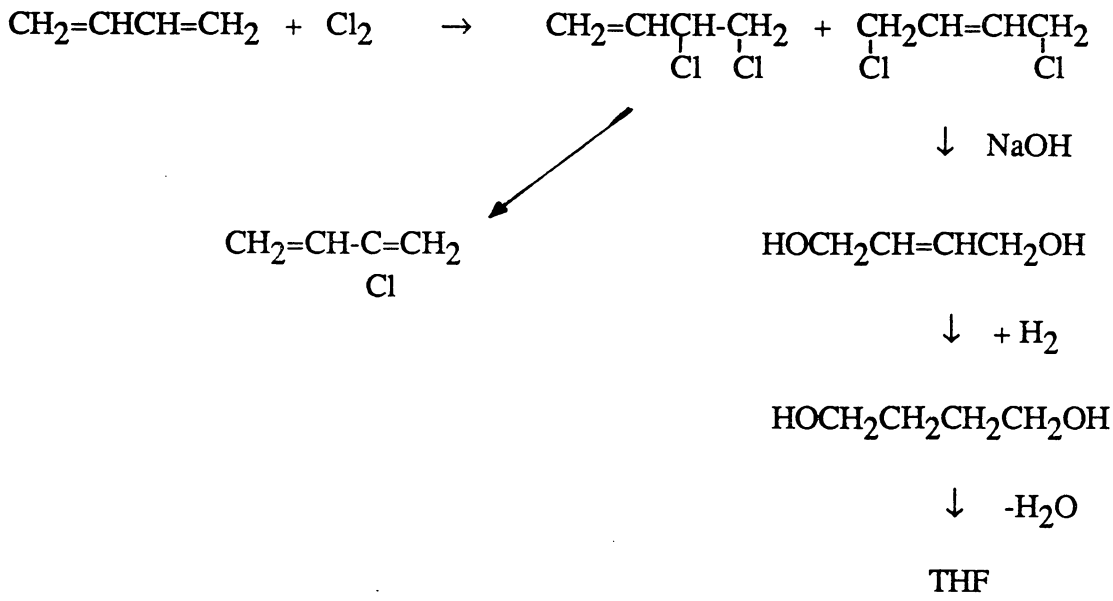

5.2.4.2. Polymerization:

Tetrahydrofuran (THF), is a Lewis base and can only be polymerized by cationic or onium ion methods. Requirements for a successful polymerization include: pure, dry reagents; dry apparatus and exclusion of air by the use of either high vacuum or an inert atmosphere such as dry nitrogen.

Such a possible route for THF polymerization is reviewed in Figure 5.7 [67]. The monomer **I** can be attacked either by a stable oxonium ion such as **II** or a proton source to generate the initiated species **III**. The oxonium ion thus produced can be interact with monomer **I** to generate, essentially, a living polymerization. The terminal unit of **IV** should still bear an oxonium ion unit. Propagation would involve nucleophilic attack of **I** at the carbon adjacent to the oxonium ion. Termination with water, for example, would produce

a hydroxyl group at one end of the chain. The kinetics and mechanisms of such processes are extremely interesting and have been discussed in a number of books [71, 119] as well as by Penczek [100, 103-105].

The propagating species in THF polymerization is a tertiary oxonium ion:

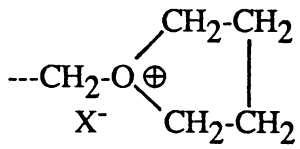

an counterion X^- must be associated with a negatively charged species, for reasons of electrical neutrality. The early work of Meerwein and coworkers [70] has shown that polymerization continues only if the propagation rate is faster than the rate of irreversible reaction of the oxonium ion with its accompanying anion. More firmly bonded elements in a complex ion lead to more stable and more suitable counterions for THF polymerizations and fewer side reactions. The elements that comprise stable counterions for THF polymerizations are found almost exclusively among the nometals in groups VA, VIA and VII A [71].

In ionic polymerization, active centers exist in the form of free ions, ion pairs and their associates. This accounts for the strong dependence of the process parameters (kinetics, molecular weight characteristics and compositions of the reactants) on the nature of the reaction medium. The effects of the medium on the rate and on the extent of polymerization can be summarized as follows [72]:

(1). ion pair - free ion equilibrium.

(2). solvation (electrostatic and specific) of the active center and the counter-ion altering the reactivities of both forms.

(3). Partial separation of the reaction components due to predominant

concentration near the active center either of the more polar or of the more electrodonating component of the solution.

(4). effect of the dielectric medium on chain propagation, i.e. the dipole-ion pair, or dipole-ion reations.

All these effects are closely interrelated and represent in fact different aspects of one phenomenon - the solvation.

Consideration of the expected dissociation constants [73] of the polymerizing oxonium salts in cholorated hydrocarbon solvents would suggest that several percent free ions could well be present. The dissociation constants of such salts have been measured in methylene chloride solution [74] and shown to be near 4×10^{-6}, sufficiently high that a contribution to the polymerization by free ions could be expected.

Penczek and coworkers [75] have shown that both the enthalpy and entropy of polymerization are somewhat dependent on both counterion and solvent. For the $CF_3SO_3^-$ counterion , for example, ΔH_p and ΔS_p^o are respectively equal to: -25.1 ± 1.3 kJ mol^{-1} and -104,6 ± 4.2 J $mol^{-1}deg^{-1}$ in CCl_4; and -23.4 ± 0.8 kJ mol^{-1} and -82.4 ± 3.3 J $mol^{-1}deg^{-1}$ in CH_2Cl_2. The reasons for these differences are discussed in Penczek's paper and are related to structural factors and solvation.

The polymerization of THF is an equilibrium process. Hence, for every temperature there is an equilibrium monomer concentration, M_e, that is thermodynamically determined. The thermodynamics of equilibrium polymerizations have been reviewed by Sawada [79]. In the case of a ring opening polymerization a large number of monomer units must be involved in a propagation step to generate a macromolecule. The Gibbs equation, $\Delta G = \Delta H - T\Delta S$, must yield a negative free energy change for the propagation reaction if high molecular weight is to be achieved [67]. A slightly negative free energy of polymerization of about -3350 J mol^{-1} at 25°C [76] has been estimated from the experimentally derived

ΔH of -18.8 kJ mol^{-1} and ΔS of about -75.3 J $deg^{-1}mol^{-1}$. The standard free energy change is made up of enthalpy and entropy contributions which together with reaction temperatures define the magnitude and sign of the free energy.

There is also a ceiling temperature, T_c, above which no polymerization at all will occur. A plot of conversion to PTHF as a function of temperature is shown in Figure 5.8 [77]. The T_c thus derived is $83 \pm 2\ ^{o}C$. Dainton and Ivin [78] have related M_e to the absolute temperature T in the equation.

$$\ln [M_e] = \frac{\Delta H_p}{RT} - \frac{\Delta S_p^{o}}{R} = \frac{\Delta G_p}{RT}$$

Figure 5.9 [76] show that for THF polymerizations the plot of ln $[M_e]$ versus 1/T gives a straight line, where ΔH and ΔS can be derived from the slope and the intercept of the curve, respectively.

Since the conversion to PTHF at any given temperature clearly depends on the monomer concentration and is independent of the polymer concentration, inert diluent reduces the conversion to polymer at a given temperature. There are practical limits to how low a temperature can be used. Below ca $-20^{o}C$, the rate of propagation becomes so slow that prohibitively long times are required for significant conversions to PTHF.

No termination would occur if the counterion was stable with respect to a single propagating THF-oxonium ion [80,81]. Szwarc [82] has given the name "living" to this type of polymerizations. In living chain polymerization, termination and transfer reactions are absent and the polymerization is described by initiation and propagation reactions only. If the initiation reaction is faster than propagation, the resulting molecular weight distribution is narrow. The molecular weight of a polymer isolated from a "living" system

depends only on the number of growing centers and the amount of monomer available for polymerization. Another consequence of a "living" system is that eventually a steady state is attained where the "living" polymers are in equilibrium with their monomer, and the rate of propagation becomes equal to the rate of depolymerization.

The "living" nature of THF polymerization provides opportunity for the synthesis of PTHF of any desired molecular weight with a narrow molecular weight distribution and with controlled end groups. However, a careful balancing of thermodynamic, kinetic and mechanistic considerations is essential if this goal is to be achieved. The subjects of the cationic polymerization of THF and the conditions required to produce a living PTHF having one cationically active end group per chain have been comprehensively reviewed [71, 83].

A "macromer" can be synthesized by a proper choice of the nucleophile to terminate the living oxonium ions. "Macromers" are short polymer molecules with functional ends, that is polymerizable in turn. Copolymerization of a vinylic (or acrylic) monomer with a macromer should result in a graft copolymer, the macromer units constituting the grafts. Growing interest has been recently paid to the synthesis of macromers for their potential applications as intermediates for the synthesis of graft copolymers [84-86].

Polytetrahydrofuran macromers have been investigated by many groups around the world [87-89]. Unsaturated nucleophiles used for the termination of living oxonium ions have included sodium p-vinylbenzyloxide [89] and potassium p-isopropenylbenzyloxide [87].

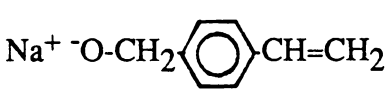

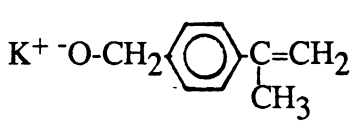

They have proved to be effective for the PTHF macromer synthesis. An alternate method reported by Sierra-Vargas et al. [88], which they utilized unsaturated oxocarbenium salt to initiate the polymerization of THF. The reaction is illustrated as follow:

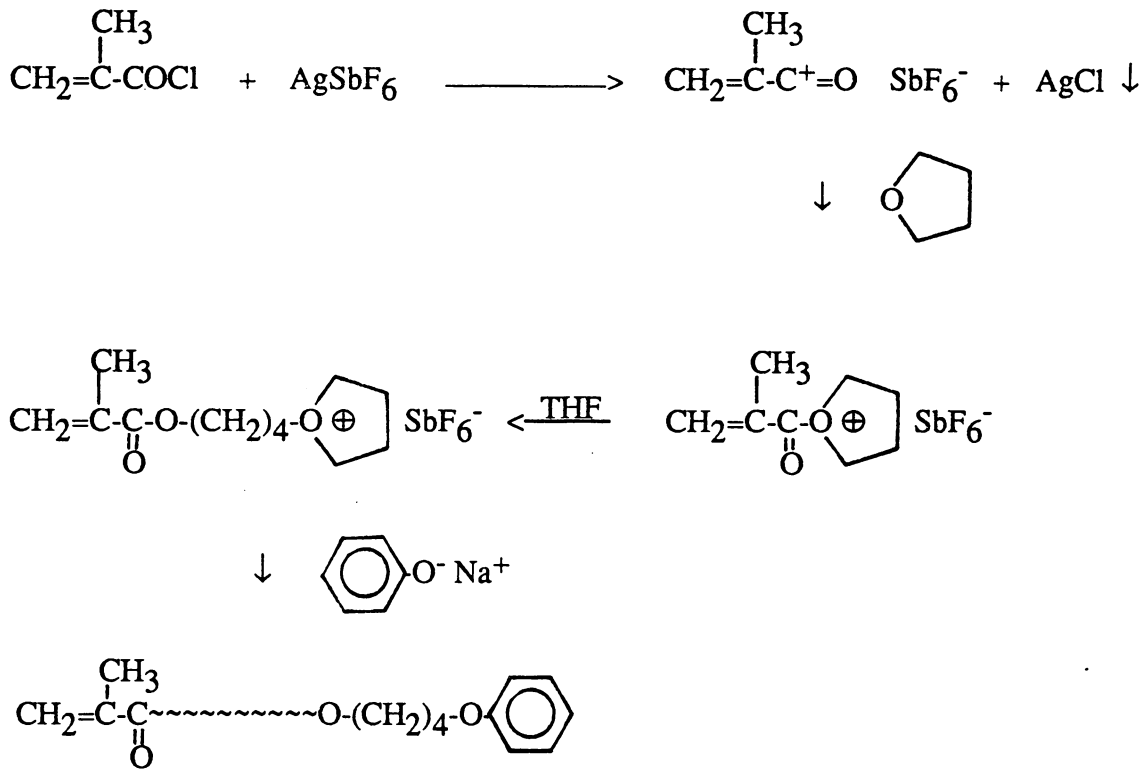

The macromers obtained were found to be well defined, of narrow molecular weight distribution and with quantitatively polymerizable terminal double bonds.

Telechelic liquid polymers, oligomers with exactly two functional end groups, constitute an important class of polymeric materials that have gained significance in practical applications as well as in scientific research. Commercial polyurethanes and polyesters containing PTHF are based on α,ω-diprimary diols of relatively low molecular

weight, with Mn ranging from 650 to 3000.

The traditional as well as the simplest and most direct method of preparing PTHF glycol is to initiate the polymerization of THF with protonic acid which leads to the formation of an OH head group and termination of the polymerization with water which produces an OH end group.

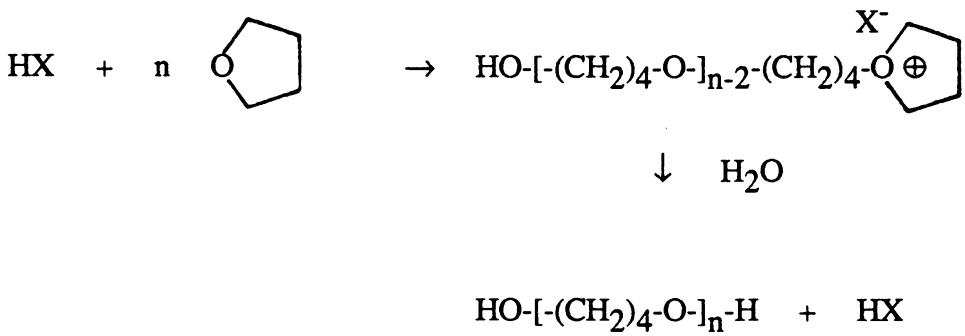

This process have several disadvantages, e.g. the acids cannot be recovered and reused. Moreover, the presence of hydroxyl groups during polymerization markedly increased the molecular weight and broadens the molecualr weight distribution [90].

Many of the problems associated with the direct preparation of PTHF glycol can be overcome by preparation of a diacetate ester intermediate. This is accomplished by polymerization of THF with strong protonic acid in the presence of acetic anhydride [91-93]. In the presence of acetic anhydride, the hydroxyl is quickly converted to an acetate, and transfer reactions with acetic anhydride cause formation of stable acetate end groups and molecular weight control. For detail information, readers can refer to the references cited.

All the a α,ω-diprimary diols utilized in the synthesis of polyurethane elastomers are based on DuPont's Teracol Polyether Glycols. Therefore, it is necessary to mention how

Teracol has been prepared industrially. The strong acid catalyst that DuPont may be used commercially for the synthesis of hydroxy-terminated PTHF is Nafion resin ($NfSO_3H$) [94]. In its free acid form this resin has the structure:

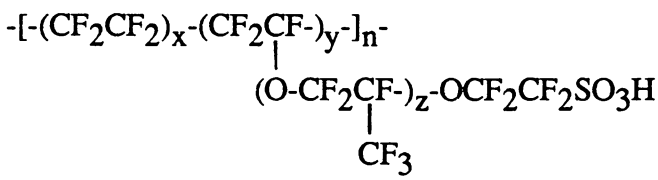

When PTHF glycols are prepared using this resin the reaction mixture normally includes acetic anhydride and acetic acid in addition to THF [95]. The reaction scheme is shown in Figure 5.10 [71]. Many reactions probably occur simultaneously and in a competing manner in the course of this synthesis. For example, similar reactions would occur with HSO_3F-acetic anhydride-acetic acid mixtures, except that free acid would be one of the products of the termination step. The diprimary glycol can be obtained from the diacetate ester by alcoholysis or hydrolysis of the diacetate by boiling 2-3 h with 0.5N alcoholic KOH [109]. Polytetrahydrofuran glycols with molecular weights of up to ca 10,000 can be purified by dissolving in ethyl ether and washing with water.

Other difunctional initiators lead to PTHF with oxonium ions on both ends of the chain such as 2,2'-octamethylene-bis-1,3-dioxolenium perchlorate [96,97], trifluoromethane sulfonic acid anhydride [62,98], phosphorous pentafluoride [99], terephthaloyl and adipoyl salts [100], xylene dibromide and silver salts [101], and silenium dication [102]. When these difunctional PTHF oxonium ions are treated with water, PTHF diol is formed:

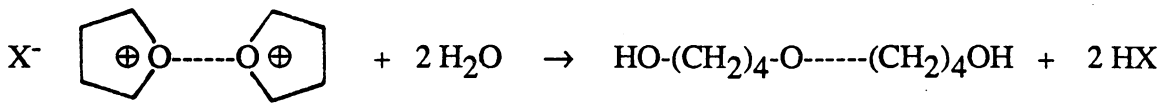

Among these difunctional initiators mentioned, special emphasis will be focused on trifluoromethane sulfonic acid anhydride, $(CF_3SO_2)_2O$, which was reported by Smith and Hubin [62]. The use of the anhydrides presents an exciting new development since it allows the very simple preparation of dicationic systems. This initiator was utilized throughout this research. The growing interest in both academic and industrial environment can be easily appreciated by the number of papers published related to the application of this catalyst.

Initiation involves an O-sulfonation of THF to generate an oxonium salt, as shown below:

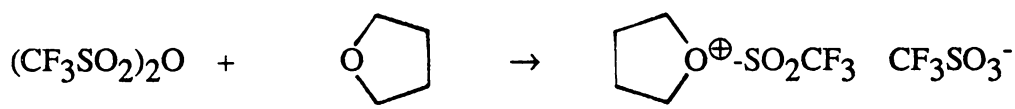

Propagation involves the progressive nucleophilic attack of THF monomer at the α-carbon atom of the oxonium ion chain end, as indicated:

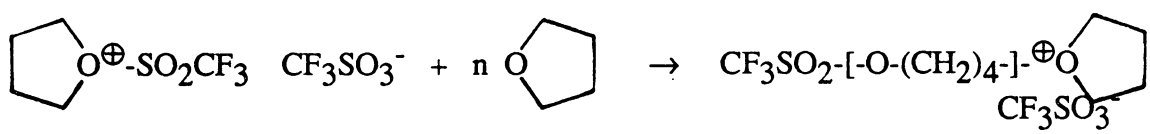

Both Saegusa [106] in Japan and Penczek [75, 103-105] in Poland have proposed some

interesting new chemistry. An understanding of the important ion-ester equilibrium is required:

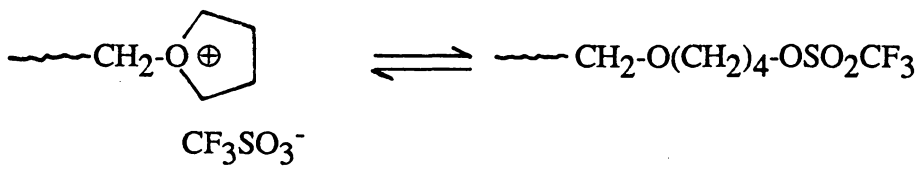

Both macroion and macroester forms appears to be capable of sustaining polymer growth at both ends, albeit at considerably different rates. The oxonium ion is appreciably much more reactive than the ester end group in the polymer propagation process. The relative equilibrium concentrations of the ester and oxonium ion end groups in a variety of solvents with wide variation in dielectric constant have been determined by using ^{1}H [104], ^{19}F [98], and ^{13}C [107]. Penczek et al. found that [104] the macroester form dominates (96%) in CCl_4 and only 8% of macroester could be detected in nitromethane. In CH_2Cl_2, both species coexist in comparable concentrations, [macroion] : [macroester] = 1 : 3. The increase in the dielectric constant of the medium would, of course, be expected to shift the equilibrium in the direction of macroion formation.

Polymers with active cations at both chain ends open up a host of possibilities for preparing block copolymers and polymers with functional end groups. Many of these possibilities had been recognized and were explored by Smith and Hubin [62]. The coupling reaction between "living" dianions and dications is not a new subject in the literature. Saegusa and Matsumoto [113] developed the phenoxy end-capping method for the determination of the concentration of the cationic living end. They proved that the occurrence of quantitative ion coupling between sodium phenoxide and PTHF cation. Berger et al. [120] suggest the possibility of mutual termination of both anionic and

cationic "living" systems to form block copolymers. However, they were not particularly successful in ion coupling of PTHF dioxonium ion and polystyrene dianion. The presence of a dication is necessary when multiblock chains are to be prepared. Yamashita et al. have reported on the preparation and use of bis-dioxolenium perchlorate [97]. The product which is formed by the polymerization of THF in the presence of this initiator contains two ester groups which might be preferably attacked by the carbanion end of the polystyrene chain. Yamashita et al. [121, 122] therefore transformed the carbanions to less basic carboxylate ions by treating the former with CO_2. Although the procedure is rather complicated these authors first obtained multiblock copolymers by the process of combination. Besides the already mentioned bis-dioxolenium perchlorate also some other different dications have been described in the literature [62,101,102].

The combination of living PTHF with base anions suggests that coupling might also occur with bases such as tertiary amines to form polymeric quaternary ammonium salts [66,108].

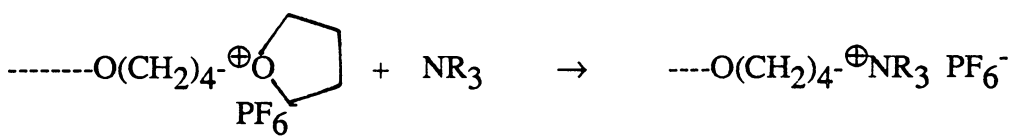

Quaternary ammonium salts are generally stable compounds and to the extent that the reaction (written as an equilibrium between molecules of different base strength) lies to the right, it is expected that polymerization of THF will stop. Cunliffe et al. [66,108] have shown that pyridine reacts quantitatively with living cationic PTHF to yield terminal pyridinium groups. The reaction between living PTHF and pyridine is rapid, being probably complete in 1 to 2 min at -10°C.

It is interest to note that the introduction of a pyridinium end grouping to the PTHF has little apparent effect in their bulk viscosities in comparison with the equivalent methoxy terminated PTHF [108]. This is marked contrast to the dramatic increases in viscosity which have been observed on quaternization of terminal pyridine units attached at the 4-position to one or both ends of polybutadiene chains [123]. These changes were ascribed to association of the ionic ends into micelles in the presence of the non-polar polymer matrix, thereby producing with monofunctional polybutadiene a material with the physical characteristics of a high molecular weight product, and with the two ended species a pseudo-crosslinked network. PTHF, however, being a polyether is a good cation solvating agent and participates in the solvation of the quaternary ammonium group. This interaction, therefore, limits the association of polymer molecules both by minimizing the ion pair interactions electrostatically and by blocking, at least partly, the approach of another ion pair.

Cunliffe et al. [66] also suggested that tertiary diamines could be used as effective chain coupling agents. The tertiary amines studied are tetramethylethylene diamine (TMEDA), 4,4'-bipyridyl, and pyrazine. The coupling efficiency of the diamines found is in the order TMEDA > 4,4'-bipyridyl >> Pyrazine. Attempts to couple bipyridyl and pyrazine with PTHF dication to high molecular weights were not successful and further work was not continued. Their failure may be due to the unstability of the counterion, PF_6^-.

The research interest is focussed on the coupling reactions of PTHF dioxonium ions, produced from $(CF_3SO_2)_2O$ and THF, with ditertiary amines such as 4,4'-bipyridyl, which produce an ionene elastomer. Similar work has been carried out nearly simultaneously also in another laboratory. Kohjiya et al. [61] have already published an interesting communication. However, no systematic work has been done so

far on the subject of stucture-property relationships of PTHF ionenes. Their primary interest was in introducing photochromic groups such as 4,4'-bipyridyl into polymers. The photochromic material has potential applications in variable light filtering devices. 4,4'-Bipyridinium salts are known as viologen, and represents oxidation-reduction chromophores. Viologens undergo two separate one-electron reduction steps as shown below [36]

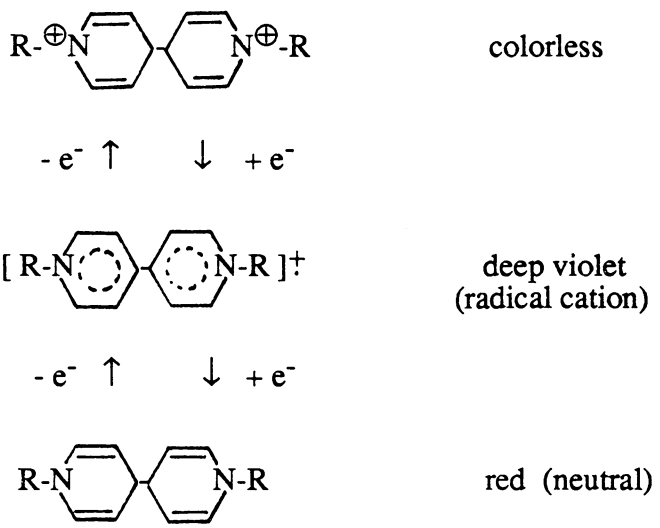

PTHF ionenes, with 4,4'-bipyridinium salts (along the polymer backbone) in between every two PTHF segments, were prepared by Kohjiya et al. [61] using the following approach

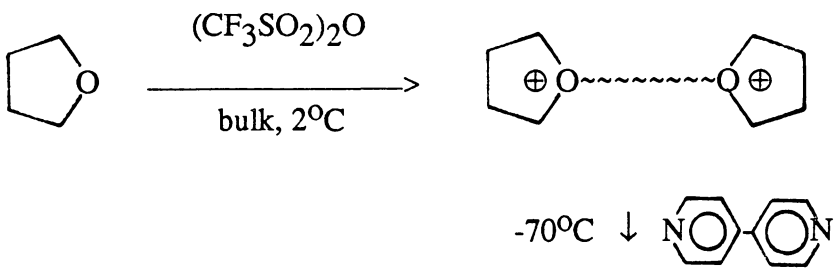

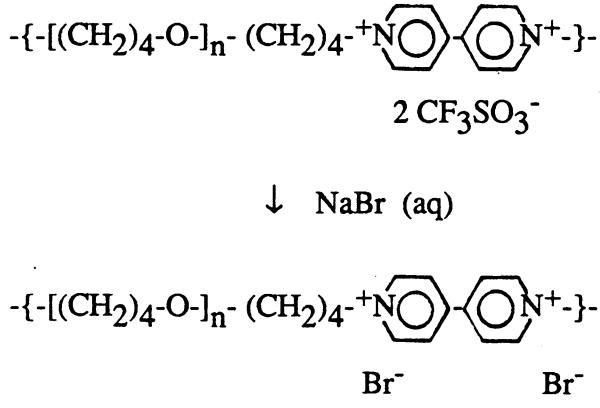

They have observed photochromism on the PTHF ionenes and their results are shown in Table 5.1.

5.2.3.3. Physical and Chemical Properties:

Typical properties of PTHF are summarized in Table 5.2 [83]. Polymers of moderately high molecular weight crystallize readily at, or below room temperature. Upon crystallization the sticky viscous fluid or tacky rubber, depending on molecular weight, becomes an easily handled tack-free wax or plastic-like material.

The only PTHFs of commerce are diprimary low molecular weight polytetramethylene ether glycols or their derivatives. The glycols are soluble in aromatic and chlorinated hydrocarbons, alcohols, esters, ketones, and nitroparaffins and are very slightly soluble in aliphatic hydrocarbons. Like THF, the PTHF glycols normally contain ca 150-250 ppm of butylated hydroxytoluene (BHT) to prevent peroxide formation.

Number-average molecular weights, Mn, of PTHF have been determined by standard techniques. For polymers of low molecular weight, Mn has been calculated primarily from data obtained by end-group analysis. Depending on the nature of the end group, the methods used include titration [110], NMR [111,112], IR [110], UV

[110,113], elemental analysis [110,114], liquid scintillation counting of ^{14}C-labeled end groups [115], and fluorescence spectroscopy [114].

Molecular weight distributions of PTHF have been determined from Mw/Mn ratios derived from gel-permeation chromatography (GPC) [101]. Although the refractive index increments (dn/dc) for PTHF in THF solvent is small, ca 0.064 ml/g, it is large enough so that THF can be used as the elution solvent for a GPC equipment with a differential refractometer as the detector.

PTHF is quite stable to attack by bases but is somewhat acid sensitive. As a polyether, it is subject to oxidative attack and subsequent breakdown, analogous to a monomeric aliphatic ether. The viscosity of a benzene solution heated in air drops steadily in the absence of an antioxidant [116]. In the presence of an antioxidant, eg. 0.5 wt% 2,6-di-t-butyl-4-methyl phenol, the viscosity falls initially but thereafter is constant. When heated in air at constant temperature, the viscosity of PTHF decreases continuously until complete degradation of the polymer occurs. In vacuum, temperatures well over 150^{o}C are needed to degrade the polymer completely. The activation energy for degradation in vacuum reported was 189 kJ/mol (45 kcal/mol) [116]. This value is comparable with that of PPO (46 kcal/mol) but low compared to hydrocarbon polymers, for which the activation energy for degradation is 60-70 kcal/mol. The corresponding value for degradation of PTHF in air is 122 kJ/mol (29 kcal/mol).

Elastomers based on PTHF glycols have excellent fungal resistance, provide good tensile strength and tear and abrasion resistance, and exhibit high vapor transmission and low hysteresis loss. High molecular weight PTHF currently has no commercial applications, although its use as an impact modifier has been suggested [117,118].

5.3. EXPERIMENTAL:

5.3.1. Purification of Monomers:

THF (Fisher, stabilized with 0.1% quinol) was purified by refluxing over fresh sodium for several hours. Addition of benzophenone permitted the deep purple sodium-benzophenone complex to form, which indicates an oxygen-free dried THF. The THF was distilled under dry nitrogen immediately prior to use. Only the middle fraction was collected directly to a flame-dried polymerization reactor - a two-necked round bottomed flask.

Pyridine (FW. 79.10, mp. -42^{o}C, bp. 115^{o}C, d. 0.978 g/cm^{3}), a colorless liquid, was purchased from Aldrich Chemical Co. It was distilled, then treated with calcium hydride under reduced pressure until degassing was complete. A middle cut was obtained by distillation through a glass wool plug prior to use.

Pyrazine (FW. 80.09, mp. 54-56^{o}C, bp. 115-116^{o}C, d. 1.031 g/cm^{3}), was obtained from Aldrich Chemical Co. It was purified by vacuum distillation.

4,4'-Methylenebis(N,N'-dimethylaniline) (FW. 254.38, mp. 88-89^{o}C), a pale-yellow color powder, was obtained from Aldrich Chemical Co. It was purified by recrystallization three times from petroleum ether. A shiny flake-like crystal was obtained after drying in a vacuum oven at 50^{o}C for 24 hours.

4,4'-Dipyridyl (FW. 156.19, mp. 105-108^{o}C, bp. 305^{o}C) of 98% purity was obtained from Aldrich. Purification was easily carried out by recrystallization from hexane for three times. A nice needle-like crystal was obtained in pure form. It was stored in a

desiccator until use.

1,2-Bis(4-pyridyl)ethane (FW. 184.24, mp. 107-110°C) with 97% purity was purchased from Aldrich. Petroleum ether was utilized as the solvent for recrystallization.

5.3.2. Synthesis of the Initiator:

Triflic acid anhydride (TFAH) was used as the initiator for the ring opening polymerization of THF. It allows the very simple preparation of "living" PTHF dicationic systems. TFAH (FW. 282.13) is available thru Aldrich Chemical Co. for the relatively expensive price (ca $77.7/50g) in comparison with its free acid form, CF_3SO_3H (FW. 150.07, bp. 162°C), which is more reasonable ($28/50g).

The method for the preparation of TFAH has been previously described in the literature [124]. The anhydrous triflic acid (50g) and phosphoric oxide (50g) were mixed in a 250 ml one-necked round bottom flask and kept at room temperature for 1 hr. Then the volatile products were distilled through a short Vigreux column to afford trifluoromethane sulfonic acid anhydride, b.p. 78-80°C. No magnetic stirrer is necessary, since trifluoromethane sulfonic acid was homogeneously mixed with powdered P_2O_5. The overall yield is about 65%. The product was tightly capped in a glass bottle and stored in the freezer before use. TFAH is a mobile, hygroscopic liquid, readily hydrolyzed by water, and decomposed appreciably after being kept for a few days, with evolution of sulfur dioxide and formation of a brown, viscous, immiscible liquid.

5.3.3. Synthesis of "Living" PTHF Dioxonium Ions:

Experiments were conducted under nitrogen and exposure of prepared reagents to air was avoided. The apparatus used for the synthesis is pictured in Figure 5.11. All the glassware was flame-dried and then cooled under nitrogen blanket immediately prior to use. A septum was used to provide a good seal and as a port for later transfer of chemicals.

Freshly distilled THF monomer was transfered directly from the distillation set-up to the reactor. The reaction flask was precalibrated in order to know the exact amount (100 ml) of THF charged. A dry box filled with dry nitrogen was utilized throughout the experiment for transferring and weighing chemicals. A reaction temperature of $2^{o}C$ was achieved by using an ice/salt water bath. The 250ml reaction flask containing known amounts of purified THF monomer was initially put into the ice bath and stirred for half an hour under nitrogen in order to obtained an equilibrium reaction temperature.

Initiation induced by syringing the desired amount of TFAH to the stirred-THF solution at $2^{o}C$ produced a clear colorless solution. The ratio of [monomer] / [initiator] was maintained constant for all experiments at about 123 ([12.3moles/liter] / [0.1moles/liter]). The polymerization rate of THF is dependent on the monomer / initiator concentration and the polymerization temperature. In living chain polymerization, termination and transfer reactions are absent and therefore the molecular weight of the resulting living polymer has a linear relationship with monomer conversion. In other words, the molecular weight of PTHF can be controlled by terminating the polymerization at a given time period with a suitable nucleophile.

5.3.4. Coupling Reactions of Living PTHF with Pyridine and Ditertiary Amines:

A solution of tertiary amines (either mono- or di- functional) with a concentration of 0.1 moles/liter in THF was injected at 2°C to the living PTHF solution. A colorless solution resulted in most cases. In the case of 4,4'-methylenebis- (N,N'-dimethylaniline), a light sky-blue color was developed as soon as it mixed with living PTHF solution. In general, coupling reactions were allowed to continue for one hour although the magnetic stirrer was stopped due to the high viscosity in some cases 1~2 minutes after injection of the tertiary amine. Perfect stoichiometry between initiator and ditertiary amine is required to obtain high molecular weight polymer, as would be predicted for a condensation polymerization.

The viscous polymer solution was then slowly poured with vigorous stirring into a 1000 ml beaker containing 600 ml of nearly boiling hexane. Hexane is a non-solvent for the resulting polymer and it was heated for the purpose of removing any possible unreacted ditertiary amines. The terminated polymer was coagulated as a "big rubber ball" and can be quantitatively recovered. Polymers were carefully dried in a vacuum oven at 60°C for 24 h. Due to the hydrophilic nature of the ionic bonds, materials were stored in a desiccator immediately after drying. Polymer conversions were measured by weighing dried polymers in a dry box. Film samples for mechanical testing were prepared by solvent casting from methanol. Films were dried in the vacuum oven at 60°C for 24 hours and then stored in a desiccator before testing.

Among the ditertiary amine chain extenders studied, 4,4'-dipyridyl and 1,2-bis-(4-pyridyl)ethane based polymers are colorless. However, in the cases of pyrazine and 4,4'-methylenebis- (N,N'-dimethylaniline) based polymers, dark green and blue colors are developed, respectively, as soon as polymer solutions contact to air. Nevertheless, mechanically strong polymers were obtained in every case. Pyrazine based polymer was

found to be the least thermally stable and room temperature vacuum drying is essential in this case.

5.3.5. Characterization Techniques:

5.3.5.1. Reduced Viscosity Measurements.

All viscosity measurements were carried out in an Ubbelhode Viscometer at 25.0 ± 0.1^{o}C. The solvent for this study was methanol which was purified by drying over 3A molecular sieves, following by simple distillation over calcium hydride.

The bulb was filled with 10ml of polymer solution with a concentration of 1g/dl and diluted to a total volume of 400ml (0.025 g/dl). Reduced viscosities were taken on solutions with 10 different concentrations from 1g/dl to 0.025 g/dl. Polyelectrolytic behavior of the polymer solution was usually observed at very dilute concentrations.

5.3.5.2. Spectroscopic Analysis:

Structural characterization of the PTHF ionenes was obtained with a Nicolet MX-1 FT-IR Spectrometer linked to a Nicolet Data Station. IR spectra were taken on polymer films prepared directly by casting methanol solution onto the KBr pellet.

Nuclear magnetic resonance (NMR) spectra were measured with an IBM 270SY Spectrometer. Polymers were dissolved in deuterated acetone (~10% wt/vol) and tetramethylsilane (TMS) was used as the internal reference. Number Average molecular weight of the PTHF segment can be (indirectly) derived from the ratio of peak intensities

related to the PTHF and ionic portions.

5.3.5.3. Thermal Analysis:

Differential scanning calorimetry (DSC) thermograms were recorded by using a Perkin-Elmer DSC-II over the temperature range of -100°C to 50°C. A constant flow of helium gas was employed throughout the measurements. The data were derived from second heating cycles in order to provide a constant thermal history. Glass transition temperatures were determined as the temperature corresponding to one half the increase in heat capacity at the transition (eg. the midpoint). Crystallization and melting temperatures were selected as the peaks minimum and maximum, respectively.

Thermal mechanical analysis (TMA) on polymer films was performed on a Perkin-Elmer Thermal Mechanical Analyzer over the temperature range -100 to 250°C. The experiments were carried out at a heating rate of 10°C/min under a constant load of 10 gm. Transition temperatures were estimated as the intersection of the two lines tangent to the curve preceding and following the region of softening.

Thermogravimetric analysis (TGA) is used for the thermal degradation studies which began at 50°C to where the polymers degrade completely. TGA runs were performed under nitrogen with a heating rate of 10°C/min on a Perkin-Elmer TGS-2.

5.3.5.4. Dynamic Mechanical Analysis:

The dynamic mechanical data were recorded using Rheovibron DDV-IIC Viscoelastomer (Toyo Measuring Instruments) at a frequency of 11 Hz. The samples were rapidly cooled down to -150°C and the measurements were made with a heating rate of

2°C/min up to 300°C.

5.3.5.5. Tensile Testing:

Uniaxial stress-strain experiments were performed on dog-bone specimens using an Instron Tensile Tester (Model 1122) at room temperature. These experiments were carried out at a strain rate of 200% per minute based on the initial sample length. Dog-bone shaped specimens 10mm long were punched from solvent-cast films using special dies. All data are averages of at least 3 tests on different samples.

5.3.5.6. Nomenclature:

The ionene elastomers were all based on PTHF soft segment of various segment molecular weights. Thus, a system obtained with 1350 molecular weight PTHF is referred to as PTHF-1350-X, where X indicates the type of ditertiary amine utilized as the coupling agent.

5.4. RESULTS AND DISCUSSION

5.4.1. Reaction of Living PTHF with Pyridine

Table 5.3 summarizes results obtained from an experiment in which an excess

amount of pyridine was added to samples of living PTHF isolated at the indicated time intervals. The polymerization had been initiated at 2°C and allowed to react for a further 30 minutes at that temperature. Excess pyridine and unreacted THF monomer were then stripped off under vacuum at 60°C for 24 hr.

The theoretical molecular weights of the resulting pyridinium salt terminated PTHFs were calculated on the basis of percent monomer conversion versus the concentration of initiator. They are compared with the molecular weights estimated from ^{1}H NMR spectra. A typical spectrum of pyridinium salt terminated PTHF is shown in Figure 5.12. All assigments of the corresponding protons are as indicated in the Figure. The triplets appearing at 8.3 and 8.7 ppm results from H_e and H_f of the pyridine ring, respectively. The doublet at 9.3 ppm is due to the H_d of the pyridine ring. This is in accordance with the integration of signals observed at 8.3 (2H), 8.7 (1H), and 9.3 (2H), respectively. Furthermore, the triplet at 4.9 ppm is due to the terminal methylene unit bonded to the quaternary nitrogen. The rest of the methylene protons are attributed to tetramethylene oxide units appearing over a wide range from 1.6 to 3.5 ppm. Two peaks at around 2.0 and 2.8 ppm can be ignored since they are due to the presence of undeuterated acetone and water, respectively. A control deuterated acetone ^{1}H NMR spectrum is shown in Figure 5.17.

The average number of repeating units of tetramethylene oxide for each polymer chain can be obtained, approximately, by ratioing the peak integrations related to tetramethylene oxide and pyridinium salt. The molecular weight of oligomeric PTHF thus calculated from ^{1}H NMR results are further plotted versus % monomer conversion as shown in Figure 5.13. The increase of molecular weight linearly with conversion suggests the living nature of this system. Moreover, it was clearly demonstrated that pyridine could be used as an effective nucleophile to terminate the living PTHF. The reaction between

living PTHF with a counter ion of PF_6^- and pyridine is rapid, and has been reported by Cunliffe et el. [108] that reaction is probably complete in 1 to 2 min at -10°C .

The open circles in Figure 5.14 demonstrates the time-conversion relationships for the polymerization at 2°C of bulk THF (12.3 moles/liter) using $(CF_3SO_2)_2O$ at concentration level of 0.1 moles/liter. Within experimental error, the polymerization rate remains linear, at least in the time period studied and is expected to be proportional to anhydride concentration.

5.4.2. Coupling Reactions of Living PTHF with Ditertiary Amines

In this section, the reactions of living PTHF with ditertiary amines were examined to establish whether it can be utilized synthetically to prepare high molecular weight "ionene" copolymer. Four ditertiary amines have been studied as coupling agents for living PTHF chains - 4,4'-methylene-bis-(N,N'-dimethylaniline), pyrazine, 4,4'-dipyridyl, and 1,2-bis-(4-pyridyl)-ethane. The structures of these diamines are illustrated below:

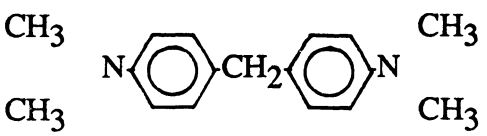

4,4'-methylene-bis-(N,N'-dimethylaniline) (BDMA)

Pyrazine (PY)

4,4'-Dipyridyl (DIPY)

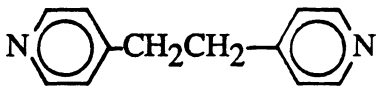

1,2-bis-(4-pyridyl)-ethane (BPE)

BDMA was found to react with living PTHF at a slow rate under the conditions described. One hour of reaction time is usually required to obtain high molecular weight polymer. The slow coupling rate is probably due to its weak basicity and steric hindered structure. This is not a desirable situation in the sense that living PTHF may still be polymerizing during coupling and a wide distribution of PTHF segment length could result. The copolymer shows poor mechanical strength and an unpredictable structure. Moreover, polymers thus obtained displayed a characteristic color of blue to green. If the coupling reaction of BDMA with living PTHF was allowed to proceed at temperatures below -70°C, a temperature where the PTHF propagation rate is very low, one may speculate that ionene polymers with controlled structure may still be prepared. Since it would involve liquid nitrogen temperature, one might consider the route impractical.

Ditertiary amines with stronger basicity are generally better nucleophiles, and were therefore necessary for efficient coupling reactions with living PTHF. Ionene polymers with controlled structure can only be prepared when the coupling reaction is quantitative and the coupling rate is rapid.

Pyrazine has been also utilized by Cunliffe et el. [66] as a chain coupling agent for living difunctional PTHF. They found that the living PTHF with a counterion of PF_6^- reacted completely with a slight (~10%) excess pyrazine within 15 min to form the monoadduct exclusively. Attempts to use the amine as a coupling agent therefore failed. Presumably, the basicity of the second nitrogen is reduced by the formation of the quaternary nitrogen bond on the same ring. Its interaction with the oxonium ion of the second polymer molecule is limited to solvation rather than bond formation by nucleophilic replacement of the THF molecule.

Similar experiments were conducted in our laboratory except that $CF_3SO_3^-$ was the counter-ion instead. Despite the slow coupling rate, a high molecular weight polymer was obtained after ca 15 min. The superior stability of $CF_3SO_3^-$ complex with quaternary ammonium cation is presumably responsible for such a drastic improvment over Cunliffe's work. The slow coupling rate may be due to the fact that the second nitrogen was deactivated by reaction of the first. The polymerization was homogeneous throughout the experiment and polymer solution became a clear, transparent "jello" at the end of the reaction. A dark-green color spontaneously developed as soon as the solution contacted air. The color remains even after the removal of residual THF under vacuum at 40°C for 24 hr.

Regardless of the presence of the unusual color, the product was nevertheless a tough rubbery material at room temperature, quite different from the normal waxy PTHF. A black char-like material resulted after further drying the sample overnight at 80°C under vacuum. The cause of the instability could be a poor charge separation, since two single-positive charges are on the same aromatic ring. No further work was carried out to identify causes for the color change, although that may be interesting for certain applications.

4,4'-Bipyridyl was found to be most effective in coupling with the living PTHF to form high molecular weight polymer. The magnetic stirring bar was stopped immediately after the addition of bipyridyl due to high solution viscosity. The high coupling rate indicates that there is possibly no interaction between two seemingly conjugated pyridine rings. If conjugation exists after the first pyridine reacted, the nucleophilicity of the second will be dramatically reduced due to the partial positive nature of the second. One possible explanation for this behavior may be that the two pyridine rings are not coplanar, after the first one has reacted with living PTHF this could significantly reduce the interactions

between two individual rings. The product shows good oxidative stability and no color change during the polymer work-up. Since the coupling rate is fast, an ionene with controlled PTHF segment molecular weight and possibly narrow molecular weight distribution can be prepared. This also provides a good supporting evidence for the fact that $(CF_3SO_2)_2O$ is such an effective difunctional initiator for THF polymerization as suggested earlier by Smith et al [62]. The coupling efficiency and difunctionality of PTHF are proved to be quantitative by the fact that high molecular weight polymer only formed when a perfect stoichiometry was achieved.

Confirmation that this material was the high molecular weight coupled product expected with narrow molecular weight distribution could not, easily be obtained by GPC. The GPC traces showed nothing but solvent (THF) peaks, although ionenes are soluble in THF if PTHF segment molecular weights higher than 1350. The failure of the injected ionene to elute is probably due to the highly interaction between the multiple-charged high molecular weight polymer with the column. Indeed, these effects may be strong evidence for such a product. This behavior has also been found on similar materials by Cunliffe et el. [66].

PTHF ionenes with a wide range of properties can be prepared by allowing different polymerization times, followed by coupling with ditertiary amine,. The PTHF conversions steadily increased with time as shown in Figure 5.14. This in good agreement with data (open circles) obtained from a control experiment under the same conditions. It is necessary to point out here that the term "conversion" used throughout this work representing only the amount of THF monomer consumed at a certain time. In other words, the weights of "heavy" counterion and 4,4'-bipyridyl have been removed from the polymer recovery weight during the calculation of conversion. The molecular weights of 4,4'-bipyridyl and two $CF_3SO_3^-$ counterions appeared on each repeating segment are 156

and 282, respectively. Obviously, the weight contribution from ionic groups to the total weight of polymer is reduced as the PTHF segment molecular weight is increased. The conversion values thus obtained are more meaningful and reflect the true nature of the THF polymerization.

High molecular weight ionenes with useful physical strength can only be prepared when PTHF segment molecular weight higher than 1000. The reason is solely due to the premature precipitation for samples which contained high ionic concentration.

A typical FT-IR spectrum of PTHF ionene is shown in Figure 5.15. IR cannot be used to identify the presence of quaternary ammonium salts, since there is no characteristic IR absorptions observed. However, the C-H stretching band at 3027 cm^{-1} of bipyridyl apparently shifted to higher wavenumbers 3063 cm^{-1} after quaternization. The peak intensity increased with increasing bipyridinium salt content in the polymer. This provides evidence for such a product, although the analysis not straightfoward. The peaks appeared at 2938 and 2853 cm^{-1} are due to asymmetric and symmetric C-H vibration of PTHF segment, respectively.

The most informative characterization tool, in terms of structural identification, appears to be NMR. A typical ^{1}H NMR spectrum is given in Figure 5.16. Deuterated acetone was utilized as the solvent for NMR analysis since PTHF ionenes are not chloroform soluble. The NMR spectrum of bipyridyl is shown in Figure 5.17. The shift of bipyridyl proton peaks downfield after quaternization enables clean differentiation between free diamine (if present) and quaternary products. They are 9.5 and 8.9 ppm for the quaternized ring and 8.8 and 7.8 ppm for the non-quaternized ring. The absence of bipyridyl peaks again support a quaternary ammonium structure. Slightly different shifts may be observed for different solvents and counterions.

The peak at 3.4 ppm is due to the $-CH_2O$ protons and an equal intensity peak at 1.7

ppm is related to the two middle methylene units (-CH_2CH_2-) in PTHF. Those four methylene units directly bound to pyridinium cation appear at slightly higher shifts as a shoulder of the main peak. Integrations indicate two protons are associated with each peak.

Proton NMR also can be used to estimate the PTHF segment molecular weight between two ionic groups provided the PTHF segments are short enough. In each repeating segment contains one bipyridinium salt and a certain number n repeating units of tetramethylene oxide. The number n therefore can be approximately estimated by comparison of the integration of peaks at 8.9 ppm (4H) and 3.4 ppm (4H).

The estimated PTHF segment molecular weight (not total polymer molecular weight) for a series of PTHF ionenes are gathered in the last column of Table 5.4. The calculated values from ^1H NMR are in good agreement with those values estimated on the basis of THF conversion. The accuracy of ^1H NMR proved to be acceptable for this purpose.

The linear relationship between calculated PTHF segment molecular weights and THF conversions (shown as solid circles) is demonstrated in FIgure 5.13. This suggested the "living" character of THF polymerization and more importantly, the high coupling rate between 4,4'-bipyridyl and living PTHF. A deviation from linearity may otherwise be observed, if the coupling rate is slow. Because the data are collected on samples prepared in five separate experiments, the informations provided are only qualitative, although the same reaction conditions were employed in all cases. This may also be responsible for the deviation from the control pyridine termination experiment (shown as open circles in Figure 5.13) in which samples from the same batch were taken periodically with time.

Figure 5.18 showed the PTHF segment molecular weight is a function of the time allowed for THF polymerization before coupling. This plot can be utilized for PTHF segment length determination by using an extrapolation method. For each different condition, i.e. concentrations and temperature, construction of a new calibration curve was

required for this purpose. The capability of molecular weight determination by using proton NMR as described before was limited when PTHF molecular weight exceeded ca 5000.

The chemical composition of these PTHF ionenes can be represented by

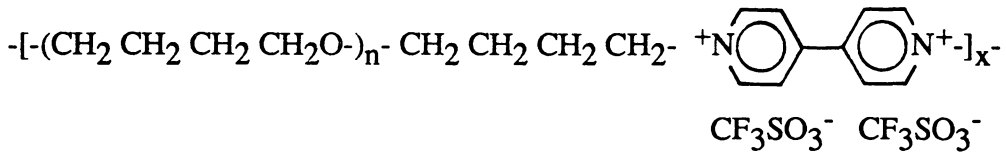

The mole fraction of ionic groups (triflic acid pyridinium salts) contained on the polymer backbone is approximately equal to the value of 2/n+2 where n is the number of repeating units of tetramethylene oxide with respect to each bipyridinium salt and "2" represents the number of ionic groups on each repeating segment. The calculated ionic concentrations of PTHF ionenes with various PTHF segment molecular weights were tabulated in Table 5.5. As the molecular weight of PTHF segment increases, the ionic concentration therefore decreased.

Due to the rigid nature of the bipyridinium salt structure it can be considered as the hard segment unit with respect to the PTHF segment. The counter-ion - triflic acid anion, has a molecular weight of 149, which is twice as large as its counterpart (pyridinium cation). Therefore, it is interesting to know the hard segment contents with and without considering the weight of the counter-ion. Those numbers are listed in Table 5.5.

The BPE based PTHF-ionenes were prepared by using a similar approach as bipyridyl based ionenes. Initially, the coupling reaction of BPE with living dioxonium ions was expected to proceed at a comparable rate as BP coupled reactions since the two

pyridine rings are basically separated and will not interact with each other by conjugation. Therefore, the second pyridine should react with living PTHF as fast as the first pyridine. However, a slower coupling rate was found in the case of BPE reactions. High molecular weight polymer formed approximately 15 minutes after the addition of BPE. The slower coupling rate imparts possibly a broad PTHF segment molecular weight distribution.

The PTHF segment molecular weight is a function of reaction time, temperature, and concentrations as has been discussed previously, and were determined by ^{1}H NMR. A typical ^{1}H NMR spectrum along with peak assignments is shown in Figure 5.19.

5.4.2.1. Solution Properties

The resulting PTHF ionenes can be easily dissolved in methanol and acetone, and indirectly in water. The solution of PTHF ionene/methanol forms a homogeneous mixture with water. Water is miscible with methanol in all proportions. The polymers stay in the water solution even after the removal of methanol. Therefore, a wide range concentrations of aqueous PTHF ionene solution can be prepared if necessary. This observation can be interpreted as follows: The hydrophilic quaternary ammonium groups has a low probability of encountering water molecules before dissolving in the methanol, since they are initially surrounded by the hydrophobic PTHF segments. Water, has a high dielectric constant, which solvates quaternary ammonium groups even after the removal of methanol. The ionic association can therefore be reduced, which imparts the solubility of PTHF-ionenes in water.

The solvent polarity is no doubt an important factor affecting the solution viscosity of polymers. In Figure 5.20, the reduced viscosity of PTHF ionene with molecular weight

of 1350 measured in methanol was plotted versus concentrations (from 1 g/dl to 0.025 g/dl). It was found that the smaller the concentration, the higher the reduced viscosity. This polyelectrolyte behavior in methanol reveals the ionic nature of PTHF ionene. The sharply rising viscosity at very dilute concentrations indicates an increase in the degree of ionization of the polymer. Solution viscosity depends on the size of the polymer chain, i.e. the hydrodynamic volume. Therefore, increasing viscosity at low concentrations represents an uncoiling polymer chain. The charges on the backbone become less shielded by the counterions in high dielectric medium at low concentraions, leading to an increase in intramolecular repulsion. This mutual repulsion of their charges causes expansion of the chain.

It is expected that when PTHF ionenes are dissolved in nonionizing solvents such as chloroform (if soluble) they would behave in completely normal fashion, i.e. viscosity is decreased linearly with increasing dilution. By contrast, in ionizing solvents, the size of the polyelectrolyte random coil is a function of the polymer concentrations as well as their ionic concentrations, since both influence the degree of ionization. It is therefore expected that a more pronounced polyelectrolyte behavior, will be observed in PTHF ionenes with shorter PTHF segment with respect to ionenes with higher PTHF segment molecular weight. This is because of the ionic concentration is decreased with the PTHF segment molecular weight. Considering the ionizing power of the medium, the viscosity of PTHF ionene could be expected to be higher in water than in methanol, since water has a higher dielectric constant than methanol.

5.4.2.2. Thermochromic Behavior

An attempt was made to exchange the monovalent counterion, $CF_3SO_3^-$, to a divalent anion, $SO_4^=$. A 10% methanol solution of the BP based PTHF-ionene was dripped into a large amount of the saturated aqueous solution of sodium sulfate with agitation. The mixture initially became a milky-like solution and then precipitation of polymer occured. The precipitated polymer was collected as a rubber-ball-like material and was washed successively with distilled water several times in order to remove residual salts. Film samples were prepared by solvent casting from a 10% methanol polymer solution on a Teflon mold. The majority of methanol was removed in a nitrogen purged dry-box at room temperature, before further vacuum-drying.

The vacuum-drying was conducted at 60°C. An interesting phenomenon was observed after approximately one hour at 60°C. The polymer film turned to a dark-brown color and a light-brown color remained after it was slow cooled in air. The color change was observed to be reversible and has been termed thermochromic behavior. The nature of the thermochromic behavior is not clear and certainly is of interest for further investigation

.

5.4.2.3. Thermal Analysis

A. Thermal Gravimetric Analysis (TGA)

Thermal stability is of important for thermal processibility and applications in heated enviornments. TGA thermograms of PTHF ionenes are shown in Figure 5.21. The measurements were accomplished at a heating rate of 10°C/min under nitrogen atmosphere.

The initial decomposition temperatures all exceeded 220°C and were clearly dependent on the ionic concentrations. A limit ca 290°C is reached as the ionic contents were above 10 mole %. The primary catastrophic weight loss was due to the decomposition of the PTHF segment. There is a good correlation between the percentage of weight left after the primary decomposition with the hard segment (bipyridinium salt) contents shown in Table 5.5. This interesting correlation strongly suggested the residual could be a 4,4'-bipyridinium triflate salt with a structure shown below

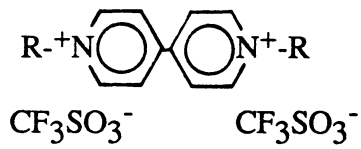

where R could be a proton or an alkyl group. The structural identification of such a product has not been conducted yet. Such a possible quaternary ammonium compound is thermally stable even up to the temperature of ca 400°C where the secondary decomposition was initiated. For reference purpose, the boiling points of 4,4'-bipyridyl and triflic acid are 305°C and 162°C, respectively.

At the same temperature of ca 470°C for all ionenes, the quaternary ammonium compound was completely dissociated and there is no char formation. Indeed this provides a further evidence that a common residual was remained for all samples after primary decomposition.

Despite a highly conjugated structure of 4,4'-bipyridinium salt, there is essentially no interaction between the π-electron systems of the two rings. Each of the positive charge are only delocalized on the ring where they belong.

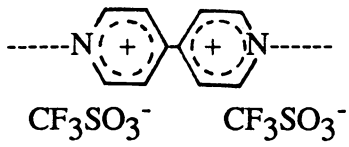

If two single-positive charges are delocalized on the same ring, such a structure would be considered thermally unstable as in the case of pyrazine based ionene system. It is therefore that the charge separation is the prime concern for the thermal stability of ionenes.

Figure 5.22 shows the thermogravimetric curves of BPE based ionenes. There is no noticeable weight loss until 280°C. Interestingly, BPE based PTHF-ionenes are generally 40°C more thermally stable than the BP based polymers from TGA studies. Again, this may be due to the charge separation of two single-positive charges. The further apart the common charges the more stable the polymer is.

B. Differential Scanning Calorimetry (DSC)

DSC curves as a function of PTHF segment molecular weight are presented in Figure 5.23. The value of T_g was taken from the measured curves by the midpoint method. This has been suggested as the most appropriate way to determine the glass transition temperature since it is the temperature at which the great mass of units in a polymer has become activated [125]. It also is more precisely readable than the onset temperature. Crystallization and melting temperatures were selected as the peaks minimum and maximum, respectively.

Ionic groups such as quaternary ammonium salts are highly polar in nature. As it

became a part of polymer backbone and bonded to a less polar flexible segment such as PTHF, the formation of ionic clusters are expected. A high degree of phase separation is therefore expected. However, this point need to be proved morphologically by using small angle X-ray spectroscopy (SAXS) which is under thorough investigation in Professor Wilkes's laboratory.

From these traces, the dependence of thermal behaviors to the PTHF segment length can be easily visuallized. The soft segment crystallization was observed when the PTHF segment molecular weight is greater than 750. There is about 10°C increase in melting temperature when the PTHF molecular weight increased from 1350 to 2550. The increase of melting temperature probably indicated that the soft segment crystallites are bigger for larger PTHF segment length.

It is noted that the soft segment glass transition temperature was systematically decreased with increasing PTHF segment molecular weight. This is probably due to the anchoring effects for the soft segment end group restrictions. As the soft segment length between two anchoring points (ionic domains) decreased, the chains became less mobil. As a result of that, the ease of soft segment crystallization also may be retarded.

It is generally thought that the presence of crystallites in the soft segment matrix will restrict the mobility of the soft segment, i.e. a rising T_g should be observed. Interestingly, the increased soft segment crystallinity was not caused the increased soft segment T_g of PTHF-ionenes. This may suggest that the T_g of PTHF soft segment having large crystallites will show a minimum or no dependence on the degree of crystallinity.

Another interesting point in these traces is the location of the soft segment crystallization peaks (T_c). The T_c was shifted toward T_g as the so-called T_g-T_m window was opened up. One is usually noted that as the crystallization temperature approaches T_g, i.e., high supercooling (large value of T_m-T_c), the ability of a molecule to diffuse to a

growing crystal is decreased due to the viscosity increase. However, a sharp crystallization peak immediately followed the T_g of soft segment for the sample PTHF-2550-BP was observed, which suggests the ease of chain mobility. The mobility of PTHF may became less restricted as with increasing PTHF segment length.

The transition temperatures and other thermal characteristics are summarized in Table 5.6. The values of ΔC_p , ΔH_c and ΔH_f listed in Table 5.6 were calculated per miligram of soft segment by taking into account the quantity of PTHF soft segment actually present in the polymer. Clearly, the magnitude of the heat capacity change (ΔC_p) at the soft segment T_g is a function of both the relative amount of the participating amorphous phase and the difference of conformation entropy between the glassy and rubbery state. It is noted that ΔC_ps of samples PTHF-550BP and PTHF-750-BP are apparently larger than the rest of samples with higher PTHF segment molecular weights. This indicates a possible phase mixing between PTHF soft segment and the 4,4'-bipyridinium unit in these samples with shorter PTHF segment length. A small amount of ionic segment solubilized in the PTHF phase caused the increase of ΔC_p of amorphous phase. As a result of phase mixing, the crystallizability of PTHF was hampered due to the presence of "impurity" in the soft segment phase. The structural heterogeneity of the soft phase was also indicated by a large glass transition zone width. The dipole-dipole interaction between the low molecular weight ether and ionic groups may be responsible for the partial solubilization of these two in each other.

It is noted in the case of PTHF-1350-BP that the ΔH_c of crystallization is equal to ΔH_f of fusion. This indicates a fully amorphous structure of the quenched product. For samples PTHF-1700-BP and PTHF-2550-BP, there are some estimated amount of 23% of the PTHF soft segment were crystallized even under fast cooling of 320^{o}C/min as

evaluated by the difference between ΔH_c and ΔH_f. The narrow T_g zone width observed on those polymers suggests a high degree of stuctural homogeneity.

In light of the above rationale, we therefore view the changes in soft segment glass transition temperatures as arising from the degree of phase separation as well as the restrictions imposed by the ionic junction points. To better display the observed relationships, the T_gs were plotted versus the PTHF segment molecular weights and ionic concentrations as are shown in Figure 5.24 and Figure 5.25, respectively. Interestingly, a break-point was observed in both cases at 1350 molecular weight of PTHF and/ or 9.6 mole% ionic concentration. This distinct change in properties possibly suggests a critical ionic concentration of PTHF segment molecular weight for the onset of complete phase separation. The polarity difference between two phases will be increased with the PTHF molecular weight. On the other hand, the restrictions imposed by the ionic domains became less effective when the PTHF length between juctions is increased.

In Figure 5.24, the curve is extropolated to infinite PTHF molecular weight. A value of ca -89^{o}C was obtained and is predicted to be the ultimate glass transition temperature of PTHF. A similar result was also obtained when extropolation is extended to zero ionic concentration as indicated in Figure 5.25. The value of -86^{o}C is generally reported in the literature [126] as the glass transition temperature of PTHF.

Two melting endotherms are generally observed for crystallizable PTHF. The position of the endotherm is a function of PTHF molecular weight. In the literature [129], the low-temperature endotherm is generally attributed to the melting of metastable crystallites while the higher temperature endotherm is associated with crystallites at equilibrium state. This behavior clearly also observed in the ionenes as illustrated in Figure 5.26 and PTHF-2550-BP is utilized as the example. The effect of thermal history is no doubt an important consideration in interpretating the later characterization data.

The sample was aged in a desiccator for 60 days before the DSC scans were recorded. In the first run, the sample was fast cooled (320°C/min) to -120°C from room temperature. The DSC behavior was recorded at a heating rate of 10°C/min. A sharp endotherm in conjunction with a relatively small crystallization peak and a diffused glass transition suggests the sample is crystalline before quenching. This is understandable if scan is taken in the winter time when the room temperature is below the melting temperature of PTHF. The sample was then quenched to -120°C from a temperature above the equilibrium T_m after the first run. The PTHF phase thus obtained has about 80% of amorphous content as discussed previousely. It is observed that the melting endotherm is broader in the second run while the measured ΔH_f are almost equal as in the first run. This may explained as the presence of metastable PTHF crystallites along with the equilibrium crystallites. The temperature of 19°C was assigned to the melting of equilibrium PTHF crystllites with molecular weight of 2550. The third run is recorded as a similar fashion as the second run. The peak at 12°C is attributed to the melting of metastable PTHF crystallites.

High temperature DSC of those ionenes are also of interest. The traces of the first and second run of DSC scans from 50°C to 230°C are provided in Figure 5.27. All scans are recorded at a heating rate of 20°C/min, which enables a better sensitivity than lower heating rates.

A broad crystallization peak was observed in all the first run scans. The intensity of the peak is regularly decreased by increasing the ionic concentration. Despite the peak intensity, the onset and end temperatures of crystallization are similar for all polymers which are 98°C and 195°C. respectively. A similar crystallization temperature of around 156°C, taken as the peak minimum, was also noticed. The crystallization of ionic segments has been further confirmed by using the electron diffracton technique. It was

observed that sharp rings appeared in the electron diffraction pattern when sample was heated to temperatures above 100°C.

The melting temperature of ionic crystallites was not observed in the temperature range studied and is obviously above 230°C. The upper temperature limit of 230°C was selected due to the precautions on considering the thermal degradation of PTHF. Since the DSC scans are stopped and then quenched to room temperature before the melting of ionic crystallites, a highly oriented ionic structure is expected to persist in the second run. A weak broad glass transition at around 153°C was observed for all polymers. Again, the transition is more noticeable for polymer with lower ionic concentration. This indicates a small amount of ionic unit probably exists in the amorphous form even after thermal induced crystallization. The observed T_g values are closely related to the T_c observed in the first run. This temperature is, perhaps representing the amount of energy required to overcome the rotaional barrier of two pyridinium ring over each other.

Clearly, a stable bipyridinium conformation with better packing efficiency results during the crystallization process. The effect of structure conformation on the polymer properties will be discussed in more detail in the section of dynamic mechanical analysis.

DSC scans of BPE based PTHF-ionenes are collected in Figure 5.28 and their characteristics are summarized in Table 5.7. At comparable ionic concentration, BPE based ionenes apparently have a higher amorphous content in the PTHF phase than the BP based ionenes which is judged by the ΔH_f values. This may be attributed to the weaker ionic association and a possible broader PTHF length distribution in the BPE based ionenes.

C. Thermomechanical Analysis (TMA)

Use of the penetrometer mode of TMA for detection of transitions in polymers has

been widely used in the literature. TMA scans on PTHF ionenes with different ionic concentration are shown in Figure 5.29. A low temperature transition in the neighborhood of -70°C was observed for all samples. This temperature can be assigned to the glass transition temperature of PTHF segment although is about 10°C higher than the values obtained from DSC. The cause of difference can be attributed to the sensitivity of instruments. In general, correlation with DSC is required in order to identify penetration with a transition. The low temperature T_gs are generally followed the same trend as observed from DSC. The highest T_g was observed in polymer with the shortest PTHF segment.

However, a broad low temperature transition was obtained for polymer with 2550 PTHF segment molecular weight and seemingly a higher T_g than the rest. To explain this contradiction, it is necessary to recognize that the thermal transition behaviors observed from TMA on samples without any preliminary heat treatment can only be correlated to the first run scans of DSC at the same heating rate. Most of the DSC transitions reported are based on the second run in order to provide a constant thermal history. As discussed before, there is no significant difference between first and second runs of DSC scan for all polymers except PTHF-2550 ionene. Three consecutive runs of DSC scan on PTHF-2550 ionene have been provided in Figure 5.26. Again, a diffuse low temperature transition was observed in the first run DSC scan which is in good agreement with TMA result.

The initial temperature of polymer flow appeared to be a function of the ionic concentration. Polymer starts flowing at a lower temperature with increased PTHF segment molecular weight. Basically, all polymers exhibited a wide service temperature which is judged by the broadness of the rubbery plateau. One interesting phenomenon that deserves some attention is the slope of the penetration curves at high temperatures. For

PTHF-2550 ionene, the probe penetrated through the polymer at a slow rate while penetration occured at a much faster fashion in PTHF-750 ionene. The slow penetration suggests that some kind of structure persists at higher temperatures; perhaps ionic clusters. The complete penetration or flow was observed at a similar temperature around 250°C for all polymers. At that temperature, thermal agitation overcomes the interchain ionic interactions and thus polymer chains can flow freely over one another.

No transition was detected between the soft segment T_g and polymer flow temperature, indicating the absence of any soft segment crystallinity in PTHF-750 ionene. A significant penetration appeared at ca 50°C in PTHF-1350 ionene. This is may be due to the volume reduction caused by the conformational interconversion of ionic segment which will be discussed in detail in the dynamic mechaincal analysis section. A similar transition was also observed in PTHF-2550, however, with a much lower degree of penetration. The possibility of PTHF crystallites melting is unlikely since a bigger drop should be observed for the PTHF-2550-BP than PTHF-1350-BP on the basis of soft segment crystallinity. Another noticeable transition occured at ca 0°C may be due to the melting of PTHF crystallites.

To pursue further understanding the effects of ionic bonding in comparison with hydrogen bonding on the physical properties of polymers, a control polyurethane with a perfect alternating segmented structure

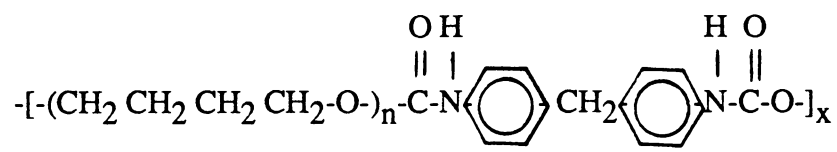

was therefore synthesized by reacting stoichiometric amount of PTMO-2000 with 4,4'-methylene diphenylisocyanate (MDI). The polymer obtained was a soft tacky rubber

and flowed completely at around 70°C as judged by TMA. More than 100°C difference in polymer flow temperature was observed between ionene and control polyurethane with similar PTHF segment molecular weight. Apparently, ionic bonding provides much stronger interchain cohesive forces than the hydrogen bonding impart higher softening temperature. The influence of phase mixing between hard and soft segment of polyurethane on polymer flow temperature could be small. A reasonably good phase separation has been achieved in this polymer with a low temperature T_g around -71°C from DSC analysis.

5.4.2.4.Tensile Properties

The stress-strain curves of the PTHF ionenes are shown in Figure 5.30. Table 5.8 summarized the tensile properties of the ionenes studied including Young's modulus, % elongation, and ultimate tensile strength. The initial modulus clearly is a function of ionic concentrations which is increases with increasing the ionic content. The increase is due to the greater rigidity imposed by the hard segment (ionic segment). The stress level during extension also increases with ionic concentration, again showing the reinforcing effects of the less mobil ionic segment domains. However, the data of elongation to break (for those three samples with higher PTHF segment molecular weight) increase with increased ionic concentration, which is not expected and will be discussed later.

PTHF-550-BP exhibits poor mechanical strength. This is, however, cannot be considered as the true tensile behavior of this structure. The polymer film prepared by using solvent casting from methanol solution, was brittle which probably because of relatively low molecular weight.

Elastomeric behavior was observed on PTHF-750-BP, with an elongation of 700% at break. Again, low tensile stress at failure indicates the polymer is not a high molecular weight product for the reason described in the synthesis section. Clearly, the reduction of ionic concentration by increasing the PTHF segment molecular weight eventually improves the solubility of polymer in THF. In other words, high molecular weight polymer can only be prepared when PTHF segment molecular weight exceeds approximately 1000. An ultimate tensile strength in the range of 30 MPa was observed for those three samples with higher PTHF segment length. Polymers are no doubt high molecular weight products.

Interestingly, a slope change occured at 300% elongation for all high molecular weight polymers, suggests the initiation of strain-induced crystallization. At around 400% elongation, a "modulus-reversal" behavior was observed. It is noted that polymer with higher PTHF segment length becomes more rigid at elongation above 400% than the polymer with shorter PTHF segment. In other words, the modulus increased at a faster rate in polymer which had larger PTHF segment length. Before offering an explanation of this phenomenon, one has to remember that there are two major variables in this series of ionenes, namely, ionic concentration and PTHF segment length. One parameter always varied with the other. This certainly made the data more complex than it looks. Moreover, the modulus generally is proportional to the number of polymer chains per unit volume. The more polymer chains packed in a unit volume, the higher the observed modulus would be. In addition, one needs to realize that the density of ionic domain of these ionenes may be low due to the large counterion, which prevents efficient packing. Thus, in comparison with samples which have been fully strain-induced crystallized, a lower modulus was expected to associate with ionene with shorter PTHF segment length simply due to higher ionic content (lower density).

Tensile testing was also conducted on compression molded film of sample

PTHF-2550-BP in order to justify the processability of this material. No significant difference on tensile behaviors between compression molded and solvent cast films was observed. This suggests that good flow and no chain scission occurred during compression molding at 190°C for 10 min. A lower tensile strength should be observed if the polymer undergoes thermal degradation during compression molding.

Figure 5.31 shows the tensile behavior of the BPE based PTHF-ionenes. An ultimate tensile strength of about 35 MPa with 1000% elongation was obtained for ionenes with a PTHF segment molecular weight of 1500. Due to the more irregular structure of BPE as compared with BP, a relatively weaker interchain ionic association was expected for BPE based ionenes and imparts inferior thermomechanical properties than the BP based ionenes with similar ionic concentration.

5.4.2.5. Dynamic Mechanical Properties

To investigate the compositional dependence of the local scale motion as well as cooperative segmental motion which may exist in these PTHF ionenes, dynamic mechanical spectra were obtained. The storage modulus, E', and the dissipation factor, tan δ, as a function of temperature, are displayed in Figure 5.32 and Figure 5.33, respectively. All samples are aged in a desiccator for 2 days after drying before dynamic mechanical analysis was conducted.

The low temperature loss peak at -125°C is related to the local mode motion of the $-(CH_2)_4O-$ unit. The α_a relaxation at around -70°C assigned to the onset of segmental motion associated with the glass transition of PTHF soft segment. The peak intensity of the α_a relaxation should be a function of PTHF segment molecular weight since it relates

to the amount of soft segment involved in the transition. This is true when comparison was made between PTHF-1700-BP and PTHF-1350-BP. However, a contradiction occurred with sample PTHF-2550-BP which has the highest soft segment content among polymers studied, a very weak α_a relaxation was observed instead. Again, this is in good agreement with the result which we found and discussed previously from thermomechanical as well as DSC analysis.

The T_g values of the soft segment determined at 11 Hz from the peak position of tan δ curves are about 10°C higher than those values obtained from DSC results. This has been [127] attributed to the fact that with the Rheovibron, it is not possible to increase the length of the sample during the measurement, and therefore a decrease of sample tension occurs in the vicinity of the glass transition causing a shift of the transition to a higher temperature.

On the high temperature side of α_a peak, a mechanical dispersion is indicated as a shoulder near -15°C. This transition is designated as α_c and is related to the melting of crystallites for the PTHF soft segment. The δ relaxation near 200°C ascribed to a transition of the ionic segments. A secondary transition at this temperature was also observed by DSC. This multi-transition behavior clearly indicated a two-phase system in which ionic segments formed clusters (or domains) which are dispersed in the PTHF soft segment matrix. Ionic domains act as physical crosslinks and/or filler for the flexible soft segment matrix. A better phase separation is usually translated to a more effective reinforcing filler effect.

The storage modulus curves indicated that a rubbery plateau extended beyond 200°C was exhibited for all samples. The plateau modulus increases on increasing the ionic concentration as expected. This behavior is consistent with the modulus obtained from stress-strain analysis. The drop of storage modulus occured at -80°C is due to the glass

transition of PTHF segment from a glass to a rubbery material. An increase in E' above the T_g on samples with PTHF segment molecular weight of 1700 and 1350, suggests the crystallization of the soft segment. It is no doubt that the extent of E' at this temperature is related to the amount of soft segment in the polymer which clearly to be the case. The sample, PTHF-2550-BP, shows a diffuse soft segment glass transition and no increase on E' in the crystallization region. It is thought that the ionenes with longer PTHF segment may undergo more crystallization during the initial sample cooling. However, the contribution to the soft segment crystallinity by fast cooling to temperatures well below its T_g is usually small in the cases of low molecular weight PTHF. Apparently, the soft segment already crystallized to certain extent in sample PTHF-2550-BP, due to the aged effects after sample preparation, before experiment was conducted. This has been proved to be the case by other methods described previously. The melting of soft segment crystallites in the range from -25 to 25^{o}C and this produces a decrease in storage modulus.

One unusual transition appeared at around 50^{o}C which was not expected and has not been reported in the literature. Some of the characteristics of the transition are summarized in Table 5.9. The melting temperatures of the soft segment derived from the first run of the DSC results are given for reference purpose. The onset and end temperature of the transition are designated as T_o and T_e, respectively. The extent of the storage modulus "jump" at the transition is also listed.

This transition clearly is dependent on the ionic concentration of ionenes. The extent of the E' "jump", is seen to increase regularly with the ionic content. In addition, the T_o decreases on decreasing the PTHF molecular weight. It is interesting to note that the end of the transition, all appear at a similar temperature. In other words, broadening of the transition occurred when the ionic concentration is high, or when the PTHF segment

length is short. To further understanding about the nature of the transition, the T_m of the soft segment obtained from the first run of DSC results was substracted from the onset transition temperature, T_o. The reason of doing this was because the mobility of the ionic segment was suspected to be the governing factor defining the onset of the transition temperature. At temperatures below soft segment T_m, which is molecular weight dependent, the mobility of ionic segments was restricted by the presence of the soft segment crystallites. Therefore, it is expected that the mobility of ionic segment will increase at the temperatures above the soft segment T_m. Interestingly, it is found that the values, $T_m - T_o$, are all equal to a "magic" number of 34°C. This number has no physical significance, which is only an indication of the exsistance of some sort of correlation between the transition and the T_m of soft segment. The T_m values obtained from DSC were utilized for this purpose only because a precise reading can be easily obtained, while the dynamic mechanical spectra are more complex in the region of interest. However, there is no difficulty to determine the onset temperatures of the E' "jump" from storage modulus/temperature curves.

To test the reversibility of the transition, several experiments were conducted and the results are shown in Figure 5.34. First, the sample, PTHF-2550-BP was dried under vacuum at 80°C for 12 hr and slow cooled in a desiccator for a period of 1 hr. It was then initially cooled in the Rheovibron chamber to 0°C and heated at 2°C/min to 90°C which is a temperature above the T_e. Second, the same sample as the first experiment was utilized which was slow cooled from 90°C to -100°C after the first run. The results are compared with the dynamic mechanical spectrum of aged PTHF-2550-BP as has shown in Figure 5.32. It is recognized that the PTHF soft segment crystallinity could be induced by slow

heating from a temperature below its T_g. Therefore, the sample for the first experiment perhaps possess the lowest crystallinity among three runs. Moreover, the aged sample has the highest melting temperature, because most of the crystallites are near their equilibrium state. In the sample for the second experiment, some of the crystallites are in the metastable state for the reasons discussed in the DSC section.

The transition proven to be reversible. Transitions due to the removal of absorbed moisture by the hydrophilic ionene when heated, becomes an unrealistic explanation. First of all, water, if present, is difficult to remove from an ionic compound at temperatures below its boiling point. Second, if this is the case, the transition will not be reversible. It was also found that the onset transition temperature depends on the thermal history and increases with the soft segment crystallinity. The width of the transition tends to be broaden with a possible decreasing soft segment crystallinity.

A possible explanation, which is consistent with the observations, involves the conformational interconversion of 4,4'-bipyridinium salt as illustrated in Figure 5.35. The preferred conformation of 4,4'-bipridinium salt, below soft segment T_m, is probably an anti-conformation in which two bulky triflic acid anions (twice as large as pyridine ring) are on the opposite side of the neighboring rings. This is due to a possible favored lowest energy state. Above the melting temperature of PTHF soft segment, the ionic clusters can be considered as dispersions in a polar liquid medium. Some of the anti-conformational isomers are possibly converted into the skew conformations in polar liquid medium. If this is so, the bipyridinium salt may exist in the "propellerlike" conformation, either symmetric or unsymmetric. The interconversion phenomenon has been discussed in great detail in Hallas's book entitled "organic stereochemistry" [128]. Despite the examples given in Hallas's book, nothing is directly related to the type of ionic salt as our compound, however, the basic ideas can be employed in our system. The skewed form is more

important in polar than in non-polar solvents. This is because the skewed conformation has a considerable dipole moment and solvation is known to reduce the potential energy of a dipole, thereby stabilizing this form relative to the anti-conformation. In the solid state, below the T_m of soft segment, the anti-conformations tend to be preferred over the skewed form, although both are possibly present to an appreciable extent at equilibrium. Increasing the temperature by heating may increase the populations of skew form at equilibrium due to that energy is provided externally to overcome the rotational barrier of the transition from anti to skew conformations.

The distance between two 4,4'-bipyridinium units is expected to be larger in the anti-conformation than in the skew form. In the anti- conformation, two bulky triflic acid anions tend to stay away from each other due to the repulsion between two common charges. On the other hand, the repulsion forces between common charges are reduced in the skew form simply because two triflic acid anions are not on the same plane. As a result of that, the distance between two 4,4'-bipyridinium units are minimized in the skew form which imparts stronger interchain ionic interaction than the anti-conformation.

On the basis of foregoing discussion, the phenomenon of "jump" in E' therefore can be explained by a possibly increased ionic associations above the soft segment T_m. Certainly, a higher "jump" would be observed on ionenes with higher ionic concentration. The reversibility of this behavior can also be easily understood by employing the concept of conformational interconversion of 4,4'-bipyridinium salt at the conditions described. In addition, the onset temperature of the transition, T_o, clearly is dependent on the melting temperature of PTHF matrix since PTHF behaves as a liquid when temperature is above its T_m. This model also explained the thermal history dependency on the T_o which is a function of soft segment T_m. The soft segment T_m can be varied by heat treatment as has

been discussed earlier. The transition at E' "jump" is broaden as the T_m transition of soft segment is broad.

It is recalled that a significant penetration was observed at around 50°C in TMA spectra (Figure 5.29) of samples PTHF-1350-BP and PTHF-2550-BP while no observable penetration can be detected on sample PTHF-750-BP. The degree of such penetration appeared to be larger for sample with higher ionic content. For sample PTHF-750-BP, the PTHF soft segment phase is completely amorphous as indicated by DSC spectrum. Despite high ionic concentration, the PTHF-750 segment behaves as a liquid above its T_g. Therefore, no conformational interconversion of bipyridinium salt will be observed at 50°C. Although no dynamic mechanical spectrum on sample PTHF-750-BP is provided at this moment, it is expected that no E' "jump" will be detected at 50°C. The E' "jump" transition can only be observed when the PTHF soft segment is crystallizable. Moreover, a larger volume shrinkage was expected for sample with higher ionic content, i.e. larger penetration.

One should also recall that a crystallization exotherm observed in the first run in the high temperature DSC spectra of BP based PTHF-ionenes, as shown in Figure 5.27. Such a crystallization process is not reversible in the second run if the sample quenched from a temperature below its melting temperature. This may be due to the thermally induced restructuring of the ionic domains, which is in contrast to the conformational change with medium polarity as observed in lower temperature. Keep in mind that the rotation of two pyridinium rings along the single bond may be greatly enhanced by the energy provided externally. The prefered conformation at high temperature may not have a chance to go back to the oringinal state after cooling due to the hindered rotation by bulky counterions. No E' "jump" was observed at this temperature range from dynamic mechanical spectra. This may suggest that there is no net volume change of polymer during this

thermal-induced crystallization.

It is necessary to point out here that the foregoing discussions are only speculations and are not proven. Several methods are usually used to investigate molecular conformation as well as calculations of thermodynamic properties. Some of the more important physical methods are dipole-moment measurements, X-ray and electron-diffraction studies, infrared, ultraviolet, Raman, microwave, and nuclear magnetic spectroscopy. The instruments with heating capability and the flexibility of use of solid film samples could be utilized to characterize this unusual transition behavior observed on PTHF-ionenes.

To further prove the aforementioned speculations, 1,2-bis-(4-pyridyl)- ehtane (BPE) was utilized to couple with living PTHF dioxonium ions. The basic idea is to reduce the repulsion of common charges (triflic acid anion) on neighboring pyridinium rings by introducing a "spacer", two methylene units in the case of BPE. If it does as expected, the E' "jump should be less distinct than BP based ionenes or non-exist. The data in Figure 5.36 show this to be the case. Figure 5.36 presents storage modulus data as a function of temperature for BPE and BP based ionenes with similar ionic content. However, this system may not be directly correlated to the bipyridyl system since the two methlyene units provides flexibility to the ionic segment which is therefore exhibited small stereo-conformational effects as changing the medium polarity.

The BPE based ionenes show a much lower softening temperature than the BP based polymers. The is mostly attributed to the weak ionic association due to the more irregular structure than the 4,4'-bipyridinium salt.

trans-1,2-Dipyridine ethylene, has a rigid, symmetrical structure which

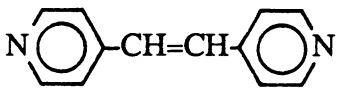

is chemically similar to the 4,4'-bipyridyl and a similar nucleophilicity toward living dioxonium ions was expected. Moreover, two pyridine rings are separated by an ethylene unit, a rigid "spacer", which can be utilized to reduced the steric tension of two large counterions as previously described. This system certainly would be of interest to investigate in the future to further clarify the proposed model.

5.5. CONCLUSION

Ion coupling of living PTHF dioxonium ion by ditertiary amine has been demonstrated to be a facile approach in synthesizing PTHF ionenes. 4,4'-Bipyridyl is the most effective coupling agent among the ditertiary amines studied. The coupling reaction is completed within minutes. Films for physical testing can be prepared by solvent casting directly from polymer solution. The polymers are also compression moldable and can be processed at 190^{o}C without losing mechanical strength. No weight loss was observed from thermogravmetric analysis up to 250^{o}C.

This approach is certainly of interest from the practical point of view. One of the problem thwarting continued rapid development in the field of ion-containing polymers is the lack of commercially available highly reactive and inexpensive ionic monomers from which suitable ion-containing polymer systems can be prepared. A more conventional approach for the preparation of PTHF ionenes is achieved by reacting ditertiary

amine-terminated PTHF oligomer with a reactive dihalide such as dibenzylhalide. Such a process is costly in the sense that it is a multistep process. The polymers thus obtained are usually not thermally stable enough for compression molding.

By using our approach, polymers with a wide range of properties can be prepared rapidly. Ionic concentration of the polymer was controlled by the PTHF segment molecular weight. PTHF-ionenes with high ionic content behave as a polyelectrolyte in high dielectric media such as methanol. A wide service temperature was noticed from -80°C to as high as 200°C. One unusual transition was observed from dynamic mechanical spectra at around 50°C. Such a transition is speculated to be related to conformational interconversion of 4,4'-bipyridinium salt from anti forms to skew conformations.

REFERENCES

1. D. Dieterich, W. Keberle, and H. Witt, Agnew. Chem. Int. Ed., 9, 40 (1970).
2. K.K.S. Hwang, C.Z. Yang, and S.L. Cooper, Polym. Eng. Sci., 21, 1027 (1981).
3. J.A. Miller, K.K.S. Hwang, and S.L. Cooper, J. Macromol. Sci., Phys. Ed., B 22 (2), 321 (1983).
4. Yu.S. Lipatov, L.V. Karabanova, L.M. Sergeyeva, and E.Ya. Gorichko, Polym. Sci. U.S.S.R., 24 (1), 126 (1982).
5. S.L.Hsu, H.X. Xiao, H.H. Szmant, and K.C. Frisch, J. Applied Polym. Sci., 29, 2467 (1984).
6. A. Rembaum, Adv. Urethane Sci. and Tech., 2, 109 (1973).
7. S.V. Laptil, V.N. Vatulev, Y.Y. Kercha, A.G. Kakovenk, V.V. Yoroshenko, A.P. Grekov, and I.Y. Litvin, Vysikomol. Soedin. Ser., 23 (10), 760 (1981).

8. A. Eisenberg, and M. King, "Ion-Containing Polymers: Physical Properties and Structure", Academic Press, New York (1977).

9. L. Holliday, Ed., "Ionic Polymers," Applied Sci., London (1975).

10. O. Lorenz, H. August, H. Hick, and F. Triebs, Angew. Makromol. Chem., 63, 11 (1977).

11. M. Rutkowska, J. Applied Polym. Sci., 31, 1469 (1986).

12. X. Yu, M.R. Nagarajan, C. Li, P.E. Gibson, and S.L. Cooper, J. Polym. Sci., B (24), 2681 (1986).

13. X. Yu, M.R. Nagarajan, T.G. Grasel, P.E. Gibson, and S.L. Cooper, J. Polym. Sci., Polym. Phys. Ed., 23, 2319 (1985).

14. H. Kothandaraman, K. Venkatarao, A. Raghavan, and V. Chandrasekaran, Polym. Bulle., 13, 353 (1985).

15. J. Economy, J.H. Mason, and L.C. Wohrer, J. Polym. Sci., A1, 8, 2231 (1970).

16. B. Lee, unpublished results.

17. M.F. Hoover and G.B. Butler, J. Polym. Sci.: Symposium No. 45, 1 (1974).

18. E.R. Littmann and C.S. Marvel, 52, 287 (1930).

19. C.F. Gibbs, E.R. Littmann, and C.S. Marvel, J. Amer. Chem. Soc., 55, 753 (1933).

20. M.R. Lehman, C.D. Thompson, and C.S. Marvel, J. Amer. Chem. Soc., 55, 1977 (1933).

21. C.F. Gibbs and C.S. Marvel, J. Amer. Chem. Soc., 56, 725 (1934).

22. C.F. Gibbs and C.S. Marvel, J. Amer. Chem. Soc., 57, 1137 (1935).

23. A. Rembaum, J. Macromol. Sci., A3, 87 (1969).

24. H. Noguchi, and A. Rembaum, J. Polym. Sci. B, 7, 383, 395 (1969).

25. J.C. Salamone, and B. Snider, J. Macromol. Sci., A1, 3495 (1970).

26. E.G. Knapick, J.A. Hirsch, and P. Ander, Macromol., 18, 1015 (1985).

27. W. Kern and E. Brenneisen, J. Prakt. Chem., 159, 194 (1941).

28. J.E. Kirby and J.F. Lontz, U.S. Patent, 2,388,614 (November 6, 1945).

29. A. Rembaum, W. Baumgartner, and A. Eisenberg, J. Polym. Sci. B, 6, 159 (1968).

30. D. Casson and A. Rembaum, Macromolecules, 5, 75 (1972).

31. D. Casson and A. Rembaum, J. Polym. Sci., 8, 773 (1970).

32. V. Hadek, H. Noguchi, and A. Rembaum, Macromolecules, 4, 494 (1971).

33. H. Noguchi and A. Rembaum, Macromolecules, 5, 253 (1972).

34. A. Rembaum and H. Noguchi, Macromolecules, 5, 261 (1972).

35. M.S. Simon, and P.T. Moore, J. Polym. Sci., Chem. ed., 13, 1 (1975).

36. A. Factor, and G.E. Heinsohn, J. Polym. Sci. Polym. Lett., 9, 289 (1971).

37. E. Jenckel and R. Heusch, Kolloid-Z. Z. Polym., 130, 89 (1953).

38. A. Eisenberg, H. Matsuura, and T. Yokoyama, Polym. J., 2, 117 (1971).

39. T. Tsutsui, R. Tanaka, and T. Tanaka, J. Polym. Sci. Polym. Phys., 13, 2091 (1975).

40. A. Blumstein, S.R. Kakivaya, K.R. Shah, and D.J. Wilkins, J. Polym. Sci.: Symposium No. 45, 75 (1974).

41. K. Sugiyama and T. Nakaya, Macromol. Chem., Rapid Commun., 7, 679 (1986).

42. F.L. Hirschfelder and G.M.J. Schmidt, J. Polym. Sci., A, 2, 2181 (1964).

43. M. Fujii, J. Polym. Sci. Polym. Phys. Ed., 24, 39 (1986).

44. K.T. Leffek and F.H.C. Tsao, Can. J. Chem., 46, 1215 (1968).

45. J.T. Burns and K.T. Leffek, Can. J. Chem., 47, 3725 (1969).

46. E.C.F. Ko and K.T. Leffek, Can. J. Chem., 48, 1865 (1970).

47. C.M. Leir and J.E. Stark, 3M Company, Macromol., in Press.

48. G.S. Manning, J. Chem. Phys., 51, 924 (1969).

49. A.J. Sonnessa, W. Cullen, and P. Ander, Macromolecules, 13, 195 (1980).

50. P. Ander, M. Casiero, T. Geer, L. Leung-Louie, J. Sapjeta, and S. Savner, Macromolecules, 15, 1333 (1982).

51. P. Ander, L. Leung-Louie, and F. Silvestri, Macromolecules, 12, 1204 (1979).

52. P. Ander, L. Leung-Louie, in "Polyamines and Ammonium Salts"; E.J. Goethals, Ed., Pergamon Press: Oxford, 1980.

53. R. Longworth, in "Developments in Ionic Polymers-1", A.D. Wilson and H.J. Prosser, Ed., Applied Science Publishers, New York, 1983.

54. J.H. Lupinski, and K.D. Kopple, Science, 146, 1038 (1964).

55. M. Watanabe, N. Toneaki, Y. Takizawa, and Isao Shinohara, J. Polym. Sci. Chem. Ed., 20, 2669 (1982).

56. M. Watanabe, N. Toneaki, and Isao Shinohara, Polym. J., 14(3), 189 (1982).

57. T.O. Paine (to NASA), "Ionene Membrane Separator," U.S. Pat. 3,629,161 (Dec. 21, 1971).

58. M. Watanabe, K. Nagaoka, M. Kanba, and Isao Shinohara, Polym. J., 14(11), 877 (1982).

59. S. Kohjiya, T. Ohtsuki, and S. Yamashita, IUPAC 6th International Symposium on Cationic Polymerization and Related Processes, Ghent, Belgium, Abstracts, 169 (1983).

60. S. Kohjiya, T. Ohtsuki, and S. Yamashita, Makromol. Chem., Rapid Commun., 2, 417 (1981).

61. S. Kohjiya, T. Hashimoto, S. Yamashita, and M. Irie, Chem. Lett., 1497 (1985).

62. S. Smith and A.J. Hubin, J. Macromol. Sci. Chem., 7, 1399 (1973).

63. M. Watanabe, N. Toneaki, and I. Shinohara, Polym. Prep. Jpn., 30, 552 (1981).

64. T. Kamiya and I. Shinohara, J. Polym. Sci., Polym. Lett. Ed., 17, 641 (1979).

65. T. Kamiya, K. Goto, and I. Shinohara, J. Polym. Sci., Polym. Chem. Ed., 17, 561 (1979).

66. A.V. Cunliffe, D.H. Richards, and F. Robertson, Polymer, 22, 108 (1981).

67. J.E. McGrath, in "Ring-Opening Polymerization: Kinetics, Mechanism and Synthesis", ACS Symposium Series No. 286 (1985).

68. K. Matsuda, Chemtech, 4, 744 (Dec. 1974).

69. S. Ushio, Chem. Eng., 78, 24 (Dec. 27, 1971).

70. H. Meerwein, G. Hinz, P. Hoffman, E. Kroning, and E. Pfeil, J. Prakt. Chem., 147, 257 (1937).

71. P. Dreyfuss, "Poly(tetrahydrofuran)", Gordon and Breach Science Publishers, New York, 1982.

72. S.G. Entelis, G.V. Korovina, and T.V. Grinevich, in "Cationic Polymerization and Related Processes", E.J. Goethals, Ed., Academic Press, New York, 1984.

73. F.R. Jones and P.H. Piesch, Chem. Commun., 1018 (1970).

74. J.M. Sangster and D.J. Worsfold, J. Macromol. Sci.- Chem., A7 (7), 1415 (1973).

75. A.M. Buyle, K. Matyjaszewski, and S. Penczek, Macromolecules, 10, 269 (1977).

76. P. Dreyfuss and M.P. Dreyfuss, Adv. Polym. Sci., 4, 528 (1967).

77. M.P. Dreyfuss and P. Dreyfuss, J. Polym. Sci. : A1 (4), 2179 (1966).

78. F.S. Dainton and K. Ivin, Quart. Rev., 12, 61 (1958).

79. H. Sawada, J. Macromol. Sci., Revs. Macromol. Chem., C8, 235 (1972).

80. W.M. Pasika and J.W. Wynn, J. Polym. Sci., A-1, 7, 1489 (1969).

81. M.P. Dreyfuss, J.C. Westfahl, and P. Dreyfuss, Macromolecules, 1, 437 (1968).

82. M. Szwarc, Fortschr. Hochpolymer. Forsch., 2, 275 (1960).

83. P. Dreyfuss and M.P. Dreyfuss, in "Encyclopedia of Chemical Technology", Vol.

13, 3rd Ed., John Wiley & Sons, Inc., 1982.

84. O. Vogl, J. Polym. Sci. Polym. Symp., No. 64, 1 (1978).

85. R. Milkovich, in "Anionic Polymerization" Edited by J.E. McGrath, ACS Symposium Series No. 166 (1981).

86. S.D. Smith and J.E. McGrath, Polym. Preprints, 27 (2), 31 (1986).

87. J. Sierra-Vargas, P. Masson, G. Beinert, P. Rempp, and E. Franta, Polym. Bull., 7, 277 (1982).

88. J. Sierra-Vargas, J.G. Zilliox, P. Rempp, and E. Franta, Polym. Bull., 3, 83 (1980).

89. R. Asami, M. Takaki, K. Kita, and E. Asakura, Polym. Bull., 2, 713 (1980).

90. A.C. Farthing, in "High Polymers", Vol. 13, Part I, N.G. Gaylord, Ed., Interscience Publishers, New York, 1963.

91. J. Guzman, M.A. Sanchez, and J.G. Fatou, An. Quim., 74 (9-10), 1155 (1978).

92. W. Stix and W. Heitz, Macromol. Chem., 180, 1367 (1979).

93. W. Ochsner and K.H. Reichert, Macromol. Chem., 150, 1 (1971).

94. G. Pruckmayr, US Patent 4,153,786 (to E. I. du Pont de Nemours and Co.), May 8, 1978.

95. D.J. Vaughan, "'Nafion', an Electrochemical Traffic Controller", E. I. du Pont de Nemours and Co., Wilmington, Del. 19898 (undated).

96. Y. Yamashita, M. Hirota, K. Nobutoki, Y. Nakamura, A. Hirao, S. Kozawa, K. Chiba, H. Matsui, and G. Hattori. J. Polym. Sci., B, 8, 481 (1970).

97. Y. Yamashita, M. Hirota, H. Matsui, A. Hirao, and K. Nobutoki, Polym. J., 2, 43 (1971).

98. S. Smith, W.J. Schultz, and R.A. Newmark, Polym. Preprints, 18, 6 (1977).

99. R. Hoene and K.H.W. Reichert, Makromol. Chem., 177, 3545 (1976).

100. E. Franta, L. Reibel, J. Lejmann, and S. Penczek, J. Polym. Sci. : Polym. Symp., 56, 139 (1976).

101. D.H. Richards, S.B. Kingston, and T. Souel, Polymer, 19, 68 (1978).

102. M. Kucera, F. Bozek, and K. Majerova, Polymer, 20, 1013 (1979).

103. K. Matyjaszewski, P. Kubisa, and S. Penczek, J. Polym. Sci., Polym. Chem., 12, 1333 (1974).

104. K. Matyjaszewski and S. Penczek, J. Polym. Sci., Polym. Chem., 12, 1905 (1974).

105. K. Matyjaszewski, P. Kubisa, and S. Penczek, J. Polym. Sci., Polym. Chem., 13, 763 (1975).

106. S. Kobayashi, H. Danda, and T. Saegusa, Macromolecules, 7, 415 (1974).

107. G. Pruckmayr and T.K. Wu, Macromolecules, 8, 954 (1975).

108. A.V. Cunliffe, D.B. Hartley, S.B. Kingston, D.H. Richards, and D. Thompson, Polymer, 22, 101 (1981).

109. Belg. Pat. 868,726, to E. I. du Pont de Nemours & Co., Jan, 4, 1979.

110. D. Sims, Makromol. Chem., 98, 235 (1966).

111. Y. Eckstein, D.P. Lee, R.P. Quirk, and P. Dreyfuss, J. Polym. Sci., Polym. Chem. Ed., 18, 2021 (1980).

112. K. Brzezinska, W. Chwialkowska, P. Kubisa, K. Matyjaszewski, and S. Penczek, Makromol. Chem., 178, 2491 (1977).

113. T. Saegusa and S. Matsumoto, J. Polym. Sci., A-1, 6, 1559 (1968).

114. Y. Eckstein and P. Dreyfuss, Anal. Chem., 52, 537 (1980).

115. D. Vofsi and A.V. Tobolsky, J. Polym. Sci., A3, 3261 (1965).

116. A. Davis and J.H. Golden, Makromol. Chem., 81, 38 (1965).

117. P. Dreyfuss, M.P. Dreyfuss, and H.A. Tucker, Adv. Chem. Ser., 128, 125

(1973).

118. T. Sakomura, T. Yoshida, Y. Fujita, and H. Shinbara, U.S. Patent 3,696,143, to Toyo Soda Manufacturing Co., Ltd., Oct. 3, 1972.
119. K.J. Ivin and T. Saegusa, Editors, "Ring Opening Polymerization" (in three volumes), Elsevier, 1984.
120. G. Berger, M. Levy, and D. Vofsi, J. Polym. Sci., B, 4, 183 (1966).
121. Y. Yamashita, K. Nobutoki, Y. Nakamura, and M. Hirota, Macromolecules, 4 (5), 548 (1971).
122. Y. Yamashita, M. Hirota,K. Nobutoki, Y. Nakamura, A. Hirao, S. Kozawa, H. Matsui, G. Hattori, and M. Okada, J. Polym. Sci., B, 8, 481 (1970).
123. F.J. Burgess, A.V. Cunliffe, and D.H. Richards, Euro. Polym. J., 14, 509 (1978).
124. J. Burdon, I. Farazmand, M. Stacey, and J.C. Tatlow, J. Chem. Soc., 2574 (1957).
125. G. ten Brinke, F.E. Karasz, and T.S. Ellis, Macromolecules, 16, 244 (1983).
126. J. Lehmann and P. Dreyfuss, Adv. Chem. Series, 176, 587 (1979).
127. R. Russo and E.L. Thomas, J. Macromol. Sci, Phys. Ed., B22 (4), 553 (1983).
128. G. Hallas, "Organic Stereochemistry", McGraw-Hill Publishing Company Ltd., London (1967).
129. C.B. Wang and S.L. Cooper, Macromolecules, 16, 775 (1983).

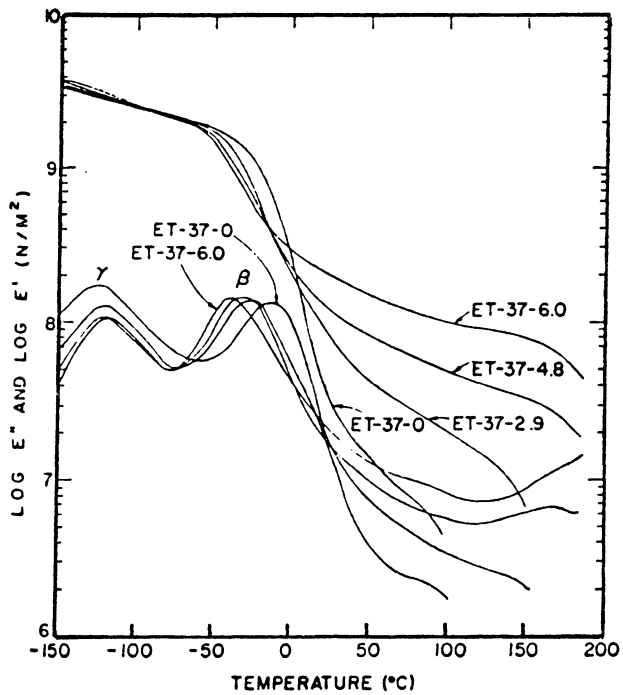

FIGURE 5.1. Dynamic Mechanical Properties of Polyurethane Zwitterionimers. [2]

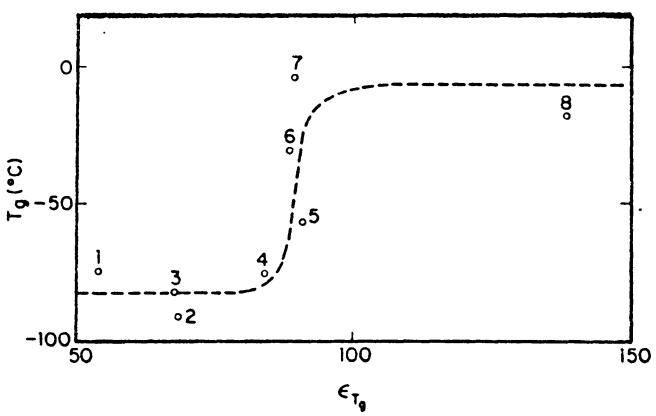

FIGURE 5.2. Glass Transition of a 6,8-ionene Using Various Plasticisers Versus Dielectric Constant of the Plasticizer. [38]

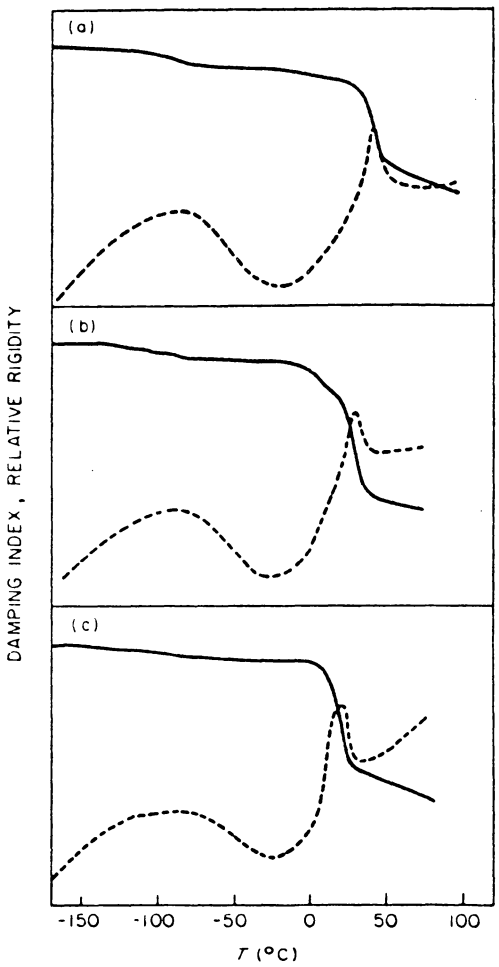

FIGURE 5.3. Temperature Dependence of Relative Rigidity (–)and Damping Index (--) of Ionenes. [39]

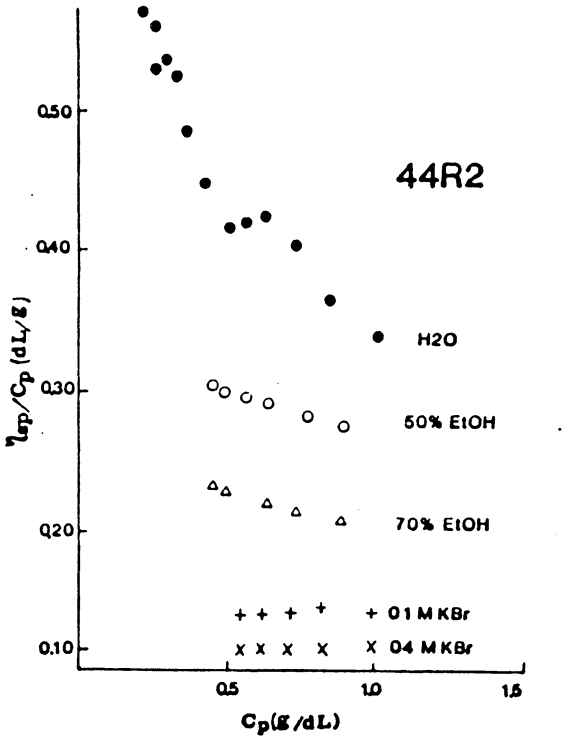

FIGURE 5.4. Concentration Dependence on the Reduced Viscosity for Ionene in Several Solvents. [26]

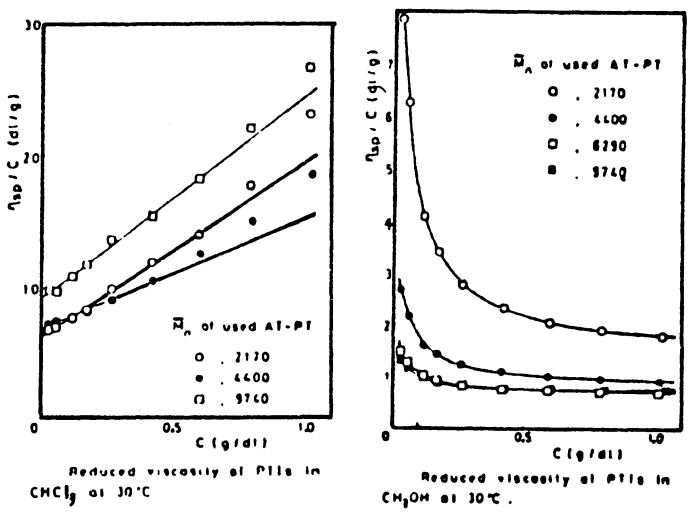

FIGURE 5.5. Solution Properties of PTHF-Ionene Elastomers. [59]

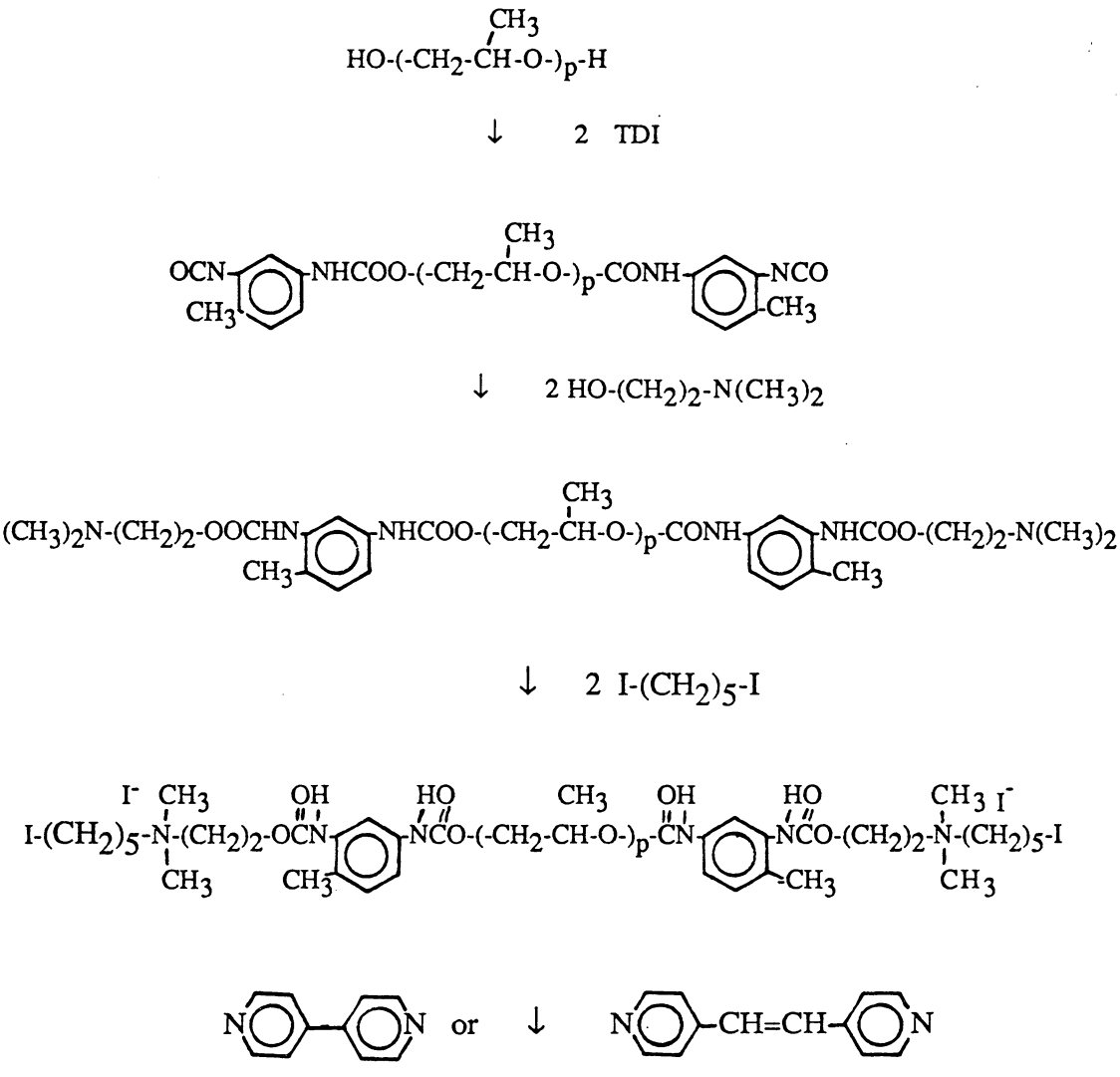

Elastomeric Ionenes

FIGURE 5.6. Procedure for Preparation of Elastomeric Ionene Polymers. [56]

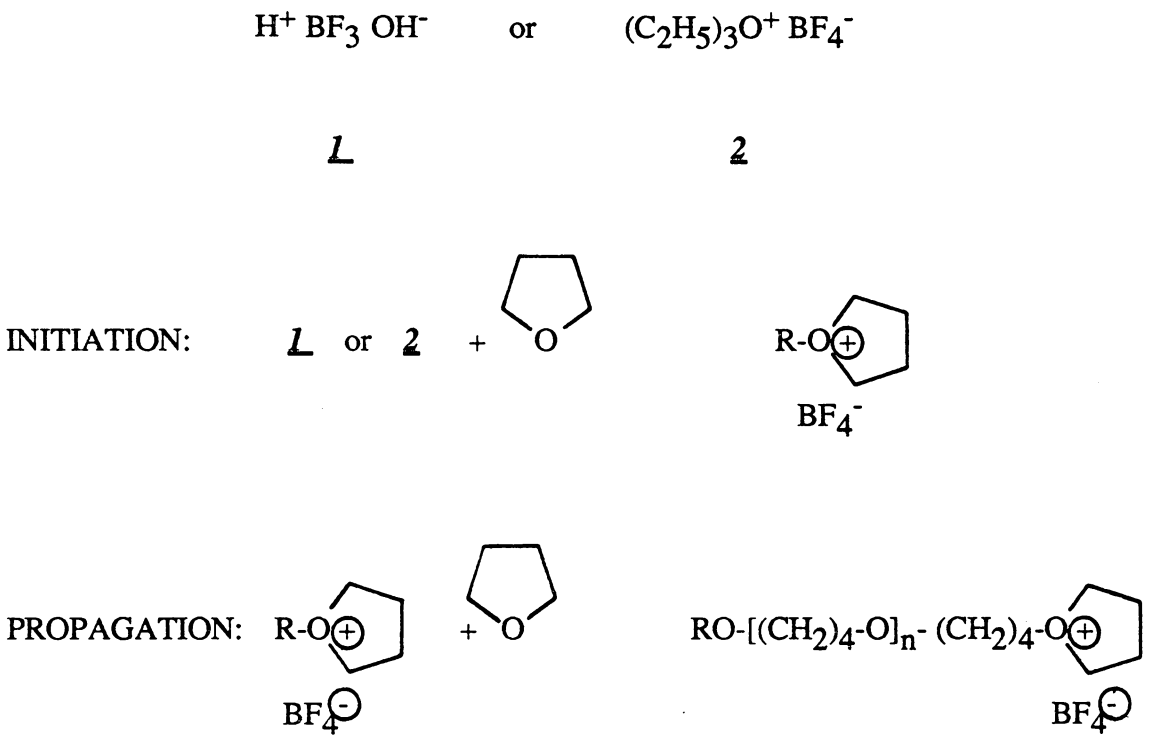

FIGURE 5.7. Cationic Initiated Polymerization of THF. [67]

$$\ln [M]_e = \frac{\Delta H_p}{RT} - \frac{\Delta S_p^0}{R} = \frac{\Delta G_p}{RT},$$

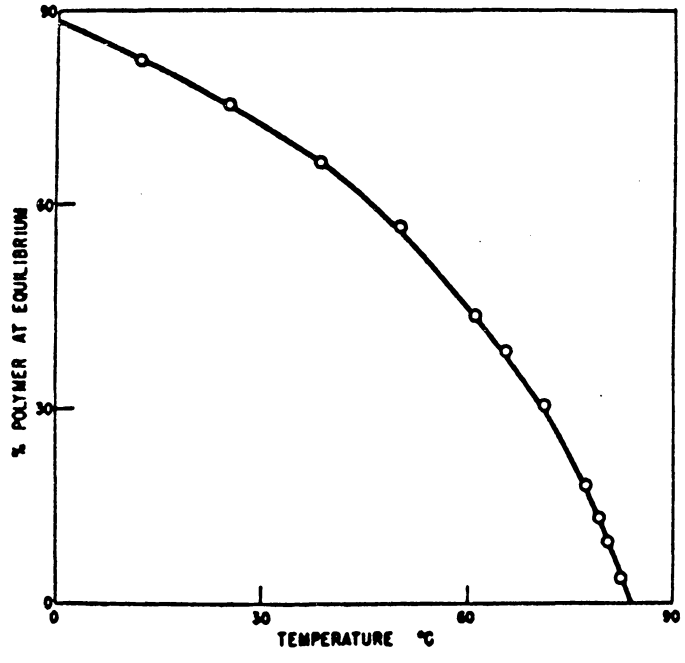

FIGURE 5.8. Effect of Temperature on Conversion to PTHF in Bulk THF polymerization.

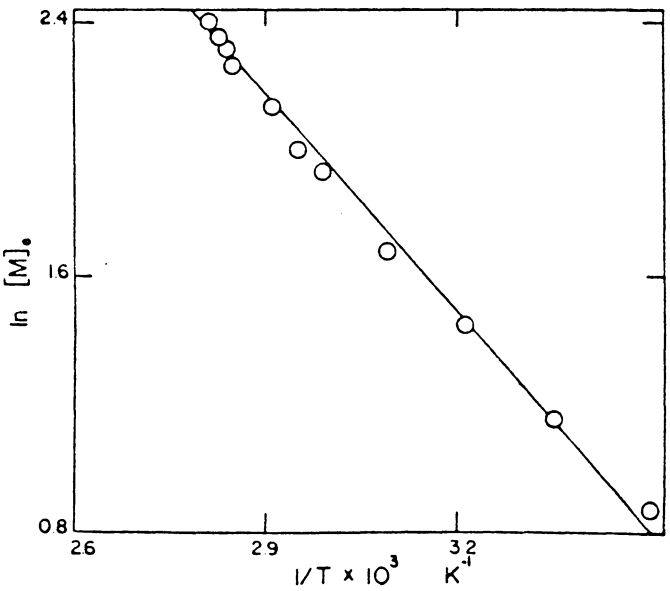

FIGURE 5.9. Equilibrium THF Concentration as a Function of Reciprocal Temperature. [76]

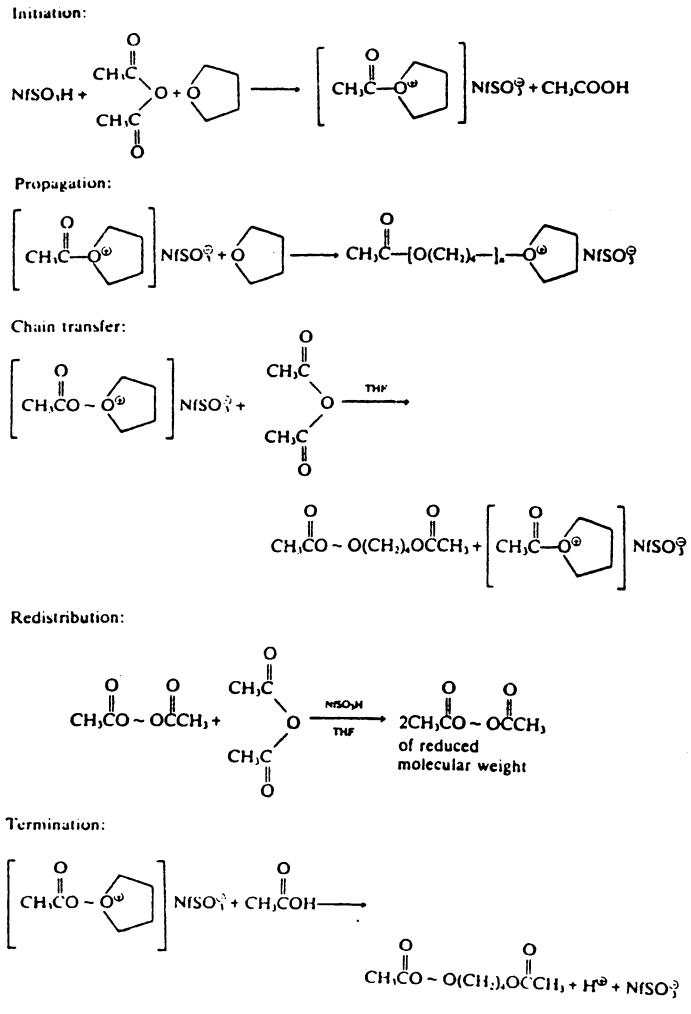

FIGURE 5.10. Commercial Route to Teracol® Polyether Polyols. [71]

TABLE 5.1. Photochromism of PTV in Solution and Solid States.

Entry	Solvent	[PTV][c] / %	Sensitizer or accelerator	Color observation
1	CH_3OH	1.3	none	remains colorless
2	"	0.18	EDTA,[d] proflavine[e]	yellow – deep green
3	NMP[f]	1.2	none	yellow – deep green
4	none	–	EDTA,[d] proflavine[e]	brown – deep brown
5	none	–	PVP[g]	light yellow – green

a) Entry Nos. 1-3. b) Entry Nos. 4 and 5. c) Concentration in g of PTV/100 cm^3 of solvent. d) Ethylenediaminetetraacetic acid tetrasodium salt. e) Mole ratio of [viologen]/[EDTA]/[proflavine] was 1/1.4/0.14. f) N-methyl-2-pyrrolidone. g) Poly(N-vinyl-2-pyrrolidone, 1.1 wt% of PTV.

TABLE 5.2. Physical Properties of PTHF.

Property	Value
melting temperature (T_m), °C	43 , 58–60
glass-transition temperature (T_g), °C	−80
density	
amorphous (at 25°C), g/cm^3	0.975
crystalline (at 25°C), g/cm^3	1.07 1.08
300% modulus, MPa	
high to low mol wt	1.6–14.3
cured plasticized high mol wt	13.7–19.0
compression modulus, MPa	
tensile strength, MPa	
high mol wt	29.0
high to low mol wt	27.6–41.4
cured	16.8–38.3
cured plasticized high mol wt	13.7–19.0
elongation, %	
high mol wt	820
high to low mol wt	300–600
cured	400–740
cured plasticized high mol wt	450–735
modulus of elasticity, MPa	97.0
heat-distortion temperature, °C	
at 1.82 MPa	
at 0.48 MPa	
Izod impact (notched, at 22.8°C), J/m	
Shore A hardness	95
Rockwell hardness	
thermal expansion coefficient (α) $= (1/V)(\partial V/\partial T)_p$, K^{-1}	4–7 × 10^{-4}
compressibility (β) $= (1/V)(\partial V/\partial T)_T$, kPa^{-1}	4–10 × 10^{-7}
internal pressure (P_i), MPa	281
ΔC_p (at T_g), J/(mol·K)[f]	
rapidly cooled	19.4
annealed	15.8
coefficient of expansion (dV_s/dT), cm^3/(g·K)	7.3 × 10^{-4}
refractive index (at 20°C)	1.48
dielectric constant (k_ϵ) (at 25°C)	5.0
solubility parameter (δ_p) (J/cm^3)$^{1/2}$ [m]	17.3–17.6
unit cell (oriented)	
monoclinic	C_2/c–C_{2n} C_2/c
a, nm	0.548–0.561
b, nm	0.873–0.892
c, nm	1.207–1.225
β, °	134.2–134.5

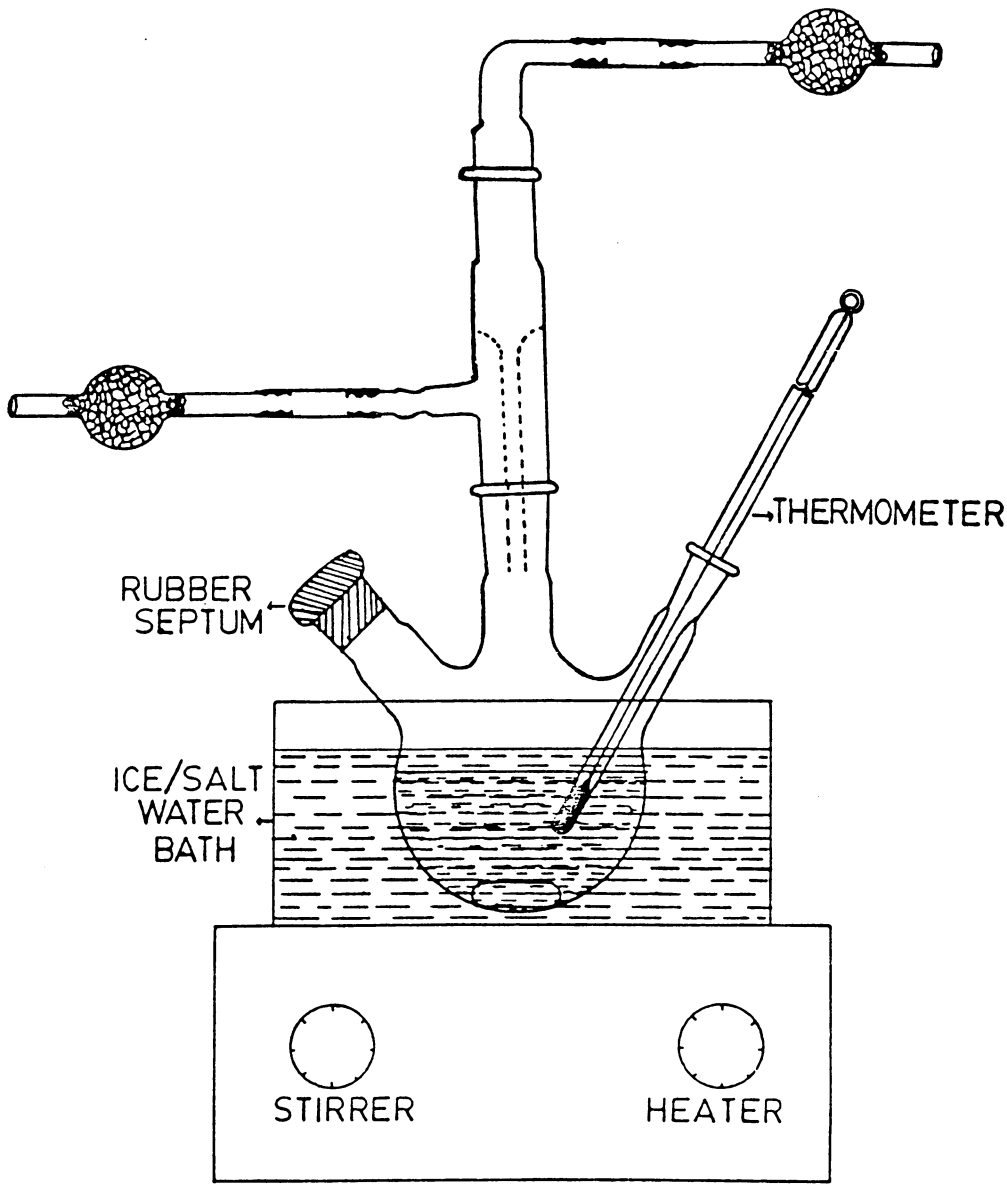

FIGURE 5.11. The Reaction Set-Up for the PTHF-Ionene Synthesis.

TABLE 5.3. Molecular Weight of Pyridine Terminated PTHF Reactions as a Function of Polymerization Time and Conversion.

TIME[1] sec.	CONV. %	Theor. PTHF[2] mol. wt.	Cal. PTHF[3] mol. wt.
430	9.5	800	950
680	15.7	1350	1300
930	20.5	1750	2100
1200	26.3	2250	2550
1500	35.9	3050	3350

1. THF Polymerization Time Before Terminated with Pyridine.
2. Based on % THF Monomer Conversion.
3. Based on ^{1}H NMR Results.

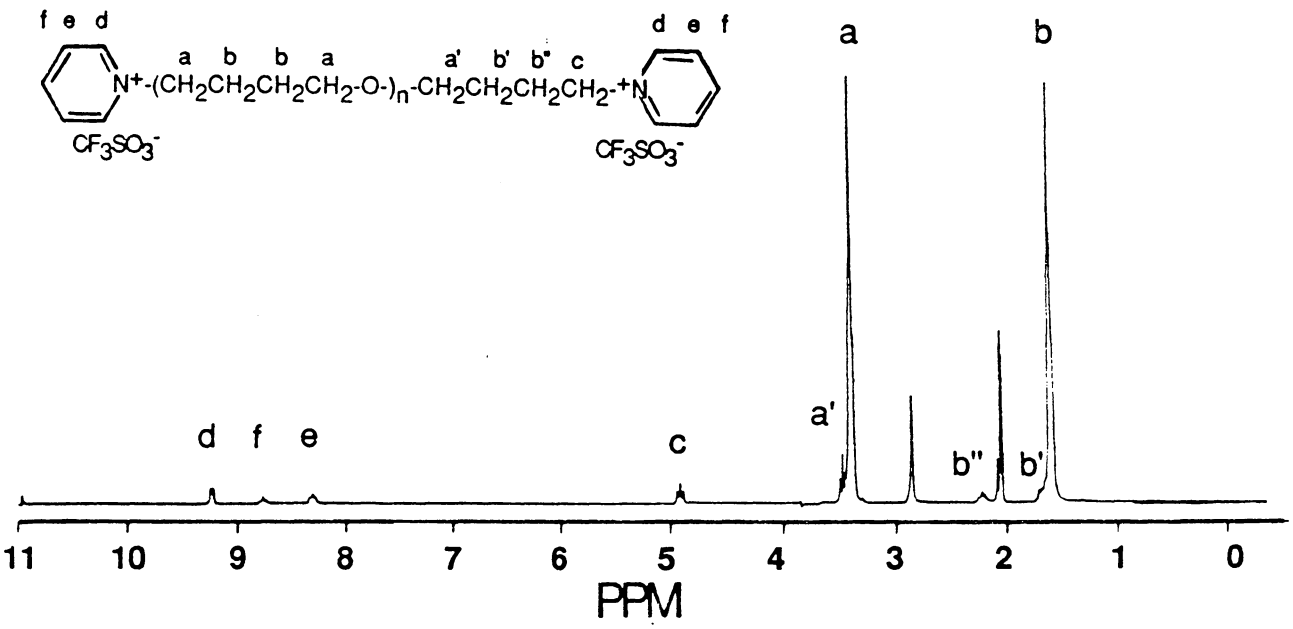

FIGURE 5.12. ^{1}H NMR of Pyridinium Salt Terminated PTHF.

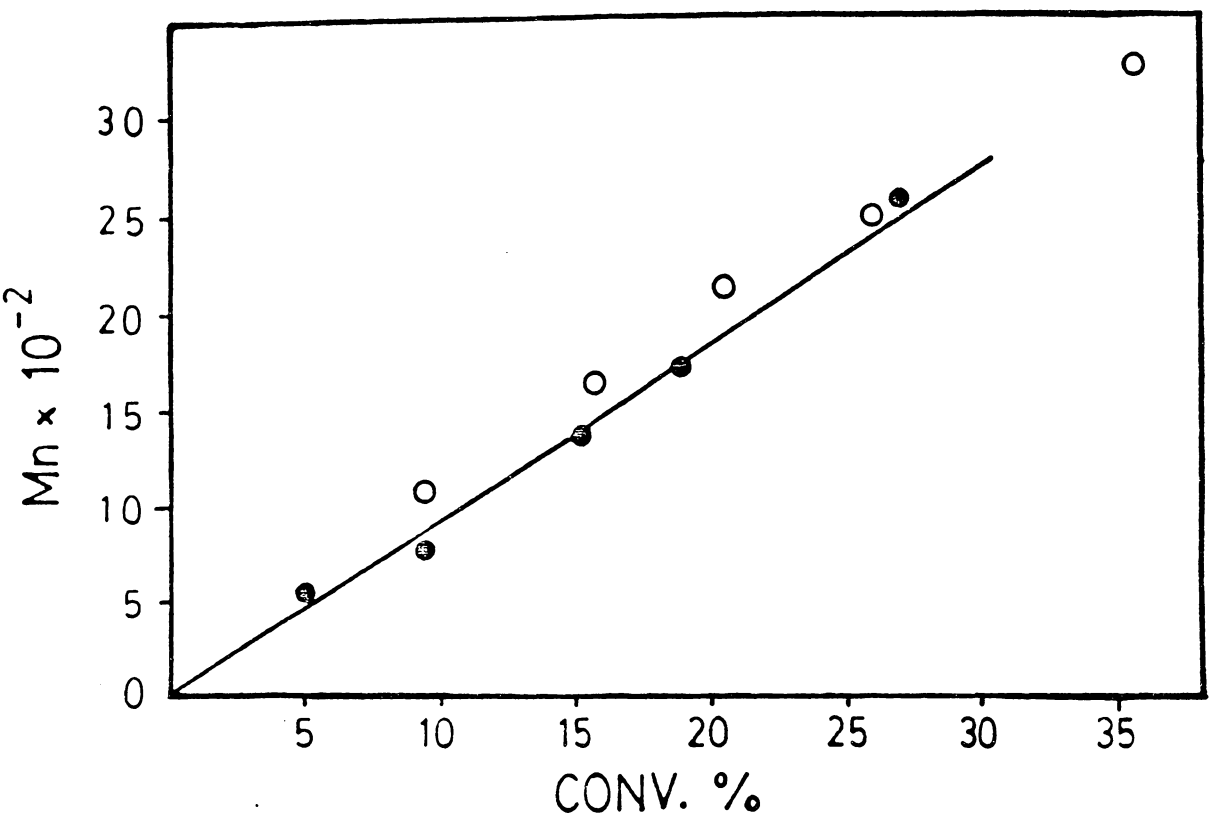

FIGURE 5.13. PTHF Segment Molecular Weight as a Function of Conversion.

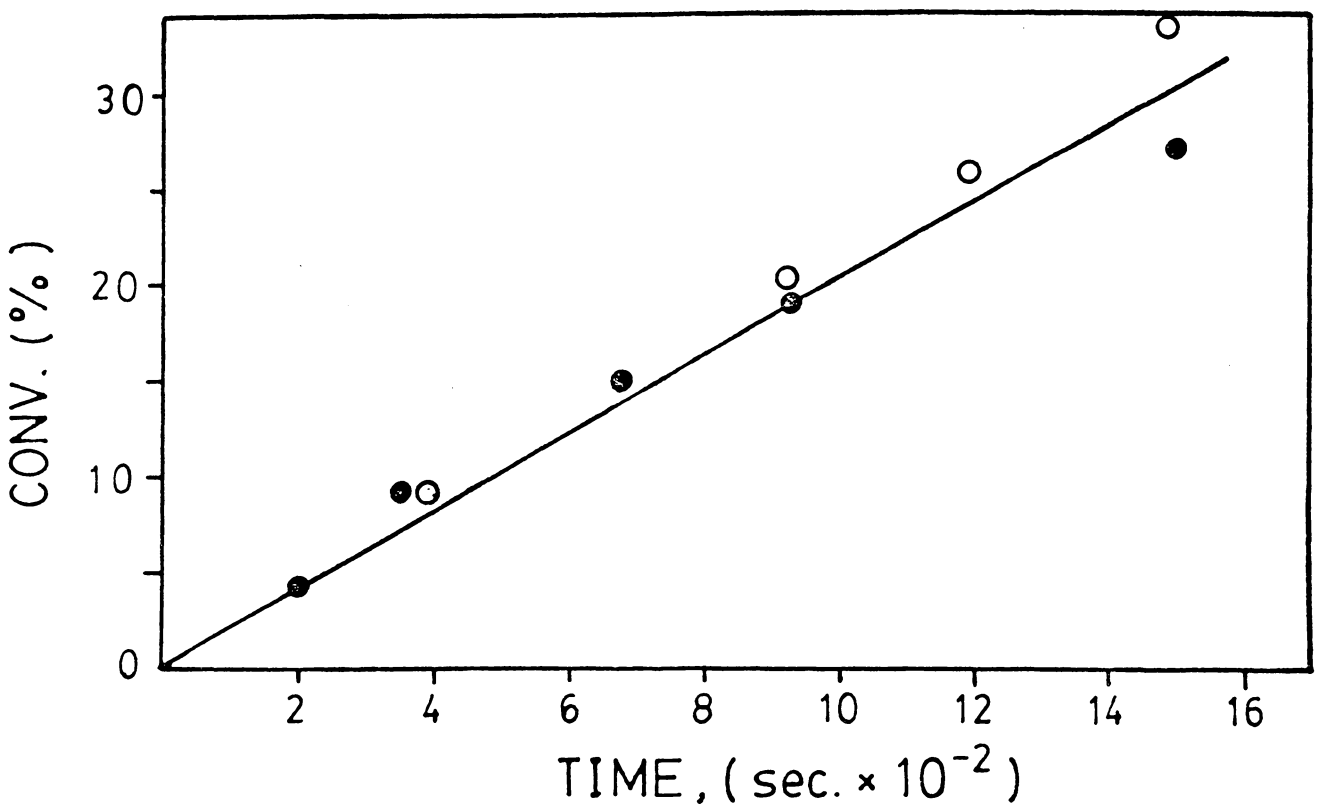

FIGURE 5.14. Monomer Conversion as a Function of Polymerization Time.

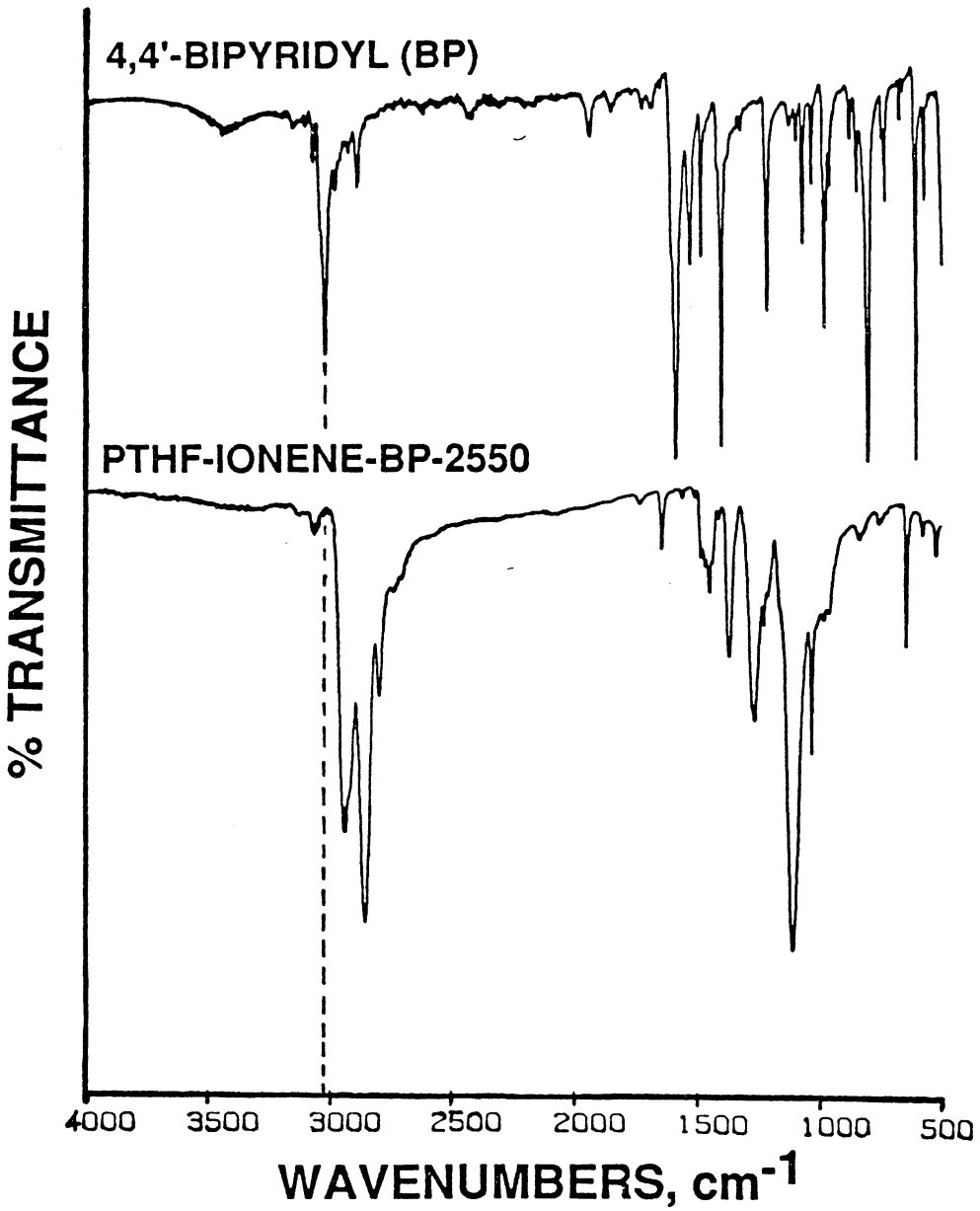

FIGURE 5.15. FT-IR Spectrum of PTHF-Ionene.

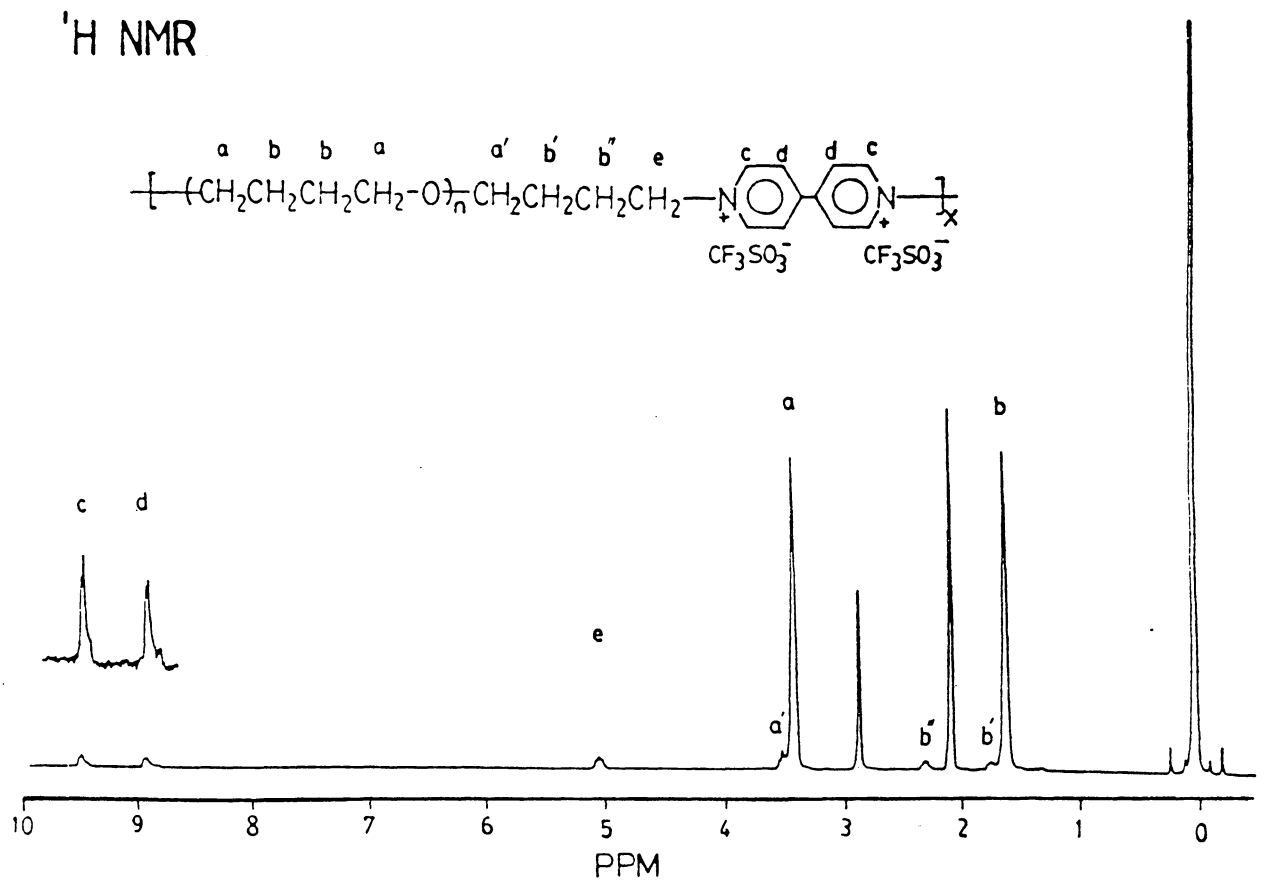

FIGURE 5.16. ^{1}H NMR of BP Based PTHF-Ionene.

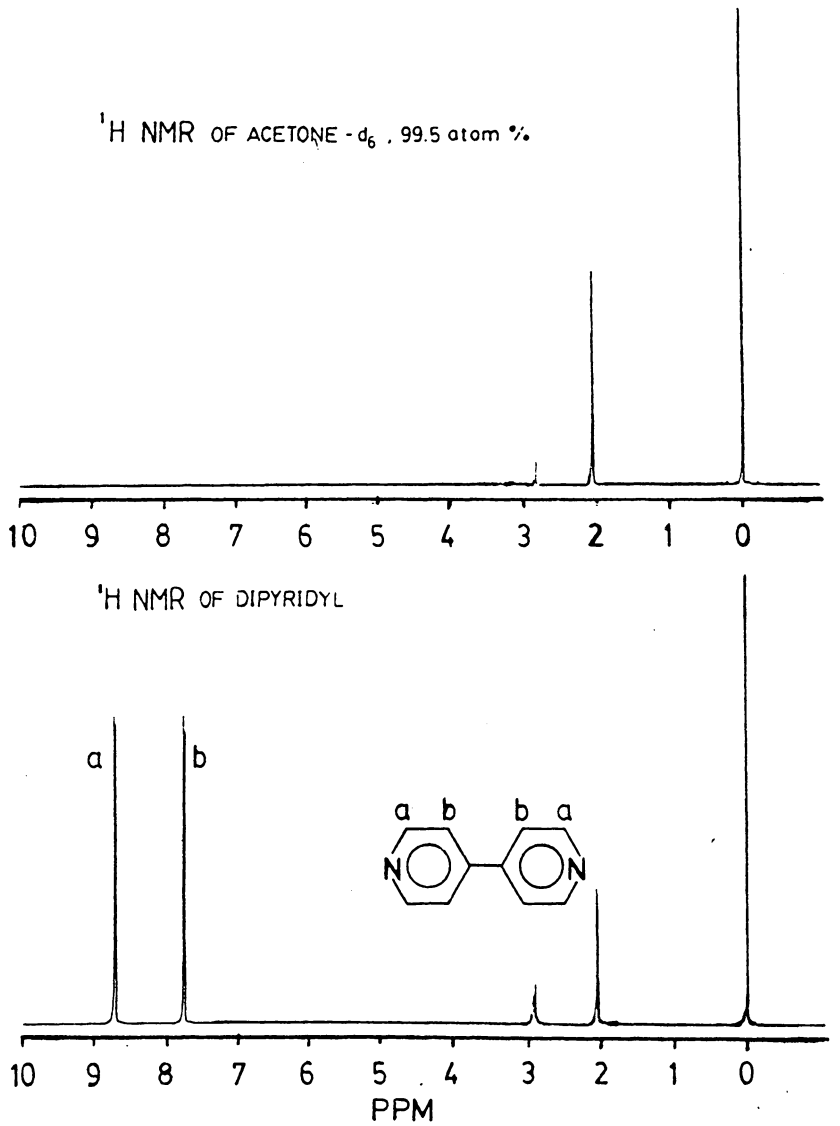

FIGURE 5.17. ^{1}H NMR of 4,4'-Dipyridyl and Acetone-d_6.

TABLE 5.4. PTHF Segment Molecular Weight as a Function of Polymerization Time Before Terminated with 4,4'-Dipyridyl.

SAMPLE	Time[1] sec.	Monomer Conversion, %	Theor. PTHF Seg. M.W.[2]	Cal. PTHF Seg. M.W.[3]
PTHF- 550-BP	200	4.7	400	550
PTHF- 750-BP	350	9.4	800	750
PTHF-1350-BP	680	15.3	1300	1350
PTHF-1700-BP	930	19.0	1600	1700
PTHF-2550-BP	1500	26.8	2500	2550

1. Allowed THF Polymerization Time Before Coupling with Ditertiary Amine.
2. Based on Monomer Conversions.
3. Based on ^{1}H NMR Results.

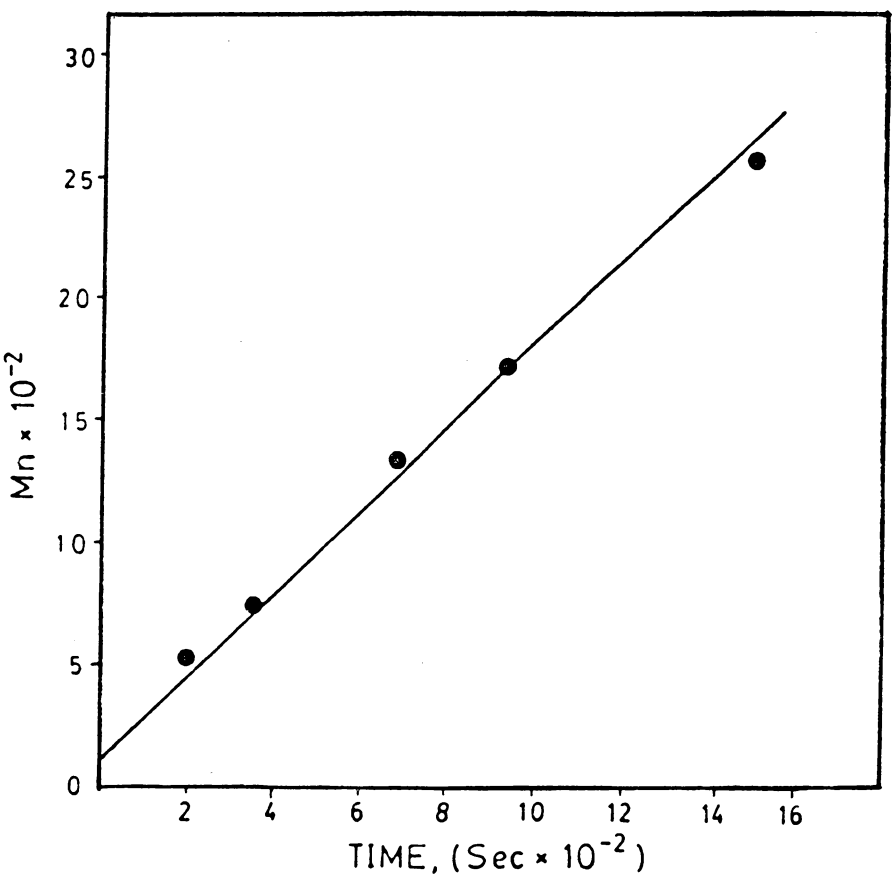

FIGURE 5.18. PTHF Segment Molecular Weight as a Function of Polymerization Time.

TABLE 5.5. Characteristics of PTHF-Ionenes Based on the 4,4'-Dipyridyl with Various PTHF Segment Molecular Weights.

SAMPLE	n* #	Hard Seg. wt.% (incl. counter ion)	Hard Seg. wt.% (w/o counter ion)	IONIC CONC.** mole %
PTHF- 550-BP	7.6	44.3	22.1	20.7
PTHF- 750-BP	10.4	36.9	17.2	16.1
PTHF-1350-BP	18.8	24.5	10.4	9.6
PTHF-1700-BP	24.6	20.5	8.4	7.5
PTHF-2550-BP	35.4	14.7	5.8	5.3

* # of tetramethylene oxide repeating unit with respect to each 4,4'-dipyridinium salt.

** Estimated ionic concentration = 2/n+2.

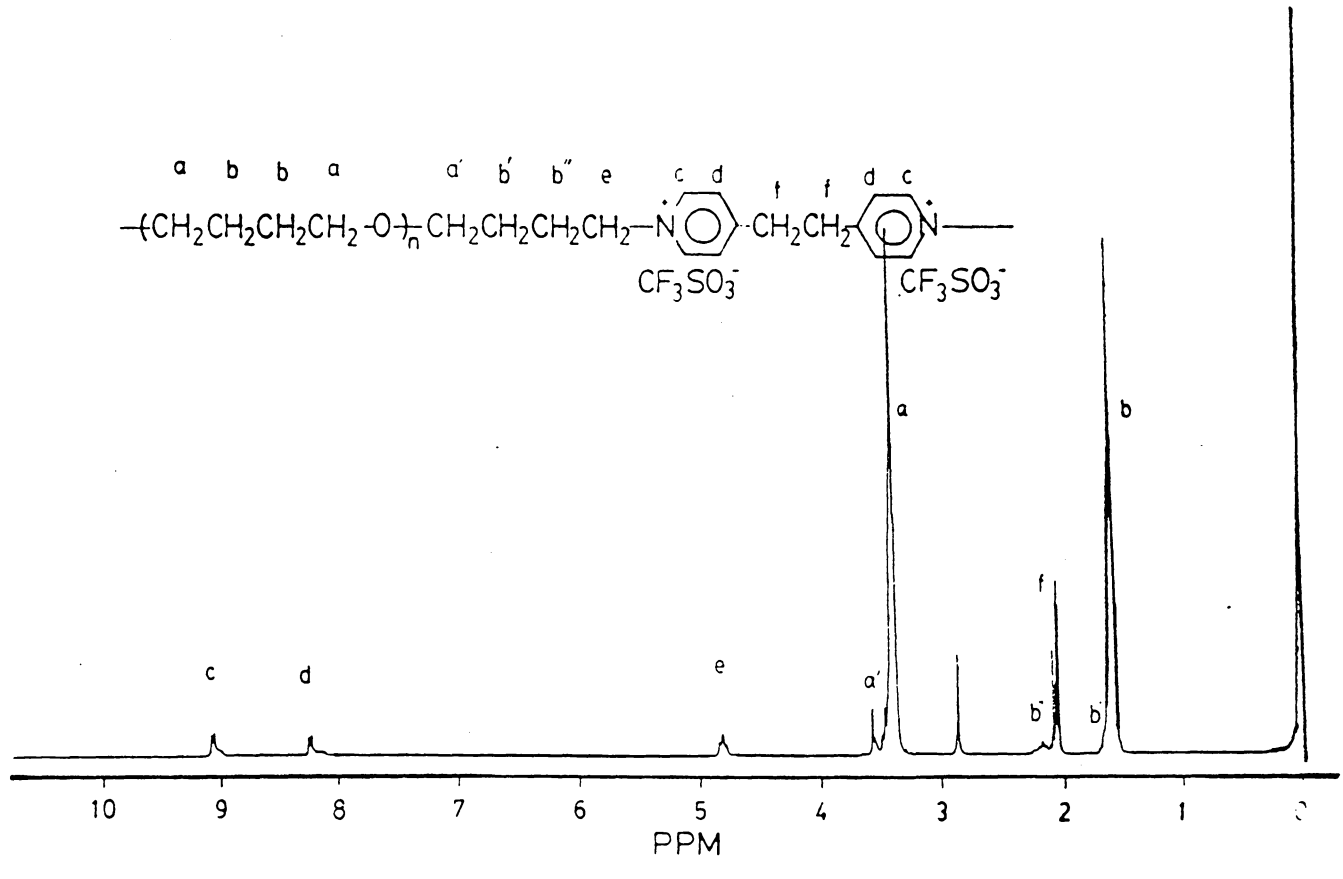

FIGURE 5.19. ^{1}H NMR of BPE Based PTHF-Ionene.

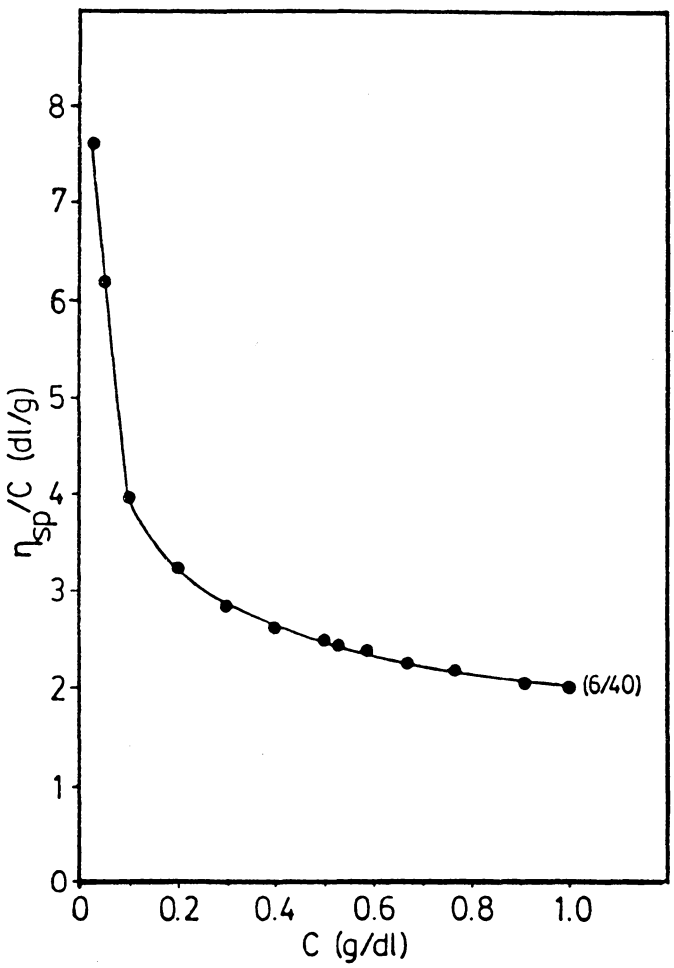

FIGURE 5.20. Solution Properties of PTHF-Ionene - Reduced Viscosity vs. Concentration.

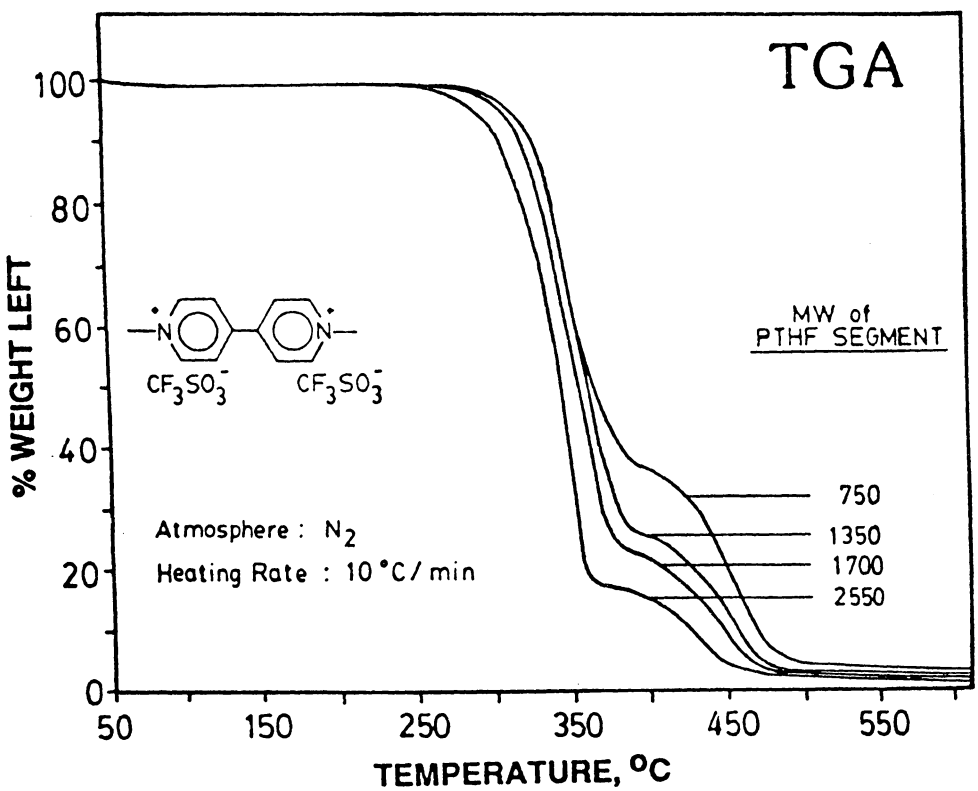

FIGURE 5.21. TGA Spectra of BP Based PTHF-Ionenes.

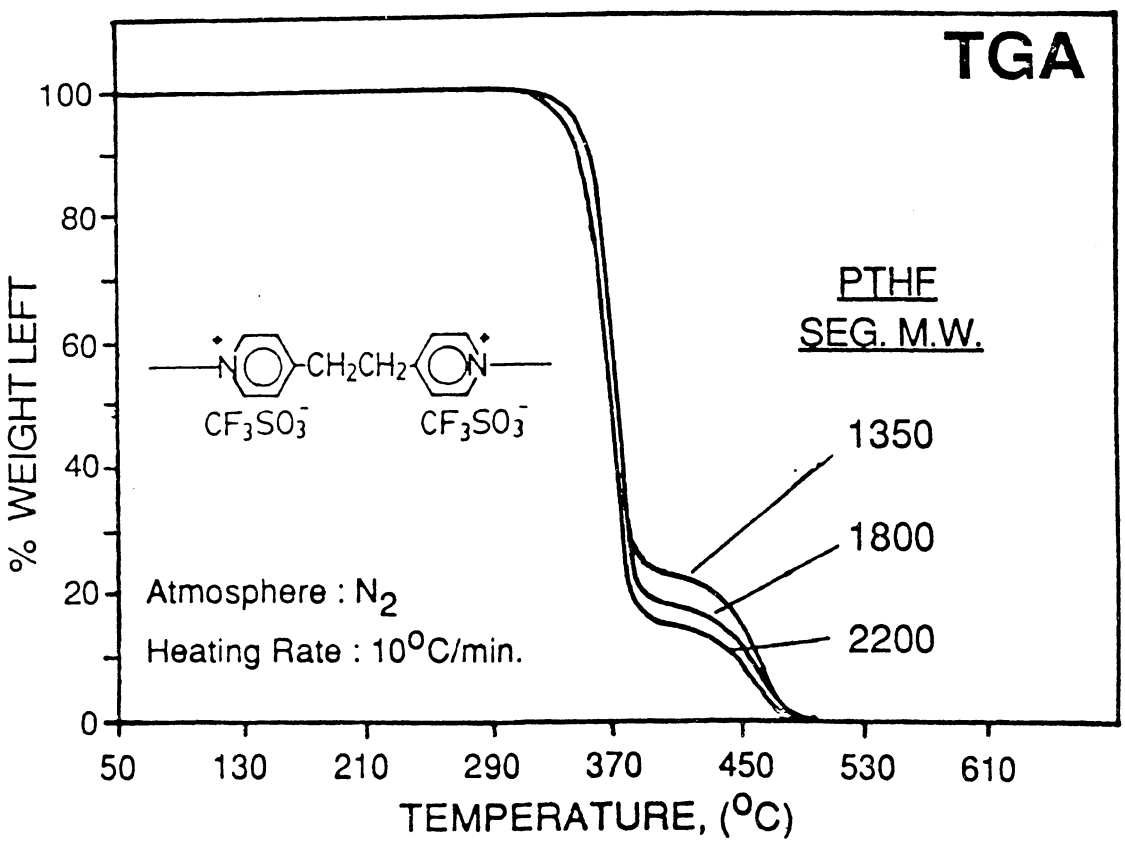

FIGURE 5.22. TGA Spectra of BPE Based PTHF-Ionenes.

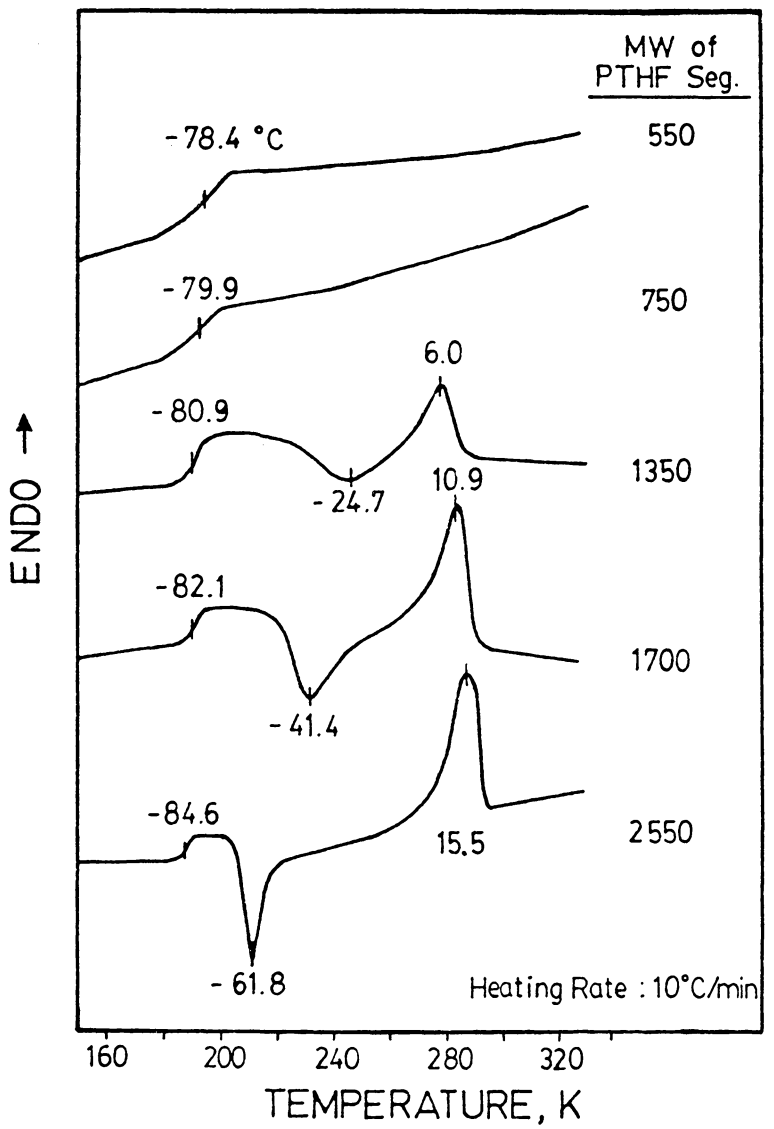

FIGURE 5.23. DSC Spectra of BP Based PTHF-Ionenes.

TABLE 5.6. Low Temperature DSC Behaviors of PTHF-Ionenes Based on the 4,4'-Dipyridyl with Various PTHF Segment Molecular Weights.

	Tg, °C					Tc		Tm	
Sample	onset	mid.	end	width	$\Delta C_p x10^{-2}$*	°C	$-\Delta H_c$*	°C	ΔH_f*
PTHF- 550-BP	-95.2	-78.4	-68.4	26.8	16.0	-	-	-	-
PTHF- 750-BP	-92.6	-79.9	-68.7	23.9	19.8	-	-	-	-
PTHF-1350-BP	-90.0	-80.9	-73.3	16.7	13.2	-24.7	2.2	6.0	2.1
PTHF-1700-BP	-90.1	-82.1	-77.8	12.3	13.3	-41.4	5.1	10.9	6.9
PTHF-2550-BP	-92.6	-84.6	-80.5	12.1	12.2	-61.8	8.7	15.5	10.4

* mcal/mg, All values of ΔC_p, ΔH_c, and ΔH_f have been normallized to the weight of the soft segment.

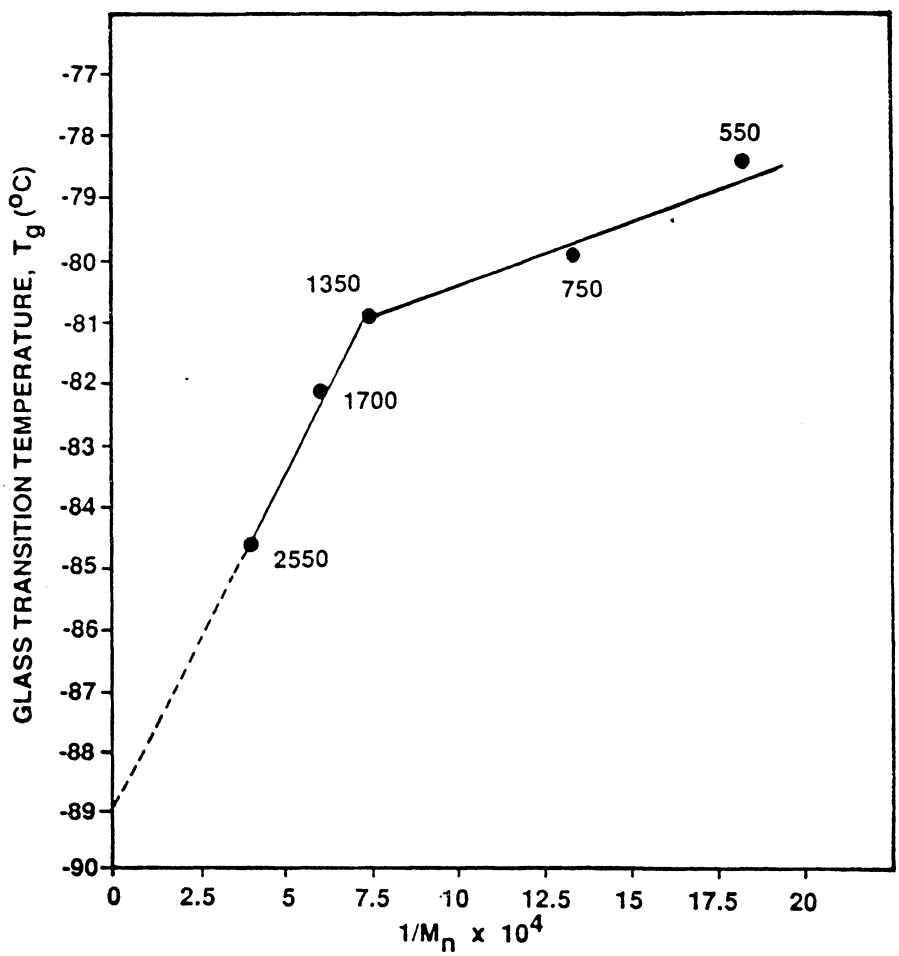

FIGURE 5.24. Glass Transition Temperatures as a Function of PTHF Segment Length.

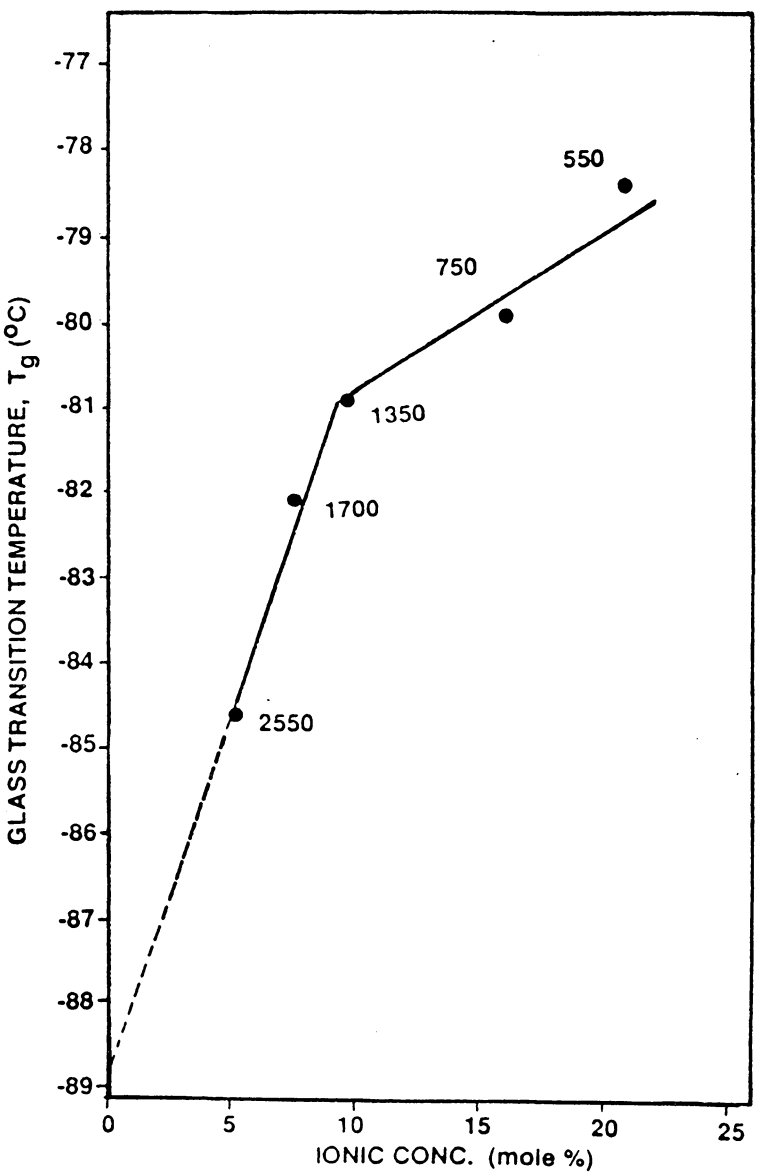

FIGURE 5.25. Glass Transition Temperatures as a Function of Ionic Concentrations.

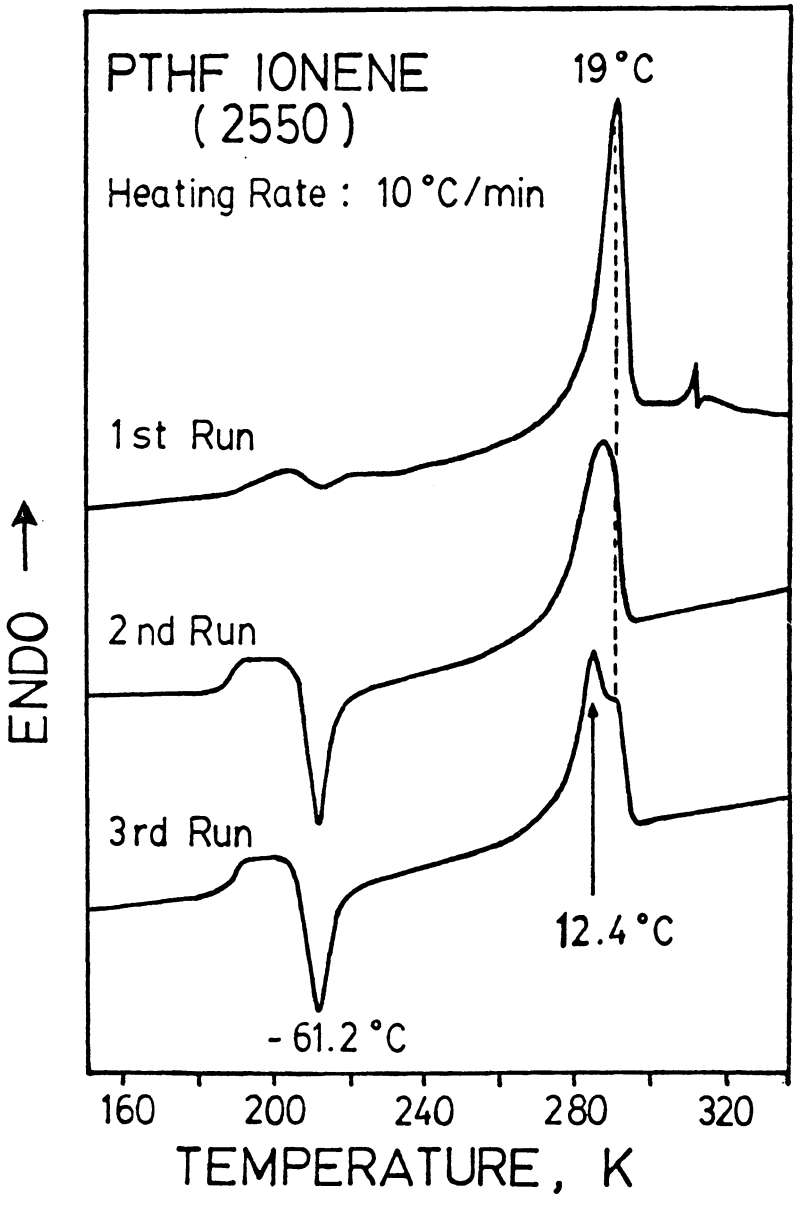

FIGURE 5.26. Thermal History Dependence of PTHF Low Temperature Transitions.

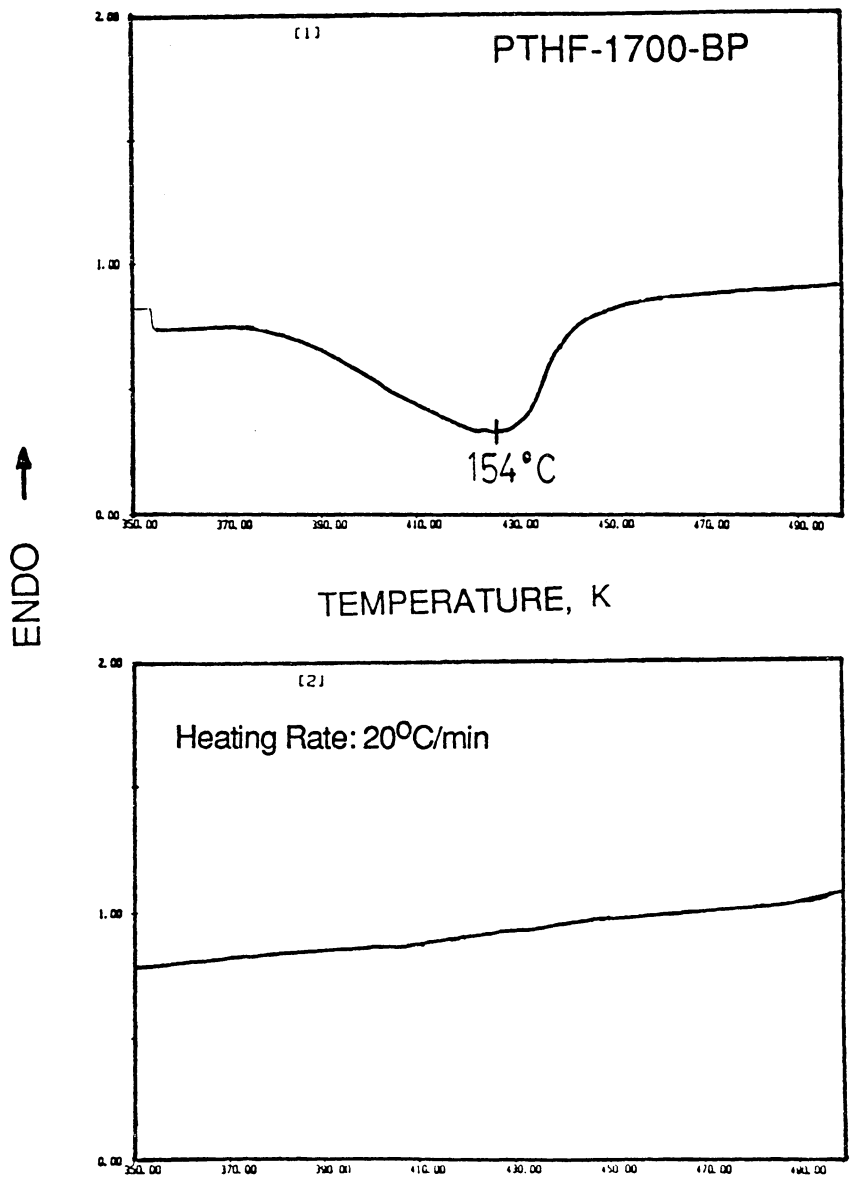

FIGURE 5.27. High Temperature DSC Transitions of BP Based PTHF-Ionenes.

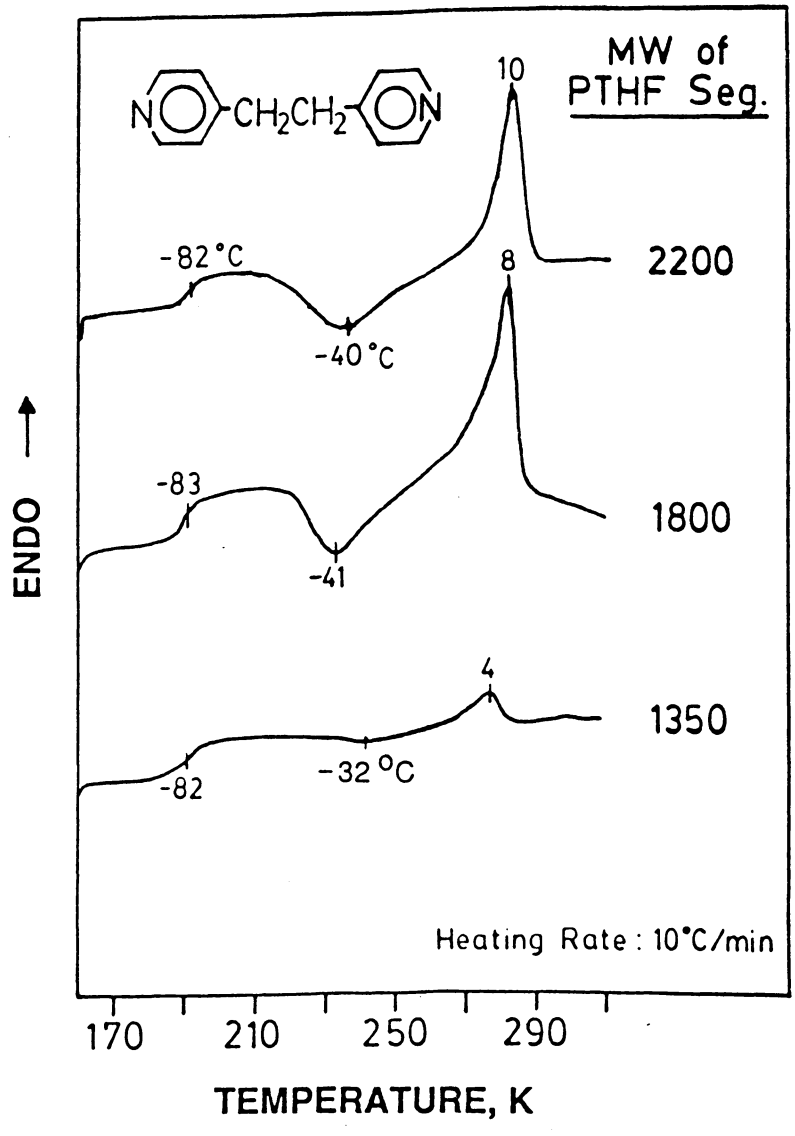

FIGURE 5.28. Low Temperature DSC Spectra of BPE Based PTHF-Ionenes.

TABLE 5.7. Characteristics of PTHF-Ionenes Based on the 1,2-Bis(4,4'-Pyridine)-Ethane with Various PTHF Segment Molecular Weights.

SAMPLE	Tg (°C) onset	mid.	end	width	$\Delta C_p x10^{-2}$*	Tc °C	Tc $-\Delta H_c$*	Tm °C	Tm ΔH_f*	Hard Seg. wt.% w/ [a]	w/o [b]	Ionic Content [c]
PTHF-1350-BPE	-91	-82	-77	14	14.1	-32	1.1	4	1.4	25.7	12.0	9.6
PTHF-1800-BPE	-89	-83	-78	11	13.6	-41	5.1	8	7.6	20.6	9.3	7.4
PTHF-2200-BPE	-87	-82	-77	10	12.1	-40	6.9	10	8.1	17.5	7.7	6.5

a. with considering the weight of counterions.

b. without considering the weight of counterions.

c. mole %, calculated as 2/2+n, where n is the number of repeating units of tetramethylene oxide with respect to each bipyridinium salt.

*. mcal/mg, All values of ΔC_p, ΔH_c, and ΔH_f have been normallized to the weight of the soft segment.

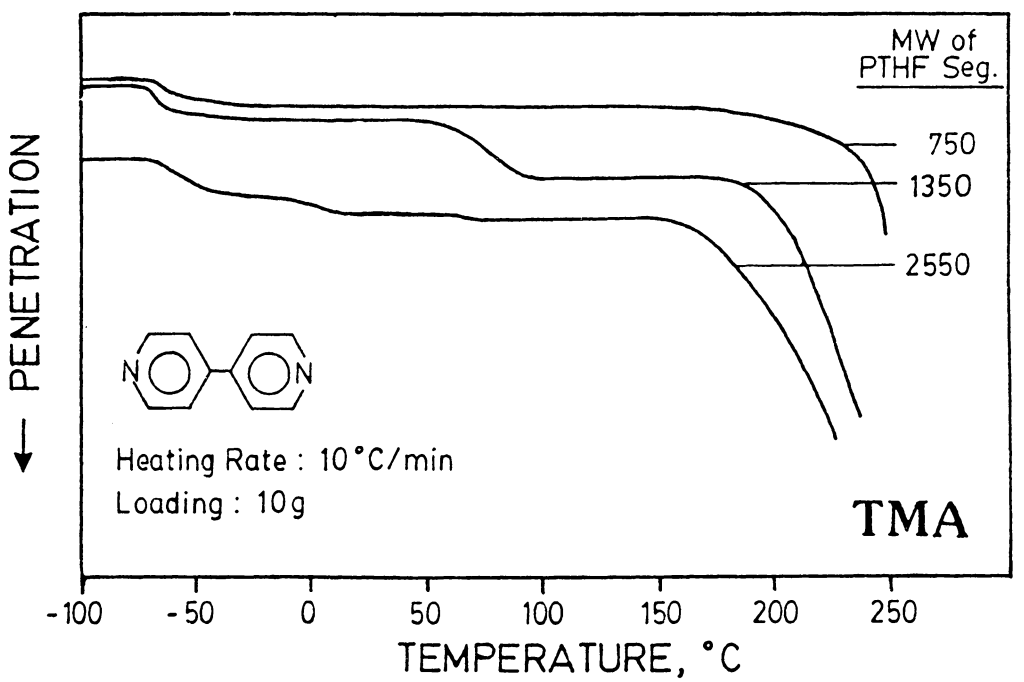

FIGURE 5.29. TMA Spectra of BP Based PTHF-Ionenes.

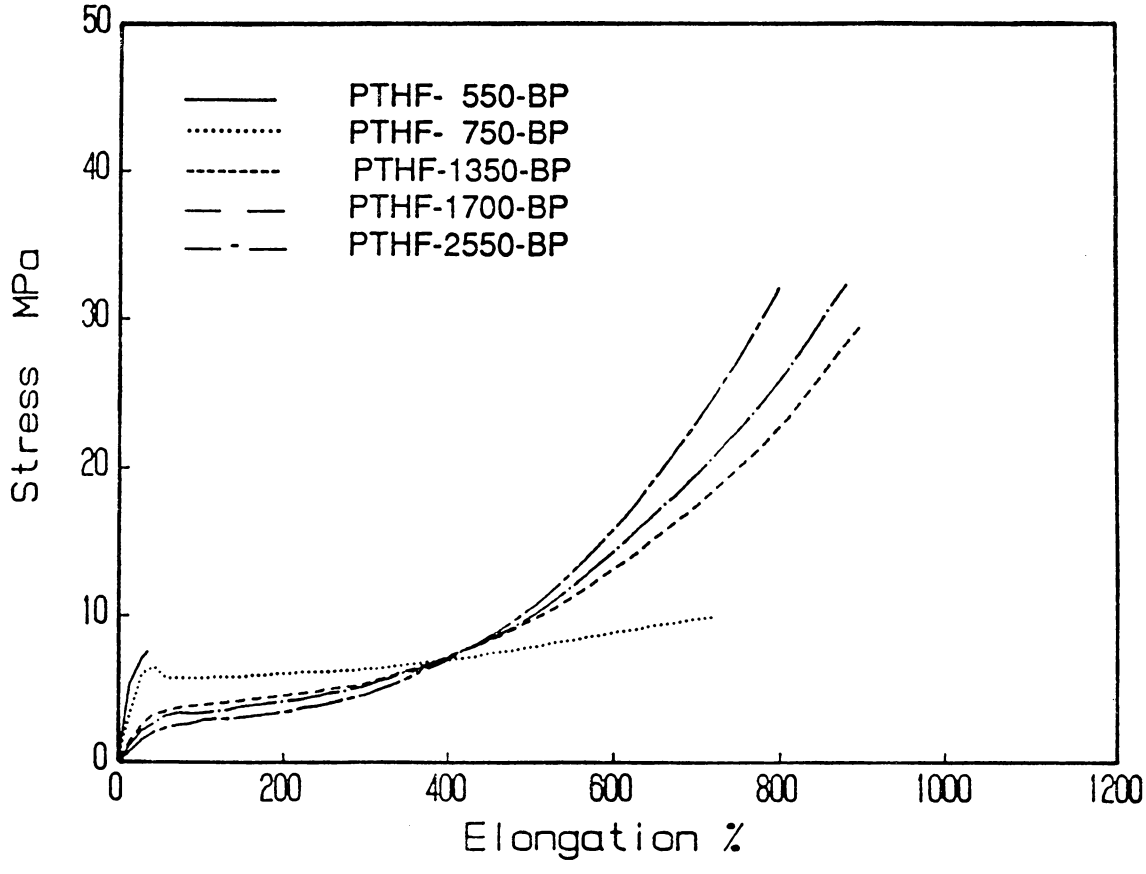

FIGURE 5.30. Stress-Strain Analysis of BP Based PTHF-Ionenes.

TABLE 5.8. Summary of Tensile Testing Results.

Sample	Elongation at Break %	Ultimate tensile strength MPa	Young's Modulus MPa
PTHF- 550-BP	30	8	26.1
PTHF- 750-BP	716	10	17.0
PTHF-1350-BP	895	30	6.7
PTHF-1700-BP	884	33	5.9
PTHF-2550-BP	800	33	4.4

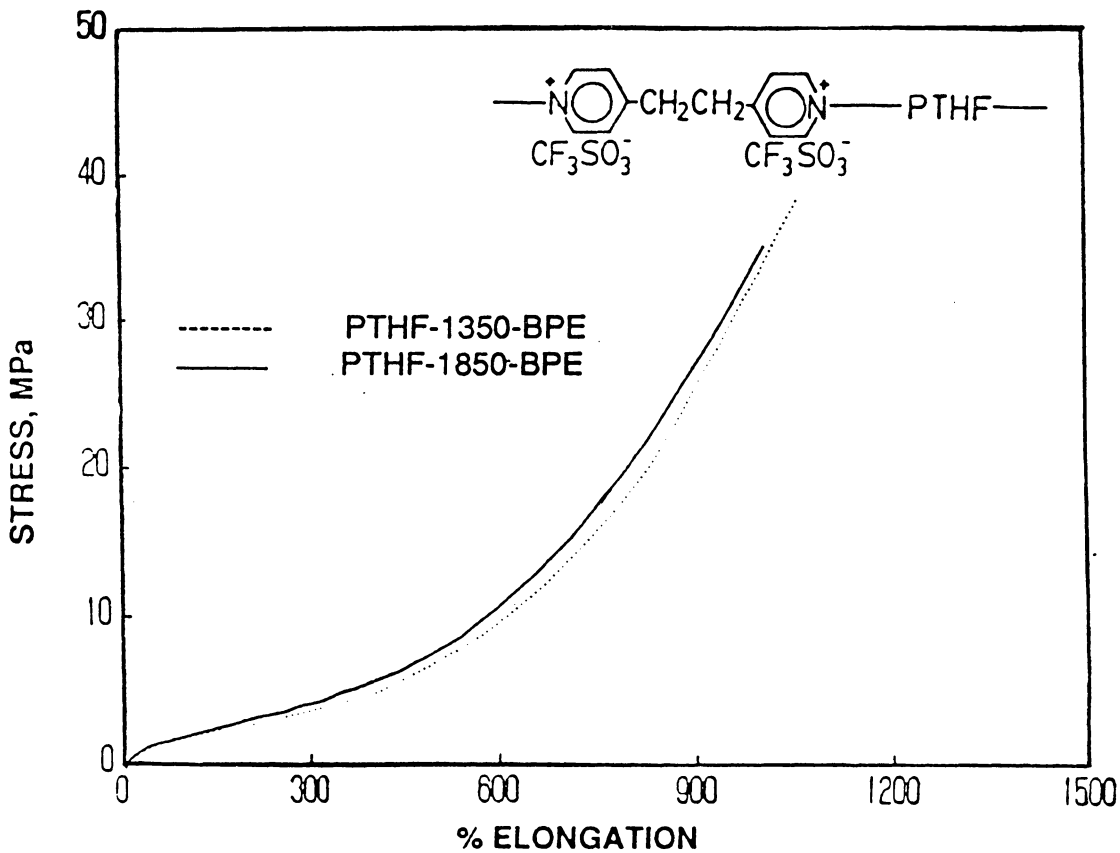

FIGURE 5.31. Stess-Strain Plot of BPE Based PTHF-Ionenes.

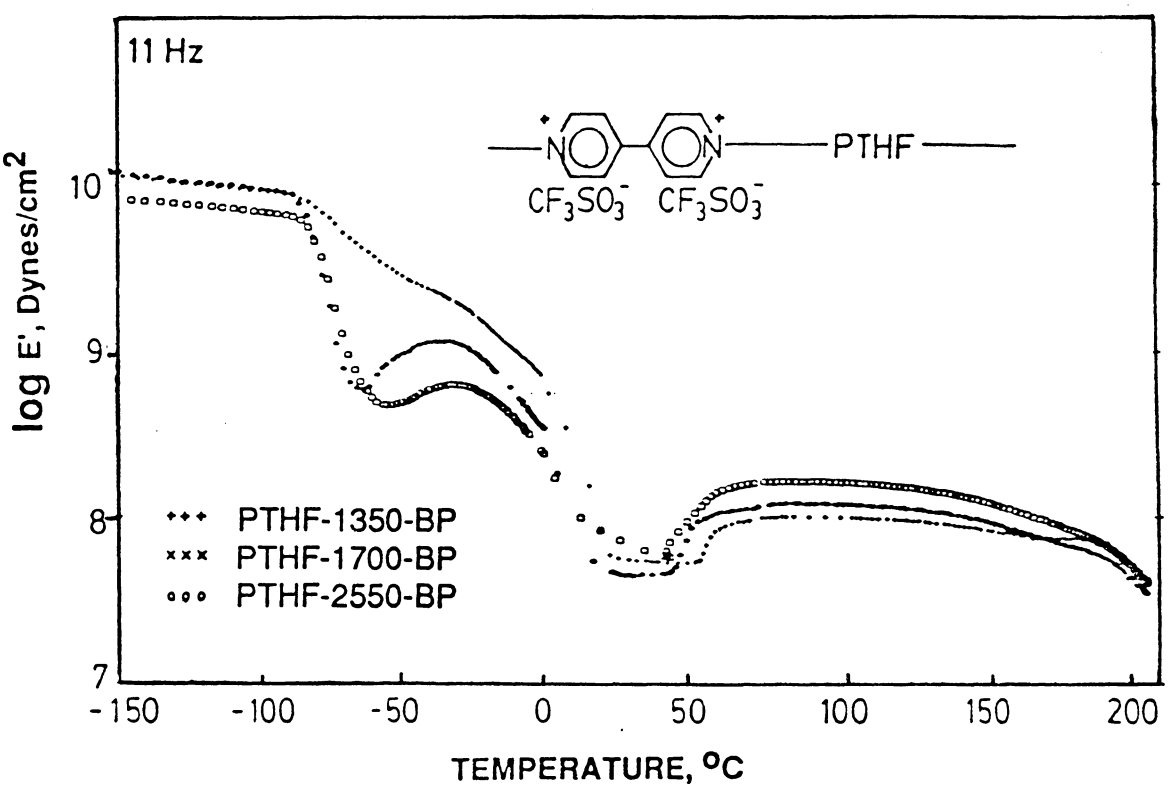

FIGURE 5.32. Storage Modulus Curves of BP Based PTHF-Ionenes.

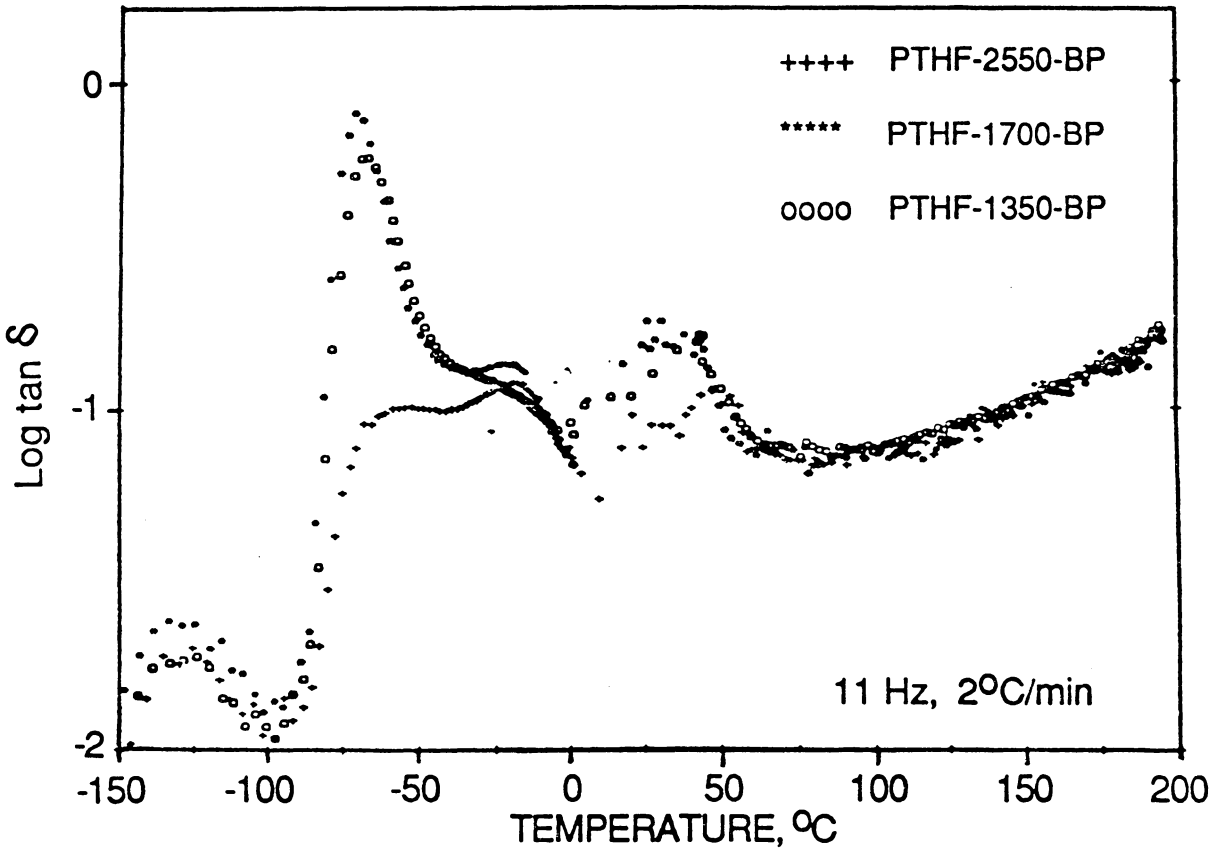

FIGURE 5.33. Tan δ vs. Temperature Curves of BP Based PTHF-Ionenes.

TABLE 5.9. Characteristics of Storage Modulus "JUMP".

Sample	Transition at "Jump"			extent of E' change	ionic conc.	T_m of PTHF [c]	$T_o - T_m$
	T_o [a]	T_e [b] (°C)	width	log E', dynes/cm^2	mole %	°C	°C
PTHF-1350-BP	40	66	25	0.45	9.6	6	34
PTHF-1700-BP	45	62	18	0.39	7.5	11	34
PTHF-2550-BP	53	62	9	0.24	5.3	19	34

a. onset temperature.

b. end temperature.

c. 1st run DSC values.

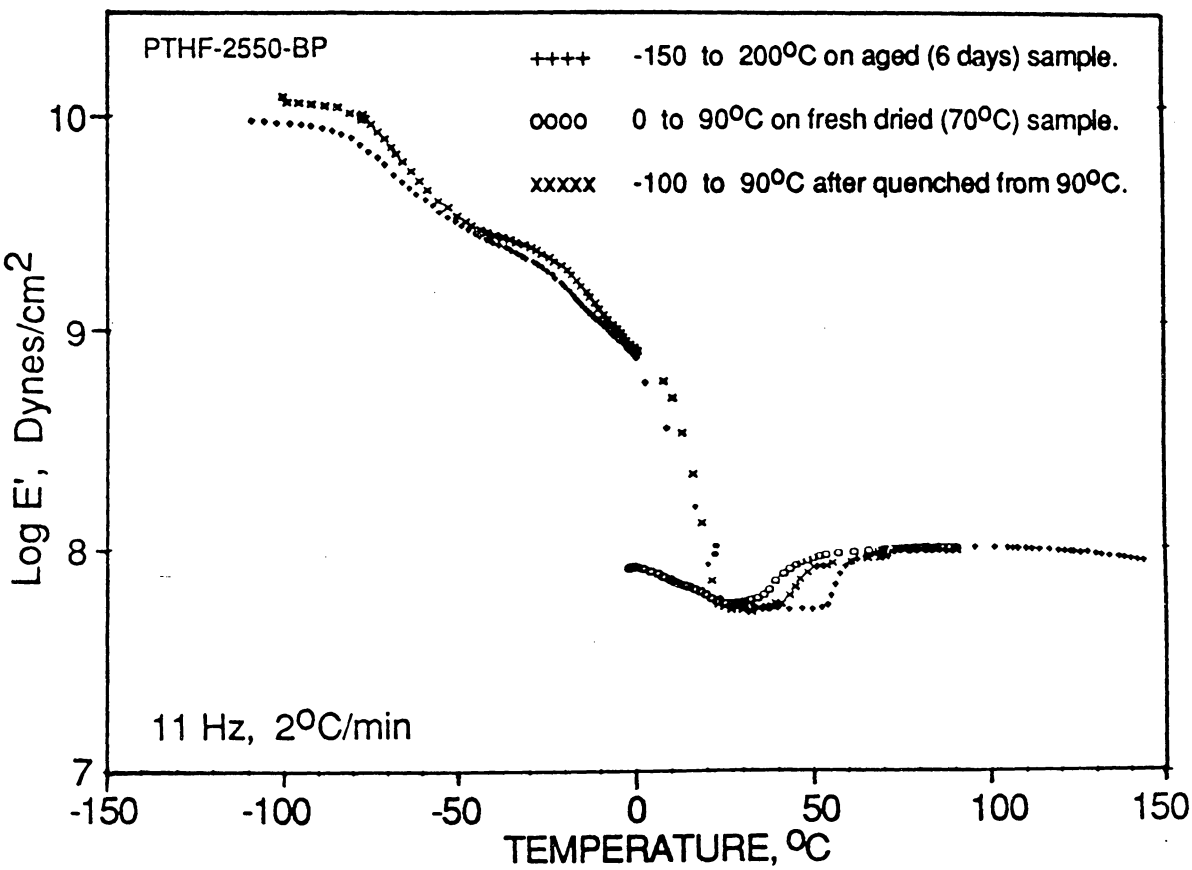

FIGURE 5.34. Thermal History Dependence of Storage Modulus "JUMP".

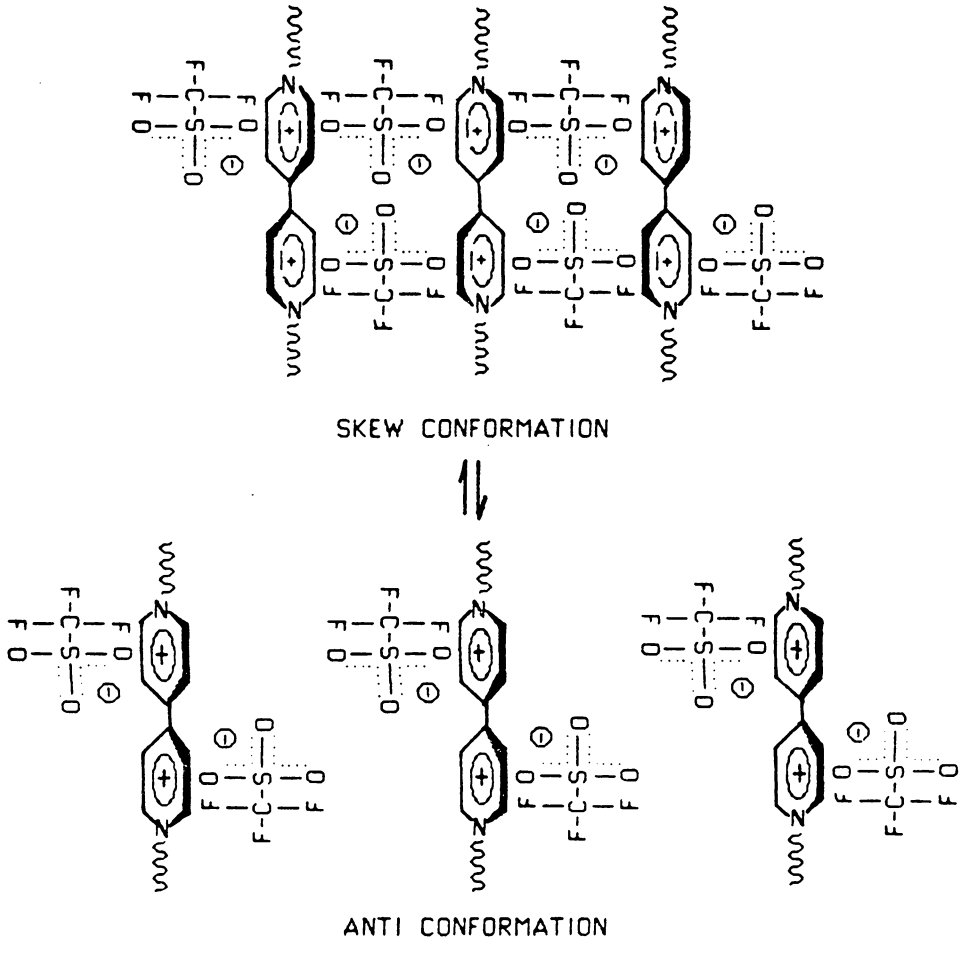

FIGURE 5.35. Conformational Interchange of Bipyridinium Salt.

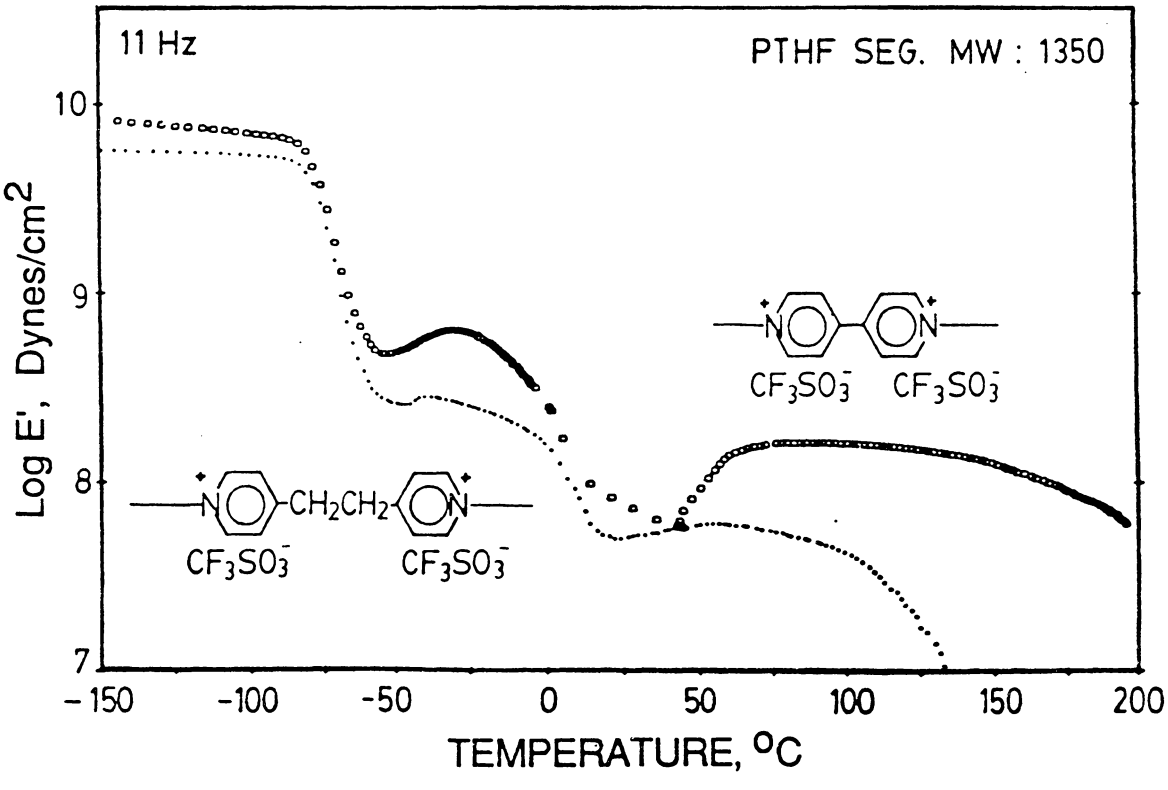

FIGURE 5.36. Dynamic Mechanical Spectra of BP and BPE Based PTHF-Ionenes with Similar PTHF Segment Molecular Weight.

6. GENERAL CONCLUSIONS

Interphase bonding between the hard and soft segments in polyurethanes and polyureas has been demonstrated to be critically important to the degree of phase separation and the cohesiveness of hard segment domain structure. Introduction of urea linkages to polyurethane elastomer systems greatly enhanced the thermal and mechanical properties of the polymer, due possibly to more extensive hydrogen bonding. Enhanced phase separation in polyurethane elastomers has been observed when the urea linkages were located on the polymer backbone. In fact, preliminary work showed that even "free" urea molecules in the polymer matrix could assist this process.

Ionic segments in polytetrahydrofuran-ionenes interact with each other by coulombic interactions, which appears to provide even stronger interchain associations than the hydrogen bonding effects. It was feasible to synthesize these materials via capping dioxonium ion terminated polytetrahydrofuran with ditertiary amines such as bipyridine. The stronger interchain interactions provide polymer with better cohesiveness of the domain structure which was reflected by a higher polymer softening temperature.

Important new polyurethane-urea and ionene elastomers, which are not easily prepared by conventional approaches, now can be synthesized by using the methods described in this thesis.

The vita has been removed from the scanned document